Advancements in minimally invasive image-guided liver therapies
Burgmans, M.C.

Citation

Burgmans, M. C. (2017, October 26). *Advancements in minimally invasive image-guided liver therapies*. Retrieved from https://hdl.handle.net/1887/54940

Cover Page

![Universiteit Leiden logo]

Universiteit Leiden

![Leiden University Repository banner]

The handle http://hdl.handle.net/1887/54940 holds various files of this Leiden University dissertation.
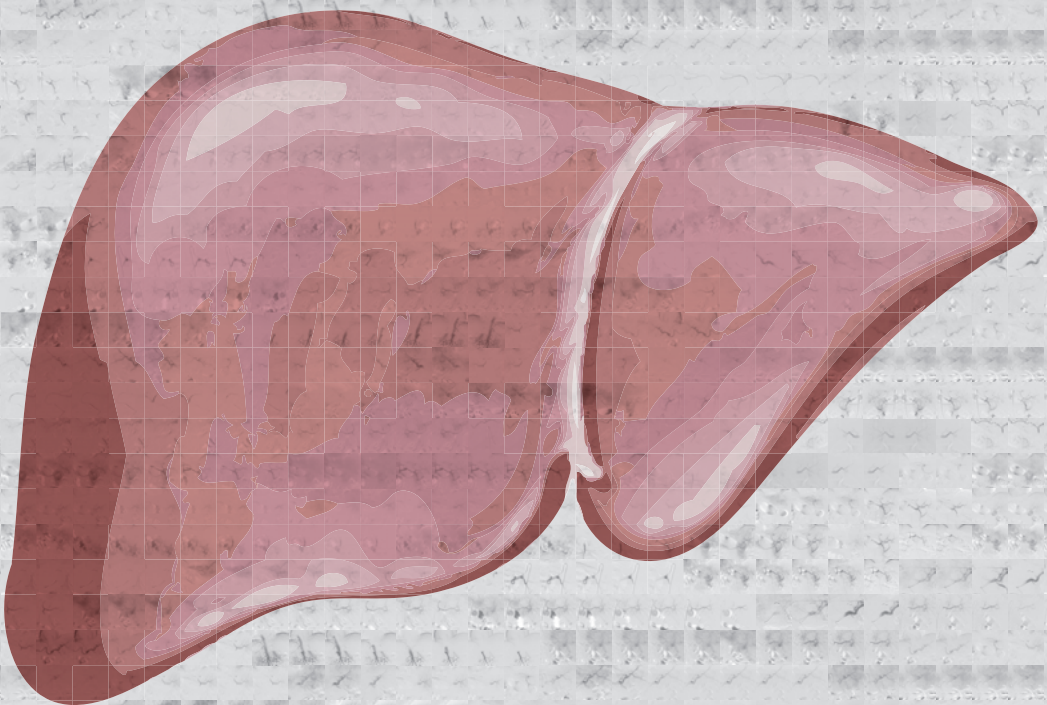
Author: Burgmans, M.C.
Title: Advancements in minimally invasive image-guided liver therapies
Issue Date: 2017-10-26

Mark Burgmans

Advancements in minimally invasive image-guided liver therapies

Advancements in minimally invasive image-guided liver therapies

Mark Burgmans

Advancements in minimally invasive image-guided liver therapies

Proefschrift

ter verkrijging van
de graad van Doctor aan de Universiteit Leiden,
op gezag van Rector Magnificus prof.mr. C.J.J.M. Stolker,
volgens besluit van het College voor Promoties
te verdedigen op 26 oktober 2017
klokke 16.15 uur

door

Mark Christiaan Burgmans

geboren te Leiden
in 1972

CONTENTS

Chapter 1

General introduction
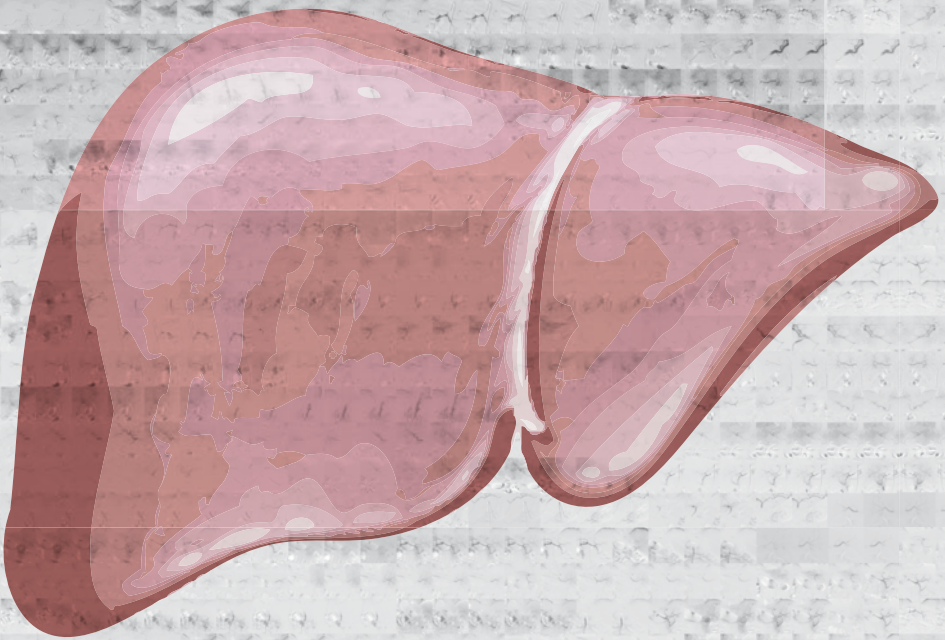
INTRODUCTION

Interventional oncology

Interventional oncology (IO) is a rapidly evolving sub-specialty of interventional radiology with increasing importance in the management of cancer patients. Over the past two decades interventional radiologists together with scientists have ridding the tidal wave of technological innovation to introduce multiple novel cancer treatments. Therapies such as percutaneous ablation, drug-eluting bead trans-arterial chemo-embolization and radioembolization have found their way to clinical practice and are now considered standard of care for various indications. As interventional radiology procedures are targeted minimally invasive therapies, complication rates are generally low and hospital admissions short. This offers clear advantages over surgical procedures and intense chemotherapeutic regimes that put a larger burden on both the health care budget and patients.

IO is a relatively new medical specialty compared to other specialties involved in cancer care, such as surgery, radiotherapy and medical oncology. Whereas many surgical procedures and chemotherapeutic therapies have gone through decades of improvements and evaluation in clinical research and trials, some of the IO procedures have only been introduced in clinical practice over recent years. There is a need for further research to optimize novel minimally invasive therapies and to determine the role in the treatment algorithms for various cancer types.

LIVER MALIGNANCIES

Liver malignancies have been at the center of attention of interventional oncologists. The liver has several unique features that can be utilized when performing minimally invasive image-guided therapies. It is the largest solid organ in the human body and occupies much of the right hypochondrial region of the upper abdomen. The location, size and texture of the liver allow excellent visualization with ultrasonography. Furthermore, the liver has a unique dual blood supply. Most of the blood supply to the hepatocytes is derived from the portal vein (70-80%) and the hepatic arteries supply the remaining 20-30%. In contrast, most hepatic malignancies have a dominant or exclusive vascular supply from the hepatic artery. The difference in vascularization between non-tumorous liver parenchyma and liver malignancies is utilized in transarterial therapies, such as transarterial (chemo)embolization, radioembolization and percutaneous hepatic perfusion.

Primary liver malignancies

Most patients in this thesis are patients with hepatocellular carcinoma (HCC). Primary liver cancer is a rare disease in the Netherlands, but the third most common cause of cancer-related death in the world (1). HCC represents more than 90% of primary liver tumors and the incidence of HCC in Europe is estimated to increase from 21.000 cases in 2008 to 78.000 cases in 2020 (1). Approximately 90% of HCC are associated with an underlying liver disease (1). At the time of diagnosis, the majority of patients with HCC are not surgical candidates. Surgical resection may not be feasible as a result of tumor location, advanced stage of disease or contra-indications such as liver cirrhosis with portal hypertension, deranged liver function or co-morbidity.

For patients who are not surgical candidates, minimally invasive image-guided therapies are often the treatment of choice. In patients with very early stage according to the Barcelona Clinic Liver Cancer (BCLC) staging system (HCC <2cm), percutaneous ablation is the treatment of choice for patients who are not a candidate for liver transplantation. Ablation is the first-line therapy for patients with BCLC early stage (≤3 HCC of ≤3cm each), if surgical resection or transplantation is contra-indicated (2). In patients with BCLC intermediate stage, the superiority of transarterial chemo-embolization (TACE) over best-alternative care has been demonstrated in two randomized controlled trials (3,4). The efficacy of transarterial radioembolization has been proven in several phase II and retrospective studies in patients with either intermediate or advanced BCLC stage (5,6).

Secondary liver malignancies

The liver is a predilection site for metastases from various malignancies. The high incidence of liver metastases may be attributed to several factors. First, the likelihood of metastatic deposits is increased as a high volume of blood perfuses the liver. The liver has an extensive capillary network and therefore blood flow in the liver is relatively slow, increasing the likelihood that tumor cells nestle in the liver (7). Second, several organs with a high incidence of malignancies, such as the colon and pancreas, drain into the portal vein through the splanchnic veins and subsequently into the capillary bed of the liver. Finally, the endothelium of the liver sinusoids lacks a basal lamina and endothelial fenestration may allow tumor cells to exit the bloodstream more easily (7).

MINIMALLY INVASIVE, IMAGE-GUIDED LIVER INTERVENTIONS

Radiofrequency ablation

Radiofrequency ablation (RFA) is the most commonly used ablation technique used for the treatment of liver tumors. After placement of a RFA probe into a tumor using a percutaneous or open approach, an alternating electrical current can be delivered through the RFA probe. This causes ionic cell agitation that results in heat generation. The heat is generated in an active zone around the tip of the RFA probe and more peripheral areas receive heat through thermal conduction. RFA is most suitable for tumors smaller than 3cm as larger tumors are associated with higher local tumor recurrence rates (8-10).

Much of the research on ablation focuses on ways to reduce recurrence rates. More accurate tumor targeting and improved response assessment is essential in achieving better outcomes after RFA. Also, on-going trials are analyzing the efficacy of combination treatment of RFA with either other locoregional therapies or systemic therapy. Furthermore, new RFA systems and alternative ablation techniques, such as microwave ablation (MWA) and irreversible electroporation (IRE), have been introduced over recent years.

Transarterial chemoembolization

Transarterial chemoembolization (TACE) was accepted as the first line treatment in patients with intermediate stage HCC after two randomized trials showed the superiority of TACE over best alternative care (3,4). TACE has not been widely adopted in the Netherlands as a treatment for secondary tumors, but there is growing scientific evidence that TACE offers symptomatic relieve and/or survival benefit in patients with liver metastases from various histologic origins (11,12). Over the past decade, there has been an increased use of TACE with drug-eluting beads. These embolic beads can be preloaded with a chemotherapeutic agent and allow a sustained, local drug release with lower systemic toxicity (13). The availability of smaller micro-catheters, allowing more selective hepatic artery catheterization, and better imaging techniques, such as cone-beam computed tomography (CBCT) and computed tomography hepatic arteriography (CTHA), has led to more accurate tumor targeting. Nevertheless, recurrence rates after TACE are high and the long-term prognosis remains poor. There is an on-going demand for improvements in patient selection, tumor targeting and response assessment.

Radioembolization

The liver has low tolerance to external radiation therapy, and cirrhosis further decreases this tolerance. External beam radiation may cause radiation-induced liver disease at a whole liver dose exceeding 40 Gray (Gy), but such a dose is generally insufficient to

cause necrosis in liver tumors (14). Radioembolization enables delivery of a high radiation dose to a liver tumor with limited radiation injury to the non-tumorous liver tissue. Radioembolization is a form of brachytherapy, in which microspheres loaded with a radionuclide are delivered to the hepatic tumors by selective hepatic arterial infusion. Currently, microspheres loaded with either yttrium-90 (SIR-spheres or Theraspheres) or Holmium-166 (QuiremSpheres) are commercially available. The infused microspheres lodge permanently within the vascular bed of the tumor to deliver high-energy ß-radiation. Each microsphere has a limited therapeutic range (mean tissue range 2.5-3.2mm; maximum 9-11mm), but radiation of the entire tumorous region can be achieved by infusion of large numbers of spheres. Radioembolization has been proven to be an effective treatment for patients with irresectable HCC and is used in clinical practice to treat intermediate and advanced stages of this disease (6,15). Also, radioembolization has gained acceptance as an effective treatment in patients with liver metastases from colorectal carcinoma and other tumors (16).

Percutaneous hepatic perfusion

The unique hepatic anatomy allows vascular isolation of the liver from the systemic blood circulation Percutaneous hepatic perfusion (PHP) is a novel minimally invasive technique that enables vascular isolation and perfusion of the liver with the use of endovascular techniques (17). This technique allows administration of a very high dose of chemotherapy to the liver with limited systemic side effects. This innovative therapy has been shown to be effective, especially in patients with hepatic metastases from ocular melanoma (17).

AIM AND OUTLINE OF THIS THESIS

The aim of this thesis is to evaluate and advance minimally invasive image-guided liver therapies. Current practices and therapies are evaluated and new imaging techniques and treatment strategies are analyzed. PART I focuses on image-guided percutaneous RFA. In chapter 2, the results are presented of a retrospective study of 279 HCC patients treated with percutaneous RFA in either a tertiary referral center in Northern-Europa or South-East Asia. The study investigates how differences in base-line patient characteristics may vary per geographical region and influence long-term outcome. Chapter 3 is a phantom study that investigates the accuracy of electromagnetic fusion of volumetric computed tomography (CT) with real-time ultrasonography (US). Such fusion imaging may enable US-guided targeting of tumors, even if lesions are inconspicuous on US. In the phantom study, manual fusion of images is compared with automatic and semi-automatic fusion and the accuracy and errors of fusion imaging are investigated. In chapter

4, the efficacy of RFA with adjuvant drug-eluting bead TACE is evaluated in patients with HCC >3cm. PART II discusses transarterial liver therapies. The subject of chapter 5 is a prospective study comparing catheter-directed contrast-enhanced ultrasound (CCEUS) and catheter-directed computed tomography hepatic arteriography (CTHA) as adjuncts to digital subtraction angiography (DSA) to guide TACE. Chapter 6 describes the feasibility and safety of yttrium-90 (Y90) infusion into the right inferior phrenic artery in large HCC tumors with extra-hepatic vascular supply, using CTHA in addition to DSA to plan and execute therapy.. The superior imaging capabilities of CTHA are also demonstrated in Chapter 7. As shown in this chapter, CTHA enables better detection of the falciform artery compared to DSA and Tc99m-macroaggregated albumin single photon emission computed tomography with integrated computed tomography (Tc99m-MAA SPECT/CT). The value of CTHA is further illustrated in Chapter 8 that discusses the development of personalized predictive dosimetry in radioembolization with the use of artery-specific SPECT/CT partition modeling. Chapter 9 is a review of the current literature on PHP. The results of a prospective pharmacological study investigating the efficacy and safety of the Delcath GEN2 filter are reported in Chapter 10. PART III is a short but indispensible part of this thesis. In Chapter 11, a prospective study is presented that evaluates the impact of an outpatient interventional radiology clinic on patient safety and satisfaction. Finally, the main conclusions of this thesis are summarized and discussed in Chapter 12.
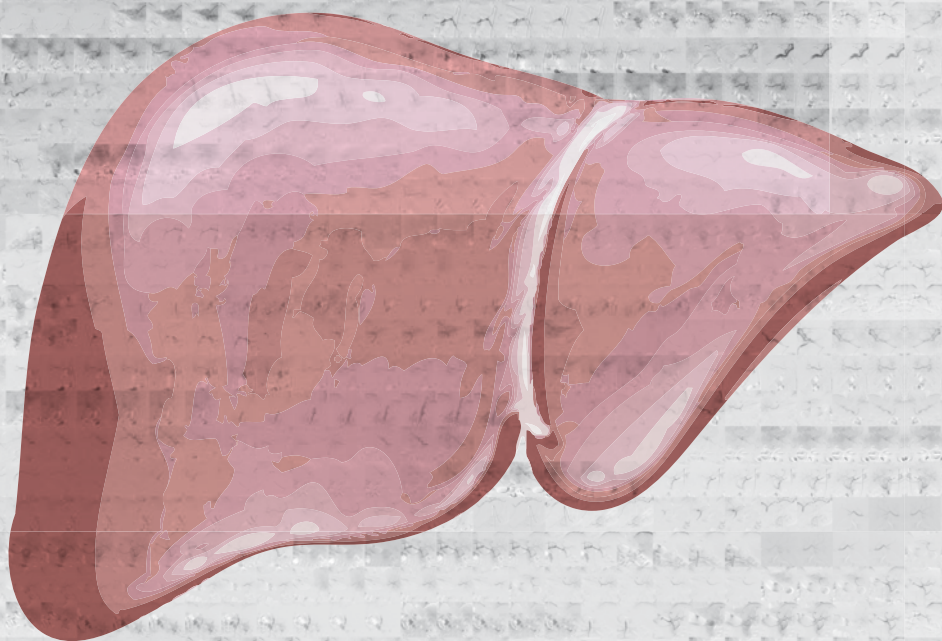
REFERENCES

1. EASL-EORT clinical practise guidelines: management of hepatocellular carcinoma. European Association for Study of Liver; European Organisation for Research and Treatment of Cancer. Eur J Cancer. 2012 Mar;48(5):599-641.

2. Forner A, Llovet JM, Bruix J. Hepatocellular carcinoma. Lancet 2012: 379:1245-55.

3. Llovet JM, Real MI, Monta.a X, et al. Arterial embolisation or chemoembolization versus symptomatic treatment in patients with unresectable hepatocellular carcinoma: a randomised controlled trial. Lancet 2002; 359: 1734–39.

4. Lo CM, Ngan H, Tso WK, et al. Randomized controlled trial of transarterial lipiodol chemoembolization for unresectable hepatocellular carcinoma. Hepatology 2002; 35: 1164–71.

5. Sangro B, Salem R, Kennedy A, Coldwell D, Wasan H. Radioembolization for hepatocellular carcinoma: a review of the evidence and treatment recommendations. Am J Clin Oncol. 2011;34:422-31.

6. Sangro B, Iñarrairaegui M, Bilbao JI. Radio-embolization for hepatocellular carcinoma. J Hepatol. 2012;56:464-473.

7. Vidal-Vanaclocha F. Architectural and functional aspects of the liver with implications for liver metastasis. In P.Brodt (ed.), Liver metastasis – biology and treatment 16, DOI 10.1007/978-94-007-029209_2, Springer Media BV 9-42.

8. Weis S, Franke A, Mössner J, Jakobsen JC, Schoppmeyer K. Radiofrequency (thermal) ablation versus no intervention or other interventions for hepatocellular carcinoma (Review). The Cochrane Library 2013, Issue 2.

9. Tiong L, Maddern GJ. Systematic review and meta-analysis of survival and disease recurrence after radiofrequency ablation for hepatocellular carcinoma. Br J Surg. 2011 Sep;98(9):1210-24.

10. Mulier S, Ruers T, Jamart J, Michel L, Marchal G, Ni Y. Radiofrequency ablation versus resection for resectable colorectal liver metastases: time for a randomized trial? An update. Dig Surg 2008;25(6):445-60.

11. Fiorentini G, Aliberti C, Tilli M et al. Intra-arterial infusion of irinotecan-loaded drug-eluting beads (DEBIRI) versus intravenous therapy (FOLFIRI) for hepatic metastases from colorectal cancer: final results of a phase III study. Anticancer Res 2012;32:1387–95.

12. Richardson AJ, Laurence JM, Lam VW. Transarterial chemoembolization with irinotecan beads in the treatment of colorectal liver metastases: systematic review. J Vasc Interv Radiol 2013;24(8):1209-17.

13. Lammer J, Malagari K, Vogl T, et al. Prospective randomized study of doxorubicin-eluting-bead embolization in the treatment of hepatocellular carcinoma: results of the PRECISION V study. Cardiovasc Intervent Radiol 2010. Feb;33(1):41-52.

14. Emami B, Lyman J, Brown A, et al. Tolerance of normal tissue to therapeutic irradiation. Int J Radiat Oncol Biol Phys. 1991 May 15;21(1):109-22.

15. Salem R, Thurston KG. Radioembolization with 90Yttrium microspheres: a state-of-the-art brachytherapy treatment for primary and secondary liver malignancies. Part 1: Technical and methodologic considerations. J Vasc Interv Radiol. 2006 Aug;17(8):1251-78.

16. van Cutsem E, Cervantes A, Adam R, et al. ESMO consensus guidelines for the management of patients with metastatic colorectal cancer. Ann Oncol 2016 Aug;27(8):1386-422.

17.   Burgmans MC, de Leede EM, Martini CH, et al. Percutaneous isolated hepatic perfusion for the treatment of unresectable liver malignancies. Cardiovasc Interv Radiol. 2016 Jun;39(6):801-14

PART I

PERCUTANEOUS RADIOFREQUENCY ABLATION

Chapter 2

Differences in patient characteristics and midterm outcome between Asian and European patients treated with radiofrequency ablation for hepatocellular carcinoma
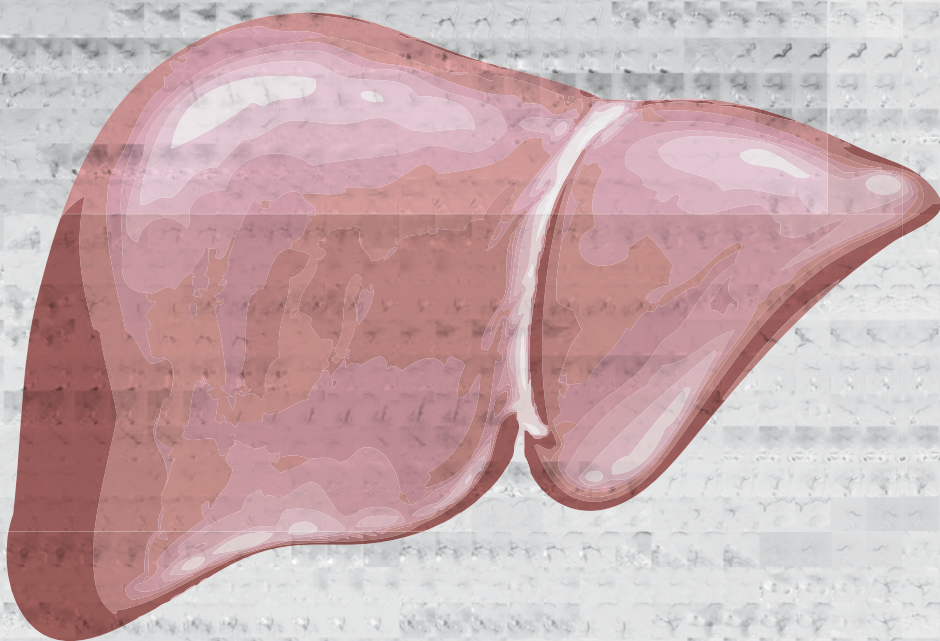
Burgmans MC, Too CW, Fiocco M, Kerbert AJC, Lo RH, Schaapman JJ, van Erkel AR, Coenraad MJ, Tan BS

ABSTRACT

Purpose

The aim of this study was to compare patient characteristics and mid-term outcome after RFA for unresectable hepatocellular carcinoma (HCC) in an Asian and European cohort

Methods

The study was based on retrospective analysis of 279 patients (mean 64.8 ± 12.1 years; 208 males) treated with RFA for de novo HCC in tertiary referral centers in Singapore and the Netherlands, with median follow-up of 28.2 months (quartiles: 13.1-40.5 months). Cumulative incidence of recurrence and death were analyzed using a competing risk model.

Results

Age was higher in the Asian group: 66.5 versus 60.1 years (p<0.0001). The most common etiology was hepatitis B in the Asian group (48.0%) and alcohol-induced cirrhosis in Europeans (54.4%); p<0.001. Asian patients had less advanced disease: 35.5%, 55.0% and 3.0% respectively had BCLC 0, A and B versus 21.5%, 58.2% and 15.2% in the European group (p=0.01). The cumulative incidence of recurrence in the Asian group at 1, 2, 3 and 5 years was 37.0%, 56.4%, 62.3% and 67.7% respectively compared to 32.6%, 47.2%, 49.7% and 53.4% in the European group (p=0.474).

At 1, 2, 3 and 5 years the cumulative incidence of death in the Asian group was 2.0%, 3.9%, 4.9% and 4.9% respectively and 7.7%, 9.2%, 14.1% and 21.0% in the European group (p=0.155).

Conclusion

Similar short-term treatment outcomes are achieved with RFA in HCC patients in the South-East Asian and Northern-European populations. Midterm recurrence and death rates differ between the groups as a result of differences in baseline patient characteristics and patient selection. Our study provides insight relevant to the design of future international studies.

INTRODUCTION

Hepatocellular carcinoma (HCC) is a heterogeneous condition with multiple variables affecting the course of the disease. The prognosis is not only determined by the tumor burden, but also by the liver function and performance status of a patient. In order to have stratification and prognostication ability, most staging systems have incorporated various prognostic factors (1-6). The Barcelona Clinic Liver Cancer (BCLC) classification system is the most widely adopted staging system for HCC worldwide and is endorsed by the European Association for the Study of the Liver (EASL) and American Association for the Study of Liver Disease (AASLD) (7,8). The Asian Pacific Association for the Study of the Liver (APASL) guidelines are based on results from many of the randomized controlled trials and cohort studies that were also used to devise the BCLC schedule, and both guidelines use similar eligibility criteria for RFA (9). Despite adherence to similar treatment guidelines, outcomes in daily clinical practice are unlikely to be the same in different parts of the world as a result of geographical differences in characteristics and etiology of HCC. In East-Asia, the incidence rates of HCC are high and most HCC cases are attributable to chronic hepatitis B infection (7,10). In Northern-European countries, HCC is not prevalent, and chronic hepatitis C and alcohol-induced liver disease are the most dominant predisposing risk factors (7,10).

Prospective clinical trials have been essential in the development of treatment guidelines, but often only recruit patients from a particular region and according to strict eligibility criteria. Real-world observational studies are needed to provide insight into how the implementation of HCC guidelines has affected patient care in different geographical regions. The aim of our descriptive study was to compare the patient characteristics and midterm outcome after RFA for unresectable, de novo HCC in an Asian and European patient cohort. In this retrospective study, the cumulative incidence of recurrence and death after RFA were analyzed in large centers both in South-East Asia and Northern Europe.

METHODS

Patients

We conducted a retrospective analysis of a patient cohort in a high-volume hospital in Singapore and the Netherlands. Both institutions were tertiary referral centers with dedicated care for hepato-biliary diseases and liver transplant programs. The local medical ethics committee of both institutions approved the retrospective study and informed consent was waived for the analysis. Between January 2009 and March 2014, 442 consecutive patients were treated with percutaneous RFA for unresectable HCC

in the radiology department of one of the two centers. Of the 442 patients, 163 had undergone previous HCC treatment, i.e. ablation, resection, transplantation or transarterial chemoembolization, and these were excluded from the analysis. All remaining 279 patients (mean age ± standard deviation (SD): 64.8 ± 12.1 years; 208 males) were treated with RFA because of newly diagnosed HCC. The diagnosis was based on either tumor histology (n=30) or on radiological imaging criteria according to guidelines by the EASL or the APASL (n=249) (7,9). For radiological confirmation of the diagnosis, multiphase contrast-enhanced computed tomography (CECT) and/or dynamic gadolinium-enhanced magnetic resonance imaging (GE-MRI) was used. Arterial hyperenhancement of a lesion with wash-out in the delayed phase was considered to be diagnostic of HCC in patients with liver cirrhosis or chronic hepatitis B/C.

Similar eligibility criteria were used in both centers for local ablation and these were in accordance with the BCLC and APASL treatment guidelines: a single tumor measuring ≤5 cm or a maximum of 3 HCCs measuring ≤3cm each and Child Pugh A or B status (7,9). In exceptional cases, RFA was offered also outside BCLC and APASL criteria. In patients with two tumors, RFA was considered if only one HCC measured more than 3cm and no more than 5 cm. Patients with Child Pugh C who were on the waiting list for liver transplantation could undergo RFA as a bridging therapy to transplantation. Contraindications for RFA were: significant and uncorrectable coagulopathy, extrahepatic metastasis, or macrovascular invasion, and severe liver dysfunction (Child-Pugh C) in a patient *not* eligible for liver transplantation.

Radiofrequency ablation

All patients gave informed consent prior to treatment. Percutaneous RFA was performed using ultrasound and/or CT guidance. In the European center, procedures were performed under general anesthesia. Local anesthesia and conscious sedation with midazolam and fentanyl were used in the Asian center.

Both centers used similar RFA equipment: either a single electrode was used (3 cm exposed tip Cooltip (Covidien, Gosport Hamspire, United Kingdom) or multiple electrodes with a switch-control system (3 or 4 cm exposed tip Cooltip). Ablation was performed for 12 (single Cooltip electrode) or 16-20 minutes (multiple Cooltip electrodes) using standard impedance controlled ablation. In the European center, CECT was performed immediately after ablation on a spiral CT (Aquilion 16, Toshiba, Tokyo, Japan). If this CT showed residual tumor enhancement, immediate re-ablation was performed. In the Asian center, CECT was performed 1 day after ablation (Aquillion 64, Toshiba, Tokyo, Japan). If the CECT showed residual tumor enhancement, re-ablation was performed during the same or subsequent admission, dependent on the patient's preference.

Follow-up

All patients were scheduled for follow-up examinations every 3 months after RFA, including liver function tests and multiphase CECT or dynamic GE-MRI. In the European center, these examinations were also performed at 6 weeks after RFA.

Recurrence was defined as local tumor progression (LTP) and/or a new intrahepatic tumor distant from the treated tumor. Recurrence was distinguished from incomplete ablation. Tumor enhancement on the CECT performed immediately or 1 day after RFA, was classified as incomplete ablation and treated with repeated RFA until complete radiological ablation was achieved. Patients were followed until last follow-up date, death, or till the end of the study.

The median follow-up for all patients was 28.2 months (quartiles: 13.1–40.5 months).

Statistical analysis

Comparisons between the two groups were done by student t-test for continuous variables and Pearson Chi-Square test for categorical variables using two-sided tests. A competing risk model with recurrence and death as competing events was used to estimate the cumulative incidence of recurrence and death per center. To study the impact of prognostic factors on recurrence the cause specific hazard ratios were estimated by employing a Cox proportional hazard regression model with transplantation as time-dependent risk factor (11). A Cox's proportional hazard model was employed to study the association between risk factors and overall survival with recurrence and transplantation as time-dependent risk factors. A difference was considered significant when $p < 0.05$. The statistical analyses were performed using SPSS 21 (IBM, Armonk, NY, USA). The competing risks analysis was performed in the R-software environment with the mstate library (12,13).

RESULTS

Patient characteristics

Baseline demographics of all patients are shown in Table 1. The median age of patients in the Southeast Asian group was slightly higher than that of the Northern European patients ($p<0.0001$). Statistically significant differences between the patient groups were also seen in underlying liver disease and BCLC stage ($p<0.0001$ and $p=0.01$ respectively). In the European patients, alcoholic liver disease was most prevalent (54.4%) followed by hepatitis C (22.7%), whereas the majority of Asian patients suffered from chronic hepatitis B (48.0%). The percentage of patients without underlying liver disease

was much higher in the Asian group compared to the European group: 19.0% versus 6.3%. The Asian group had a higher percentage of patients with BCLC very early stage: 35.5% versus 21.5% in the European group. Both the percentage of patients with BCLC early stage and intermediate stage were higher in the European group: 58.2% and

Table 1. Baseline characteristics of 279 patients treated with RFA for de novo HCC.

	Asia-Pacific; n=200 (%)	European; n=79 (%)	Total; n=279 (%)	p-value
Age (year), mean ± SD	66.5 ± 10.7	60.1 ± 14.3	64.8 ± 12.1	**<0.0001**
Male/female	144 / 56 (72,0 / 28,0)	64 / 15 (81,0 / 19,0)	208 / 71 (74,6 / 25,4)	0.78
Etiology				**<0.0001**
HBV	96 (48.0)	7 (8.9)	103 (36.9)	
HCV	26 (13.0)	18 (22.7)	44(15.8)	
Alcohol	21 (10.5)	43 (54.4)	64 (22.9)	
NASH	11 (5.5)	3 (3.8)	14 (5.0)	
Cryptogenic	38 (19.0)	5 (6.3)	43 (15.4)	
Others	8 (4.0)	3 (3.8)	11 (3.9)	
AFP (ng/mL), mean ± SD	141,4 ± 753.3[x]	346.9 ± 1600.6[#]	212.7 ± 1122.7	0.289
Child Pugh class				0.248
A	137 (68.5)	48 (60.8)	185 (66.3)	
B	49 (24.5)	27 (34.2)	77 (27.6)	
C	14 (7.0)	4 (5.0)	17 (6.1)	
Number of tumors				0.139
1	154 (77.0)	53 (67.1)	207 (74.2)	
2	39 (19.5)	24 (30.4)	63 (22.6)	
3	7 (3.5)	2 (2.5)	9 (3.2)	
Maximal diameter largest tumor (mm), mean ± SD	23.7 ± 11.3	26.8 ± 12.6	24.9 ± 12.5	0.85
Maximal diameter largest tumor				0.106
<10mm	9 (4.5)	0 (0.0)	9 (3.2)	
10-<20mm	84 (42.0)	26 (31.9)	110 (39.4)	
20-30mm	61 (30.5)	26 (32.9)	87 (31.2)	
>30mm	46 (23.0)	27 (34.2)	73 (26.1)	
BCLC stage				**0.01**
0	71 (35.5)	17 (21.5)	88 (31.5)	
A	110 (55.0)	46 (58.2)	156 (55.9)	
B	6 (3.0)	12 (15.2)	18 (6.5)	
C	0 (0.0)	0 (0.0)	0 (0.0)	
D	13 (6.5)	4 (5.0)	17 (6.1)	

SD = standard deviation HBV = hepatitis B virus. HCV = hepatitis C virus. NASH = non-alcoholic steatosis hepatitis. AFP = alpha-fetoprotein BCLC = Barcelona Clinic Liver Cancer.[x]55 missing. [#]2 missing.

15.2%, respectively, versus 55.0% and 3.0% in the Asian group. These differences in BCLC stage may be explained by the dissimilarities in Child Pugh class, number of tumors and maximal tumor diameter between the two groups. In the Asian group, a higher percentage of patients had Child Pugh A status (68.5% versus 60.8%), a single tumor (77.0% versus 67.1%), and the mean maximal diameter of the largest tumor was smaller (23.7 ± 11.3mm versus 26.8 ± 12.6mm). The differences in Child Pugh status, tumor number and tumor size did not reach statistical significance.

Treatment outcome

In 269 patients (96.4%) technical success was achieved after a single RFA procedure. In the remaining 10 patients a second ablation procedure was needed to achieve technical success.

The cumulative incidence of recurrence showed a similar trend in both the Asian and European groups during the first 1.5 years after RFA (Figure 1). At 6, 12 and 18 months, the cumulative incidence rates for recurrence in the Asian group were equal to 25.5% (95% CI: 19.5-31.6), 37.0% (95% CI: 30.3-43.8) and 49.1% (95% CI: 41.9-56.2) respectively, compared to 24.1% (95% CI: 14.7-33.5), 32.6% (95% CI: 22.0-43.2) and 45.5% (95% CI: 33.8-57.2), respectively, in the European group. The cumulative incidence of recurrence was higher in the Asian group at 2, 3 and 5 years: 56.4% (95% CI: 49.1-63.8), 62.3% (95% CI: 54.7-69.8) and 67.7% (95% CI: 58.6-76.7), respectively, compared to 47.2% (95% CI: 35.4-59.0), 49.7% (95% CI: 37.5- 62.0) and 53.4% (95% CI: 40.2-66.6), respectively, in the European group. The difference between the cumulative incidences of recurrence for the two groups was not significant (p=0.474).

The cumulative incidence of death was higher in the European population compared to the Asian group (Figure 1). At 1, 2, 3 and 5 years, the cumulative incidence rates of death were 2.0% (95% CI: 0.06-4.0), 3.9% (1.0-6.7), 4.9% (1.5-8.3) and 4.9% (1.5-8.3), respectively, in the Asian group and 7.7% (1.8-13.6), 9.2% (2.7-15.8), 14.1% (5.1-23.1) and 21.0% (9.0-33.1) in the European group. The differences in cumulative death between the two groups did not reach statistical significance (p=0.155).

Prognostic factors associated with the risk of recurrence

A maximal tumor diameter >3cm and tumor number >1 were independent risk factors for recurrence after RFA (Table 2). The cause-specific hazard ratio (csHR) was equal to 1.568 (95% CI: 1.083-2.271) for patients with HCCs >3cm. Patients with more than 1 tumor were 1.5 times more like to develop recurrence than patients with a single tumor (HR$_c$ 1.494 (95% CI: 1.031-2.163). Liver transplantation had a significant protective effect on tumor recurrence (HR$_c$ 0.065; 95% CI: 0.009-0.480).
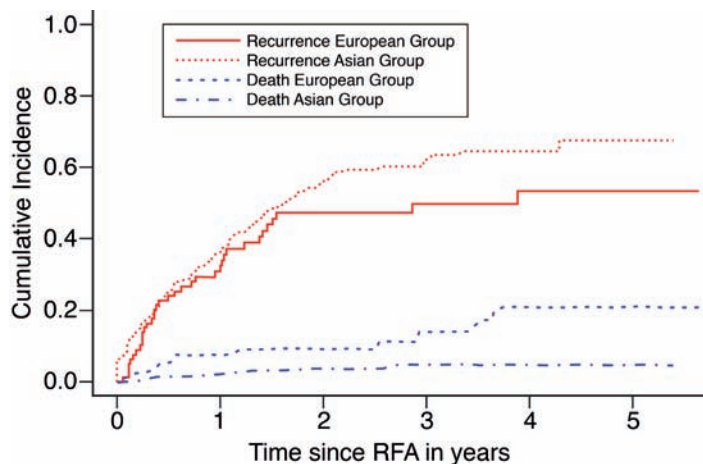
Figure 1. Cumulative incidence of recurrence and death in the South-East Asian and Northern European patient group

Cox regression model for overall survival

Child Pugh B/C status and recurrence were independent risk factors for death after RFA (Table 3). The hazard ratios (HRs) for Child Pugh B and C were equal to 2.924 (95% CI: 1.582-5.404) and 4.824 (95% CI: 2.100-11.083), respectively, with Child Pugh A status as reference category. The HR was almost 5 times increased in patients with recurrence compared to patients without recurrence (HR 4.524; 95% CI: 2.438-8.395). An increased

Table 2. Cause-specific hazard ratios to evaluate the effect of prognostic factors on risk of recurrence (multivariate analysis)

	csHR	95.0% CI for HR		p-value
		Lower	Upper	
Female (reference male)	.844	.567	1.256	0.403
Child Pugh A (reference)				0.480
Child Pugh B	.795	.535	1.181	0.256
Child Pugh C	.810	.412	1.591	0.540
Largest tumor diameter >3cm	1.568	1.083	2.271	**0.017**
Tumor number >1	1.494	1.031	2.163	**0.034**
Hepatitis B (reference)				0.739
Hepatitis C	.857	.497	1.477	0.578
Alcohol-induced	1.175	.702	1.967	0.538
Other	1.100	.692	1.750	0.686
South-East Asian center[x]	.978	.609	1.568	0.925
Liver transplantation	.065	.009	.480	**0.007**

Statistical significant *p* values are given in bold p < 0.05. csHR = cause-specific hazard ratio. CI = confidence interval. [x]The Northern-European Center was used as the reference center

HR of death was found in patients with either hepatitis C or alcohol-induced liver disease compared to hepatitis B, but the differences were not statistically significant.

Liver transplantation had a protective effect, though not statistically significant (HR 0.805; 95% CI: 0.318-2.036).

Further treatment

Table 4 provides an overview of consecutive treatments that were administered in patients with recurrent disease. No significant differences were seen between the two groups other than the higher proportion of patients in the European group receiving a liver transplantation. In the European group, 44.3% (n=35) of patients eventually underwent liver transplantation compared to 3.0% in the Asian group (n=6) (p<0.0001).

Table 3. Hazard ratios to evaluate the effect of prognostic factors on overall survival (multivariate analysis)

	HR	95.0% CI for HR		p-value
		Lower	Upper	
Female (reference male)	.968	.491	1.911	0.926
Child Pugh A (reference)				0.000
Child Pugh B	2.924	1.582	5.404	**0.001**
Child Pugh C	4.824	2.100	11.083	**0.000**
Largest tumor diameter >3cm	1.326	.714	2.462	0.372
Tumor number >1	.679	.355	1.299	0.242
Hepatitis B (reference)				0.399
Hepatitis C	1.573	.697	3.549	0.275
Alcohol-induced	1.234	.554	2.747	0.607
Other	.776	.326	1.845	0.566
South-East Asian center	.531	.269	1.049	0.068
Recurrence (time-dependent)	4.524	2.438	8.395	**0.000**
Liver transplantation	.805	.318	2.036	0.647

Statistical significant *p* values are given in bold p < 0.05. HR = hazard ratio. CI = confidence interval

Table 4. Summary of second line treatment in the South-East Asian and Northern-European patient cohort

Second line treatment	Asian group; n=97 (48.5%)	European group; n=54 (68.4%)	p-value
Resection	8 (4.0)	2 (2.5)	0.552
RFA	68 (34.0)	21 (26.6)	0.231
TACE/TARE	35 (17.5)	13 (16.5)	0.835
Liver transplantation	5 (2.5)	35 (44.3)	**<0.0001**
Sorafenib	3 (1.5)	4 (5.1)	0.89

Statistical significant *p* values are given in bold p < 0.05. TACE = transarterial chemoembolization. TARE = transarterial radioembolization

DISCUSSION

Our study provides insight in the differences in baseline characteristics and treatment outcome between a South East Asian and Northern European cohort of patients undergoing RFA for de novo HCC. The differences observed may have implications for clinical management and the design of large multicenter, international studies.

Our study confirms that hepatitis B is the leading cause of HCC in South-East Asia, whereas most HCC cases in Northern Europe are related to alcohol or hepatitis C. This is well known from the literature (7,10). The higher percentage of patients without known risk factors in the Asian study group is also consistent with previous reports (14).

In the Asian group, the number of tumors as well as Child Pugh score was lower compared to the European group. These observed dissimilarities between the two groups may, in part, reflect differences in patient selection. First of all, differences in screening between the Netherlands and Singapore may have resulted in detection of tumors at an early stage in the Asian group. In both countries, six monthly screening with ultrasonography was common practice during the study period, but the higher incidence of HCC in Asia is likely to results in higher awareness and better adherence to the screening program by Singaporean doctors and patients. Secondly, differences in baseline characteristics may be a result of differences in the EASL and APASL guidelines. According to the APASL guidelines, the diagnosis of HCC can be made regardless of the size of a lesion, if a lesion has typical arterial enhancement and portovenous 'wash-out' on diagnostic imaging. This is different from the EASL guidelines that state that non-invasive criteria only apply in patients with typical lesions >1cm. The difference in diagnostic criteria between the APASL and EASL guidelines explains the difference in baseline tumor size between the Asian and European group in our study. In the Asian group, 9 patients had a maximal tumor diameter of <1cm, whereas all European patients had a tumor larger than 1 cm. This is also reflected by the smaller mean tumor diameter of patients in the Asian group compared to that of the European patients (23.7 ± 11.3 versus 26.8 ± 12.6 respectively). As the noninvasive diagnostic accuracy is lower in lesions <1cm, there is an increased risk of a false-positive diagnosis of HCC in the Asian group in our study. It is unlikely though that this had a significant impact on the results of our study, as only 4.5% of patients in the Asian group had lesions <1cm. There is considerable overlap between the BCLC and APASL treatment algorithms with regards to selection of patients for RFA. According to both algorithms, eligible candidates are Child Pugh A/B patients with a single tumor ≤ 5cm or up to 3 nodules of ≤3cm each *and* the absence of vascular invasion or extra-hepatic disease (the EASL guidelines do not clearly give a maximal diameter for a solitary tumor, but 5cm is generally considered the limit beyond which RFA is associated with

unacceptable high recurrence rates). The EASL and APASL guidelines both recommend RFA as an alternative to resection for patients not suitable for surgery, but do not use the same criteria to select surgical candidates (15). The EASL guidelines recommend resection for patients with a single tumor with very well preserved liver function, defined as normal bilirubin with either hepatic vein pressure gradient <10mmHg or platelet count ≥100x 10^9/L. According to the APASL guidelines, surgical resection should be considered for single or multifocal disease, anatomically resectable, and with satisfactory liver function reserve without strict cut-off values. As a result of the more conservative criteria for resection in the EASL guidelines, patients may have been referred for ablation in the European center, whereas the same patients may still have been surgical candidates in the Asian institution. This may have contributed to a higher percentage of patients in the European group with Child Pugh B status and >1 tumor. Following the APASL guidelines, decisions on resectability in South-East Asia are more contingent on age and functional capacity of a patient. This may also explain the significantly higher age of patients in the Asian cohort.

The differences in cumulative incidence of recurrence and death between the Asian and European group are likely related to a multitude of variables, such as patient selection, baseline patient characteristics, pathogenesis and histopathology of tumors, differences in clinical management and treatment of underlying liver disease. Patients in the European group had an insignificant higher midterm cumulative incidence of death. As the recurrence rate in the European patients was not higher than in the Asian patients, the poorer survival rate is probably attributable to factors other than disease progression. It is likely that the significantly higher baseline Child Pugh score had a negative impact on survival. A higher Child Pugh score has been shown to be associated with poorer overall survival in previous studies (16-23). The lower Child Pugh score may also reflect a difference between the two groups in the proportion of patients with cirrhosis, as the development of HCC in the absence of cirrhosis tends to be more common in Asian patients. Another factor could be the differences in therapeutic options for the underlying liver disease. Anti-viral agents such as lamivudine, adefovir dipivoxil or entecavir may improve overall survival after RFA in hepatitis B patients, whereas therapeutic options for hepatitis C and alcohol-induced liver cirrhosis were limited during the study period (24,25). Finally, differences in molecular pathogenesis of HCC between regions and races may result in differences in outcome (26).

Although previous studies have shown that liver transplantation improves survival in patients with HCC, such a survival benefit was not found in our study (27). Transplantation did have a significant protective effect on tumor recurrence, but the protective

effect on survival did not reach statistical significance. This is likely to be related to the relatively small number of patients that were transplanted in our study (14.3%).

Our study findings are of importance when interpreting published studies on RFA in HCC patients. Comparison of studies that have been conducted in different parts of the world is complicated by the differences in patient characteristics, selection and clinical management. Results obtained in an Asian population cannot be extrapolated to a European population without notion of these differences, and vice versa. Our results may also have important implications for the design of new international studies. Based on our results, the impact of RFA on survival may be more difficult to determine in a Northern-European population than in a South-East Asian cohort as factors other than tumor progression play a more important role in the first group of patients. European patients eligible for RFA are likely to have risk factors other than tumor recurrence that are associated with poorer survival, such as hepatitis C or alcohol-induced liver cirrhosis, and higher BCLC stage. To demonstrate survival benefit of RFA in a group of European patients with unresectable HCC, one may thus need a larger sample size than in an Asian patient group.

Our descriptive study has several limitations. The first limitation is the retrospective design of the study. Secondly, the numbers of centers included in our analysis is limited and therefore the data may not be representative for all centers in the geographical regions that were compared. Thirdly, some predicting factors that may have been different between the two cohorts were not analyzed, for example co-morbidity, tumor histology, and anti-viral treatment of hepatitis. Fourthly, a small numbers of patients in the Asian and European group were treated outside APASL and EASL criteria respectively. This may have resulted in differences between the groups that are not attributable to differences in the regional guidelines. Finally, we did not analyze the cause of death. The poorer survival rate in the European patients may have been related to causes other that progression of tumor or underlying liver disease. It is not unlikely that the proportion of patients with tobacco abuse and poor nutritional status was higher in the European group given the higher prevalence of alcohol abuse.

In conclusion, the baseline characteristics of patients treated with RFA for de novo HCC differ between Northern-European and South-East Asian patients. Despite these differences similar short and midterm treatment outcomes are achieved by applying regional recommendations for RFA in HCC patients. Midterm recurrence and death rates differ between the two groups and this may be explained by differences in underlying liver disease, screening, and the more conservative approach to resection in European countries.

REFERENCES

1. Okuda K, Ohtsuki T, Obata H, Tomimatsu M, Okazaki N, Hasegawa H, Nakajima Y, Ohnishi K. Natural history of hepatocellular carcinoma and prognosis in relation to treatment. Study of 850 patients. Cancer 1985;56:918-28.

2. Llovet JM, Brú C, Bruix J. Prognosis of hepatocellular carcinoma: the BCLC staging classification. Semin Liver Dis 1999;19:329-38.

3. A new prognostic system for hepatocellular carcinoma: a retrospective study of 435 patients: the Cancer of the Liver Italian Program (CLIP) investigators. Hepatology 1998;28:751-5.

4. Kudo M, Chung H, Osaki Y. Prognostic staging system for hepatocellular carcinoma (CLIP score): its value and limitations, and a proposal for a new staging system, the Japan Integrated Staging Score (JIS score). J Gastroenterol 2003;38:207-15.

5. Leung TW, Tang AM, Zee B, Lau WY, Lai PB, Leung KL, Lau JT, Yu SC, Johnson PJ. Construction of the Chinese University Prognostic Index for hepatocellular carcinoma and comparison with the TNM staging system, the Okuda staging system, and the Cancer of the Liver Italian Program staging system: a study based on 926 patients. Cancer 2002;94:1760-9.

6. Chevret S, Trinchet JC, Mathieu D, Rached AA, Beaugrand M, Chastang C.. A new prognostic classification for predicting survival in patients with hepatocellular carcinoma. Groupe d'Etude et de Traitement du Carcinome Hépatocellulaire. J Hepatol 1999;31:133-41.

7. European Association For The Study Of The Liver; European Organisation For Research And Treatment Of Cancer. EASL-EORTC clinical practice guidelines: management of hepatocellular carcinoma. J Hepatol 2012. Apr;56(4):908-43.

8. Bruix J, Sherman M, American Association for Study of Liver Diseases. Management of Hepatocellular Carcinoma: An Update. Hepatology 2011. Mar;53(3):1020-22.

9. Omata M, Lesmana LA, Tateishi R, Chen PJ, Lin SM, Yoshida H, Kudo M, Lee JM, Choi BI, Poon RT, Shiina S, Cheng AL, Jia JD, Obi S, Han KH, Jafri W, Chow P, Lim SG, Chawla YK, Budihusodo U, Gani RA, Lesmana CR, Putranto TA, Liaw YF, Sarin SK. Asian Pacific Association for the Study of the Liver consensus recommendations on hepatocellular carcinoma. Hepatol Int. 2010;4:439–474

10. Parkin DM, Bray F, Ferlay J, Pisani P. Global cancer statistics, 2002. CA Cancer J Clin 2005;55:74–108

11. Putter H, Fiocco M, Geskus RB. Tutorial in biostatistics: Competing risks and multi-state models. Stat Med 2007 May 20: 26 (11): 2389–2430

12. De Wreede LC, Fiocco M, Putter H. Mstate: an R package for the analysis of competing risks and multi-state models. J. Stat. Softw 2011;38:1-30.

13. De Wreede LC, Fiocco M, Putter H. The mstate package for the estimation and prediction in non and semi-parametric multi-state and competing risks models. Comput Methods Programs Biomed 2010 Sep;99(3):261-74

14. Bruix J, Sherman M, Llovet JM, Beaugrand M, Lencioni R, Burroughs AK, Christensen E, Pagliaro L, Colombo M, Rodés J; EASL Panel of Experts on HCC.. Clinical management of hepatocellular carcinoma. Conclusions of the Barcelona-2000 EASL conference. European Association for the Study of the Liver. J Hepatol 2001;35:421– 430

15. Chow PK. Resection for hepatocellular carcinoma: is it justifiable to restrict this to

the American Association for the Study of the Liver/Barcelona Clinic for Liver Cancer criteria? J Gastroenterol Hepatol. 2012 Mar;27(3):452-7.

16. Choi D, Lim HK, Rhim H, Kim YS, Lee WJ, Paik SW, Koh KC, Lee JH, Choi MS, Yoo BC. Percutaneous radiofrequency ablation for early-stage hepatocellular carcinoma as a first-line treatment: long-term results and prognostic factors in a large single-institution series. Eur Radiol 2007;17(3):684–692.

17. Shiina S, Tateishi R, Arano T, Uchino K, Enooku K, Nakagawa H, Asaoka Y, Sato T, Masuzaki R, Kondo Y, Goto T, Yoshida H, Omata M, Koike K. Radiofrequency ablation for hepatocellular carcinoma: 10-year outcome and prognostic factors. Am J Gastroenterol 2012;107(4):569–577.

18. Tateishi R, Shiina S, Teratani T, Obi S, Sato S, Koike Y, Fujishima T, Yoshida H, Kawabe T, Omata M. Percutaneous radiofrequency ablation for hepatocellular carcinoma: an analysis of 1000 cases. Cancer 2005;103(6):1201–1209.

19. Raut CP, Izzo F, Marra P, Ellis LM, Vauthey JN, Cremona F, Vallone P, Mastro A, Fornage BD, Curley SA. Significant long-term survival after radiofrequency ablation of unresectable hepatocellular carcinoma in patients with cirrhosis. Ann Surg Oncol 2005;12(8):616–628.

20. Lencioni R, Cioni D, Crocetti L, Franchini C, Pina CD, Lera J, Bartolozzi C.. Early stage hepatocellular carcinoma in patients with cirrhosis: long-term results of percutaneous image-guided radiofrequency ablation. Radiology 2005;234(3):961–967.

21. Lam VW, Ng KK, Chok KS, Cheung TT, Yuen J, Tung H, Tso WK, Fan ST, Poon RT. Risk factors and prognostic factors of local recurrence after radiofrequency ablation of hepatocellular carcinoma. J Am Coll Surg 2008;207(1):20–29.

22. Xu HX, Lu MD, Xie XY, Yin XY, Kuang M, Chen JW, Xu ZF, Liu GJ. Prognostic factors for long-term outcome after percutaneous thermal ablation for hepatocellular carcinoma: a survival analysis of 137 consecutive patients. Clin Radiol 2005;60(9):1018–1025.

23. Guglielmi A, Ruzzenente A, Battocchia A, Tonon A, Fracastoro G, Cordiano C. Radiofrequency ablation of hepatocellular carcinoma in cirrhotic patients. Hepatogastroenterology 2003;50(50):480–484.

24. Chuma M, Hige S, Kamiyama T, Meguro T, Nagasaka A, Nakanishi K, Yamamoto Y, Nakanishi M, Kohara T, Sho T, Yamamoto K, Horimoto H, Kobayashi T, Yokoo H, Matsushita M, Todo S, Asaka M. The influence of hepatitis B DNA level and antiviral therapy on recurrence after initial curative treatment in patients with hepatocellular carcinoma. J Gastroenterol 2009;44: 991-999.

25. Hann HW, Coben R, Brown D, Needleman L, Rosato E, Min A, Hann RS, Park KB, Dunn S, DiMarino AJ. A long-term study of the effects of antiviral therapy on survival of patients with HBV-associated hepatocellular carcinoma (HCC) following local tumor ablation. Cancer Med 2014;3: 390-396.

26. Song TJ, Fong Y, Cho SJ, Gönen M, Hezel M, Tuorto S, Choi SY, Kim YC, Suh SO, Koo BH, Chae YS, Jarnagin WR, Klimstra DS. Comparison of hepatocellular carcinoma in American and Asian patients by tissue array analysis. J Surg Oncol. 2012 Jul 1;106(1):84-88.

27. Mazzaferro V, Regalia E, Doci R, Andreola S, Pulvirenti A, Bozzetti F, Montalto F, Ammatuna M, Morabito A, Gennari L. Liver transplantation for the treatment of small hepatocellular carcinomas in patients with cirrhosis. N Engl J Med. 1996 Mar 14;334(11):693-699.

Chapter 3

Phantom study investigating the accuracy of manual and automatic image fusion with the General Electric Logiq E9: implications for use in percutaneous liver interventions
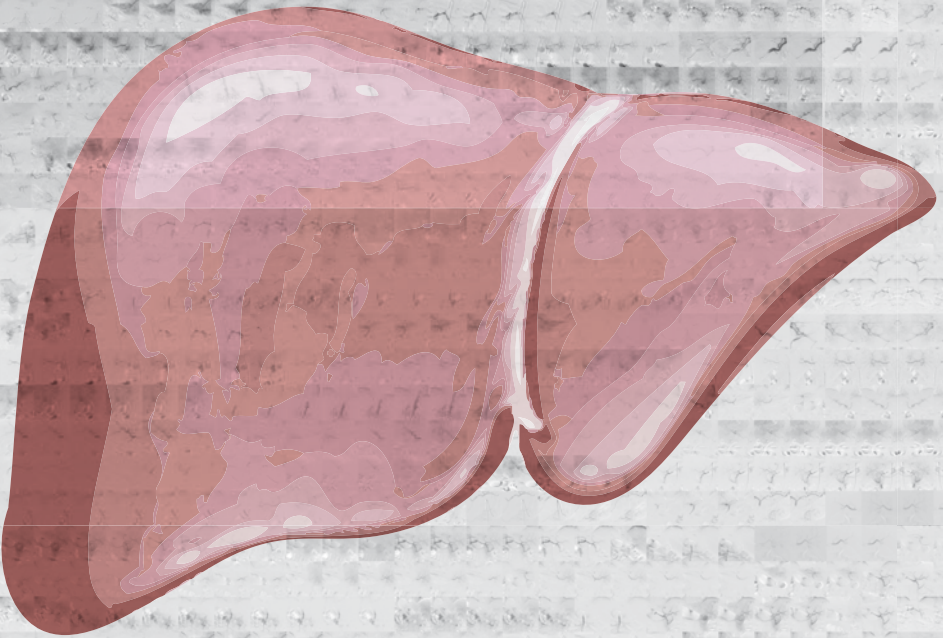
Burgmans MC, Harder JM, P. Meershoek P, Chan SXJM, van de Berg NS, van Leeuwen FWB, van Erkel AR

ABSTRACT

Purpose

To determine the accuracy of automatic and manual co-registration methods for image fusion of three-dimensional computed tomography (CT) with real-time ultrasonography (US) for image-guided liver interventions.

Methods

CT images of a multi-modality skills phantom with lesions were acquired and co-registered to real-time US using GE Logiq E9 navigation software. Manual co-registration was compared to automatic and semi-automatic co-registration using an active tracker. Also, manual point registration was compared to plane registration with and without an additional translation point. Finally, a comparison was made between manual and automatic selection of reference points. The residual displacement was measured in phantom lesions to determine the registration accuracy of different methods. In each experiment the accuracy of the co-registration method was determined by measurement of the residual displacement in phantom lesions by two independent observers.

Results

Mean displacements for a superficial and deep liver lesion were comparable after manual and semi-automatic co-registration: 2.4mm and 2.0mm vs. 2.0mm and 2.5mm, respectively. Both methods were significantly better than automatic co-registration: 5.9mm and 5.2mm residual displacement ($p<0.001$ and $p<0.01$). The accuracy of manual point registration was higher than that of plane registration, the latter being heavily dependent on accurate matching of axial CT and US images by the operator. Automatic reference point selection resulted in significantly lower registration accuracy compared to manual point selection despite lower root mean square deviation (RSMD) values.

Conclusion

The accuracy of manual and semi-automatic co-registration is better than that of automatic co-registration. For manual co-registration using a plane, choosing the correct plane orientation is an essential first step in the registration process. Automatic reference point selection based on RSMD values is error-prone.

INTRODUCTION

Image guidance using ultrasonography (US) offers important advantages over computed tomography (CT) guidance for targeting of liver lesions during minimally invasive procedures such as biopsies and percutaneous ablations (1). US allows real-time imaging, is not associated with radiation, and offers the interventional radiologist a free choice of plane for needle placement. However, up to one fifth of liver lesions are inconspicuous on US (2).

US systems with fusion imaging are commercially available from different vendors (3,4,5,6). Three dimensional (3D) computed tomography (CT) or magnetic resonance (MR) image data can be acquired before the intervention and uploaded onto these US systems for image fusion with real-time US images, using an electromagnetic transmitter and electromagnetic sensors attached to the transducer (7,8). To the interventional radiologist, the fusion-imaging technology may be of great value as it allows targeting of lesions that are inconspicuous on US with reduced radiation exposure. Several clinical studies have demonstrated the usefulness of US-CT/MRI image fusion in targeting liver tumors that are inconspicuous on US (1-6).

For safe and accurate use of these navigation systems, accurate matching (co-registration) of the 3D image datasets with the real-time US images is essential. Inaccuracies in co-registration may lead to technical failure or inadvertent ablation of healthy liver tissue. Co-registration can be performed either manually or automatically. Manual co-registration requires indication of reference points or planes by the operator in the real-time US data and their corresponding positions or planes in the 3D dataset (9,10). It can be challenging, requires experience and does not compensate for patient movement. A variable learning curve is experienced for obtaining consistent and accurate manual co-registration. Automatic co-registration by the ultrasound machine on the other hand either makes use of automatic image recognition or of a frame with fiducial markers, attached to the patient's body (11,12). Automatic co-registration saves time, can compensate for patient movement and is feasible even if ultrasonographic visualization of the liver is compromised, due to e.g. obesity, overlying air, steatosis or cirrhosis. Though automatic co-registration offers an easier to use and learn platform than manual co-registration, the accuracy of automatic registration has not been determined.

In this study we compared the accuracy of manual and automatic co-registration for liver lesions in a phantom using the General Electric Logiq E9 system (General Electric (GE) Healthcare, Wauwatosa, WI, USA). Additional experiments demonstrate the benefits and caveats of different manual co-registration methods. Based on these experiments we aim to provide recommendations for efficient, reliable and accurate co-registration.

METHODS

Equipment

A General Electric Logiq E9 ultrasound system with XDclear platform (General Electric (GE) Healthcare, Wauwatosa, WI, USA) and multi-modality abdominal CIRS model 057 phantom (CIRS, Norfolk, VA, USA) were used to conduct the experiments. GE Volume Navigation software, a C1-6-D convex transducer and an electromagnetic signal trans-mitter (Ascension Technology, Shelburne, VT, USA) were used to allow fusion of US and CT images (Figure 1 and 2). An omniTRAX™ Active Patient Tracker (CIVCO Medical Solutions, Kalona, IA, USA) was fixed on the anterolateral side of the phantom (Figure 1). CT of the phantom was acquired using a Toshiba Aquilion 64 scanner (Toshiba Medi-cal Systems, Otawara, Japan) with the following scanning parameters: tube voltage of 120 kVp, 1.0 mm slice thickness and in-plane resolution of 0.78 mm × 0.78 mm. The CT data was uploaded to a GE Logiq E9 ultrasound system (Figure 1) prior to image fusion.

Measurement of co-registration accuracy

Several phantom experiments were conducted (see below). In each experiment the accuracy of the co-registration method was determined. Accuracy was determined by measurement of the residual displacement by two independent observers (PM and CH). High accuracy corresponded to low residual displacement, i.e. low registration mismatch between the US and CT images. Inaccuracy referred to high residual displacement, i.e. large discrepancies between US and CT images. To measure the residual displacement, a marker was placed in the center of a lesion on the US images, i.e. center$_{US}$. Then, the cen-ter of the lesion was identified on the CT images, i.e. center$_{CT}$, and the distance between center$_{US}$ and center$_{CT}$ was measured in millimeters.

For manual co-registration methods, the root mean square deviation (RSMD) was re-corded. The RSMD is an established method to quantify the reliability of image fusion, as it is the standard deviation of the mean distance between the corresponding registration points on CT and US. The RSMD for a set of n reference points is given by the formula:

$$\text{RMSD} = \sqrt{\frac{\sum_{i=1}^{n} \left| \vec{x}_{i,CT} - \vec{x}_{i,US} \right|^2}{n}}$$

where $\vec{x}_{i,CT}$ and $\vec{x}_{i,US}$ are the position of the reference point i on CT and US respectively
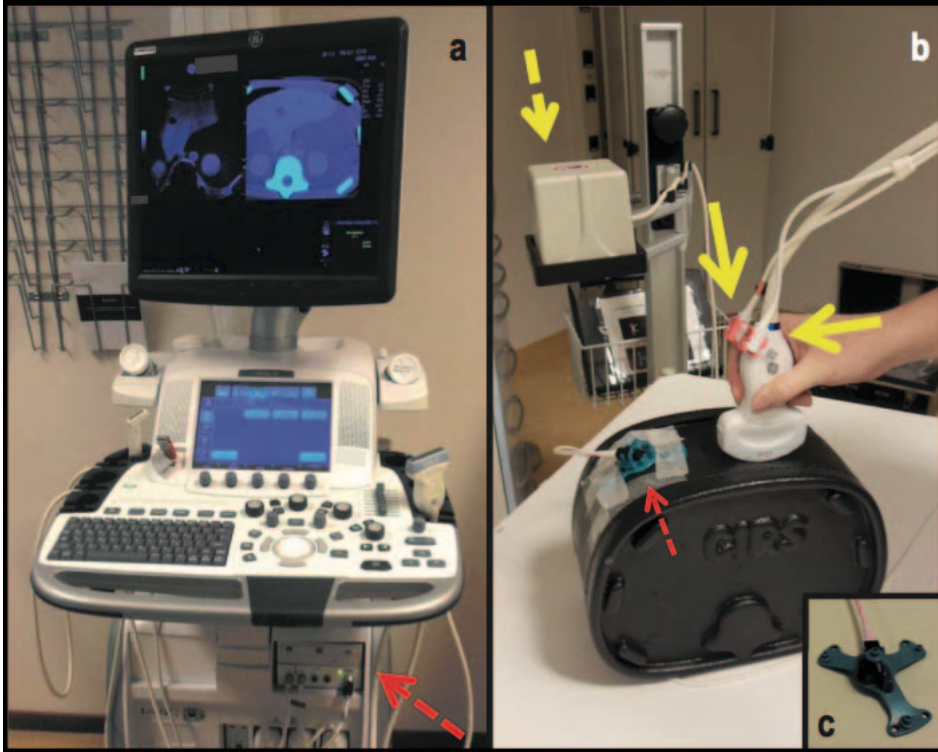
Figure 1. Volume navigation system and phantom setup: (a) GE Logiq E9 US system with volume navigation module (dashed arrow). (b) C1-6-D convex transducer equipped with two electromagnetic sensors (solid yellow arrows). The electromagnetic transmitter is positioned next to the phantom (yellow dashed arrow) and the active tracker with four radio-opaque fiducial markers and an additional electromagnetic sensor is attached to the phantom (red dashed arrow). (c) omniTRAX™ Active Patient Tracker with electromagnetic sensor

Experiments

Experiment A. Manual versus automatic versus semi-automatic co-registration
In the first experiment, the registration accuracy of manual point co-registration was compared with that of automatic co-registration and semi-automatic co-registration. Figure 3A provides a graphical overview of the different co-registration methods used in this experiment.

For manual point co-registration, three reference points were selected manually on both the US and CT images using the "point/all" registration option of the GE Logiq E9 system. The center of each kidney and a well identifiable point of the left hepatic vein were chosen as reference points. Automatic co-registration was established using automatic detection of the active tracker within the electromagnetic field by the US system. Semi-automatic co-registration was realized by automatic co-registration and an additional

Figure 2. Example of automatic co-registration of US and CT images in a 65-year old male with colorectal liver metastases. Two sub-centimeter lesions were characterized as metastases with the use of MRI (not shown), but were not found on pre-procedural ultrasonographic examination. The patient was scheduled to undergo ablation using the GE Logiq E9 navigation system. CT with intravenous contrast was obtained with the omniTRAX™ Active Patient Tracker attached to the patient. The images show adequate co-registration of US (left) and CT (right) with matching po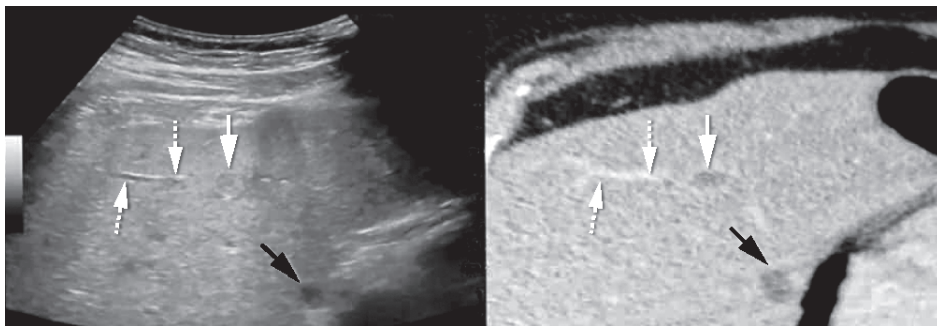sition of a portal vein branch (dotted arrows) and liver cyst (black arrows). After image fusion, the liver metastases were vaguely seen (white arrow; second lesion not shown) and could be targeted with a radiofrequency probe. Post-ablation CT showed a good location of the ablation zone and no recurrence has occurred during follow-up.

translation correction by manual indication of a well identifiable point in the left hepatic vein. Thus, automatic and semi-automatic co-registration are similar except for the following: in semi-automatic co-registration an additional reference point is placed manually after the automatic registration process to optimize the co-registration.

To compare the accuracy of the three different registration techniques, the residual displacement was measured for two different lesions in the phantom: a superficial target lesion at 50 mm from the surface and a target lesion at 80 mm from the surface. The co-registrations and measurements were repeated twenty times by each of the two observers.

Experiment B. Manual point-registration versus plane-registration
In the second experiment, two methods of manual co-registration were compared (Figure 3B). The first method was manual co-registration using three reference points as described above. In the second method, manual co-registration was established by so-called 'plane registration'. After choosing an axial CT image, the phantom was scanned with the ultrasound probe in axial plane to find a matching US image. By pressing the 'lock plane' button on the US machine, the US image was fused to the corresponding CT image. After this, correction of the image fusion was restricted to translational corrections. Then, a translation point was placed in order to optimize the co-registration.

The co-registrations and measurements were repeated five times by each of the two observers.

Experiment C. Pitfalls of co-registration, part I
The third experiment further examined co-registration using a plane (Figure 3C). In this experiment a deliberate mismatch was created between the CT and US plane. The transducer was positioned at an angle of roughly twenty degrees to the axial plane around the left-right axis, while the CT images were maintained axial without angulation. Then, subsequent translation points were set to try to correct the registration mismatch: first at a well-identifiable point in the left hepatic vein and then in the center of the right kidney.

As the last part of this experiment, the transducer was carefully positioned axially on the phantom, but at an in-plane rotation of roughly twenty degrees around the feet-head axis. The same two subsequent translation points were set as described above trying to correct the registration mismatch.

Each step of the experiment was repeated five times by each of the two observers with measurement of the registration accuracy for the superficial lesion and the center of the right kidney during each step.

Experiment D. Pitfalls of co-registration, part II
The last experiment examined manual co-registration using the "Point/best3" option of the GE Logiq E9 system (Figure 3D). This option allows automatic selection of reference points by the US system: when more than three reference points are manually selected by the operator, the US system automatically selects the three reference points that result in the lowest RSMD.

In the first step of this experiment, reference points were manually selected in the center of each kidney and at a well identifiable point of the left hepatic vein The left hepatic vein reference point was deliberately displaced 8 mm too far anteriorly in the sonogram to test a clinical scenario of operator-dependent misregistration. The second step was to evaluate whether the addition of a fourth reference would improve the co-registration accuracy. A fourth reference point was placed on the left edge of the spine, in line with the reference points in the kidneys. Finally, the "Point/best3" option was selected on the US system to activate selection of the best three out of the four reference points by the US system based on RSMD calculations. As a result of the displacement of the middle hepatic vein reference point, a preference was enforced for automatic selection by the system of the three reference points that were in line.
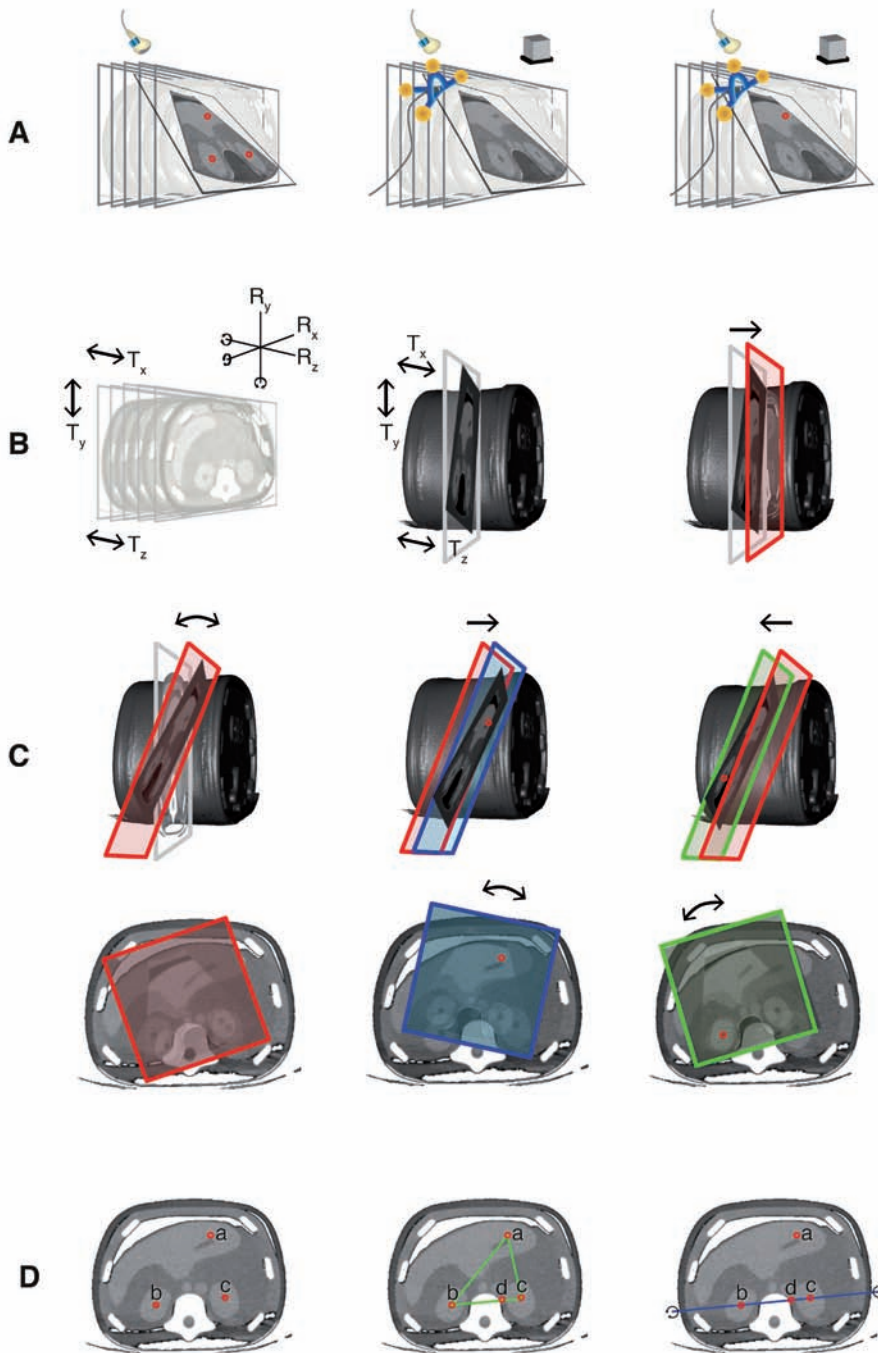
Figure 3. Graphical overview of the phantom experiments. A. Comparison of manual point co-registration (left), automatic co-registration (middle) and semi-automatic co-registration (right). B. Comparison of two manual co-registration methods: point co-registration (not shown; see A, left) and plane-registration. Prior

to plane-registration, the orientation of the ultrasound plane could be changed by both rotation (Rx, Ry and/or Rz) and translation (Tx, Ty and/or Tz) (left). After fusion of the CT and US image by pressing the 'lock plane' button on the US machine, correction of the image fusion was restricted to translational movements (middle). A single translation point was placed to optimize the co-registration (right) C. Plane-registration was conducted with deliberate mismatch between the CT and US plane. The US transducer was positioned at an angle of roughly twenty degrees to the axial plane around the left-right axis (above) or at an in-plane rotation of roughly twenty degrees around the feet-head axis (below). The angulated US plane was fused to an axial CT image. After this, correction of the co-registration was attempted by placing a well-identifiable point in the left hepatic vein (middle) and then in the center of the right kidney (right). D. Comparison of manual selection of three reference points (left) or four reference points (middle) and automatic selection of three out of four reference points (right). As the left hepatic vein reference point (a) was deliberately placed 8mm anteriorly, a system preference was enforced for the three reference points that were in line (as these resulted in the lowest RSMD). Rotation of the registration plane was restricted by the triangular orientation of the reference points (middle) in the experiments with operator-dependent point selection, whereas rotational errors around the blue line (right) occurred with automatic point selection

After each step the reported RMSD was recorded and the residual displacement was measured in the superficial lesion. All steps and measurements were repeated five times by each of the two observers.

Statistical analysis

Statistical analyses were performed using SPSS version 23.0 (IBM, Armonk, NY, USA). For all measurements, mean and standard deviation were derived as well as 95% confidence intervals (CI) of the mean. Using a 2-way analysis of variance (ANOVA) the dependency of the accuracy on the position of the lesion and the co-registration method (manual using reference points, automatic, and semi-automatic) was determined. Additionally, a one-way ANOVA was used to analyze the dependency of the accuracy on the position of the lesion for each of these co-registration methods separately. A one-way ANOVA was also used to determine the dependency of the registration accuracy on the number of reference points. A p-value < 0.05 was considered statistically significant.

RESULTS

For all co-registration experiments, measurements are listed in Table 1.

Experiment A. Manual versus automatic versus semi-automatic co-registration
A significantly higher mean residual displacement was found with automatic co-registration compared to manual co-registration: 5.9 mm and 5.2 mm for the superficial and deep liver lesion respectively, compared to 2.4 mm and 2.0 mm (Figure 4). The accuracy of automatic co-registration improved significantly after applying a translation correction, i.e. semi-automatic co-registration (p<0.0005). The residual displacement

Table 1. Reported RMSD and residual displacement for different co-registration methods: mean, standard deviation and 95%CI of the mean.

	Measure	Target	mean ± std.dev. (mm)	95%CI (mm)
Experiment A				
Manual point	RMSD		1.0 ± 0.4	0.8 - 1.1
	Residual displacement	Superficial lesion	2.4 ± 0.5	2.2 - 2.5
		Deep lesion	2.0 ± 0.6	1.9 - 2.2
Automatic	Residual displacement	Superficial lesion	5.9 ± 0.7	5.7 - 6.1
		Deep lesion	5.2 ± 0.6	5.0 - 5.4
Semi - automatic	Residual displacement	Superficial lesion	2.0 ± 0.7	1.8 - 2.3
		Deep lesion	2.5 ± 0.7	2.2 - 2.7
Experiment B				
Plane only	Residual displacement	Superficial lesion	13 ± 3	11 - 15
		Left kidney	13 ± 3	11 - 16
TP1: superficial	Residual displacement	Superficial lesion	1.9 ± 0.8	1.4 - 2.5
		Left kidney	4.5 ± 1.8	3.2 - 5.7
Experiment C				
20^0 angulation around L-R axis				
Plane only	Residual displacement	Superficial lesion	17 ± 11	9 - 26
		Left kidney	33 ± 4	30 - 36
TP1: superficial	Residual displacement	Superficial lesion	4.7 ± 2.6	2.8 - 6.6
		Left kidney	34 ± 3	32 - 36
TP2: deep	Residual displacement	Superficial lesion	34 ± 3	32 - 36
		Left kidney	5.9 ± 1.8	4.6 - 7.2
20^0 rotation around F-H axis				
Plane only	Residual displacement	Superficial lesion	35 ± 5	31 - 38
		Left kidney	54 ± 8	49 - 60
TP1: superficial	Residual displacement	Superficial lesion	18 ± 4	15 - 21
		Left kidney	26 ± 5	23 - 30
TP2: deep	Residual displacement	Superficial lesion	28 ± 6	24 - 32
		Left kidney	35 ± 7	30 - 40
Experiment D				
Three	RMSD		2.5 ± 0.5	2.1 - 2.8
	Residual displacement	Superficial lesion	6.2 ± 1.1	5.5 - 7.0
Four	RMSD		2.4 ± 0.5	2.0 - 2.7
	Residual displacement	Superficial lesion	5.5 ± 1.3	4.5 - 6.4
Best three of four	RMSD		0.9 ± 0.4	0.6 - 1.1
	Residual displacement	Superficial lesion	40 ± 26	21 - 58

TP = translation point; L-R = left-right; F-H = feet-head; RSMD = root mean square deviation
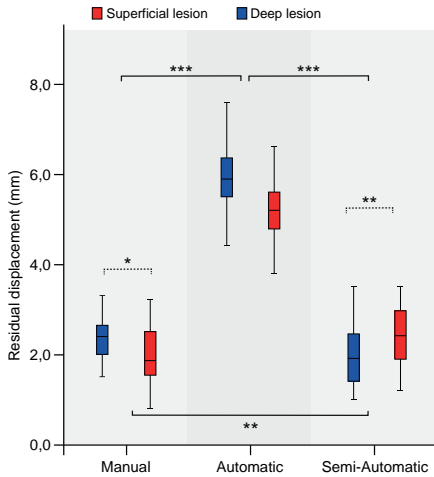
Figure 4. Comparison of manual, automatic and semi-automatic co-registration. Accuracy is expressed as residual displacement between US and CT measured for a superficial lesion (blue) and a deep lesion (red). Centerlines in boxplots indicate the median, box edges indicate the 25th and 75th percentile. Uninterrupted brackets indicate comparisons between co-registration methods. Dotted brackets indicate comparison between lesions for a single co-registration method. *p<0.05, **p<0.01,***p<0.001.

of semi-automatic co-registration was similar to the displacement found after manual co-registration: 2.0mm and 2.5mm for the superficial and deep lesion, respectively.

The accuracy depended on both the co-registration method and the position of the lesion. After manual co-registration, the mean displacement was significantly larger for the superficial lesion than for the deep lesion (p=0.027). Conversely, the semi-automatic co-registration resulted in a larger displacement for the deep lesion than for the superficial lesion (p=0.002).

Experiment B. Manual point-registration versus plane-registration
After manual co-registration using a plane, a high residual displacement was found for both the superficial lesion and the left kidney (13.3 ± 3mm for both). Upon placing a translation point, this accuracy improved to 1.9 ± 0.8mm and 4.5 ± 1.8mm respectively (Figure 5A).

Experiment C. Pitfalls of co-registration, part I
Manual co-registration using a deliberately angulated plane resulted in poor registration accuracy with a wide range (Figure 5).

Placement of a translation point did improve registration accuracy, but only for one of the two points of measurement (Figure 5B). If the translation point was placed in the left hepatic vein, registration accuracy improved for the liver lesion but not for the center of the right kidney. If the translation point was placed in the right kidney, only the registration accuracy for center of the right kidney improved substantially.
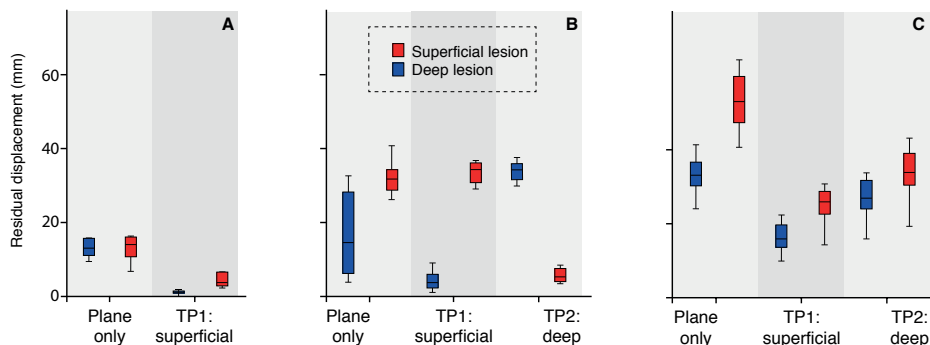
Figure 5. A. Comparison of plane co-registration without (right) and with (left) additional translation point. Registration accuracy was measured for a superficial lesion (blue) and deep lesion (red). B. Plane co-registration using a plane deliberately angulated around the left-right axis (left) resulted in poor registration accuracy with a wide range. Placement of a superficial translation point (TP1) resulted in improved registration accuracy for the superficial lesion, but not for the deep lesion (middle). Placement of a deep translation point (TP2) resulted in high registration accuracy for the deep lesion, but not for the superficial lesion (right). C. Plane co-registration with a plane deliberately rotated around the feet-head axis resulted in poor registration accuracy with a wide range (left). Placement of a superficial translation point (TP1) or deep translation point (TP2) did not result in acceptable registration accuracies (middle and right).
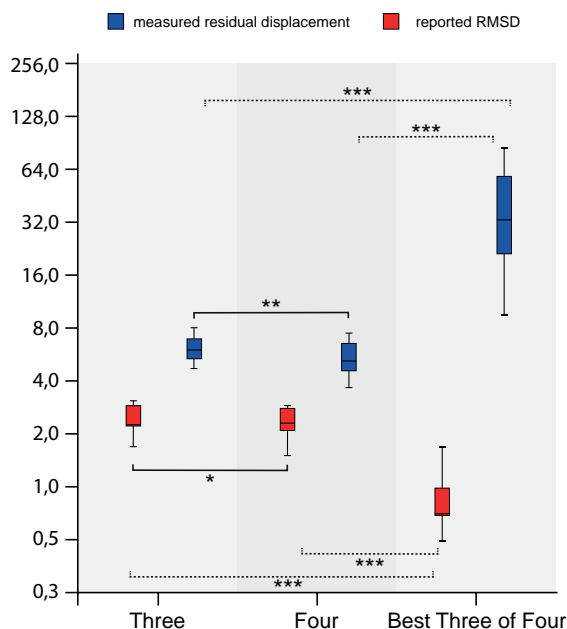
Figure 6. Comparison of manual point registration using three reference points (left), four reference points (middle) and software-based selection of three out of four reference points based on root mean square deviation (RMSD) (right). The registration error expressed as RMSD (red) does not correspond with the actual residual displacement (blue). Centerlines in boxplots indicate the median, box edges indicate the 25th and 75th percentile. Uninterrupted brackets indicate comparison of measured residual displacement for different co-registration methods. Dotted brackets indicate comparisons between reported RSMD. *$p<0.05$, **$p<0.01$, ***$p<0.001$.

After deliberate in-plane rotation of the US transducer around the feet-head axis, a substantial in-plane displacement was measured at both the superficial lesion and the right kidney (Figure 5C). Again, assigning translation points led to an acceptable

co-registration only near the most recently chosen translation point. Objects at other locations remained misaligned.

Experiment D. Pitfalls of co-registration, part II
Deliberate misplacement of one of the reference points during manual co-registration led to a high residual displacement in the superficial lesion (6.2 ± 1.1mm) (Figure 6). Adding a fourth reference point led to a non-significant (p=0.91) improvement in registration displacement (5.5 ± 1.3mm) (Figure 6). Selection by the US system of the best three of four reference points resulted in a significantly worse residual displacement compared to either using three or four reference points (p<0.0005, Figure 6). The mean reported RMSD, however, was significantly smaller in this case compared to the two co-registration methods with operator-dependent selection of reference points (p<0.0005).

DISCUSSION

Basic knowledge of fusion technology and potential pitfalls is essential when using US systems with fusion imaging. We did not investigate the GE Logiq E9 navigation system in a clinical setting, so the implications of our phantom study for use of the system in patients are open to discussion. Nevertheless, it is likely that many of our study findings also apply in a clinical system. A co-registration method that is inaccurate in a phantom study is likely to have a higher co-registration mismatch in patients.

Our results demonstrate that automatic co-registration is significantly less accurate than manual co-registration when using the GE Logiq E9 navigation system (p<0.0005). Based on our findings we consider this registration method insufficient for routine use in clinical practice. The residual displacement of automatic co-registration was >5mm. This increases the risk of technical failure (i.e. incomplete treatment or insufficient margins) in liver tumor ablation or of a sampling error in a percutaneous biopsy of a liver lesion. We therefore consider manual co-registration to be the preferred registration method. The accuracy of manual co-registration with the GE Logiq E9 has also been demonstrated in previous experiments, both in phantom studies as in healthy volunteers (2-10).

Semi-automatic co-registration is a valuable alternative in patients where manual registration is complicated by compromised ultrasonographic visibility and difficulties in identification of reference points. In our phantom study, the registration accuracy of semi-automatic co-registration was comparable to that of manual co-registration. Semi-automatic has an important disadvantage over manual co-registration. It requires acquisition of a contrast-enhanced CT or MRI just prior to the intervention with the tracker

attached to the patient (same applies to automatic co-registration). This increases the procedure time as well as the radiation dose and contrast volume for the patient.

Based on our study findings, manual selection of reference points using the "Point/all" mode offers the most accurate and reliable co-registration of the different manual co-registration methods of the GE Logiq E9 navigation system. Co-registration using a plane depends on the operator's ability to identify an identical axial plane on the US images and the pre-intervention data. In clinical practice, matching the plane orientations in the first step of the registration process may be prone to errors as the positioning of the patient during the intervention may be different from that during the acquisition of the CT or MRI. As shown in our study, an initial mismatch between the CT and US plane cannot be sufficiently corrected by adding translation points. The addition of a translation point does shift the plane in the X-, Y- and/or Z-axis, but does not allow rotation of the plane. The registration accuracy may thus only be sufficient close to the intersection line between the US and CT plane. We therefore advise to use co-registration with plane registration with caution and only if placement of a translation point close to the target lesion is feasible.

From the current study it was also found that assignment of reference points by the operator was more accurate than automatic selection of three reference points by the US system. The system's selection algorithm is based on the lowest RSMD, which does not necessarily result in the best registration accuracy.

Similar to previous study findings, the current study shows that the accuracy is dependent on the position of the target lesion (9). After manual co-registration, the residual displacement was slightly larger for the superficial target lesion than for the deep lesion. This is expected to be a direct consequence of the compression of the phantom by the transducer, which influences the position of a superficial lesion more than that of a deep lesion (13). Conversely, semi-automatic co-registration was found to be less accurate for the deep target lesion than for the superficial lesion, which suggests that the accuracy decreases with increasing distance between the lesion and the active tracker. Preferably, both the active tracker and the translation point are placed close to the target lesion for improved accuracy.

Our study has several limitations. The performance of the US system in clinical practice may differ from the results obtained in our phantom study. Registration inaccuracies are expected to be greater in patients for all co-registration methods as motion, breathing and tissue compressibility may induce registration errors (14,15). Furthermore, patient positioning may have a negative impact on registration accuracy, as it may lead to

increased mismatches due to deformation of tissue (13,16,17). Another limitation of the study is that we only investigated the performance of the GE Logiq E9 and study findings may thus not be extrapolated to other systems and registration methods. Finally, reference points were chosen within the phantom kidneys for manual co-registration, because these could be identified more easily than other landmarks due to the limited anatomical detail in our phantom. In patients, reference points are preferentially placed within the liver when performing percutaneous liver interventions.

In conclusion, manual and semi-automatic co-registration result in low registration inaccuracies in a phantom model and are preferred over fully automatic co-registration. Point-registration is preferentially performed using all operator-assigned reference points rather than using automatic point selection by the US system. Plane registration is an alternative method, provided that the plane orientation is correctly chosen during the first step of the registration process.

REFERENCES

1. Kim YJ, Lee MW, Park HS: Small hepatocellular carcinomas: ultrasonography guided percutaneous radiofrequency ablation. Abdom Imaging 2013; 38:98–111.

2. Mauri G, Cova L, De Beni S, Ierace T, Tondolo T, Cerri A, Goldberg SN, Solbiati L: Real-time US-CT/MRI image fusion for guidance of thermal ablation of liver tumors undetectable with US: results in 295 cases. Cardiovasc Intervent Radiol 2015; 38(1):143-151.

3. Minami Y, Kudo M. Ultrasound Fusion Imaging of Hepatocellular Carcinoma: A Review of Current Evidence. Dig Dis 2014;32:690–695.

4. Min JH, Lim HK, Lim S, Kang TW, Song KD, Choi SY, Rhim H, Lee MW. Radiofrequency ablation of very-early-stage hepatocellular carcinoma inconspicuous on fusion imaging with B-mode US: value of fusion imaging with contrast-enhanced US. Clin and Mol Hepatol 2014; 20:61-70.

5. Makino Y, Imai Y, Igura T, Ohama H, Kogita S, Sawai Y, Fukuda K, Ohashi H, Murakami T. Usefulness of the Multimodality Fusion Imaging for the Diagnosis and Treatment of Hepatocellular Carcinoma. Dig Dis 2012; 30:580-587.

6. Xu ZF, Xie XY, Kuang M, Liu GJ, Chen LD, Zheng YL, Lu MD. Percutaneous Radiofrequency Ablation of Malignant Liver Tumors with Ultrasound and CT Fusion Imaging Guidance. J Clin Ultrasound 2014; 42:321–330.

7. Crocetti L, Lencioni R, DeBeni S, See TC, Pina CD, Bartolozzi C. Targeting Liver Lesions for Radiofrequency Ablation. An Experimental Feasibility Study Using a CT–US Fusion Imaging System. Invest Radiol 2008; 43:33–39.

8. Hakime A, Deschamps F, De Carvalho EGM, Teriitehau C, Auperin A, De Baere T. Clinical Evaluation of Spatial Accuracy of a Fusion Imaging Technique Combining Previously Acquired Computed Tomography and Real-Time Ultrasound for Imaging of Liver Metastases. Cardiovasc Intervent Radiol 2011; 34(2):338-344.

9. Ewertsen C, Ellegaard K, Boesen M, Torp-Pedersen S, Bachmann Nielsen M. Comparison of Two Co-Registration Methods for Real-Time Ultrasonography Fused with MRI: a Phantom Study. Ultraschall in Med 2010; 31:296–301.

10. Ewertsen C, Hansen KL, Henriksen BM, Nielsen MB. Improving Accuracy for Image Fusion in Abdominal Ultrasonography. Diagnostics 2012; 2:34-41.

11. Roche A, Pennec X, Malandain G, Ayache N. Rigid registration of 3D ultrasound with MR images: a new approach combining intensity and gradient information. IEEE Trans Med Imaging 2001; 20(10):1038–1049.

12. Wein W, Brunke S, Khamene A, Callstrom MR, Navab N. Automatic CT-ultrasound registration for diagnostic imaging and image-guided intervention. Med Image Anal 2008; 12:577–585.

13. Brouwer OR, van den Berg NS, Mathéron HM, Wendler T, van der Poel HG, Horenblas S, Valdés-Olmos RA, van Leeuwen FWB. Feasibility of Intraoperative Navigation to the Sentinel Node in the Groin Using Preoperatively Acquired Single Photon Emission Computerized Tomography Data: Transferring Functional Imaging to the Operating Room. J Urol 2014; 192:1810-1816.

14. Brouwer OR, Buckle T, Bunschoten A, Kuil J, Wendler T, Vahrmeijer AL, Valdés-Olmos RA, van der Poel HG, van Leeuwen FWB. Image navigation as a means to expand the boundaries of fluorescence-guided surgery. Phys Med Biol 2012; 57:3123-3136.

15. Baumhauer M, Feuerstein M, Meinzer HP, Rassweiler J. Navigation in endoscopic soft

tissue surgery: perspectives and limitations. J Endourol 2008; 22(4): 751-766.

16.   van den Berg NS, Engelen T, Brouwer OR, Mathéron HM, Valdés-Olmos RA, Nieweg OE, van Leeuwen FWB. A pilot study of SPECT/CT-based mixed-reality navigation towards the sentinel node in patients with melanoma or Merkel cell carcinoma of a lower extremity. Nucl Med Commun 2016; 37(8):812-817.

17.   Navab N, Blum T, Wand L, Okur A, Wendler T. First deployments of augmented reality in operating rooms. Computer 2012; 45(7):48-55.

Chapter 4

Local tumor progression and survival rates after combined radiofrequency ablation and drug-eluting bead chemoembolization in unresectable hepatocellular carcinoma
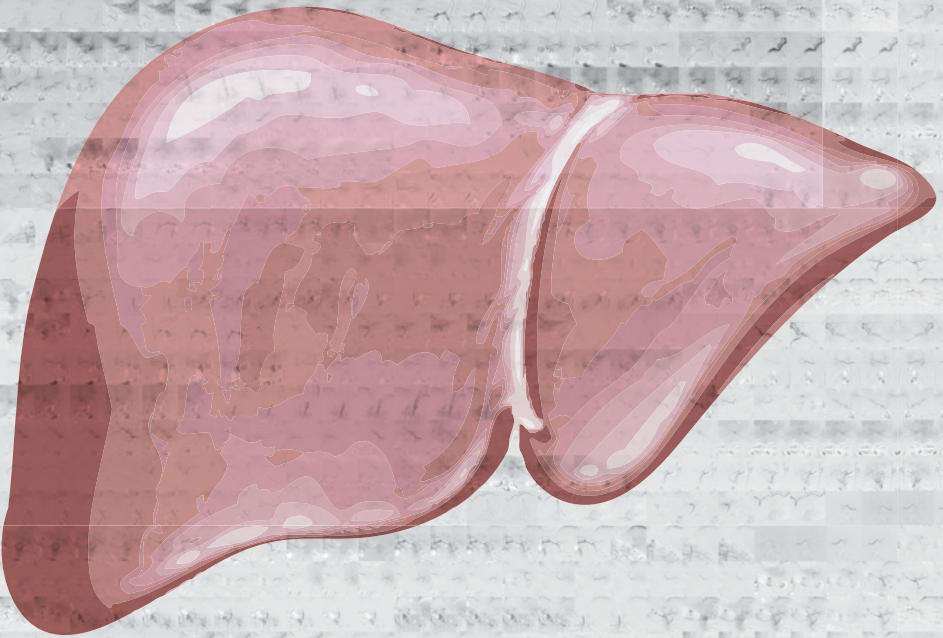
Burgmans MC, Schaapman JJ, Wolterbeek R, van Rijswijk CSP, Coenraad MJ, van Erkel AR

ABSTRACT

Purpose
Local tumor progression (LTP) rates after radiofrequency ablation (RFA) are higher in hepatocellular carcinoma (HCC) >3cm compared to HCCs ≤3cm. Combined RFA and drug-eluting-bead transarterial chemoembolization (DEBTACE) can achieve larger ablation zones compared to RFA alone. This retrospective study describes 3-year LTP free-survival (LTPFS) and overall survival (OS) after RFA and combined RFA-DEBTACE for HCC ≤3 cm and >3cm respectively.

Methods
Local medical ethics committee approved the study. 54 patients (42 males; median 66 years (range: 29-82 years)) were treated with RFA for de novo unresectable HCC. Thirty-nine patients received RFA only. Fifteen patients with HCC >3-7cm underwent RFA-DEBTACE. LTPFS and OS were analyzed using Kaplan-Meier and Cox regression analysis.

Results
In the RFA-group, LTPFS and OS rates at 1-, 2- and 3-years were 81.4%, 66.0% and 59.4% and 87.2%, 81,6% and 69.8% respectively. The LTPFS and OS rates were lower in the RFA-DEBTACE-group: 26.9%, 17.9% and 17.9% and 73.3%, 66.7% and 53.3% respectively.

Conclusion
LTPFS rates after RFA-DEBTACE for HCC >3-7cm are low compared to the results reported after combination therapy of conventional TACE followed by RFA for HCC with similar size.

INTRODUCTION

Hepatocellular carcinoma (HCC) is the third most common cause of cancer-related death in the world (1,2). Surgical resection is the first line treatment for patients with solitary HCC and a well-preserved liver function (1,2). Unfortunately, many patients with HCC are not eligible for surgical resection due to underlying liver disease, i.e. cirrhosis with portal hypertension. Liver transplantation is the preferred treatment for patients with liver cirrhosis and tumors within Milan criteria (single tumor <5cm or up to 3 tumors <3cm) who are unsuitable for resection (1,2). Radiofrequency ablation (RFA) is an effective alternative for surgical resection and may be used as a 'bridge-to-transplant' for patients on the waiting list for liver transplantation (1,2).

Local tumor progression rates after RFA are significantly higher in tumors >3 cm compared to smaller tumors (1-5). Different strategies have been advocated to reduce local tumor progression rates after RFA in tumors >3cm. Several Asian studies have shown promising results of conventional transarterial chemoembolization (cTACE) as a neo-adjuvant treatment preceding RFA. Yet, cTACE has been abandoned in many European centers after a prospective randomized trial (Precision V) comparing cTACE and TACE with doxorubicin-eluting beads (DEBTACE) (6). This trial showed a better safety profile and favorable response rates of DEBTACE compared to cTACE.

There is a paucity of publications on combined treatment with RFA and DEBTACE. In a pilot study, it has been shown that RFA followed by DEBTACE resulted in significant increase in the volume of ablation necrosis compared to RFA alone (7). However, data on long-term results for combined RFA and DEBTACE is absent.

In our institution, a treatment protocol was implemented in January 2009 whereby patients with HCC >3cm were treated with combined RFA-DEBTACE and patients with HCC ≤3 cm were treated with RFA only. The objective of the study was to analyze three year local tumor progression free-survival and overall survival data of patients treated by RFA and combined RFA-DEBTACE for HCC ≤3 cm and >3-7cm respectively.

METHODS

Patients

The institutional review board (IRB) approved the study and informed consent was waived for the retrospective analysis. All patients gave informed consent to undergo treatment. Between January 2009 and July 2012, 54 consecutive patients (42 males;

median age 66 years (range: 29-82 years)) were treated in our institution with RFA for de novo unresectable HCC. The diagnosis was based either on tumor histology or on radiological imaging criteria, according to guidelines by the European Association for Study of the Liver (8). For radiological confirmation of the diagnosis, 4-phase contrast-enhanced computed tomography (CECT) and/or dynamic gadolinium-enhanced magnetic resonance imaging (GE-MRI) was used. All patients were discussed in a multi-disciplinary meeting of hepatologists, surgeons, radiologists and oncologists and consensus about the given treatment was reached in all cases.

Eligibility criteria for local ablation were: Child Pugh A or B, Child Pugh C in a patient eligible to undergo liver transplant, Eastern Cooperation Oncology Group performance status (ECOG) <2, single tumor measuring <7 cm or a maximum of 3 HCCs measuring ≤3cm. Ineligibility criteria were: radiologic evidence of vascular invasion into portal/hepatic vein branches, extrahepatic metastases, severe liver dysfunction (Child-Pugh C) *and* no eligibility for liver transplantation, significant and uncorrectable coagulopathy (International Normalized Ratio (INR) >1.7, platelet count <50x 10^9/mm^3). Patients with a HCC >3cm were scheduled to undergo RFA followed by DEBTACE the next day. All other patients underwent RFA only.

The following baseline information was retrieved from the electronic patient records and Picture and Archiving Computer System (Sectra, Linköping, Sweden): (a) age, (b) gender, (c) size of lesion, (d) number of lesions, (e) baseline serum albumin, (f) baseline serum bilirubin, (g) baseline INR, (h) etiology cirrhosis, (i) Child Pugh status, (j) tumor stage according to Barcelona Clinic Liver Cancer (BCLC) criteria.

The median follow-up for all patients was 23.8 months (quartiles: 15.5-36.9 months).

Radiofrequency ablation

Percutaneous RFA was performed under general anesthesia under ultrasound and/or CT guidance. A single electrode was used (3 cm exposed tip Cooltip (Covidien, Gosport Hamspire, United Kingdom) or StarBurst XL (AngioDynamics, Amsterdam, Netherlands) or multiple electrodes with a switch-control system (3 or 4 cm exposed tip Cooltip). Ablation was performed for 12 (single Cooltip electrode) or 16 minutes (multiple Cooltip electrodes) using standard impedance controlled ablation. Temperature-based ablation was accomplished with the StarBurst XL electrode. CECT was performed immediately after ablation on a 16-slice spiral CT (Toshiba, Tokyo, Japan). Technical success was defined as absence of tumor enhancement after ablation. If the CECT showed residual tumor enhancement, re-ablation was performed in the same session.

Transarterial chemoembolization

TACE was scheduled 1 day after RFA. After introduction of a 5F/6F vascular sheath in the common femoral artery, angiography was performed from the common, lobar and (sub) segmental hepatic arteries. Cone-beam CT (CBCT) was performed in individual cases to better delineate vascular tumor supply (XperCT, Philips Healthcare, Best, Netherlands). TACE was performed as selective as possible using 100-300 micrometer and 300-500 micrometer DC Bead® with a total of 100mg doxorubicin (Biocompatibles UK Limited, Surrey, United Kingdom). Endpoints for embolization were complete administration of 2 vials of DC Bead® or arterial flow stasis. Hepatic angiography was performed immediately after embolization. Technical success was defined as successful delivery of DC Bead® into the tumor feeding artery with absence of tumor blush on the completion angiogram.

Complications

Complications were evaluated according to the Common Terminology Criteria for Adverse Effects version 4.0 (CTCAE 4.0).

Follow-up

Four-phase CECT or dynamic GE-MRI was performed 6 weeks after treatment and repeated every 3 months thereafter. Local tumor progression was defined as the presence of tumor enhancement on a follow-up scan at the location of the treated tumor. Local tumor progression was distinguished from distant recurrence (i.e. a new intrahepatic tumor distant from the treated tumor). Patients were followed until last follow-up date, death or the end of the study. The endpoints were local tumor progression-free survival and overall survival.

Statistical analysis

The statistical analyses were performed using SPSS 21 (IBM, Armonk, NY, USA). Comparisons between the two groups were done by student t-test for continuous variables and the Chi-square test for categorical variables. Survival curves for overall survival and local tumor progression-free survival were constructed by the Kaplan-Meier method and compared with the Cox regression analysis. The impact of liver transplantation on overall survival was assessed using a time-dependant covariate with a log-rank test. All statistical tests were two-sided, and a difference was considered significant when $p < 0.05$.

RESULTS

Patient characteristics

Baseline demographics of all patients are shown in Table 1. All patients had hepatocellular carcinoma in the setting of liver cirrhosis. Of the 54 patients, 39 patients were treated with RFA and 15 with RFA-DEBTACE.

Table 1. Baseline patient and tumor characteristics of 54 patients.

Characteristic	Value
Median age (range)	66 years (29-82 years)
Male gender	42
ECOG	
0	53 (98.1)
1	1 (1.9)
Cause of cirrhosis (n (%))	
Hepatitis B	6 (11.1)
Hepatitis C	14 (25.9)
Alcohol	31 (57.4)
Other	11 (20.4)
Child Pugh score (n (%))	
A	48 (88.9)
B	4 (7.4)
C	2 (3.7)
No. nodules per patient (n (%))	
1	40 (74.1)
2	11 (20.3)
3	3 (5.6)
Maximal tumor diameter in mm (n=71)	Median 22.0 Range 8-69

* The sum of percentages is >100% as the etiology of cirrhosis may be multifactorial. ECOG = Eastern Cooperative Oncology Group

Baseline parameters per group are described in Table 2. The mean maximal diameter of tumors at baseline was 45.7 mm in the combined RFA-DEBTACE group and 21.5 mm in the RFA group. In one patient in the RFA-DEBTACE group the maximal diameter of the largest tumor was <3cm. This patient had two tumors in segment 6 of respectively 24 mm and 22 mm that were in close relation to each other. It had been decided to consider the two tumors as one larger tumor area and perform RFA combined with DEB-TACE. In the RFA-DEBTACE group, the percentage of patients with multifocal disease (>1 lesion)

Table 2. Baseline patient and tumor characteristics per treatment group.

	RFA (n=39)	RFA and TACE (n=15)
Median age (range)	62.5 years (29-79 years)	65.2 years (47-82 years)
Male gender (%)	30 (76.9)	12 (80.0)
ECOG (n (%))		
0	38 (97.4)	15 (100)
1	1 (2.6)	0 (0)
Cause of cirrhosis in (n (%))*		
Hepatitis B	3 (7.7)	3 (20.0)
Hepatitis C	10 (25.6)	4 (26.7)
Alcohol	23 (59.0)	8 (53.3)
Other	9 (23.1)	2 (13.3)
Child Pugh score (n (%))		
A	34 (87.2)	14 (93.3)
B	3 (7.7)	1 (6.7)
C	2 (5.5)	0 (0)
Nodules per patient (no. of patients per arm (%))		
1	31 (79.5)	9 (60.0)
2	6 (15.4)	6 (33.3)
3	2 (5.1)	1 (6,7)
Mean maximal diameter of largest tumor (mm)	21.5 Range 10-30	45.7 Range 24-67

* The sum of percentages is >100% as the etiology of cirrhosis may be multifactorial. ECOG = Eastern Co-operative Oncology Group

was 40.0%. In the RFA group, 20.5% of patients had multifocal disease. The difference between the two groups was not statistically significant (p=0.175).

Treatment outcome

Technical success was achieved in 98.1% (n=53) of RFA procedures and 100% (n=15) of TACE procedures.

Figure 1 shows the local tumor progression-free survival of the RFA and RFA-DEBTACE group. The mean local tumor progression-free survival for all patients was 30.7 months (95% CI: 23.9-37.5 months). Patients in the RFA group had a mean local tumor progression free-survival of 36.9 months (95% CI: 29.6-44.3 months). Mean local tumor progression free-survival in the RFA-DEBTACE group was 11.0 months (95% CI: 2.8-19.4 months). The difference between the two groups was statistically significant: HR 0.211; 95% CI: 0.094-0.471. In the RFA group, the local tumor progression free-survival rates at 1-, 2- and 3-years were 81.4%, 66.0% and 59.4% respectively. These rates were 26.9%, 17.9%
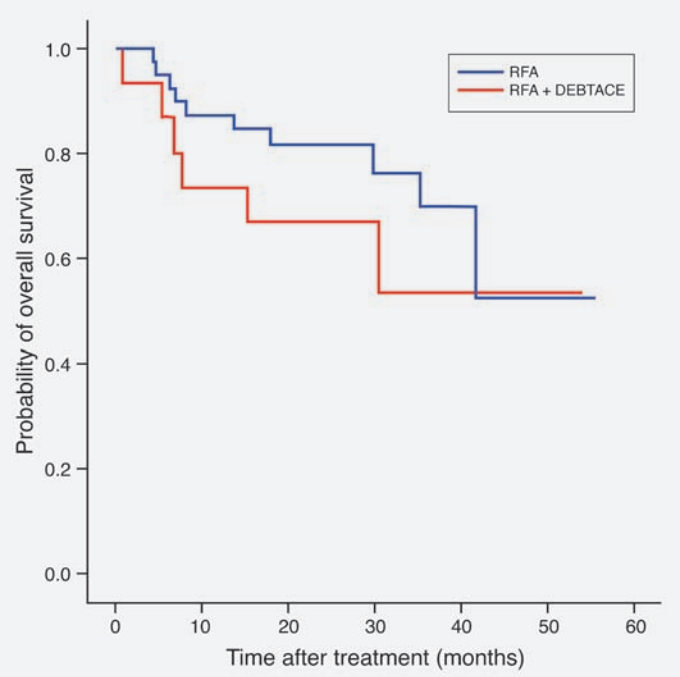
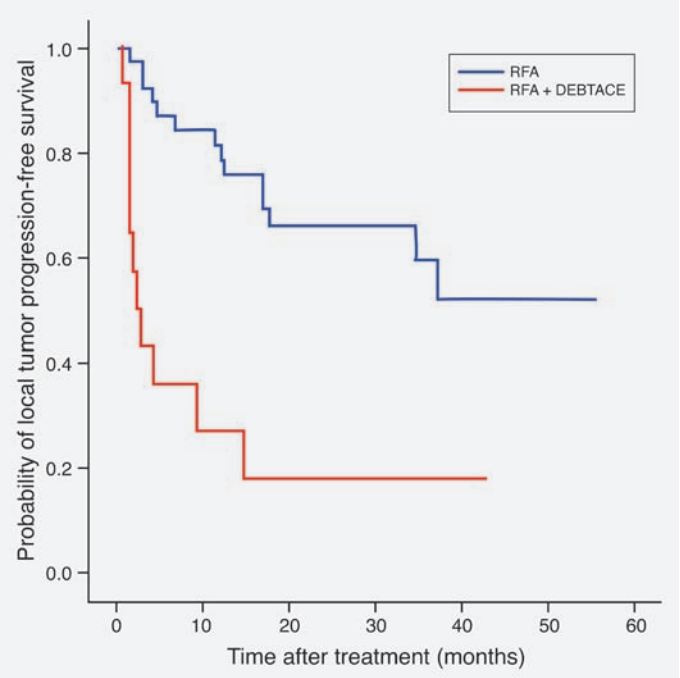**Figure 1.** Overall survival rate per treatment group

Figure 2. Local tumor progression-free survival rate per treatment group

and 17.9% respectively in the RFA-DEBTACE group. The differences in local tumor progression free-survival rates at 1-, 2- and 3-years were statistically significant (p=0.0001, p=0.0004 and p=0.0045 respectively).

Figure 2 shows the overall survival of the RFA and RFA-DEBTACE group. The mean overall survival of all patients was 40.4 months (95% CI: 34.5-46.2 months). The mean overall survival in the RFA group was 41.6 months (95% CI: 34.6-48.6 months) and 34.8 months (95% CI: 23.5-46.1 months) in the RFA-DEBTACE. The overall survival at 1-, 2- and 3-years was 87.2%, 81,6% and 69.8% respectively in the RFA group. In the RFA-DEBTACE group, these rates were 73.3%, 66.7% and 53.3%. The difference in overall survival between the two groups at 1-, 2- and 3-years was not statistically significant (p=0.27, p=0.28 and p=0.36 respectively).

Complications

CTCAE grade 3-4 complications occurred in one patient in the RFA group (2.6%) and 2 patients in the RFA-DEBTACE group (13.3%). The patient in the RFA group had a puncture site bleeding, which was treated successfully with transarterial embolization. One patient in the RFA-DEBTACE group developed a liver abscess 6 days after the ablation and was successfully treated with percutaneous drainage and antibiotics. The other patient in the DEBTACE group had a 47mm HCC high up in the dome of the liver. The RFA procedure was complicated by a right-sided pneumothorax for which a chest-tube was inserted. The next day, TACE of the liver dome tumor was performed. Five days after the TACE, the patient developed sepsis as result of Escherichia coli peritonitis. Despite treatment with percutaneous drainage of the ascites and intravenous antibiotics, the patient passed away 23 days after RFA as a result of sepsis and hepatorenal syndrome.

Consecutive treatment

Twenty-two patients (40.7%) underwent liver transplantation with a median of 7.0 months (range 0.3-28.6 months) after the first RFA treatment. The transplant rate for patients in the RFA group was 43.6% and 33.3% in the RFA-DEBTACE group. The difference in transplantation rate between the groups was not statistically significant (p=0.551). None of the patients that were transplanted had recurrent HCC. Liver transplantation resulted in a non-significant increase in survival with a hazard ratio of 0.452 in favor of transplantation (95% CI: 0.116-1.768).

Nineteen out of 54 patients (35.2%) received additional loco-regional treatment after the initial RFA or RFA-DEBTACE. In the RFA group, 28.2% patients underwent further loco-regional treatment after the initial RFA compared to 53.3% in the RFA-DEBTACE group (table 3). The difference between the two groups was statistically significant (p=0.022).

Table 3. Additional treatment during follow-up per treatment group

	RFA n (%)	RFA-TACE n (%)	Overall n (%)
Transplantation	17 (43.6)	5 (33.3)	22 (40.7)
Resection only	1 (2.6)	0 (0)	1 (1.9)
Resection and RFA and TACE	1 (2.6)	0 (0)	1 (1.9)
RFA only	3 (7.7)	3 (20.0)	6 (11.1)
RFA and TACE	3 (7.7)	2 (13.3)	5 (9.3)
TACE only	3 (7.7)	3 (20.0)	6 (11.1)

RFA = radiofrequency ablation. TACE = transarterial chemotherapy

DISCUSSION

To our best knowledge, this is the first reported study on the long-term efficacy of combined treatment with RFA and DEBTACE in patients with unresectable HCC. In our institution, we performed RFA for HCCs ≤3cm with a maximum of 3 tumors and combined treatment for HCCs >3-7cm. This treatment strategy was adopted on the premise that adjuvant DEBTACE would result in similar outcomes in patients with larger tumors compared to those with tumors ≤3cm. Despite the additional treatment with DEBTACE however, patients in the combined treatment group had significantly lower mean local tumor progression free-survival rates compared to the RFA-only group at 1, 2 and 3-years: 81.4%, 66.0% and 59.4% versus 26.9%, 17.9% and 17.9% respectively. The overall survival rate at 1, 2 and 3-years was also lower in the RFA-DEBTACE group compared to the RFA group, but the difference between the two groups did not reach statistical significance.

Clearly, direct comparison between the two groups in our study is flawed because of selection bias. Treatment selection was dependent on tumor size and as a result the mean maximal tumor diameter in the RFA-DEBTACE group was significantly larger than in the RFA group. Tumor size >3cm is a known risk factor for tumor recurrence after RFA and this is confirmed by our study (1-5). Different strategies are have been studied trying to reduce HCC recurrence rates after RFA and the debate is still open on what the best strategy is. Most studies have used a combination of RFA and TACE, but others have combined RFA with ethanol injection or sorafenib (9-12). In our study, RFA was performed first followed by DEBTACE the next day. After RFA-DEBTACE, the local tumor progression-free survival at 3 years was 17.9%. This compares favorable to previous studies that have reported 3-year recurrence free-survival rates of only around 10% after RFA for HCC >3cm (13,14). Yet, our results are poorer than those reported in studies that used a sequence whereby cTACE was performed prior to RFA (4,15-19). In a randomized controlled trial by Peng et al. in patients with unresectable HCC with ≤3 nodules smaller

than 7cm, cTACE followed by RFA (n = 94) was significantly better than RFA alone (n = 95) (15). For patients with tumor diameters of 3.1–5.0 cm, the 3-year recurrence free survival rate was 40% for the combined treatment group (compared to 10% for the RFA group). In a smaller randomized controlled study by Morimoto et al. (4), patients with solitary HCC of >3-5cm were allocated to treatment with either cTACE followed by RFA (n=19) or RFA only (n=18). Local tumor progression at the end of the third year in the cTACE-RFA group was 6% compared to 39% in the RFA group (p = 0.012).

Comparison of the results of the studies by Peng and Morimoto with our study results suggests that better outcomes may be achieved with a sequence of cTACE followed by RFA rather that with RFA followed by DEBTACE. It can be debated whether the better outcome after cTACE-RFA is a result of the difference in the type of TACE or of the difference in the treatment sequence.

In our opinion, the type of TACE is less likely to have significant impact on treatment outcome. In the Precision V trial, the objective response rate after DEBTACE was higher than after cTACE, but the difference between the two treatments did not reach statistically significance (6). We believe that differences in efficacy between cTACE-RFA and RFA-DEBTACE are more likely due to the difference in treatment sequence. It has been a long lasting debate in the interventional radiology community whether TACE should be performed before or after RFA when combining both treatments. The rationale for one or the other sequence is different. RFA induces hyperemia in a marginal zone between the ablated area and surrounding tissue. This marginal zone encompasses the periphery of the tumor in which viable tumor cells may be present as well as the area where most satellite nodules tend to be (20). When TACE is performed within several days after RFA, the hyperemia can be used to deliver a high dose of the chemotherapeutic agent to this marginal zone. This marginal zone is not specifically targeted when TACE precedes RFA. The most important theoretical advantage of this sequence is that it may reduce local tumor progression caused by heat sink. Embolization of the hepatic arteries feeding the tumor will result in reduced intra- and perilesional blood flow during the ablation. When TACE is performed after RFA, nothing is done to prevent heat-sink during the ablation. Our study results now allow comparison of long-term results of RFA-DEBTACE with those of cTACE-RFA. Local tumor progression free-survival rates in our study were lower compared to those reported in studies on cTACE-RFA. The most likely explanation for this would be that cTACE-RFA reduces the risk of tumor recurrence due to heat-sink, whereas RFA-DEBTACE does not prevent this type of recurrence. To date, there is limited data on the efficacy of combined RFA and TACE for inoperable HCC. The optimal treatment strategy in HCCs >3cm is yet to be determined and further studies are warranted. Based on a comparison of our results with results of studies using cTACE-RFA, we would argue

that a sequence of TACE followed by RFA should be the preferred sequence in further studies combining both treatments.

The retrospective nature of our study and the relatively small number of patients are limitations of this study. We did not randomize patients to treatment with either RFA or RFA-DEBTACE and therefore direct comparison between the two treatments is not possible. Furthermore, we were only able to compare our results of RFA-DEBTACE with historical data on cTACE-RFA.

In conclusion, local tumor progression free-survival rates for HCC >3cm-7cm are low compared to those after RFA for smaller tumors. The 3-year local tumor progression free-survival rate after RFA-DEBTACE was 17.9% in our study and this is low compared to results reported after cTACE-RFA for HCC with similar size.

REFERENCES

1. European Association For The Study Of The Liver; European Organisation For Research And Treatment Of Cancer. EASL-EORTC clinical practice guidelines: management of hepatocellular carcinoma. J Hepatol 2012. Apr;56(4):908-43.

2. Bruix J, Sherman M, American Association for Study of Liver Diseases. Management of Hepatocellular Carcinoma: An Update. Hepatology 2011. Mar;53(3):1020-22.

3. Kim YS, Rhim H, Cho OK, Koh BH, Kim Y. Intrahepatic recurrence after percutaneous radiofrquency ablation of hepatocellular carcinoma: analysis of the pattern and risk factors. Eur J Radiol 2006. Sept;59(3):432-41.

4. Morimoto M, Numata K, Kondou M, Nozaki A, Morita S, Tanaka K. Midterm outcomes in patients with intermediate-sized hepatocellular carcinoma: a randomized controlled trial for determining the efficacy of radiofrequency ablation combined with transcatheter arterial chemoembolization. Cancer 2010. Dec;116(23):5452–60.

5. Nouso K, Matsumoto E, Kobayashi Y, Nakamura S, Tanaka H, Osawa T, et al. Risk factors for local and distant recurrence of hepatocellular carcinomas after local ablation therapies. J Gastroenterol Hepatol 2008. Mar;23 (3): 453-58.

6. Lammer J, Malagari K, Vogl T, Pilleul F, Denys A, Watkinson A, et al. Prospective randomized study of doxorubicin-eluting-bead embolization in the treatment of hepatocellular carcinoma: results of the PRECISION V study. Cardiovasc Intervent Radiol 2010. Feb;33(1):41-52.

7. Lencioni R, Crocetti L, Petruzzi P, Vignali C, Bozzi E, Della Pina C, et al. Doxorubicine-eluting bead-enhanced radiofrequency ablation of hepatocellular carcinoma: a pilot clinical study. J Hepatol 2008. Aug;49(2):217-22.

8. Bruix J, Sherman M, Llovet JM, Beaugrand M, Lencioni R, Burroughs AK, et al. EASL Panel of Experts on HCC. Clinical management of hepatocellular carcinoma. Conclusions of the Barcelona-2000 EASL conference. European Association for the Study of the Liver. J Hepatol 2001. Sep;35(3):421–30.

9. Huang G, Lin M, Xie X, Liu B, Xu Z, Lencioni R et al. Combined radiofrequency ablation and ethanol injection with a multipronged needle for the treatment of medium and large hepatocellular carcinoma. Eur Radiol. 2014 Jul;24(7):1565-71.

10. Chen MS1, Zhang YJ, Li JQ, Liang HH, Zhang YQ, Zheng Y. Randomized clinical trial of percutaneous radiofrequency ablation plus absolute ethanol injection compared with radiofrequency ablation alone for small hepatocellular carcinoma. Zhonghua Zhong Liu Za Zhi. 2005 Oct;27(10):623-5.

11. Kurokohchi K, Watanabe S, Masaki T, Hosomi N, Funaki T, Arima K, et al. Combined use of percutaneous ethanol injection and radiofrequency ablation for the effective treatment of hepatocellular carcinoma. Int J Oncol. 2002 Oct;21(4):841-6.

12. Feng X, Xu R, Du X, Dou K, Qin X, Xu J, et al. Combination therapy with sorafenib and radiofrequency ablation for BCLC Stage 0-B1 hepatocellular carcinoma: a multicenter retrospective cohort study. Am J Gastroenterol. 2014 Dec;109(12):1891-9.

13. Guglielmi A, Ruzzenente A, Valdegamberi A, Pachera S, Campagnaro T, D'Onofrio M, et al. Radiofrequency ablation versus surgical resection for the treatment of hepatocellular carcinoma in cirrhosis. J Gastrointest Surg 2008. Jan;12(1):192-98.

14. Vivarelli M, Gugliemlmi A, Ruzzenente A, Cuchetti A, Bellusci R, Cordiano C, et al. Surgical resection versus percutaneous radiofrequennncy ablation in the treatment

of hepatocellular carcinoma on cirrhotic liver. Ann Surg 2004. Jul;240(1):102-07.

15. Peng ZW, Zhang YJ, Liang HH, Lin XJ, Guo RP, Chen MS. Recurrent hepatocellular carcinoma treated with sequential transcatheter arterial chemoembolization and RF ablation versus RF ablation alone: a prospective randomized trial. Radiology 2012. Feb;262(2):689-700.

16. Shibata T, Isoda H, Hirokawa Y, Arizono S, Shimada K, Togashi K. Small hepatocellular carcinoma: is radiofrequency ablation combined with transcatheter arterial chemoembolization more effective than radiofrequency ablation alone for treatment? Radiology 2009. Sep;252(3):905-13.

17. Kim JW, Kim JH, Won HJ, Shin YM, Yoon HK, Sung KB, et al. Hepatocellular carcinomas 2-3 cm in diameter: transarterial chemoembolization plus radiofrequency ablation vs. radiofrequency ablation alone. Eur J Radiol 2012. Mar;81:189-93.

18. Kim JH, Won HJ, Shin YM, Kim SH, Yoon HK, Sung KB, et al. Medium-Sized (3.1–5.0 cm) Hepatocellular Carcinoma: Transarterial Chemoembolization Plus Radiofrequency Ablation Versus Radiofrequency Ablation Alone. Ann Surg Oncol 2011. Jun;18(6):1624-29.

19. Peng ZW, Chen MS, Liang HH, Gao HJ, Zhang YJ, Li JQ, et al. A case-control study comparing percutaneous radiofrequency ablation alone or combined with transcatheter arterial chemoembolization for hepatocellular carcinoma. Eur J Surg Oncol 2010. Mar;36(3):257-63.

20. Pulverenti A, Garbagnati, Regalia E, Coppa J, Marchiano A, Romito R, et al. Experience with radiofrequency ablation of small hepatocellular carcinomas before liver transplantation. Transplant Proc 2001. Feb-Mar;33(1-2):1516-17.

PART II

TRANSARTERIAL LIVER THERAPIES
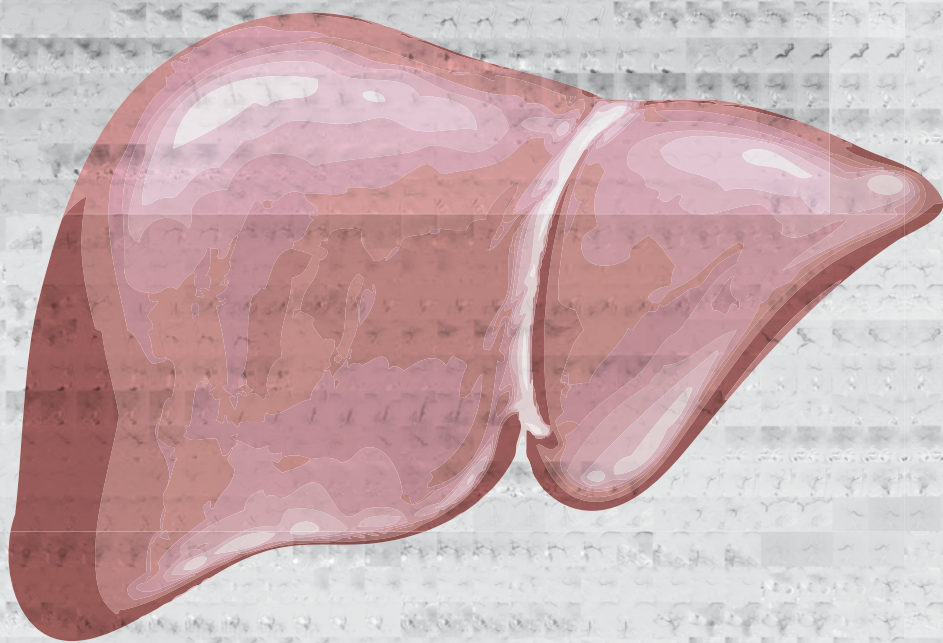
Chapter 5

Pilot study evaluating catheter-directed contrast-enhanced ultrasound compared to catheter-directed computed tomography hepatic arteriography as adjuncts to digital subtraction angiography to guide transarterial chemoembolization
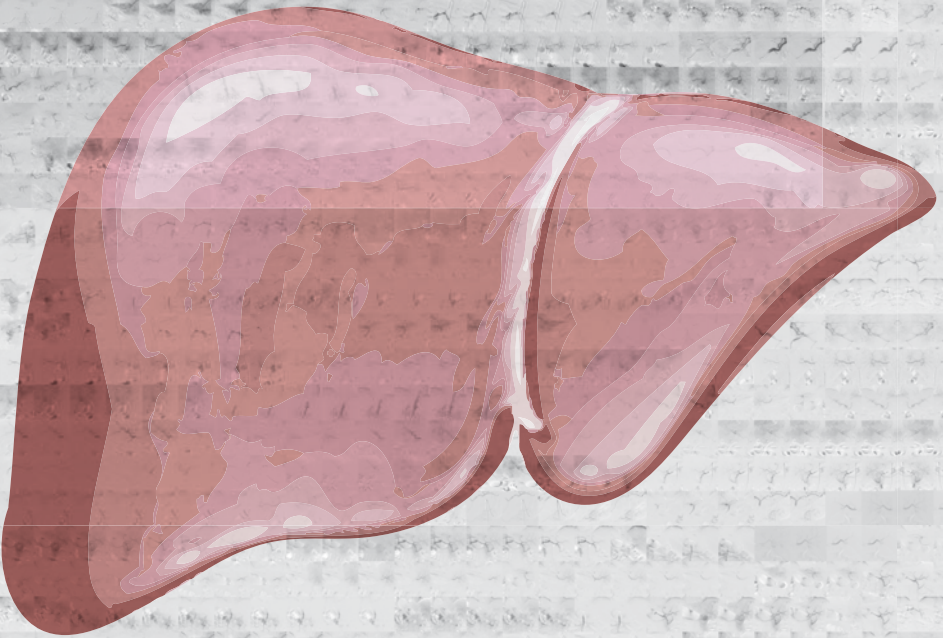
Burgmans MC, van Erkel AR, Too CW, Coenraad MJ, Lo RHG, Tan BS.

ABSTRACT

Purpose

To investigate the feasibility and procedural value of catheter-directed contrast-enhanced ultrasound (CCEUS) compared with catheter-directed computed tomography hepatic arteriography (CTHA) in patients undergoing transarterial chemoembolization (TACE) guided by digital subtraction angiography (DSA).

Methods

From December 2010 to December 2011, a pilot study was conducted including 9 patients (mean age 66.6 years; SD 8.3 years; seven men) undergoing TACE with drug-eluting beads for unresectable hepatocellular carcinoma (HCC). Both CCEUS and CTHA were performed in addition to DSA. Alterations of treatment plan based on CCEUS were recorded and compared with CTHA.

Results

CCEUS provided additional information to DSA altering the treatment plan in 4 out of 9 patients (44.4%). In these four patients, CCEUS helped to identify additional tumor feeders (n=2) or led to a change in catheter position (n=2). The information provided by CCEUS was similar to that provided by CTHA.

Conclusion

CCEUS is a potentially valuable imaging tool in adjunction to DSA when performing TACE and may provide similar information as CTHA.

INTRODUCTION

Transarterial chemoembolization (TACE) improves survival in patients with intermediate stage hepatocellular carcinoma (HCC) (1-3). Traditionally, TACE is guided by digital subtraction angiography (DSA). Yet the information obtained with DSA is limited as DSA only allows two-dimensional imaging. Different studies have shown the value of catheter-directed computed tomography hepatic arteriography (CTHA) and cone-beam computed tomography (CBCT) when performing transarterial liver therapies (4-8). These techniques allow accurate multi-planar visualization of tumor enhancement and improve identification of tumor-feeding arteries. The image quality of CTHA is superior to CBCT as a result of higher soft tissue contrast resolution and CTHA allows imaging with a larger field of view (9).

Contrast-enhanced ultrasound with catheter-directed intra-arterial injection (CCEUS) may potentially be a good alternative to CTHA or CBCT. CCEUS enables real-time visualization of tumor enhancement in multiple directions. Moreover, it is widely available and does not expose the patient to radiation. The aim of this prospective pilot study was to evaluate the procedural impact of CCEUS when used in addition to DSA to guide TACE with drug-eluting beads (DEB-TACE) in patients with intermediate stage HCC and to compare CCEUS with CTHA.

METHODS

Patients

The study was approved by the local ethics committee. Informed consent was obtained for all study patients. From December 2010 to December 2011, nine consecutive patients with HCC were included in the study (mean age 66.6 years; SD 8.3 years; seven men). Inclusion criteria for the study were: unresectable HCC, Child-Pugh A or B and ECOG performance status <2. The diagnosis of HCC was confirmed according to American Association for the Study of Liver Diseases (AASLD) practice guidelines criteria (10). Exclusion criteria were age < 18 years, diffuse HCC or more than 5 lesions, previous treatment with TACE or radioembolization, advanced stage disease according to Barcelona Clinic Liver Cancer (BCLC) criteria (11), total bilirubin >3 mg/dL, uncorrectable coagulopathy, end-stage renal failure, any contra-indication for doxorubicin, known hypersensitivity to sulphur hexafluoride (SF6) micro-bubbles, known right-to-left intra-cardiac shunts, severe pulmonary hypertension, pregnancy.

All patients provided written informed consent. The study was performed in accordance with the Declaration of Helsinki, the International Conference on Harmonization Guideline on Good Clinical Practice and relevant local laws and regulations.

Design and procedures

All patients enrolled in the study underwent grey-scale ultrasonography in the angiography room prior to TACE. In addition to this, contrast enhanced ultrasound was performed with injection of 2.4ml SF6 microbubbles (SonoVue, Bracco International, Amsterdam, The Netherlands) through a cannula in the median cubital vein (IVCEUS). Additional boluses of 2.4ml of microbubbles were given, if the distance between different tumors was such that the enhancement of each tumor could not be analyzed optimally during a single injection. Sufficient time was allowed in between injections for the first bolus of microbubbles to be cleared from the body.

The right groin and upper abdomen were cleansed with iodine and the patient was draped under sterile cloths with exposure of the right groin and upper abdomen. Vascular access was created through the right common femoral artery using a 6F vascular sheath. Using a 5F C2 catheter (Terumo, Tokyo, Japan) selective DSA from the celiac axis (CA), common hepatic artery (CHA) and proper hepatic artery (PHA) was performed with pump injection of a contrast agent (Omnipaque 300; GE Healthcare, Shanghai, China). Angiography from the superior mesenteric artery (SMA) was performed in individual cases when hepatic tumor supply from an aberrant right hepatic artery or other SMA branches was expected based on pre-procedural CT or magnetic resonance imaging (MRI). Immediately after DSA from the PHA and using the same catheter position, CCEUS was performed followed by CTHA. A 2.2F or 2.7F Progreat catheter (Terumo, Tokyo, Japan) was then used to catheterize the lobar artery of the tumor bearing lobe(s) and selective DSA was performed. Again, this was followed by CCEUS and then CTHA with the micro-catheter in the same position. Finally, the (sub)segmental arteries were catheterized using the micro-catheter and sequential DSA, CCEUS and CTHA were performed. In patients with bilobar disease, imaging at a lobar and (sub)segmental level was first performed on one side followed by TACE of the tumors in that lobe. After that, images were obtained at a lobar and (sub)segmental level on the other side and the tumors in the other lobe were treated.

DSA images were obtained with breath-hold, 3 frames/sec and 50mAs/120kV for anteroposterior projections. Using a Mark V ProVis injector (Medrad Inc, Warrendale, PA, USA), contrast medium was injected at 6ml/sec for 25ml for the CA, 5ml/sec for 15ml for the PHA, 3ml/sec for 12ml for lobar injections and 1-2ml/sec for 6-10 ml for (sub)segmental injections. CCEUS was performed using contrast harmonic imaging on a high-perfor-

mance processor (Aplio, Toshiba Medical Systems, Tokyo, Japan) with a multifrequency curved-array probe (2–5 MHz). SF6 micro-bubbles were slowly hand-injected. Injections of 1ml were used for the PHA, 0.5ml for the lobar artery and 0.3-0.5ml for (sub)segmental arteries. During the injection, the entire tumor volume was scanned to assess the presence of unenhancing areas. CTHA was performed using a hybrid 16-slice Aquilion CT/ Infinix VC-1 angiography system (Toshiba Medical Systems, Tokyo, Japan). Pump-injections were used with an injection rate similar to that used for DSA. The injected contrast volume for CTHA was calculated using the equation:

volume = (scan delay + scan time) x flow rate

with the scan delay being the time between the start of injection and enhancement of the region of interest at DSA. CTHA images were acquired using the following parameters: collimation 16x1.0, pitch factor 15, helical pitch 0.938, 120kV and 160 effective mAs. The radiation dose used to perform CTHA was recorded as dose length product (DLP) per patient.

All patients underwent super-selective TACE with the micro-catheter placed as selectively as possible. TACE was performed with DC-Bead (Biocompatibles, Surrey, UK). First 1 vial of 100-300 μm beads was injected, followed by 1 vial of 300-500 μm beads. The beads were loaded with a total of 150mg of doxorubicin (75mg per vial) and mixed with contrast medium prior to injection.

All patients underwent repeated IVCEUS immediately after TACE. Both IVCEUS and CCEUS were performed by the interventional radiologist performing the procedure. All IVCEUS and CCEUS images were archived digitally for review as cine loops in Windows Media Videos (Microsoft, Redmont, WA, USA).

Imaging analysis
At the time of the procedure, DSA images were analyzed by the interventional radiologist performing the procedure and a treatment plan was formulated. Then CCEUS images were analyzed to see if CCEUS provided additional information to DSA. CCEUS images were compared to pre-procedural IVCEUS images. If incomplete tumor enhancement was seen at CCEUS from the hepatic arteries, this prompted a search for extra-hepatic feeding arteries. If tumor enhancement was incomplete upon CCEUS from a lobar or (sub)segmental artery, but not upon CCEUS from a more proximal hepatic artery injection, the catheter was repositioned more proximally prior to injection of DC-Bead. The information obtained with CCEUS was classified into three categories: 1. no change in treatment plan; 2. identification of additional tumor feeding arteries; 3. alteration in

location of injection of the drug-eluting beads. After this, CTHA images were analyzed to see if CTHA provided information not evident on DSA and CCEUS.

IVCEUS images obtained before and after TACE were retrospectively compared to see if complete devascularization of tumors was achieved.

RESULTS

Patient and tumor characteristics are summarized in Table 1. Nineteen HCCs were identified on pre-procedural cross-sectional imaging (CT and/or MRI) with an average of 2.1 (range 1-5) tumor per patient. The mean maximal tumor size was 45.3 mm (range 10-145 mm).

Table 1. Baseline patient and tumor characteristics.

Patient and tumor characteristics	Value
Age	Mean age 67 years
	Range 58-79 years
Sex	M=7
Performance status (n=9)	
0	8 (88.9)
1	1 (11.1)
Cause of cirrhosis (n=9)	
Hepatitis B	6 (66.7)
Alcohol	2 (22.2)
NASH	1 (11.1)
Child Pugh score (n=9)	
A	8 (88.9)
B	1 (11.1)
Tumor burden (n=9)	
Unilobar	6 (66.7)
Bilobar	3 (33.3)
No. nodules (n=9)	
1-3	8 (88.9)
>3	1 (11.1)
Tumor diameter (n=19)	
1-3cm	10 (52.6)
3-5cm	2 (10.5)
5-10cm	3 (15.8)
>10cm	4 (21.1)

In four patients (44.4%), the information provided by CCEUS was not evident at DSA and led to a change of treatment plan. In two of these four patients (22.2% of total) CCEUS led to identification of additional tumor feeding arteries. Both patients had a right liver lobe tumor with a dominant vascular supply from the right hepatic artery. At DSA from the right hepatic artery, incomplete tumor enhancement was not evident. Yet, at CCEUS, there was incomplete enhancement of the tumor and this eventually helped in identifying additional tumor supply from the middle hepatic artery (Figure 1). In the two other patients (22.2%), CCEUS provided information that led to a change in the decision on where to inject the DC Bead. In these cases CCEUS allowed a more selective chemoembolization while ensuring that the entire tumor was accurately targeted (Figure 2).

In four patients where CCEUS provided information that led to a change in treatment, CTHA provided the same information (Figure 1 and 2). CTHA did not provide additional information that led to a change in treatment plan.
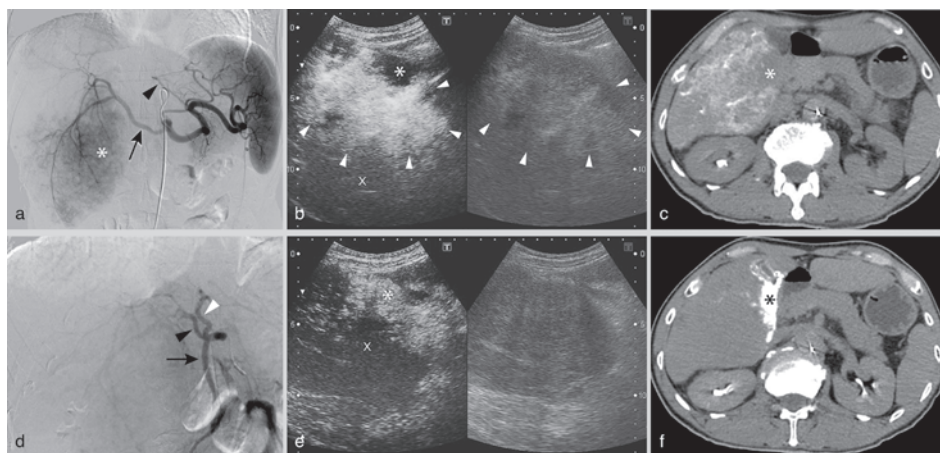
Figure 1. 58-yearr-old male with right liver lobe HCC with a maximal diameter of 12 cm. (a) DSA from the celiac axis (CA) shows tumor enhancement (asterix) through the right hepatic artery (RHA) (arrow). There is a left hepatic artery (LHA) that originates from the left gastric artery (arrowhead). No middle hepatic artery (MHA) is seen. (b) CCEUS (left) and B-mode (right) image during injection of SF6 microbubbles into the RHA. Marked arterial enhancement of the tumor (arrowheads) is seen compared to the non-tumorous liver parenchyma (cross-mark). Absent enhancement is seen in part of the tumor (asterix) (c) CTHA from the RHA also shows absent enhancement in part of the tumor (asterix). (d) DSA from the superior mesenteric artery shows retrograde flow through the gastroduodenal artery (GDA) (arrow) and opacification of the MHA (black arrowhead) and a second LHA (white arrowhead). This MHA and LHA have an origin from the CA that was not opacified at DSA from the CA due to the reversed flow through the GDA. (e) CCEUS (left image) from the MHA shows tumor supply (asterix) through the MHA with absent enhancement in the rest of the tumor (cross-mark). (f) CTHA from the MHA also shows enhancement of part of the tumor through the MHA.
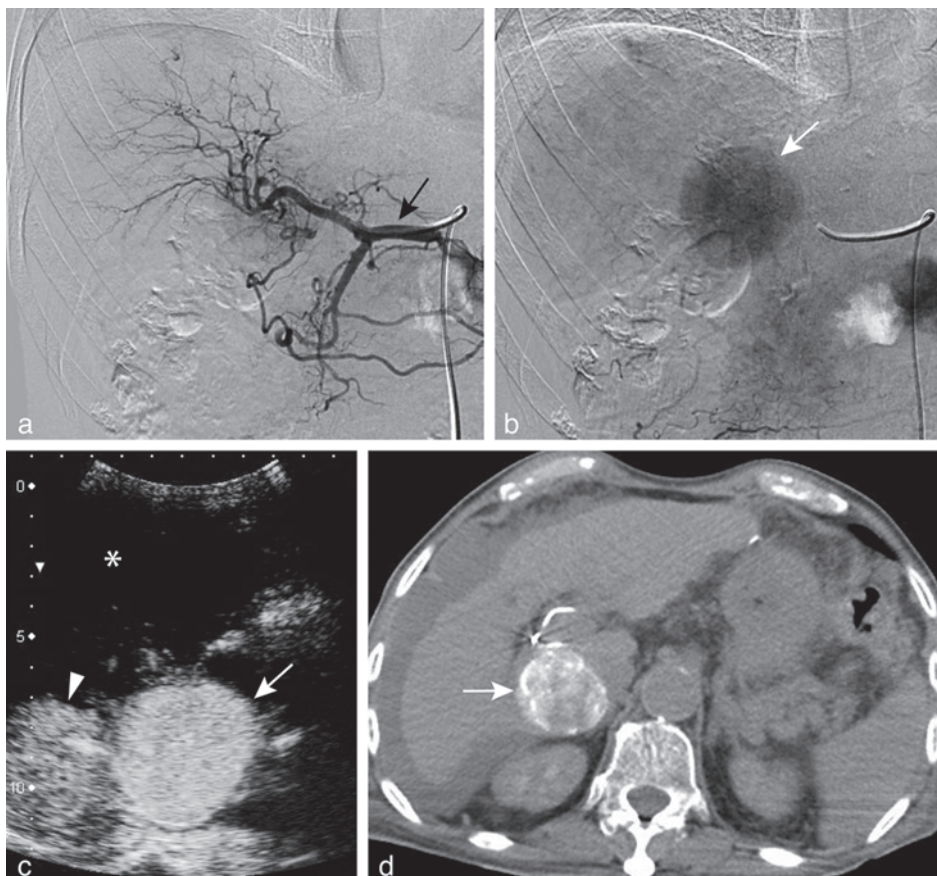
Figure 2. 79-year-old man with a 4.5 cm HCC at the border of segment 6 and the caudate lobe. (a-b) DSA from the common hepatic artery (black arrow) in arterial (a) and parenchymal (b) phase with opacification of the tumor (white arrow). (c) CCEUS from the subsegmental artery showed complete tumor enhancement (white arrow) with enhancement of a small portion of non-tumorous liver parenchyma (arrowhead) and no enhancement of most of the right liver lobe (asterisk). (d) CTHA confirmed enhancement of the entire tumor upon injection of contrast into the subsegmental artery. CCEUS and CTHA thus ensured complete tumor targeting by injection of drug-eluting beads into the subsegmental artery. IVCEUS directly after treatment and CT at 6 weeks showed complete devascularization of the tumor (not shown).

The use of CTHA did result in additional information on extra-hepatic enhancement that was not provided by DSA and CCEUS. In four patients (44.4%), CTHA revealed enhancement of the gallbladder (GB) (n=1), the hepatic falciform artery (HFA) (n=2) or both the GB and HFA (n=1) when contrast was injected from the intended location of release of the drug-eluting beads. This information did not alter the treatment plan. None of these 4 patients developed complications related to injection of drug-eluting beads into the cystic artery or HFA.

IVCEUS immediately after TACE showed complete devascularization of liver tumors in 5 patients (55.6%). The 4 patients with residual enhancement at IVCEUS all had large liver tumors (>10cm). In these patients, vascular stasis was not achieved after delivery of the full dose of drug-eluting beads and the decision was made to treat the remaining viable tumor during a second TACE procedure. The area of residual enhancement on IVCEUS corresponded to the vascular territory of the supplying artery that was not completely embolized, indicating that residual enhancement was not a result of failure to detect additional tumor feeding arteries.

The mean DLP per patient was 921.5 mGy•cm (SD 371.7 mGy•cm)

DISCUSSION

The objective of TACE is to accurately target the entire tumor while preserving the non-tumorous liver parenchyma and extra-hepatic organs. To achieve this, it is generally recommended to deliver the beads as selective as possible (12). Super-selective injection, i.e. into the segmental or sub-segmental arteries, is associated with better treatment outcomes compared to lobar or whole liver chemo-embolization (13).

DSA is used to guide the delivery of the drug-eluting beads. Yet, DSA only enables two-dimensional imaging. As a result, incomplete tumor enhancement may not be detected during hepatic DSA. This is especially true if the non-enhancing tumor parts are located anterior or posterior as hepatic DSA images are usually obtained in posterior-anterior or moderately oblique projections.

There are two important causes for incomplete tumor enhancement during hepatic DSA. The most important cause is the presence of extra-hepatic feeding arteries. Unfortunately, up to 37% of patients with HCC may have a collateral tumor supply through extra-hepatic arteries (5). Second, incomplete tumor enhancement may be due to a highly selective catheter position. Treatment at a (sub)segmental level carries the risk that the catheter is placed distally to additional hepatic feeders. Failure to detect absent enhancement of tumor parts during hepatic DSA may thus result in incomplete tumor treatment.

Different studies have shown that catheter-directed cross-sectional imaging such as CTHA and CBCT allow accurate multi-planar visualization of tumor enhancement and may improve tumor targeting (4-8). In the present study we compared CCEUS and CTHA as an adjunct to DSA to guide TACE. CCEUS proved to be safe and feasible. In 44.4% of patients, CCEUS provided information that was not evident on DSA and altered the treatment ap-

proach. The additional information provided by CCEUS was similar to that provided by CTHA. Although the number of patients in our study is limited, the findings suggest that CCEUS may improve trans-arterial liver tumor targeting, as does CTHA. In a viable tumor incomplete enhancement upon contrast injection from the hepatic arteries may indicate extra-hepatic tumor supply. Complete tumor enhancement upon contrast injection from a super-selective hepatic artery position allows the operator to feel confident that the entire tumor is targeted, whereas incomplete enhancement may prompt the search for additional feeding hepatic arteries. CCEUS offers an important advantage over CTHA. It can be repeated multiple times without increasing iodinated contrast volume or radiation, whereas computed tomographic imaging during TACE results in significant increase of the radiation dose to both the patient and operating staff (14,15).

Few centers have access to a hybrid CT/angiography system that allows CTHA images to be obtained without moving a patient between rooms. CBCT is available to many more interventional radiologists and is much more frequently used as an adjunct to DSA during TACE. CCEUS and CBCT were not compared in the present study. Yet, CCEUS may offer several additional advantages over CBCT. CBCT has a relatively long acquisition time (8-20sec) making this technique more susceptible to breathing artifacts, whereas breathing is not an issue in CCEUS. Another drawback of CBCT is the limited field of view (FOV). CCEUS is less hindered by limitations in the FOV as it can be repeated multiple times to cover larger areas without radiation or risk of contrast-induced nephropathy.

The standard volume of SF6 microbubbles of hepatic IVCEUS in our institution at the time of the study was 2.4ml. Modern high-end ultrasound machines enable good quality IVCEUS imaging with lower dosages and may therefore also allow the use of lower volumes of microbubbles for CCEUS then those used in this study.

The main limitation of our study is the limited number of patients. Second, the usefulness of CCEUS was not compared with CBCT, which is more widely used than CTHA. Yet, CTHA was used as the gold standard in the present study as this technique has better image quality and a larger field of view compared to CBCT. Furthermore, CCEUS was inferior to CTHA in providing information on extra-hepatic enhancement. Yet, the information provided by CCTA did not alter the treatment strategy and no extra-hepatic organ injury was seen.

In conclusion, CCEUS is a potentially useful imaging tool in adjunction to DSA when performing TACE. It may provide similar multi-planar information on tumor enhancement as CTHA without increasing iodinated contrast volume or radiation, yet further studies are warranted to determine the role of CCEUS.

REFERENCES

1. Llovet JM, Real MI, Montana X, et al. Arterial embolisation or chemoembolization versus symptomatic treatment in patients with unresectable hepatocellular carcinoma: a randomised controlled trial. Lancet. 2002; 359(9319):1734–1739.

2. Lo CM, Ngan H, Tso WK, et al. Randomized controlled trial of transarterial lipiodol chemoembolization for unresectable hepatocellular carcinoma. Hepatology. 2002; 35(5):1164–1171.

3. Llovet JM, Bruix J. Systematic review of randomized trials for unresectable hepatocellular carcinoma: Chemoembolization improves survival. Hepatology. 2003 Feb;37(2):429-442.

4. Burgmans MC, Kao YH, Irani FG, et al. Radioembolization with infusion of Y90 microspheres into a right inferior phrenic artery with hepatic tumor supply is feasible and safe. J Vasc Interv Radiol. 2012 Oct;23(10):1294-1301.

5. Kao YH, Tan AEH, Burgmans MC, et al. Image-guided personalized predictive dosimetry by artery-specific SPECT/CT partition modeling for safe and effective Yttrium-90 radioembolization. J Nucl Med. 2012 Apr; 53(4):559-566.

6. Miyamaya S, Yamashiro M, Okuda M et al. Usefullness of cone-beam computed tomography during ultraselective transcatheter arterial chemoembolization for small hepatocellular carcinomas that cannot be demonstrated on angiography. Cardiovasc Intervent Radiol. 2009; 32:255-264.

7. Miyamaya S, Yamashiro M, Hattori Y et al. Efficacy of cone-beam computed tomography during transcatheter arterial chemoembolization for hepatocellular carcinoma. Jpn J Radiol. 2011; 29:371-377.

8. Takayasu K, Muramatsu Y, Maeda T, et al. Targeted transarterial oily chemoembolization for small foci of hepatocellular carcinoma using a unified helical CT and angiography system: analysis of factors affecting local recurrence and survival rates. American Journal of Roentenology 2001; 176:681-688.

9. Orth RC, Wallace MJ, Kuo MD. C-arm cone-beam CT: general principles and technical considerations for use in interventional radiology. J Vasc Interv Radiol. 2008 Jun;19(6):814-820.

10. Bruix J, Sherman M. American Association for the Study of Liver Diseases. Management of hepatocellular carcinoma: an update. Hepatology. 2011 Mar;53(3):1020-2.

11. Llovet JM, Brú C, Bruix J. Prognosis of hepatocellular carcinoma: the BCLC staging classification. Semin Liver Dis. 1999; 19(3):329-338.

12. Lencioni R, de Baere T, Burrel M et al. Transcatheter treatment of hepatocellular carcinoma with doxorubicine-loaded DC Bead (DEB-DOX): technical recommendations. Cardiovasc Intervent Radiol. 2012; 35:980-985.

13. Raoul JL, Sangro B, Forner B, et al. Evolving strategies for the management of intermediate-stage hepatocellular carcinoma: Available evidence and expert opinion on the use of transarterial chemoembolization. Cancer Treat Rev. 2011 May 37(3):212-220.

14. Kothary N, Abdelmaksoud MH, Tognolini A, et al. Imaging guidance with C-arm CT: prospective evaluation of its impact on patient radiation exposure during transhepatic arterial chemoembolization. J Vasc Interv Radiol. 2011 Nov;22(11):1535-43.

15. Schulz B, Heidenreich R, Heidenreich M, et al. Radiation exposure to operating staff during rotational flat-panel angiography and C-arm cone beam computed tomography (CT) applications. Eur J Radiol. 2012 Dec;81(12):4138-42.

Chapter 6

Radioembolization with infusion of Y90 microspheres into a right inferior phrenic artery with hepatic tumor supply is feasible and safe
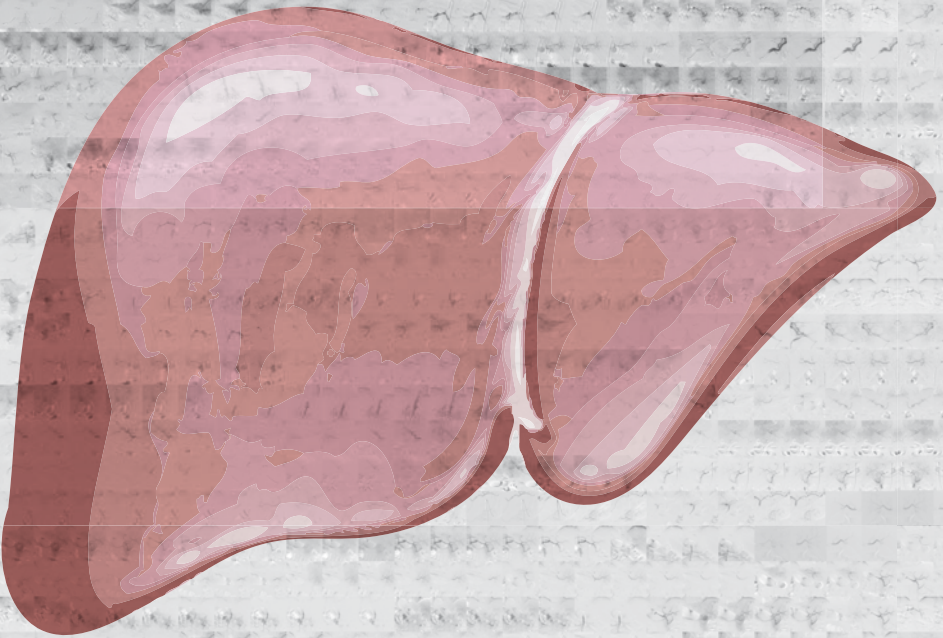
Burgmans MC, Kao YH, Irani FG, Dames E, Teo TK, Goh ASW, Chow PKH, Tay KH, Lo RHG

ABSTRACT

Purpose

To evaluate the feasibility and safety of yttrium-90 (Y90) radioembolization through the inferior phrenic arteries (IPAs).

Methods

Retrospective analysis of 108 patients referred for radioembolization to treat primary (n=103) or secondary (n=5) liver malignancy was performed. Five patients had their hepatic malignant tumors supplied by the IPA and met the inclusion criteria for infusion of Y90 spheres into the IPA. DSA, catheter-directed computer tomography hepatic angiography (CTHA) and technetium-99m macroaggregated albumin (Tc-99m MAA) SPECT/CT were used to plan treatment. Bremsstrahlung SPECT/CT was performed 1 day after radioembolization. Follow-up included clinical and biochemical tests and cross-sectional CT or MRI.

Results

Parasitized extra-hepatic arteries were detected in 37.0% (n=40) of patients. Of these, 62.5% (n=25) had tumor supply through an IPA. Of the patients with IPA supply, 20% (n=5) underwent infusion of Y90 into the right IPA. Reasons for disqualifying patients for infusion into the IPA were less than 10% tumor supply (n=11), failed catheterization of IPA (n=3), arterioportovenous shunt (n=2), failed identification of IPA at pre-treatment angiography (n=1), and gastric or esophageal enhancement on CTHA (n=3). In all 5 patients technical success was demonstrated on Y90 imaging, with no significant extra-hepatic radionuclide activity. No adverse events related to IPA radioembolization occurred at mean follow-up of 4.5 months (range 2.2-10.1 months).

Conclusions

Delivery of Y90 microspheres through the right IPA is feasible and safe with the use of CTHA in addition to DSA and Tc-99m MAA SPECT/CT in patients with tumors with greater than 10% IPA supply.

INTRODUCTION

Radioembolization with yttrium-90 (Y90) microspheres is an effective treatment for patients with unresectable primary and secondary liver malignancy (1, 2). Microspheres are delivered to the hepatic tumors by selective hepatic arterial infusion. The infused microspheres lodge permanently within the vascular bed of the tumor to deliver high-energy ß-radiation (3). As each microsphere has a limited therapeutic range (mean tissue range 2.5mm; maximum 11mm), adequate deposition of microspheres throughout the entire tumorous region is essential to achieve optimal treatment results. This may be difficult or impossible to achieve in patients with tumors supplied by parasitized extra-hepatic arteries (PEAs). Unfortunately, 17-30.8% of patient with liver malignances may have tumor supply through PEAs (4-7). The inferior phrenic arteries (IPAs) are responsible for the extra-hepatic supply in the vast majority of cases (4,6,8). Infusion of Y90 into the IPAs is generally considered not to be feasible because of the risks of non-target radiation injury (6,9).

We hypothesized that selective radioembolization into the IPAs is feasible and safe in selected patients when using a combination of digital subtraction angiography (DSA), catheter-directed computed tomography hepatic angiography (CTHA) and technetium-99m macroaggregated albumin (Tc-99m MAA) single photon emission computed tomography with integrated low-dose computed tomography (SPECT/CT) to plan and guide treatment. We retrospectively reviewed the feasibility and safety of infusion of Y90 microspheres directly into the IPAs.

METHODS

Approval by the Institutional Review Board (IRB) of our institution was obtained for this retrospective study.

Patients

We retrospectively reviewed reports and images of all pre-treatment and treatment angiograms performed between May 2010 and December 2011. In this period, pre-treatment angiography with Tc-99m MAA injections were performed in 108 patients for the following indications: hepatocellular carcinoma (HCC) in 99 patients (91.7%), metastasis from colorectal carcinoma in 4 patients (3.7%), cholangiocarcinoma in 2 patients (1.9%), hepatic angiosarcoma in 2 patients (1.9%) and metastasis from adrenocortical carcinoma in 1 patient (0.9%). Patient age ranged from 36-85 years (mean, 63.1 years) and 90 patients were male.

Among the 108 patients, 81 patients (75.0%) proceeded to have at least one treatment session with radioembolization. Seven patients underwent a second radioembolization treatment during the study period. All radioembolization procedures were performed with Y90 resin microspheres with a diameter of 20-60 µm (SIR-Spheres®, Sirtex Medical Limited, New South Wales, Australia).

Pre-treatment angiography and Tc-99m MAA

In all patients cross-sectional images obtained with either computed tomography (CT) and/or magnetic resonance imaging (MRI) were available and reviewed before the procedure. The angiographic protocol included selective DSA from the superior mesenteric artery, the celiac axis and hepatic arteries. All patients underwent CTHA using a hybrid 16-slice CT/angiography system (Toshiba, Tokyo, Japan). Selective inferior phrenic DSA and CTHA were performed in cases where tumor supply from the IPAs was suspected based on the pre-procedural cross-sectional imaging or if incomplete tumor enhancement was seen on DSA and/or CTHA from the hepatic arteries.

Selective DSA of the IPA was performed with a 5F Cobra catheter (Terumo, Tokyo, Japan) or 4F Sidewinder catheter (Terumo or Cordis, Miami Lakes, FL, USA). Subsequently, a 2.2F or 2.7F Progreat catheter (Terumo) was introduced co-axially through the 4F/5F catheter and DSA and CTHA were performed. CTHA from the IPA was performed using an injection rate of 1-3 ml/sec. The injected contrast volume for CTHA was calculated by adding the scan delay and scan time and multiplying the sum by the flowrate, with the scan delay being the time between the start of injection and enhancement of the region of interest at angiography.

Patients underwent standard coil embolization of hepaticoenteric anastomoses either on the day of the pre-treatment angiography or the day of radioembolizaton. In patients in whom radioembolization from the IPA was considered, angiography and CTHA images were carefully reviewed to identify the presence of IPA branches such as inferior vena cava, adrenal, esophageal, gastric and diaphragmatic arteries. If feasible, coil embolization of such arteries was performed with 0.018-inch coils (2mm Figure-8 or 3mm Diamond-shaped VortX, Boston Scientific, Natick, Massachusetts, USA).

At the end of the procedure, CTHA images were reviewed to visually estimate the contribution to tumor perfusion for each supplying artery as a percentage of total tumor perfusion. The Tc-99m MAA (total 5mCi in 3ml; particle size of 10-90µm) was then divided into corresponding portions and slowly hand-injected into each supplying artery. For the IPA, the injected volume of Tc-99m MAA ranged between 0.5-1ml (0.8-1.7mCi). All patients underwent Tc-99m MAA planar scintigraphy and SPECT/CT using a hybrid

SPECT/CT scanner (Philips Precedence, Amsterdam, Netherlands) for calculation of liver-to-lung shunt fraction and tumor-to-normal liver ratio and to exclude any non-target extrahepatic shunting of Tc-99m MAA. Predictive radiation dosimetry was performed by Medical Internal Radiation Dose (MIRD) macrodosimetry (ie, 'partition model').

Infusion of microspheres into IPA

Before infusion of Y90 microspheres, hepatic angiography and CTHA were repeated. Moderate enhancement of the adrenal gland or IVC was not considered to be a contra-indication for infusion of Y90 microspheres into the IPA. The activity of Y90 microspheres injected into the IPA was determined by Tc-99m MAA SPECT/CT predictive dosimetry, in accordance with target tissue masses determined by CT volumetry guided by CTHA of the IPA. Y90 microspheres were manually infused until the entire calculated dose was delivered or angiographic stasis was reached.

Safety assessment and follow-up

All patients underwent Y90 imaging one day after radioembolization. Y90 imaging of the abdomen was performed by bremsstrahlung SPECT/CT alone or in combination with Y90 internal pair production time-of-flight (TOF) positron emission tomography with integrated CT (PET/CT) as part of an unrelated research project. Also, planar liver-to-lung bremsstrahlung scintigraphy was performed. Special attention was paid to Y90 activity in the tumor area supplied by the IPA versus the rest of the tumor. Liver and renal function tests were routinely performed before discharge for all patients. Follow-up cross-sectional imaging by CT or MRI was routinely planned 3 months after treatment and approximately every 3 months thereafter. Adverse effects were classified into grade 1 to 5 in accordance with the common terminology criteria for adverse events version 3.0 (CTCAE v3) (10).

RESULTS

Identification of PEAs

Vascular tumor supply through PEAs was detected in 40 of 108 patients (37.0%) who underwent preparatory hepatic angiography with Tc-99m MAA injection. Of these 40 patients, 37 (92.5%) had HCC. Most patients (65.0%) were found to have only one PEA (Table 1). A total of 71 PEAs were detected. The IPAs were the most common source of extra-hepatic blood supply, seen in 38% of all PEAs (Table 1). Twenty-five patients (62.5% of patients with PEAs) had blood supply through one or both IPAs.

Table 1. Parasitized extra-hepatic arteries (PEAs): number per patient and types

Number of PEAs per patient		n (total = 40)	%
	1 artery	26	65.0
	2 arteries	8	20.0
	>2 arteries	6	15.0

Identified PEAs		n (total = 71)	%
Inferior phrenic		27	38.0
	Right	21	29.6
	Left	6	8.5
Right middle and/or inferior adrenal		7	9.9
Pancreaticoduodenal arcade		6	8.5
Right renal capsular		6	8.5
Right gastro-epiploic		5	7.0
Cystic		4	5.6
Right gastric		4	5.6
Gastroduodenal branch		3	4.2
Superior mesenteric branch		3	4.2
Intercostal		2	2.8
Superior phrenic		1	1.4
Supraduodenal		1	1.4
Left gastroepiploic		1	1.4
Splenic artery branch		1	1.4

Parasitized extra-hepatic supply through the IPA

The demographics of the 25 patients with tumor supply through an IPA are given in Table 2. The mean maximum diameter of liver tumors supplied by the IPA was 13.5cm (range 5.8- 20.0 cm). Tumor supply through the right IPA was detected in 19 of the 25 patients (76.0%), through the left IPA in four patients (16.0%) and through both the right and left IPA in two patients (8.0%). Five patients with right IPA supply (26.3%) had a right liver lobe tumor with extension to the diaphragm, three (15.8%) had tumor extension to the bare area, and 11 (57.9%) had tumor extending to both the diaphragm and the bare area. All patients with left or bilateral IPA supply had a liver tumor extending to both the diaphragm and the bare area. In 11 (44.0%) patients there was vascular tumor supply through at least one other PEA in addition to the IPA supply.

Treatment IPA

In 17 of the 25 patients with blood supply through one or both IPAs (68.0%), the option of infusion of radioactive microspheres through the IPA was rejected without performing CTHA from the IPA (Table 3). The feasibility of performing radioembolization from

Table 2. Demographics patients with inferior phrenic artery (IPA) supply (n=25)

Characteristic		Value	
Age		mean 62.4 yrs	
		range 39-83 yrs	
Sex		n (total =25)	%
	Male	22	
	Female	3	
Tumor type		n	%
	HCC	25	100
Tumor distribution		n	%
	Bilobar	16	64.0
	Unilobar	9	
Child-Pugh score		n	%
	A	20	80.0
	B	5	20.0
Vascular invasion		16	64%
Lymph node metastasis		2	8%
Distant metastasis		0	0%
BCLC stage			
	A	7	28.0%
	B	2	8.0%
	C	16	64%

BCLC stage = Barcelona Clinic Liver Cancer staging system, HCC = hepatocellular carcinoma

the IPA was not further evaluated in these patients because of IPA supply less than 10% (n=11), failed catheterization of the IPA (n=3), arterioportovenous shunting (n=2), or failed identification of the IPA supply at the time of pre-treatment angiography (n=1). Eight patients did undergo CTHA from the IPA to evaluate the safety of microsphere infusion into the IPA.

In three of the eight patients who underwent CTHA from the IPA, Y90 microspheres infusion into the IPA was not considered safe based on imaging findings and Tc-99m MAA was therefore not injected into the IPA. In one patient, CTHA from the left IPA showed marked gastric enhancement through several small IPA branches. There was also tumor supply seen through the right IPA, but this was estimated to be less than 10% of the overall tumor

burden. Transarterial embolization (TAE) of both the right and left IPA was performed us-
ing 250-355 µm polyvinyl alcohol (PVA) particles (Contour; Boston Scientific) in the same
setting as radioembolization through the hepatic arteries. In another patient, CTHA from
the right IPA showed a small area of esophageal enhancement and marked enhancement
of the right adrenal gland. In the third patient, reflux with enhancement of the adrenal
glands and esophagus was seen at catheter-directed cross-sectional imaging from the
right IPA. In the second and third patients, coil embolization of the IPA was performed
in order to re-establish intrahepatic antegrade flow to the tumor area supplied by the
IPA. Yet, in both patients we failed to demonstrate satisfactory re-establishment of flow

Table 3. Tumor characteristics, IPA supply and treatment of IPA territory

Parameter	Value		
Diameter of tumor with IPA supply	Mean 13.5cm (range 5.8 to 20.0 cm)		
Location of tumor supplied by IPA	n (total =25)		%
In contact with diaphragm	5		20.0
Bare area	3		12.0
In contact with diaphragm and bare area	17		68.0
Area supplied by IPA			
<10% of entire tumor volume	11		44%
10-20%	7		28.0%
20-30%	4		16.0%
30-40%	3		12.0%
Treatment IPA territory per patient	n (total =25)	% (of total)	Rationale not to attempt RE through IPA
No treatment	15	60.0%	
	11	44.0%	<10% supply
	3	12.0%	Failed catheterization IPA
	1	4.0%	Large APV shunt
TACE	1	4.0%	IPA supply not identified at preparatory DSA. Disqualified from RE because of lung shunt
TAE	2	8.0%	
	1	4.0%	Shunt IPA to PV
	1	4.0%	Gastric enhancement on CCTA
Coil-embolization	2	8.0%	
	2	8.0%	Esophageal enhancement on CCTA
Radioembolization	5	20%	

RE = radioembolization; TACE = trans-arterial chemo-embolisation; TAE = transarterial embolisation; PV =
portal vein; CCTA = catheter-directed computer tomography angiography

through intra-hepatic collaterals to the IPA territory using DSA, CTHA and SPECT/CT. In five of the 25 patients (20%), Y90 microspheres were infused directly into the right IPA.

Infusion of Y90 microspheres into the IPA

Y90 microspheres were infused into the right IPA in all five cases with radioembolization through the hepatic arteries in the same session. Two patients had been treated with radioembolization once before, but without infusion of microspheres into the IPA. In one patient, the IPA supply was not identified during the first treatment. The other patient had undergone treatment twice with conventional TACE prior to the first radioembolization. Uncomplicated TACE had been performed from the right IPA during the second TACE session.

All 5 patients had large hypervascular right liver lobe tumors (mean diameter 18.2 cm; range 15.1-20.0 cm). Selective angiography and CTHA showed good forward flow and absence of reflux in all 5 cases. The mean activity of Y90 microspheres infused into the IPA was 0.6 GBq (range 0.3-0.8 GBq). In three patients (60.0%), coil embolization was
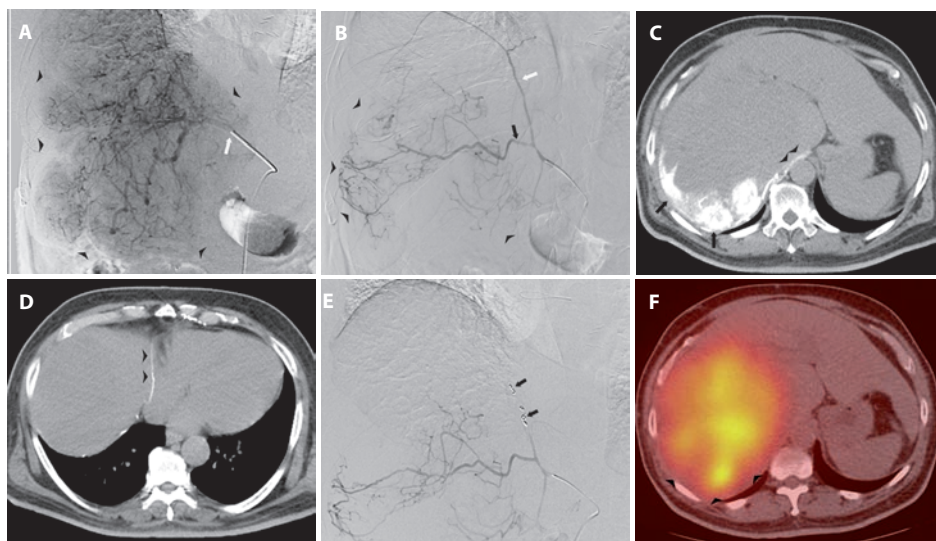
Figure 1. Images from a 64-year-old male with a large HCC. (a) DSA from the right hepatic artery (RHA) (white arrow) shows enhancement tumor (arrowheads). CTHA from the RHA showed absent enhancement of the posterior portion of the tumor (not shown). (b) DSA from the right IPA shows tumor supply (arrowheads) through the descending branch of the IPA (black arrow) and no obvious tumor supply from the ascending IPA branch (white arrow). (c+d). CTHA from the IPA shows enhancement of the posterior portion of the tumor (arrows) and the diaphragmatic crus (arrowheads) (c). The ascending IPA branch (arrowheads) does not supply the tumor (d). (e) Coils (black arrows) have been placed in the ascending IPA branch before infusion of Y90 microspheres into the RHA and right IPA. (f) Bremsstralung scan shows Y90 activity in the entire tumor, including the IPA territory (arrowheads).

performed of a diaphragmatic branch that was shown to supply the diaphragm and no tumor (Figure 1).

In one of the five patients, a small adrenal artery with tumor supply was seen to originate from the right IPA branch (Figure 2). TAE of this adrenal artery was performed with 150-250 µm PVA particles (Contour, Boston Scientific, Natick, MA, USA), and Y90 microspheres were infused into the IPA from a more distal position. In three of the five patients
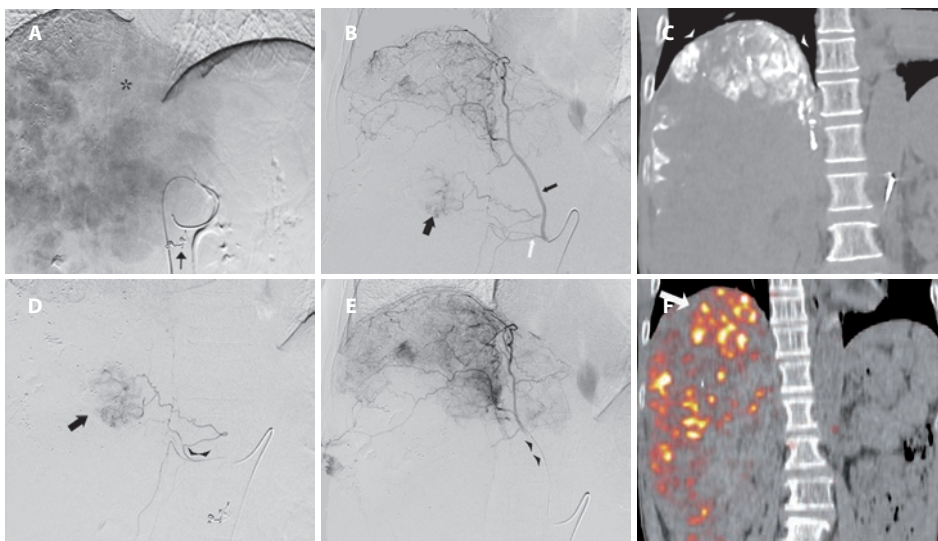

Figure 2. Images from 52-year-old male with a HCC in segment 4, 5, 6, 7 and 8. (a) DSA from the proper hepatic artery shows the large hypervascular tumor. Poor enhancement of the cranio-medial area is seen (asterix). Embolization of the gastroduodenal artery and right gastric artery has been performed with respectively an Amplatzer vascular plug 4 and microcoils (black arrow). (b) DSA from the right IPA (small black arrow) shows enhancement of the cranial portion of the tumor and supply to a small tumor area (large black arrow) through a proximal adrenal artery branch (white arrow). (c). CTHA from the IPA shows enhancement of the cranial tumor part (arrowheads). (d) DSA from the adrenal artery through a microcatheter (arrowheads) shows the small area of tumor enhancement (arrow). The adrenal artery was embolized using PVA particles. (e) After placement of the microcatheter (arrowheads) more distally into the IPA, Y90 microspheres were infused. This was followed by infusion into the proper hepatic artery. (f) PET/CT performed 1 day after radioembolization shows higher Y90 activity in the IPA territory (arrow) compared to the rest of the tumor.

(60.0%), CTHA from the IPA showed mild to moderate enhancement of the right adrenal gland. In 2 patients (40.0%) moderate enhancement of the IVC was seen in addition to this.

Y90 activity in IPA territory

All five patients who underwent infusion of microspheres into the IPA showed Y90 activity in the IPA territory on bremsstralung SPECT/CT. In three patients, homogenous activity was seen in the entire IPA territory. In the patient who underwent TAE of the adrenal artery, the small area supplied by this artery did not show Y90 activity. In another patient there was good Y90 activity in the medial portion of the IPA territory, but unsatisfactory activity in the lateral portion. Before infusion of microspheres, TAE of a right renal capsular artery was performed with 355-500 μm PVA particles (Contour, Boston Scientific). This capsular artery also showed competing supply to the lateral area of the IPA territory and the lack of Y90 activity was thought to be a result of the TAE.

Safety of radioembolization into IPA

One of the five patients who underwent radioembolization into the IPA developed a small puncture site hematoma during the procedure. No other intra-procedural complications were encountered in these five patients. In all five patients radioembolization was performed under local anesthesia and none of the patients required additional administration of analgesics during or after the procedure.

The mean follow-up duration for the five patients was 4.5 months (range, 2.2-10.1 months). One patient who had come from overseas for medical treatment in our institution was lost to follow-up. He was well at the time of discharge from the hospital and returned to his home country 7 days after radioembolization. None of the patients developed adverse effects attributable to radioembolization into the IPA.

DISCUSSION

Radioembolization through PEAs is generally considered to be contraindicated because of the high risk of non-target radiation (6,9). Unfortunately, up to 30.8% of patients with a hepatic malignancy will have vascular tumor supply through one or more PEAs (4-7). In our study, 37.0% of patients had one or more PEAs supplying part of their hepatic neoplasms. The IPAs are the most frequent source of extrahepatic collateral blood supply to hepatic tumors (4-6,8). In the present study, 62.5% of patients with PEAs had tumor supply through one or both IPAs. Particular risk factors for parasitized supply through the IPAs are a tumor location in the bare area and contact of the tumor with the diaphragm (11).

The right and left IPA divide into an ascending and descending branch and give rise to superior suprarenal and middle suprarenal branches. The right IPA may give rise to

arteries to the IVC, whereas the left IPA can give rise to accessory splenic, gastric and esophageal branches (11, 12). Potentially, the IPA can communicate with systemic arteries such as the internal mammary, intercostal, musculophrenic and pericardiophrenic arteries (12,13). Transpleural intercommunication with the pulmonary arteries can also exist, usually in patients with underlying chronic lung inflammation (14).

Administration of Y90 microspheres into the IPAs has been deemed unsafe because of the potential risks of radiation injury to the diaphragm and adrenal glands (6,9). In addition to this, spheres that are infusion into the right IPA could theoretically find their way through branches supplying the IVC, causing radiation injury to the IVC. Infusion of Y90 into the left IPA could theoretically result in radiation injury to the spleen, stomach or distal esophagus. In addition, reflux could occur into the communicating systemic arteries or into the vessel from which the IPA originates. Patients with intercommunication of the IPA and pulmonary vessels are at risk of radiation pneumonitis or even diffuse systemic irradiation if the microspheres shunt into the pulmonary veins (6).

Different strategies can be adopted in patients with PEAs. TAE and TACE have been successfully performed through different PEAs, although TACE from the IPA may be complicated by pleural effusion and atelectasis (7,11,15-22). Although TAE and TACE are feasible treatments to address parts of the hepatic malignancy supplied by PEAs, they are not the preferred option. Those patients that are assessed to undergo radioembolization, often have been selected either because of disease progression after TACE or a contra-indication to TACE such as portal vein embolization. Another option to address parasitized extra-hepatic supply was recently reported by Abdelmaksoud et al. in a study including 35 patients with 73 PEAs (6). Prior to Y90 microspheres infusion, the authors attempted to eliminate parasitic perfusion and restore intrahepatic blood supply to liver tumors by embolizing the PEAs with large particles and coils. After this method had been employed, successful re-establishment of antegrade flow through intra-hepatic collateral vessels into tumor areas previously supplied by PEAs was confirmed by both DSA and C-arm CT in 94% of territories and by scintigraphy in 96%. They also observed symmetric regional tumor response in 94% of patients and this was inferred as successfully delivery of microspheres to the territories previously supplied by PEAs. The method of embolization of PEAs offers an important advantage, as the risk of nontarget radiation is substantially lower when Y90 microspheres are infused into the hepatic arteries instead of into a PEA. However, there are uncertainties with regards to the approach of coilembolization. In the study of Abdelmaksoud et al., there was no histological confirmation of successful delivery of microspheres in the areas supplied by the PEAs. Only surrogates to measure microspheres implantation were used, such as contrast enhancement, Tc-99m MAA uptake, and tumor response. Furthermore, many patients

in the study by Abdelmaksoud et al. had also received adjuvant systemic therapy after radioembolization. Tumor response may therefore not only be a result of successful implantation of Y90 microspheres in the PEA territories. The biggest disadvantage of the method of embolizing the PEAs is that the success of microspheres delivery to the PEA territories remains unpredictable and accurate predictive radiation dosimetry for the PEA territories is therefore difficult.

In our study, five patients underwent radioembolization with direct infusion into the IPA. In all 5 cases infusion of microspheres was performed from the right IPA. None of the five patients experienced serious adverse events at a mean follow-up of 4.5 months. The use of CTHA was considered to be crucial in selecting patients for radioembolization via the IPA. CTHA provides the necessary complementary information to DSA with better image quality and spatial resolution than cone-beam CT and Tc-99m MAA scintigraphy. Furthermore, CTHA enables the vascular territory of a particular artery to be accurately delineated. Artery-specific CT volumetry guided by CTHA achieves accurate tissue mass estimates for improved radiation dosimetry to the IPA territory – a current practice at our institution (23).

Limitations of our study are the retrospective nature and the small number of patients. Further studies are needed to confirm the safety of infusion of radioactive microspheres into the IPA.

In conclusion, this study shows that the delivery of beta-emitting microspheres through the right IPA is feasible and safe in selected patients. The use of CTHA in addition to DSA and Tc-99m MAA scintigraphy is crucial in minimizing the risk of non-target radiation injury. The study does not support any conclusions on the infusion of Y90 microspheres into the left IPA or other PEAs. The risk of radiation injury to the esophagus or stomach is likely to be significantly higher when infusion of spheres would be performed from the left IPA versus the right IPA.

REFERENCES

1. Sangro B, Salem R, Kennedy A, Coldwell D, Wasan H. Radioembolization for Hepatocellular Carcinoma: A Review of the Evidence and Treatment Recommendations. Am J Clin Oncol 2011; 34:422-43.

2. Salem R, Thurston KG. Radioembolization with Y90ttrium Microspheres: A State-of-the-Art Brachytherapy Treatment for Primary and Secondary Liver Malignancies. Part 1: Technical and Methodologic Considerations. J Vasc Interv Radiol 2006; 17:1251-1278.

3. Murthy R, Nunez R, Szklaruk J, et al. Yttrium-90 Microsphere Therapy for Hepatic Malignancy: Devices, Indications, Technical Considerations, and Potential Complications. RadioGraphics 2005; 25:S41–S55.

4. Miyayama S, Matsui O, Taki K, et al. Extrahepatic Blood Supply to Hepatocellular Carcinoma: Angiographic demonstration and Transcatheter Arterial Chemoembolization. Cardiovasc Intervent Radiol 2006; 29:39–48.

5. Chung JW, Kim HC, Yoon JH, et al. Transcatheter arterial chemoembolization of hepatocellular carcinoma: prevalence and causative factors of extrahepatic collateral arteries in 479 patients. Korean J Radiol 2006; 7:257–266.

6. Abdelmaksoud MHK, Louie JD, Kothary N, et al. Embolization of Parasitized Extrahepatic Arteries to Reestablish Intrahepatic Arterial Supply to Tumors before Yttrium-90 Radioembolization. J Vasc Interv Radiol 2011; 22:1355-1362.

7. Miyayama S, Yamashiro M, Okuda M, et al. The March of Extrahepatic Collaterals: Analysis of Blood Supply to Hepatocellular Carcinoma Located in the Bare Area of the Liver After Chemoembolization. Cardiovasc Intervent Radiol 2006; 29:39–48.

8. Kim HC, Chung JW, Lee W, Jae HJ, Park JH. Recognizing extrahepatic collateral vessels that supply hepatocellular carcinoma to avoid complications of transcatheter arterial chemoembolization. Radiographics 2005; 25:S25–S39.

9. Riaz A, Lewandowski RJ, Kulik LM, et al. Complications following radioembolization with yttrium-90 microspheres: a comprehensive literature review. J Vasc Interv Radiol 2009; 20:1121–1130.

10. Trotti A, Colevas AD, Setser A, et al. CTCAE v3.0: development of a comprehensive grading system for the adverse effects of cancer treatment. Semin Radiat Oncol 2003; 13:176–181.

11. Gwon DI, Ko GY, Yoon HK, et al. Inferior Phrenic Artery: Anatomy, Variations, Pathologic Conditions, and Interventional Management. Radiographics 2007; 27:687–705.

12. Loukas M, Hullett J, Wagner T. Clinical anatomy of the inferior phrenic artery. Clin Anat 2005; 18 (5):357-365.

13. Webb WR, Jacobs RP. Transpleural abdominal systemic artery-pulmonary artery anastomosis in patients with chronic pulmonary infection. Am J Roentgenol 1977; 129:233-236.

14. Do KH, Goo JM, Im JG, Kim KW, Chung JW, Park JH. Systemic Arterial Supply to the Lungs in Adults: Spiral CT Findings. Radiographics 2001; 21:387–402.

15. Soo CS, Chuang VP, Wallace S, Charnsangavej C, Carrasco H. Treatment of hepatic neoplasm through extrahepatic collaterals. Radiology 1983; 147:45–49.

16. Kim JH, Chung JW, Han JK, Park JH, Choi BI, Han MC. Transcatheter arterial embolization of the internal mammary artery in hepatocellular carcinoma. J Vasc Interv Radiol 1995; 6:71–77.

17. Duprat G, Charnsangavej C, Wallace S, Carrasco CH. Inferior phrenic artery

embolization in the treatment of hepatic neoplasms. Acta Radiol 1988; 29:427–429

18. Kodama Y, Shimizu T, Endo H, et al. Spontaneous rupture of hepatocellular carcinoma supplied by the right renal capsular artery treated by transcatheter arterial embolization. Cardiovasc Intervent Radiol 2002; 25:137–140.

19. Miyayama S, Matsui O, Nishida H, et al. Transcatheter arterial chemoembolization for unresectable hepatocellular carcinoma fed by the cystic artery. J Vasc Interv Radiol 2003; 14:1155–1161.

20. Miyayama S, Matsui O, Taki K, et al. Transcatheter arterial chemoembolization for hepatocellular carcinoma fed by the reconstructed inferior phrenic artery: Anatomical and technical analysis. J Vasc Interv Radiol 2004; 15:815–823.

21. Kim HC, Chung JW, An S, Seong NJ, Son KR, Jae HJ, Park JH. Transarterial chemoembolization of a colic branch of the superior mesenteric artery in patients with unresectable hepatocellular carcinoma. J Vasc Interv Radiol 2011; 22:47-54.

22. Tajima T, Honda H, Kuroiwa T, et al. Pulmonary complications after hepatic artery chemoembolization or infusion via the inferior phrenic artery for primary liver cancer. J Vasc Interv Radiol 2002; 13:893–900.

23. Kao YH, Tan EH, Burgmans MC et al. Image-guided personalized predictive dosimetry by artery-specific SPECT/CT partition modeling for safe and effective Y90 radioembolization. J Nucl Med. 2012; 53:1-10.

Chapter 7

Computed tomography hepatic arteriography has a hepatic falciform artery detection rate that is much higher than that of digital subtraction angiography and 99mTc-MAA SPECT/CT: implications for planning Y90 radioembolization
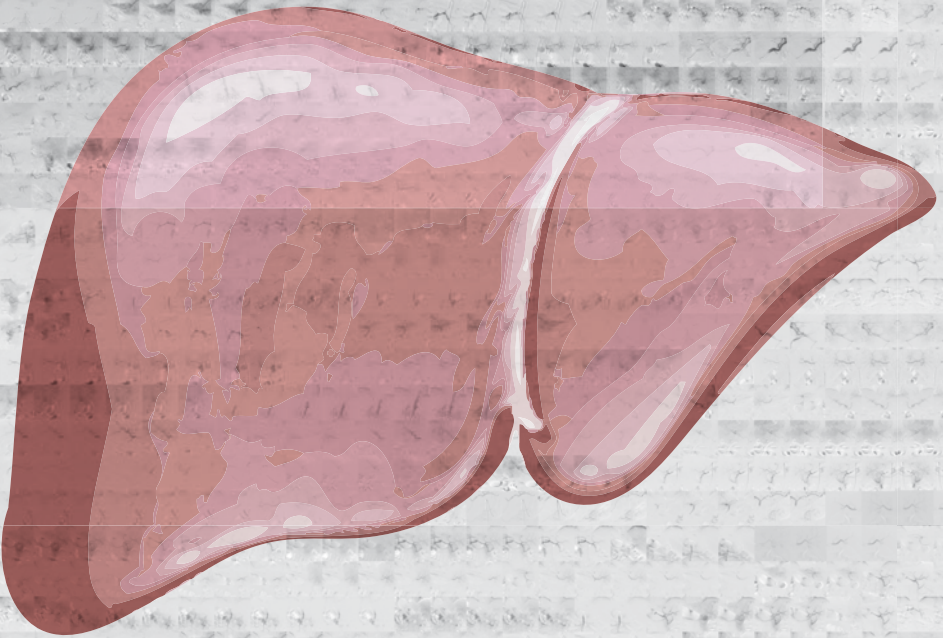
Burgmans MC, Too CW, Kao YH, Goh ASW, Chow PKH, Tan BS, Tay KH, Lo RHG.

ABSTRACT

Purpose

To compare the hepatic falciform artery (HFA) detection rates of digital subtraction angiography (DSA), computed tomography hepatic arteriography (CTHA) and 99mTc-macroaggregated albumin (99mTc-MAA) single photon emission computed tomography with integrated CT (SPECT/CT) and to correlate HFA patency with complication rates of yttrium-90 (Y90) radioembolization.

Methods

From August 2008 to November 2010, 79 patients (range 23-83 years, mean 62.3 years; 67 male) underwent pre-treatment DSA, CTHA and 99mTc-MAA scintigraphy (planar, SPECT/CT) to assess suitability for radioembolization with Y90 resin microspheres. Thirty-seven patients were excluded from the study, because CTHA was performed with a catheter position that did not result in opacification of the liver parenchyma adjacent to the falciform ligament. DSA, CTHA and 99mTc-MAA SPECT/CT images and medical records were retrospectively reviewed.

Results

A patent HFA was detected in 22 of 42 patients (52.3%). The HFA detection rates of DSA, CTHA and 99mTc-MAA SPECT/CT were 11.9%, 52.3% and 13.3% respectively (p<0.0001). An origin from the segment 4 artery was seen in 51.7% of HFAs. Prophylactic HFA coil-embolization prior to Y90 microspheres infusion was performed in 2 patients. Of the patients who underwent radioembolization with a patent HFA, none developed supra-umbilical radiation dermatitis. One patient experienced epigastric pain attributed to post-embolization syndrome and was managed conservatively.

Conclusions

The HFA detection rate of CTHA is superior to that of DSA and 99mTc-MAA SPECT/CT. Complications related to non-target radiation of the HFA vascular territory rarely occur, even in patients undergoing radioembolization with a patent HFA.

INTRODUCTION

Radioembolization with yttrium-90 (Y90) microspheres is an effective locoregional treatment for patients with unresectable primary or secondary liver malignancies (1). The microspheres are delivered by selective trans-arterial catheter-directed infusion. The microspheres lodge permanently within the vascular bed of the tumor and deliver high-energy ß-radiation over a limited range (mean tissue penetration 2.5mm; maximum 11mm). Non-target radiation to the lungs or gastro-intestinal tract may result in severe complications (2-4). To minimize the risk of such complications, all patients will undergo pre-treatment hepatic angiography with a test injection of 99mTc-macroaggregated albumin (99mTc-MAA) prior to the actual treatment. During the angiography, the vascular liver anatomy is meticulously skeletonized to identify hepatico-enteric anastomoses. If present, coil embolization of such anastomoses is performed in order to prevent inadvertent flow of microspheres to the gastro-intestinal tract. A test injection of 99mTc-MAA and subsequent planar scintigraphy and/or single photon emission computed tomography with integrated low-dose computed tomography (SPECT/CT) of the abdomen and lungs are then used to estimate the lung shunt fraction as a result of tumor-related pathological arteriovenous shunting. 99mTc-MAA SPECT/CT of the abdomen can also accurately detect inadvertent extrahepatic deposition of 99mTc-MAA, prompting additional coil embolization during the radioembolization session (2-4).

An uncommon form of non-target radiation injury can result from the flow of Y90 microspheres into the hepatic falciform artery (HFA) (5). Through the HFA, the microspheres may deposit along the anterior abdominal wall, causing supra-umbilical skin rash, epigastric pain and skin necrosis. Although this complication is rare, prophylactic coiling of the HFA generally is recommended if the HFA is identified at angiography or if deposition of 99mTc-MAA in the HFA trajectory is detected on SPECT/CT (2-4,6).

However, the reported prevalence of the HFA is much lower in most angiographic and 99mTc-MAA studies compared to anatomical studies (7-11). This suggests that the HFA may remain undetected by digital subtraction angiography (DSA) and 99mTc-MAA scintigraphy in a large number of patients. These patients would potentially be at risk of non-target radiation injury to the vascular territory of the HFA.

Cone-beam computed tomography (CBCT) and computed tomography hepatic arteriography (CTHA) are increasingly used in addition to DSA to perform transarterial liver therapies. In both imaging modalities, cross-sectional images are obtained during catheter-injection of a contrast medium into the hepatic arteries. Both CBCT and CTHA

allow detection of extra-hepatic perfusion with high sensitivity and specificity, but CTHA is the modality with higher resolution and less artefacts (12,13).

The aim of our study was to compare the HFA detection rate of CTHA with that of DSA and 99mTc-MAA SPECT/CT of the abdomen, and to correlate the detection rates with clinical outcomes.

METHODS

Approval by the Institutional Review Board (IRB) of our institution was obtained for this retrospective study.

Patients

From August 2008 to November 2010, 79 patients were referred to the Interventional Radiology department of our institution for a pre-treatment angiogram and 99mTc-MAA simulation to evaluate suitability for radioembolization. Patient age ranged from 23 to 83 years (mean, 62.3 +/- 11.7 years) and 67 patients were male. In 78 patients (98.7%), the indication for referral was hepatocellular carcinoma (HCC). One patient (1.3%) was referred for metastasis from colorectal carcinoma. Thirty-seven patients were excluded from the study, because CTHA was performed with a catheter position that did not result in opacification of the liver parenchyma bordering the falciform ligament.

Pre-treatment angiography, CTHA and Tc99m-MAA test injection

The angiographic protocol included selective DSA with pump injection of a contrast agent (Omnipaque 300; GE Healthcare, Shanghai, China or Visipaque 270; GE Healthcare, Shanghai, China) from the superior mesenteric artery (SMA), the celiac axis (CA), proper hepatic artery (PHA), left hepatic artery (LHA), right hepatic artery (RHA) and, if present, middle hepatic artery (MHA). Angiographic images were obtained with breath-hold, 3 frames/sec and 50mAs/120kV for antero-posterior projections. Using a Mark V ProVis injector (MEDRAD INC, Warrendale, PA, USA), contrast medium was injected at 6ml/sec for 25ml for the SMA and CA, 5ml/sec for 15ml for the PHA and 3ml/sec for 12ml for lobar injections.

Patients underwent CTHA using a hybrid 16-slice Aquilion CT/ Infinix VC-1 angiography system (Toshiba, Tokyo, Japan) and pump injections with a Stellant CT injector system (MEDRAD INC, Warrendale, PA, USA). Dependent on the treatment plan, CTHA was performed either with super-selective lobar or segmental contrast injections using a 2.2F or 2.7F Progreat catheter (Terumo, Tokyo, Japan) or from the PHA using a 5F C2 catheter

(Terumo, Tokyo, Japan). CTHA with super-selective lobar or segmental contrast injection was performed with an injection rate of 1-3 ml/sec. CTHA from the PHA was performed with an injection rate of 3-5 ml/sec. The injected contrast volume for CTHA was calculated using the equation "volume = (scan delay + scan time) x flow rate" with the scan delay being the time between the start of injection and enhancement of the region of interest at angiography. CTHA images were acquired using the following parameters: collimation 16x1.0, pitch factor 15, helical pitch 0.938, 120kV and 160 effective mAs. In all patients included in the study, CTHA showed opacification of the liver segments bordering the falciform ligament.

All patient would undergo standard coil embolization of hepaticoenteric anastomoses if deemed necessary to avoid non-target embolization, either on the day of the pre-treatment angiography or on the day of radioembolization. Coil embolization was performed using pushable coils (Boston Scientific, Natick, MA, USA) or an Amplatzer 4 vascular plug (AGA Medical, Golden Valley, MN, USA) for the gastroduodenal artery.

At the end of the procedure, the microcatheter was placed in a position corresponding to the intended location of future Y90 microsphere infusion. A total of 5mCi (185MBq) in 3ml 99mTc-MAA was then injected into the LHA, MHA and/or RHA, or alternatively into the PHA. All patients underwent 99mTc-MAA scintigraphy within 1 hour of 99mTc-MAA injection. Prior to September 2009, patients underwent only planar scintigraphy. After this date, 99mTc-MAA SPECT/CT of the abdomen was also performed, using a hybrid SPECT/CT scanner with a dual-head gamma camera integrated with a 16-slice multi-detector CT (Philips Precedence; Philips, Amsterdam, Netherlands). The lung shunt fraction was calculated by planar scintigraphy, whereas SPECT/CT of the abdomen was used for tumor-to-normal liver ratio (T/N ratio) calculation and to exclude any non-target extra-hepatic shunting of 99mTc-MAA. Predictive radiation dosimetry was performed by Medical Internal Radiation Dose (MIRD) macrodosimetry (i.e. 'partition model'). Patient suitability for radioembolization was decided in a multi-disciplinary manner, taking into account the potential risk-benefit based on patient-specific clinical, angiographic, CTHA and dosimetric factors.

Radioemboliation

Prior to radioembolization, hepatic angiography and CTHA were repeated. If repeated DSA or CTHA showed extrahepatic enhancement or if extrahepatic 99mTc-MAA activity was detected, additional coil-embolization was performed to prevent non-target radioembolization. If the 99mTc-MAA scan showed marked 99mTc-MAA activity in the trajectory of the HFA, identification and subsequent embolization was attempted prior to radioembolization. The infusion of Y90 microspheres was performed with the catheter

placed in an identical position as was used to infuse 99mTc-MAA. Minor changes of catheter position would be made if this would reduce the risk of non-target embolization based on DSA, CTHA and/or SPECT/CT findings. All radioembolization procedures were performed using SIR-Spheres® (Sirtex Medical Limited; New South Wales, Australia).

Bremsstrahlung scan

All patients underwent Y90 bremsstrahlung scintigraphy one day after radioembolization to assess the intrahepatic microsphere biodistribution and to exclude inadvertent extrahepatic shunting of microspheres. Planar liver-to-lung bremsstrahlung scintigraphy was performed in all patients for qualitative assessment of pulmonary Y90 activity. After September 2009, additional Y90 bremsstrahlung SPECT/CT of the abdomen was also performed.

Image interpretation

DSA and CTHA images were independently reviewed for the presence of a HFA by two interventional radiologists (MCB and RHGL), with respectively 4 and 17 years of experience with transarterial hepatic therapies. The reviewers were blinded for patient details and DSA and CTHA images were reviewed separately without cross-reference. DSA images were reviewed using an Amalga Picture Archive and Communication System (Microsoft, Redmont, WA, USA). CTHA images were reviewed using imaging software Vitrea 2 version 4.1.2.0 (Vital Images Inc, Minnetonka, MN, USA), allowing multi-planar reconstruction (MPR) and maximal intensity projection (MIP). The number of HFAs per patient and origin of the HFA was recorded for both DSA and CTHA images. Discrepancies between the two reviewers were resolved by consensus reading.

The 99mTc-MAA and Y90 bremsstrahlung scintigraphy (planar, SPECT/CT) were reviewed by a nuclear medicine physician with three years of experience in radioembolization.

Clinical correlation

Clinical follow-up including physical examination and laboratory testing was performed in all patients on days 2 and prior to discharge. Patients were routinely scheduled for clinical review at approximately 2, 6 and 12 weeks and, depending on survival, every 3 months thereafter. Contrast-enhanced 4-phase CT or MRI for patients with primary liver carcinoma and contrast-enhanced CT and/or F-18 fluorodeoxyglucose PET/CT for patients with secondary liver tumors were routinely planned at 3 months intervals.

The medical records of all patients were retrospectively reviewed for any signs of epigastric pain or discomfort, anterior abdominal wall skin rash or any other signs that could indicate non-target radiation as a result of microsphere infusion into the HFA.

Statistical analysis

The statistical significance of the HFA detection rate between DSA and CTHA and between CTHA and 99mTc-MAA was evaluated using McNemar's test. Results were considered significant when a p-value of less than 0.05 was obtained. Data analysis was performed using SPSS software version 17.

RESULTS

A patent HFA was identified in 22 (52.3%) of the 42 patients included in the study across all modalities: DSA, CTHA or 99mTc-MAA SPECT/CT. The demographics of these 22 patients are listed in Table 1.

A patent HFA was detected in 5 (11.9%) of the 42 patients with DSA (Figure 1). CTHA was positive for the presence of a patent HFA in all 5 patients in whom a HFA was detected on DSA, and further detected a patent HFA in 17 additional patients. The HFA detection rate with CTHA (52.3%) was significantly better than the detection rate with DSA (11.9%) (p<0.0001).

Table 1. Demographics of patients with a patent hepatic falciform artery

Characteristic		Value	
Age		mean 63.2 yrs (range 45-80 yrs)	
Sex		n (total = 22)	%
	Male	19	86.4
	Female	3	13.6
Tumor type			
	HCC	22	100
Tumor distribution			
	Bilobar	11	50
	Unilobar	11	50
Child-Pugh score		n	%
	A	13	59.1
	B	9	40.9
Vascular invasion/ EHD			
	Vascular invasion	7	31.9
	Lymph node metastasis	2	9.1
	Distant metastasis	1	4.5
BCLC stage			
	A	1	4.5
	B	13	59.1
	C	8	36.4

BCLC stage = Barcelona Clinic Liver Cancer staging system; EHD = extra-hepatic disease
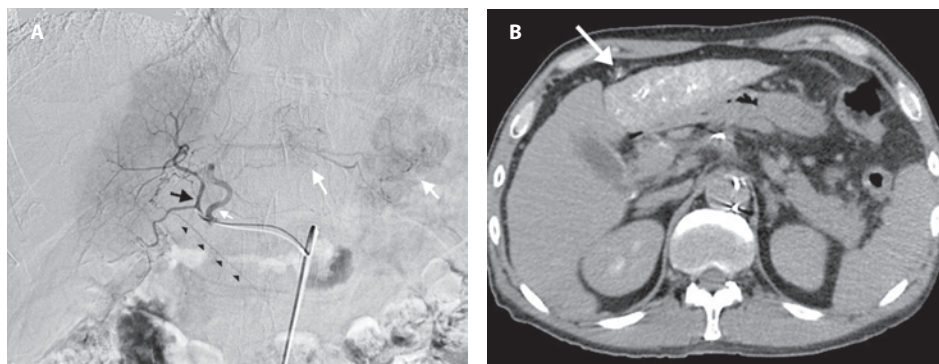
Figure 1. Patency of the hepatic falciform artery (HFA) in a 67-year old male with multifocal bilobar hepatocellular carcinoma (HCC) demonstrated on both digital subtraction angiography (DSA) and computed tomography hepatic arteriography (CTHA). a) Selective DSA from the middle hepatic artery (MHA). The MHA (black arrow) gives rise to the HFA (arrowheads). Reflux is seen into the left hepatic artery (small white arrow) with early tumor enhancement of tumors in segments 2 and 3 (large white arrows). b) CTHA also shows the HFA (arrow) to be patent. The patient was not considered to be at risk of non-target radiation to the HFA vascular territory as Y90 microspheres were infused super-selectively into the left and right hepatic artery and not the MHA.

In none of the patients, coil embolization of the HFA was performed at the time of 99mTc-MAA injection. In 6 of the 42 patients, 99mTc-MAA was injected only into the right hepatic artery and accumulation into the HFA trajectory would therefore be highly unlikely. In 6 (16.6%) of the remaining 36 patients, only 99mTc-MAA planar scintigraphy was performed. Thirty patients (83.3%) underwent both 99mTc-MAA planar scintigraphy and SPECT/CT. No HFA was detected by planar scintigraphy. With SPECT/CT, 99mTc-MAA accumulation in the trajectory of the HFA was detected in 4 (13.3%) of the 30 patients. In all 4 patients, a HFA was also detected on CTHA. In 2 of the 4 patients, DSA also detected the patent HFA. CTHA had a higher HFA detection rate than 99mTc-MAA SPECT/CT (p<0.0001). There was no statistically significant difference between the HFA detection rates of DSA versus 99mTc-MAA SPECT/CT.

A total of 29 HFAs were detected across 22 patients: 2 HFAs in 3 patients (13.6%); 3 HFAs in 2 patients (9.1%). In all patients, the HFAs originated from either the LHA or MHA. An origin from the segment 4 artery was seen in 15 (51.7%) of the 29 HFAs (Figure 2).

Of the 22 patients with a patent HFA, 3 patients (13.6%) did not proceed with radioembolization for the following reasons: high lung shunt fraction (n=1), unfavorable T/N ratio (n=1) and a combination of high lung shunt fraction and arterioportovenous shunting with unfavorable T/N ratio (n=1). The mean activity of Y90 infused in the remaining 19 patients was 2.1 ± 0.8 GBq (range 0.9 - 4.0 GBq). In the 2 patients where a patent HFA was detected on all modalities (DSA, CTHA, 99mTc-MAA SPECT/CT), coil-embolization of the
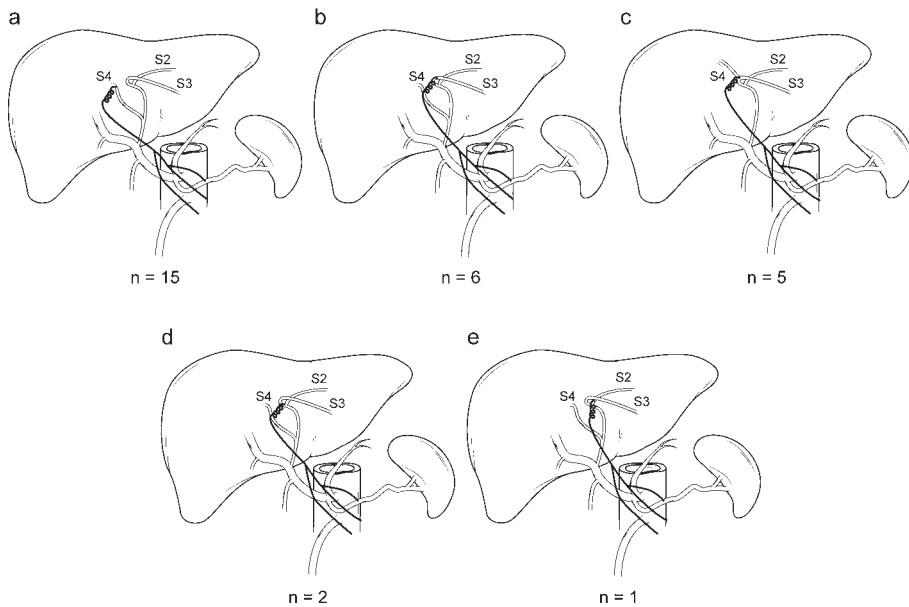
Figure 2. Schematic drawings of the origin of the 29 HFAs detected in 22 patients: a) origin from the segment 4 artery (S4) or MHA; b) origin from the segment 3 artery (S3); c) origin from a S3/S4 artery bifurcation; d) origin from the bifurcation of the segment 2 artery (S2) and S3 near the umbilical point; e) origin from S2.

HFA was performed using 2x5 mm Figure-8 micro-coils (Boston Scientific, Natick, MA, USA) just prior to selective bilobar Y90 microspheres infusion (Figure 3). Three patients had infusion of Y90 into the RHA only and were therefore not considered to be at risk of non-target irradiation of the HFA vascular territory. Therefore, 14 patients underwent radioembolization where Y90 microspheres were released proximal to a patent HFA.

Of these 14 patients, 4 patients underwent planar Y90 bremsstralung scintigraphy and the other 10 patients had additional Y90 bremsstrahlung SPECT/CT of the abdomen. None of the 14 patients had detectable non-target Y90 bremsstrahlung activity or developed anterior abdominal wall radiation dermatitis. One patient experienced epigastric pain, nausea and sub-febrile temperature following Y90 microspheres infusion. This patient was treated with bilobar infusion of spheres with a total activity of 2.5GBq for extensive bilobar HCC. The symptoms were thought to be due to post-embolization syndrome, not HFA vascular territory irradiation. The symptoms were managed conservatively and subsided after 24 hours.
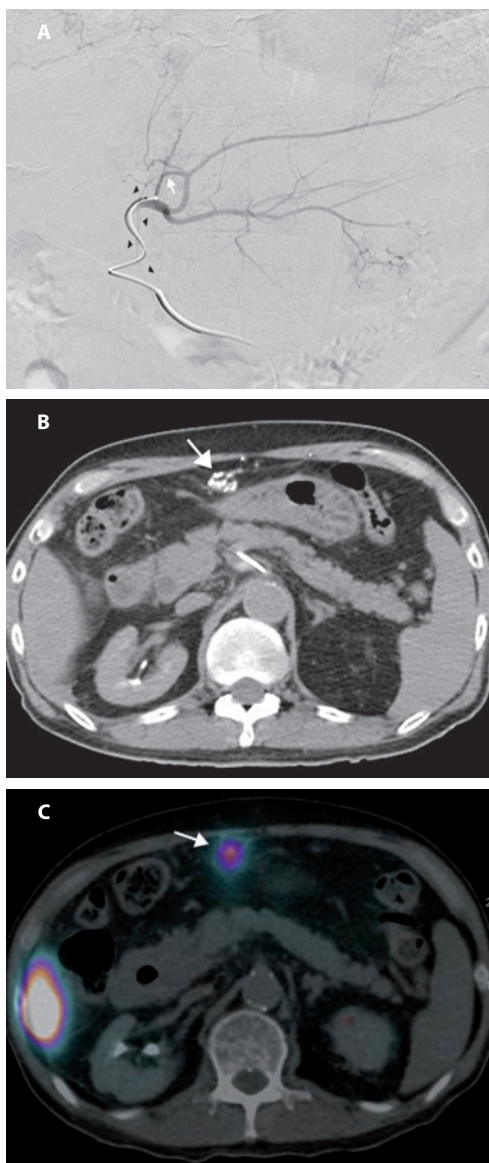
Figure 3. Patency and coil embolization of the HFA in a 74-year old male with multifocal bilobar HCC. a) Selective DSA from the left hepatic artery shows a small HFA (arrowheads) originating from a segment 4 artery (white arrow); b) CTHA performed with the same catheter position shows opacification of an anastomotic network of arteries (arrow) via the HFA. Branches of this network lead to the anterior abdominal wall (not shown); c) After injection of 99mTc-MAA into the left and right hepatic artery, SPECT/CT detected 99mTc-MAA activity in the trajectory of the HFA and the anastomotic network (arrow). At the time of actual treatment, the HFA was selectively catheterized and embolized with micro-coils prior to infusion of Y90 microspheres into the left and right hepatic artery.

DISCUSSION

There is a discrepancy in the reported prevalence of the HFA between anatomical studies and most angiographic studies. In an anatomic study by Michels, the HFA was found to be present in nearly 70% of cadaveric dissections (7). In a single study, Song et al. reported presence of the HFA on angiography in 51.6% of 250 patients (14). Yet, most

angiographic studies have reported a prevalence ranging from only 2 to 7.6% (8-11). This suggests that a prevalent HFA often remains undetected using DSA. Similarly, the reported prevalence of the HFA is low in 99mTc-MAA SPECT/CT studies compared to the study by Michels. In a study by Ahmadzadehfar et al., tracer accumulation in the anterior abdominal wall, indicating a patent HFA, was present in pre-radioembolization 99mTc-MAA SPECT/CT images in 9.3% of patients (11). In our study, the HFA detection rate of DSA and 99mTc-MAA SPECT/CT was 11.9% and 13.3%, respectively. Yet, we were able to demonstrate a patent HFA on CTHA in 52.3% of patients. Our findings are consistent with a study by Tajima et al., who found an evidently superior HFA detection rate for CTHA compared to DSA in patients undergoing transarterial chemoembolization (15). This could imply that patients undergoing radioembolization may be at risk of HFA nontarget irradiation, as DSA and 99mTc-MAA are the standard imaging modalities used for pre-treatment planning. However, complications as a result of inadvertent infusion of Y90 microspheres into the HFA appear to be uncommon with only a few reported cases in the literature (5,6,11). In our study, Y90 microspheres where released proximal to a patent HFA in 14 patients. In none of these 14 patients did the Y90 bremsstrahlung scintigraphy show suspicious activity along the anterior abdominal wall, or any symptoms that were thought to be due to non-target irradiation of the HFA vascular territory.

There could be several reasons why the majority of patients with a patent HFA did not develop symptoms of HFA non-target irradiation. All patients with a patent HFA in our study had HCC. HCCs generally are highly vascular and the preferential flow of Y90 microspheres will have been towards the liver tumors. As the HFA is a small branch, the number of microspheres (and hence the Y90 activity) actually implanted along the HFA vascular territory may have been too small to deliver a clinically significant radiation absorbed dose. Second, contrast (i.e. soluble molecules) enhancement of the HFA on CTHA may not accurately predict the flow of Y90 microspheres, which are subject to many biophysical factors such as particulate mass and momentum (16). The terminal branches of the MHA and/or LHA may have a direct pathway to the HFA or create an anastomotic network with the internal thoracic or superior epigastric arteries through the ensiform artery (10). In patients with the latter variant, predominant blood flow to the anterior abdominal wall may be through the internal thoracic or superior epigastric arteries. In patients with HCC, the direction of flow through the ensiform artery may even be hepatopedal as a result of the recruitment of blood from extrahepatic arteries by the liver tumors (10). CTHA is performed with pump-injection of a relatively high volume of a contrast medium and as a result the competing flow from the internal thoracic or superior epigastric arteries may be cancelled out. Yet, the Y90 microspheres are released by means of slow infusion. Hence, during transarterial infusion of the spheres,

the anterior abdominal wall may receive blood mainly or entirely through the internal thoracic or superior epigastric arteries in patients with a patent ensiform artery.

In two patients, the HFA was prophylactically coiled prior to radioembolization. In both cases, a patent HFA was demonstrated on DSA, CTHA and 99mTc-MAA SPECT/CT. Our study shows that the risk of complications is low if Y90 microspheres are infused proximal to a patent HFA, but we feel coil embolization of a patent HFA should nevertheless be attempted prior to radioembolization, if considered technically feasible. However, based on our study findings, we do not recommend treatment cancellation in patients with an angiographically occult HFA or in cases of failed HFA coil embolization.

A limitation of our study is its retrospective nature. Further limitation of the study involves the lack of a validated gold standard for HFA patency. The imaging findings were not correlated with anatomical dissections. Despite this, we interpreted contrast-enhancement of the HFA on CTHA as patency of the HFA. In individual patients with a patent anastomosis between the HFA and the internal thoracic or superior epigastric arteries, this may have led to what could be considered as false positives. Contrast may have been pushed into the HFA and anastomotic network by using pump-injections, whereas flow to the anterior abdominal wall would only have been through the internal thoracic or superior epigastric arteries under normal circumstances.

In conclusion, we found a significantly higher detection rate for the HFA with CTHA as compared to DSA and 99mTc-MAA SPECT/CT. However, even in patients with a patent HFA no symptoms occurred that could indicate radiation injury to the HFA vascular territory. We recommend prophylactic coil embolization of a patent HFA prior to radioembolization if technically feasible, but do not recommend cancellation of radioembolization in patients with an angiographically occult HFA or in cases of failed HFA prophylactic coil-embolization.

REFERENCES

1. Sangro B, Salem R, Kennedy A, Coldwell D, Wasan H. Radioembolization for Hepatocellular Carcinoma: A Review of the Evidence and Treatment Recommendations. Am J Clin Oncol 2011 Aug; 34(4): 422-43.

2. Salem R, Thurston KG. Radioembolization with 90-Yttrium microspheres: a state-of-the-art brachytherapy treatment for primary and secondary liver malignancies. Part 1: Technical and methodologic considerations. J Vasc Interv Radiol 2006 Aug; 17(8):1251-78.

3. Salem R, Thurston KG. Radioembolization with yttrium 90 microspheres: a state-of-the-art brachytherapy treatment for primary and secondary liver malignancies. Part 2: special topics. J Vasc Interv Radiol 2006 Sep;17(9):1425-39.

4. Lewandowski RJ, Sato KT, Atassi B, et al. Radioembolization with Y90 microspheres: angiographic and technical considerations. Cardiovasc Intervent Radiol 2007 Jul-Aug; 30(4):571-92.

5. Leong QM, Lai HK, Lo RG, Teo TK, Goh A, Chow PK. Radiation dermatitis following radioembolization for hepatocellular carcinoma: a case for prophylactic embolization of a patent falciform artery. J Vasc Interv Radiol 2009 Jun; 20(6):833-6.

6. Liu DM, Salem R, Bui JT, et al. Angiographic considerations in patients undergoing liver-directed therapy. J Vasc Interv Radiol 2005 Jul;16(7): 911-35.

7. Michels NA. Collateral arterial pathways to the liver after ligation of the hepatic artery and removal of the celiac axis. In: Michels NA, editor. Blood supply and anatomy of the upper abdominal organs. Philadelphia, PA: JB Lippincott, 1955: 317-8.

8. Baba Y, Miyazono N, Ueno K, et al. Hepatic falciform artery. Angiographic findings in 25 patients. Acta Radiol 2000 Jul;41(4): 329-33.

9. Williams DM, Cho KJ, Ensminger WD, Zeissman HA, Gyves JW. Hepatic falciform artery: anatomy, angiographic appearance, and clinical significance. Radiology 1985 Aug;156(2): 339-40.

10. Ibukuro K, Tsukiyama T, Mori K, Inoue Y. Hepatic falciform ligament artery: angiographic anatomy and clinical importance. Surg Radiol Anat 1998;20(5): 367-71.

11. Ahmadzadehfar H, Möhlenbruch M, Sabet A, et al. Is prophylactic embolization of the hepatic falciform artery needed before radioembolization in patients with 99mTc-MAA accumulation in the anterior abdominal wall? Eur J Nucl Med Mol Imaging 2011 Aug;38(8): 1477-84.

12. Louie JD, Kothary N, Kuo WT, et al. Incorporating Cone-beam CT into the Treatment Planning for Yttrium-90 Radioembolization. J Vasc Interv Radiol. 2009 May;20(5):606-13.

13. Ishigami K, Yoshimitsu K, Irie H, et al. Accessory Left Gastric Artery from Left Hepatic Artery Shown on MDCT and Conventional Angiography: Correlation with CT Hepatic Arteriography. AJR Am J Roentgenol 2006 Oct;187(4): 1002-9.

14. Song SY, Chung JW, Lim HG, Park JH. Nonhepatic arteries originating from the hepatic arteries: angiographic analysis in 250 patients. J Vasc Interv Radiol 2006 Mar;17(3): 461-9.

15. Tajima T, Yoshimitsu K, Irie H, et al. Hepatic Falciform Ligament Artery in Patients with Chronic Liver Diseases: Detection on Computed Tomography Hepatic Arteriography. Acta Radiologica 2009 Sept;50(7): 743-51.

16. Kao YH, Tan EH, Teo TKB, Ng CE, Goh SW. Imaging discordance between hepatic angiography versus Tc-99m-MAA SPECT/CT: a case series, technical discussion and clinical implications. Ann Nucl Med 2011; 25:669–76.

Chapter 8

Image-guided personalized predictive dosimetry by artery-specific SPECT/CT partition modeling for safe and effective Y90 radioembolization
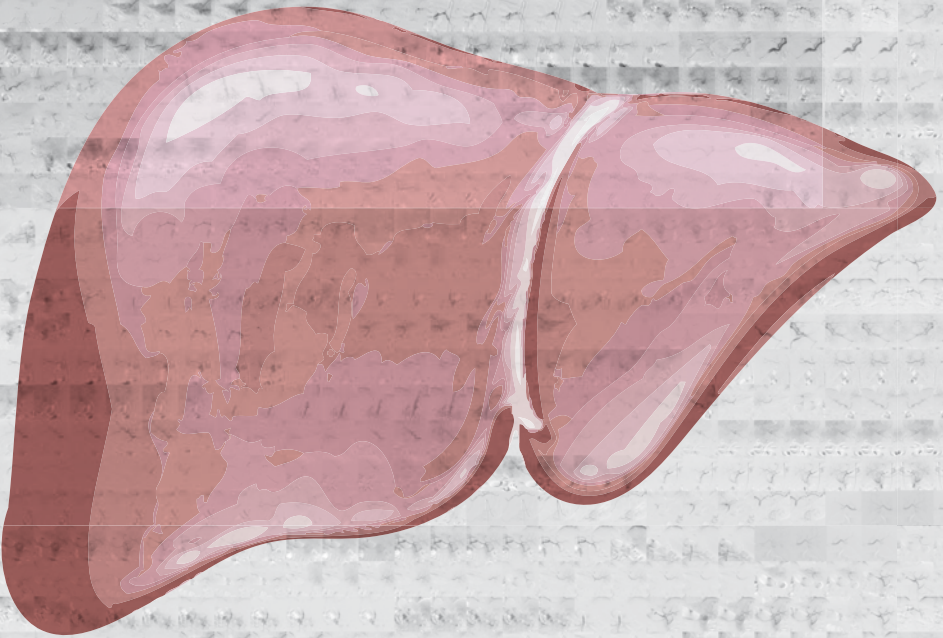
Kao YH, Tan AEH, Burgmans MC, Irani FG, Khoo LS, Lo RHG, Tay KH, Tan BS, Chow PKH, Ng DCE, Goh ASW.

ABSTRACT

Purpose

Compliance to radiobiological principles of radionuclide internal dosimetry is fundamental to the success of yttrium-90 (Y90) radioembolization. The artery-specific SPECT/CT partition model is an image-guided personalized predictive dosimetric technique developed by our institution, integrating catheter-directed computed tomography hepatic angiography (CTHA), technetium-99m-macroaggregated albumin (99mTc-MAA) SPECT/CT and partition modeling for unified dosimetry. Catheter-directed CTHA accurately delineates planning target volumes. SPECT/CT tomographically evaluates 99mTc-macroaggregted albumin (99mTc-MAA) hepatic biodistribution. The partition model is validated for Y90 resin microspheres based on Medical Internal Radiation Dosimetry (MIRD) macrodosimetry.

Methods

This was a retrospective analysis of our early clinical outcomes for inoperable hepatocellular carcinoma (HCC). Mapping hepatic angiography was performed according to standard technique with addition of catheter-directed CTHA. 99mTc-MAA planar scintigraphy was used for liver-to-lung shunt estimation, and SPECT/CT for liver dosimetry. Artery-specific SPECT/CT partition modeling was planned by experienced nuclear medicine physicians.

Results

From January to May 2011, 20 arterial territories were treated in 10 HCC patients. Median follow-up was 21 weeks (95% confidence interval (CI), 12-50). When analyzed strictly as brachytherapy, Y90 radioembolization planned by predictive dosimetry achieved index tumor regression in 8 of 8 patients, with median size decrease of 58% (95% CI, 40%-72%). Tumor thrombosis regressed or remained stable in 3 of 4 patients with baseline involvement. Best alphafetoprotein reduction ranged from 32 to 95%. Clinical success was achieved in 7 of 8 patients, including 2 by sub-lesional dosimetry, one of which had radioembolization lobectomy intent. Median predicted mean radiation absorbed doses were 106 Gy (95% CI, 105-146 Gy) to tumor, 27 Gy (95% CI, 22-33 Gy) to non-tumorous liver and 2 Gy (95% CI, 1.3-7.3 Gy) to lungs. Across all patients, tumor, non-tumorous liver and lungs received predicted ≥91 Gy, ≤51 Gy and ≤16 Gy respectively via at least one target arterial territory. No patients developed significant toxicities within 3 months post-radioembolization. The median time to best imaging response was 76 days (95% CI, 55-114 days). Median time to progression and overall survival were not reached. SPECT/CT-derived mean tumor-to-normal liver (T/N) ratios varied widely across all planning target volumes (median 5.4; 95% CI, 4.1-6.7), even within the same patient.

Conclusions

Image-guided personalized predictive dosimetry by artery-specific SPECT/CT partition modeling achieves high clinical success rates for safe and effective Y90 radioembolization.

INTRODUCTION

As a form of arterial territory-specific point-source brachytherapy, yttrium-90 (Y90) radioembolization is always effective when delivered at the right location, in the right dose, and with the right intent. Y90 radioembolization failure is invariably due to one or a combination of these three factors being incorrectly addressed. Responsibility for this triad is shared among the interventional radiologist, the nuclear medicine physician, and the referring clinician. Y90 radioembolization is complex, and a lack of coordinated care risks sub-optimum outcomes.

Contemporary techniques, outcomes, and safety data of Y90 radioembolization are well-described in recent literature (1-8). Disregard for radiobiological principles of arterial territory-specific Y90 radionuclide internal dosimetry risks toxicity and fatality (9-10). Since the 1980s, sectional imaging (e.g. computed tomography) has revolutionized the planning and delivery of external beam radiation therapy (EBRT). However to date, radiation planning for Y90 radioembolization has yet to embrace modern imaging modalities such as catheter-directed CT hepatic arteriography (CTHA) and single photon emission computed tomography with integrated low-dose CT (SPECT/CT).

Catheter-directed CTHA delineates hepatic arterial territorial margins more accurately than digital subtraction angiography (1,11). SPECT/CT is superior to both planar scintigraphy and SPECT for assessing intra-hepatic biodistribution of technetium-99m-macroaggregated albumin (99mTc-MAA), and for estimating the tumor-to-normal liver (T/N) ratio (12-14). The partition model is a validated dosimetric method for Y90 resin microspheres, scientifically superior to the 'body surface area (BSA)' method (5,10).

Accurate assessment of target liver volumes is critical because it directly affects radiation absorbed dose estimates. This is especially important when planning for selective (lobar) or super-selective (segmental or sub-segmental) Y90 radioembolization. Catheter-directed CTHA refers to the acquisition of CT with direct intraarterial injection of dilute contrast media through an angiographic catheter or microcatheter introduced into a hepatic lobar, segmental or sub-segmental artery via a percutaneous transfemoral arterial puncture (1,11). This provides superior delineation of arterial territories compared to digital subtraction angiography, enabling accurate estimation of artery-specific perfused liver volumes (1,11). Conventional Y90 radioembolization is planned on the interventional radiologists' assessment of each patient's vascular anatomy (15). However, estimation of the perfused liver volume can be challenging. Hepatic vascular anatomy has many variations (13,15-16). A main hepatic artery may supply several liver segments via its branches; conversely a single segment may be supplied by more than one arterial

branch. Couinaud segments may be distorted by large tumors, previous liver surgery or locoregional therapy – for example, ablation cavities. Aberrant arteries due to neoplastic recruitment from extrahepatic sources further complicate hepatic vascular anatomy. These factors make it difficult to reliably estimate the target volume of a diseased liver based on digital subtraction angiography alone.

This problem may be overcome by catheter-directed CTHA. With the catheter tip placed in the target artery, CT performed at the time of intra-arterial contrast injection provides superior delineation of the perfused liver volume, as compared to that shown under digital subtraction angiography. Each 'run' of catheter-directed CTHA is specific for its catheter tip position. The use of catheter-directed CTHA shifts the planning emphasis away from a conventional lobe or segment-based approach to a more patient-specific arterial territory-based approach. Catheter-directed CTHA accurately delineates each target arterial territory regardless of arterial anatomy, variant vasculature, or tissue distortion by tumor, surgery, or locally ablative treatments.

The role of SPECT/CT in diagnostic imaging and internal dosimetry is well established in nuclear medicine (17-18). In the context of Y90 radioembolization, 99mTc-MAA SPECT/CT for preradioembolization assessment has a higher detection rate for extrahepatic radiotracer activity and has greater impact on therapy planning compared to that under planar scintigraphy (14,19-20). Hepatic intraarterial 99mTc-MAA scintigraphy is a validated means of simulating the Y90 radioembolization therapy field (13-14). SPECT/CT-based dosimetry is superior to planar scintigraphy by tomographically resolving overlapping radiotracer activity, evaluating heterogeneous radiotracer uptake and detecting activity in small lesions (12,14,17). Phantom studies have shown that 99mTc-MAA SPECT/CT volume measurements are accurate and reproducible (13). To date, no standardized technique exists for the calculation of SPECT/CT-based T/N ratios, although several methods have been described (21-23).

The partition model was developed and validated for Y90 resin microspheres by Ho et al. in the 1990s (24-25). It is one of several methods recommended by the manufacturer of Y90 resin microspheres to calculate the desired Y90 activity (26). Based on Medical Internal Radiation Dosimetry (MIRD) macrodosimetry, it partitions the lungs, tumor, and non-tumorous liver into separate compartments for radiation dose modeling (24,26). This model surpasses the commonly used BSA method by incorporating absolute tissue masses and patient-specific mean T/N ratios for personalized and scientifically sound estimates of mean radiation absorbed doses to each tissue compartment (5,10,27). Technical differences between BSA methodology and partition modeling discussed elsewhere, along with limitations and clinical implications (10).

The artery-specific SPECT/CT partition model is a unified technique of personalized predictive dosimetry developed by our institution for Y90 radioembolization using resin microspheres. It integrates catheter-directed CTHA, 99mTc-MAA SPECT/CT and partition modeling for improved predictive radionuclide dosimetry. Its fundamental premise is to derive more accurate estimates of tissue masses and mean T/N ratios to optimize partition modeling. The underlying principles and limitations of MIRD macrodosimetry remain unchanged. Through the use of artery-specific SPECT/CT partition modeling, predicted mean radiation absorbed doses specific to target arterial territories are independently calculated and physician-adjusted according to patient-specific circumstances (e.g. mean T/N ratio, liver-to-lung shunt, liver reserve, prognosis, treatment intent and potential treatment benefit). The overall process yields a personalized image-guided predictive radiation plan for safe and effective Y90 radioembolization. This report provides a technical overview of this integrated dosimetric technique and details our early clinical outcomes in patients with inoperable hepatocellular carcinoma (HCC).

METHODS

Patients

The institutional review board waived the need to obtain informed consent for this retrospective study. The technique for using artery-specific SPECT/CT partition modeling to plan Y90 radioembolization was implemented at our institution as a routine clinical service in January 2011. Five months post-implementation, we had treated 22 patients with inoperable HCC. Of these, 10 patients were embargoed under an ongoing clinical trial. Two patients were planned by BSA methodology due to morphologically diffuse and infiltrative tumors that were below 99mTc-MAA SPECT/CT resolution for reliable regions-of-interest (ROI) contouring. Both these patients were excluded (10). Treatment of the remaining 10 consecutive patients was planned by artery-specific SPECT/CT partition modeling, and these patients were eligible for inclusion into this report. Retrospective review of hospital medical records was performed for these 10 patients until August 2011, the time at which the manuscript was prepared.

Patient and baseline disease characteristics were highly heterogeneous (Tables 1 and 2).

Median age was 59 years (range 48-65 years). There were 8 men and 2 women. Seven patients had chronic viral hepatitis. Five patients received prior therapy for HCC, including 2 with previous Y90 radioembolization planned by conventional planar partition modeling. Eight patients were Child-Pugh A; the remainder were Child-Pugh *B. Tumor*

Table 1. Patient characteristics

Patient No.	Age	Sex	Tumor	Risk factor	Previous Treatment	ECOG	Child-Pugh
1	58	M	HCC	HCV	Segmentectomy; sorafenib	1-2	A
2	63	M	HCC	HBV	Y90 RE; segmentectomy	0	A
3	61	F	HCC	Cryptogenic	No	3	A
4	48	M	HCC	HBV	RFA	1-2	B
5	60	M	HCC	Cryptogenic	No	0	A
6	56	M	HCC	HBV	Right hemi-hepatectomy; TACE	0	A
7	61	F	HCC	Cryptogenic	Y90 RE	1-2	A
8	65	M	HCC	HCV	No	0	B
9	56	M	HCC	HBV	No	0	A
10	52	M	HCC	HCV	No	0	A

HCC: hepatocellular carcinoma; HBV: chronic hepatitis B; HCV: chronic hepatitis C; ECOG: Eastern cooperative oncology group performance status; PV: portal vein; Y90 RE: Y90 radioembolization; RFA: radiofrequency ablation; TACE: transarterial chemoembolization

Table 2. Disease characteristics

Patient No.	UNOS T-stage	BCLC	Tumor extent	Vascular invasion	Site of hepatic intra-arterial 99mTc-MAA injection
1	T4b	C	Bilobar; infiltrative	Branch PV	Right; left *
2	rT2	A	Solitary recurrence at segment IV resection margin	No	Right; left *
3	T3	D	Central large dominant tumor; smaller satellite lesions	No	Right; left *
4	T4b	C	Right lobe; multifocal	Branch PV	Superior branch of right; posterior branch of right †
5	T4b	C	Bilobar; multifocal; subcentimeter lesions present	Branch PV	Right; accessory right; left *
6	T4b	B	Bilobar; multifocal; subcentimeter lesions present	No	Right; left *
7	T4a	B	Right lobe; large necrotic tumor; satellite lesions with ill-defined margins	No	Right; middle †
8	T4a	B	Bilobar; multifocal; subcentimeter lesions present	No	Right; middle; left *
9	T4b	C	Bilobar; multifocal;subcentimeter lesions present	Branch PV	Proper *
10	T4b	C	Large right lobe tumor with ill-defined margins; subcentimeter lesion present	Branch and main PV; right hepatic vein	Right †

UNOS: United Network for Organ Sharing staging system, all patients are N0 M0; BCLC: Barcelona Clinic Liver Cancer staging system; PV: portal vein; * Whole-liver 99mTc-MAA injection; † Selective lobar/segmental 99mTc-MAA injection

extent varied widely across all patients and were mostly bilobar and multifocal. Eight patients had T4 disease by the United Network for Organ Sharing (UNOS) staging system; none had nodal or distant metastases. Classification by the Barcelona Clinic Liver Cancer (BCLC) staging system was: 1 BCLC A; 3 BCLC B; 5 BCLC C; 1 BCLC D. Five patients had tumor vascular involvement.

Technique overview

Mapping hepatic angiography and 99mTc-MAA injection were performed according to standard technique (1, 15). Prophylactic coil embolization of vessels at risk was performed either at mapping hepatic angiography or at Y90 radioembolization, at the discretion of the interventional radiologist. The catheter tip position for 99mTc-MAA injection was decided in consensus between the interventional radiologist and nuclear medicine physician during mapping hepatic angiography. 99mTc-MAA was slowly hand-injected non-selectively (whole liver), selectively (lobar) or super-selectively (segmental or sub-segmental) depending on patient-specific circumstances. Patients were immediately transferred to the gamma camera suite for planar liver-to-lung shunt scintigraphy and SPECT/CT of the abdomen.

The following describes the essence of the technique of artery-specific SPECT/CT partition modeling. Catheter-directed CTHA guided volumes-of-interest (VOI) delineation on 99mTc-MAA SPECT/CT to obtain arterial territory-specific tissue volumes and SPECT/CT-based mean T/N ratio estimates for improved partition modeling. The term *planning target volume* is used, adapted from EBRT. All treatments were planned by a team of experienced nuclear medicine physicians, and the final prescribed mean radiation absorbed doses were guided by published dose-response relationships (5). By partition modeling, the nuclear medicine physician had full control over predicted radiation absorbed dose estimates to tumor, non-tumorous liver and lungs within each planning target volume. The overall dosimetric aim was to balance the desired mean tumor radiation absorbed dose with collateral radiation injury, in accordance to the treatment intent.

Y90 radioembolization was performed using resin microspheres (SIR-Spheres®, Sirtex Medical Limited, New South Wales, Australia) within 2 weeks of mapping hepatic angiography. Catheter tip placement was the same as that of the 99mTc-MAA injections. All patients received prophylactic omeprazole, 20mg, twice daily prior to Y90 radioembolization and this treatment continued for at least 6 weeks after radioembolization. In accord with our institutional protocol, after Y90 radioembolization all patients were observed overnight and discharged after bremsstrahlung planar scintigraphy of the lung and SPECT/CT of the abdomen the following day.

Terms and definitions

Postradioembolization bremsstrahlung SPECT/CT of the abdomen was used to determine technical success. Technical success was achieved when all targeted tumors within planning target volumes showed satisfactory bremsstrahlung activity by visual assessment, in keeping with the radiation plan (28). The success of the technique was considered indeterminate when planning target volumes included subcentimeter tumors or tumors with ill-defined margins (e.g. infiltrative HCC), below bremsstrahlung SPECT/CT spatial resolution. A technical failure occurred when targeted tumors did not exhibit visually detectable focal bremsstrahlung activity, analogous to a geographical miss in the context of EBRT.

Clinical and biochemical toxicities within 3 months after radioembolization were classified according to Common Terminology Criteria for Adverse Events (CTCAE v4.03) (28-29). The nadir in serum alphafetoprotein at any time post-radioembolization indicated the best biochemical response.

To evaluate the effectiveness of Y90 radioembolization strictly as a form of brachytherapy delivered at a single time-point, the best imaging response was defined as the greatest change in size of the targeted index (largest) tumor between baseline and follow-up diagnostic sectional imaging. Clinical success was defined as any degree of regression of targeted tumors on follow-up diagnostic sectional imaging within planning target volumes, regardless of new tumors appearing within or outside planning target volumes (28).

Overall response by Response Evaluation Criteria in Solid Tumors version 1.1 (RECIST 1.1), World Health Organization (WHO), and 2-D European Association for the Study of the Liver (2D-EASL) guidelines were used to evaluate Y90 radioembolization as a part of comprehensive multi-modality therapy for inoperable HCC, without regard to planning target volumes (28,30).

Statistical methods

Data are presented as median and 95% confidence intervals (CI), where applicable. Using Bland-Altman analysis, the total desired Y90 activities calculated by artery-specific SPECT/CT partition modeling were compared to that hypothetically derived by BSA methodology. The intra-class correlation coefficient (ICC) was calculated with values 0.8 or more considered excellent; 0.6-0.8, good; 0.4-0.6, moderate; and less than 0.4, poor. Statistical analysis was performed on Microsoft® Office Excel 2003 (Microsoft Corporation) and SPSS version 17.0 (SPSS Inc., Chicago, USA).

RESULTS

The artery-specific SPECT/CT dosimetric plans of all 10 patients are summarized in Table 3. There were a total of 20 radiation plans across 10 patients i.e. one planning target volume per target arterial territory. Two patients underwent Y90 radioembolization in a single arterial territory, 6 patients in 2 arterial territories and 2 patients in 3 arterial territories (Figure 1).

Sublesional dosimetry was performed in 2 patients; 1 of which was planned with radio-embolization lobectomy intent (Figures 2-3). Four patients underwent prophylactic coil embolization of arteries at risk: 3 gastroduodenal; 2 accessory left gastric; 2 right gastric; 1 right inferior phrenic; 1 falciform; 1 pancreatico-duodenal arcade. Technical success was achieved in 2 of 10, indeterminate in 7 of 10, and technical failure in 1 of 10 patients. Patient 8 was classified as a technical failure due to the absence of visually detectable focal bremsstrahlung activity in a targeted caudate tumor.

Median predicted mean radiation absorbed doses by artery-specific SPECT/CT partition modeling were 106 Gy (95% CI, 105-146 Gy) to tumor, 27 Gy (95% CI, 22-33 Gy) to non-tumorous liver and 2 Gy (95% CI, 1.3-7.3 Gy) to lungs. Across all patients, tumor, non-tumorous liver and lungs were predicted to have received ≥91 Gy, ≤51 Gy and ≤16 Gy respectively to at least one target arterial territory. The median artery-specific tumor and non-tumorous liver masses were 156 g (95% CI, 117-436 g) and 752 g (95% CI, 513-833 g) respectively. The median liver-to-lung shunt estimated by planar 99mTc-MAA scintigraphy was 5.4% (95% CI, 4.3%-9.0%). The median Y90 activity injected into an arterial territory was 0.6 GBq (95% CI, 0.7-1.3 GBq). Patient 2 received a mean radiation absorbed dose of 93 Gy to the left lobe nontumorous liver for Y90 radioembolization lobectomy (Table 3; Fig. 2). There was good tumor response together with slow progressive atrophy of the left lobe 6 months post-radioembolization, in keeping with the dosimetric intent. The right lobe volume, which received a mean radiation absorbed dose of 27 Gy to non-tumorous liver, remained stable over time (Figure 3).

SPECT/CT-based mean T/N ratios varied widely across all planning target volumes (median 5.4; 95% CI, 4.1-6.7), and even within the same patient (median intra-patient difference 1.9; 95% CI, 1.1-2.5). We could not find any predictive relationship between mean T/N ratios and liver tissue masses. In a sub-analysis, the total desired Y90 activities calculated by artery-specific SPECT/CT partition modeling were compared to that hypo-thetically derived by BSA methodology. Bland-Altman analysis (Figure 4) showed a wide 95% limit of agreement ranging from -1.12 to +1.41, with only moderate correlation (ICC 0.59; 95% CI, -0.71 to 0.90).

Table 3. Dosimetric data by artery-specific SPECT/CT partition modeling

Pt No.	1st Y90 RE radiation dose	Planning target volume 1	Planning target volume 2	Planning target volume 3	Artery prophylactic coil embolization	Liver-lung shunt, Gy	Total injected Y90 activity	Technical success*
1	N/A	Right hepatic artery T/N ratio 5.7 Tumor mass 259g Tumor dose 171Gy Liver mass 920g Liver dose 30Gy Y90 activity 1.6GBq	Left hepatic artery T/N ratio 8.1 Tumor mass 46g Tumor dose 177Gy Liver mass 833g Liver dose 22Gy Y90 activity 0.5GBq	N/A	No	8.3% 5Gy	2.1GBq	Indeterminate; ill-defined tumor margins †
2	Liver 70Gy; Lung 9Gy ‡	Right hepatic artery T/N ratio 6.1 Tumor mass 7g Tumor dose 164Gy Liver mass 782g Liver dose 27Gy Y90 activity 0.4GBq	Left hepatic artery § T/N ratio 1.4 Tumor mass 28g Tumor dose 133Gy Liver mass 256g Liver dose 93Gy Y90 activity 0.6GBq	N/A	No	4.5% 1Gy	1.0GBq	Yes
3	N/A	Right hepatic artery T/N ratio 6.5 Tumor mass 410g Tumor dose 92Gy Liver mass 983g Liver dose 14Gy Y90 activity 1.0GBq	Left hepatic artery T/N ratio 4.6 Tumor mass 172g Tumor dose 59Gy Liver mass 752g Liver dose 13Gy Y90 activity 0.4GBq	N/A	Accessory left gastric; gastro-duodenal ‖	4.6% 2Gy	1.4GBq	Indeterminate; subcentimeter lesions ¶
4	N/A	Right hepatic artery (superior branch) T/N ratio 8.1 Tumor mass 58g Tumor dose 241Gy Liver mass 189g Liver dose 30Gy Y90 activity 0.4GBq	Right hepatic artery (posterior branch) T/N ratio 8.4 Tumor mass 484g Tumor dose 176Gy Liver mass 825g Liver dose 21Gy Y90 activity 2.2GBq	N/A	No	10.3% 9Gy	2.6GBq	Yes

Table 3. Dosimetric data by artery-specific SPECT/CT partition modeling (continued)

Pt No.	1st Y90 RE radiation dose	Planning target volume 1	Planning target volume 2	Planning target volume 3	Artery prophylactic coil embolization	Liver-lung shunt, Gy	Total injected Y90 activity	Technical success*
5	N/A	Right hepatic artery T/N ratio 5.2 Tumor mass 337g Tumor dose 135Gy Liver mass 247g Liver dose 26Gy Y90 activity 1.1GBq	Accessory right hepatic artery T/N ratio 3.1 Tumor mass 730g Tumor dose 87Gy Liver mass 423g Liver dose 28Gy Y90 activity 1.5GBq	Left hepatic artery T/N ratio 2.3 Tumor mass 12g Tumor dose 106Gy Liver mass 595g Liver dose 47Gy Y90 activity 0.6GBq	No	3.5% 2Gy	3.2GBq	Indeterminate; subcentimeter lesions ¶
6	N/A	Right hepatic artery T/N ratio 5.6 Tumor mass 27g Tumor dose 151Gy Liver mass 460g Liver dose 27Gy Y90 activity 0.4GBq	Left hepatic artery T/N ratio 7.6 Tumor mass 40g Tumor dose 152Gy Liver mass 1196g Liver dose 20Gy Y90 activity 0.6GBq	N/A	No	8.4% 2Gy	1.0GBq	Indeterminate; subcentimeter lesions ¶
7	Liver 40Gy; Lung 10Gy ‡	Right hepatic artery T/N ratio 2.1 Tumor mass 156g Tumor dose 106Gy Liver mass 363g Liver dose 51Gy Y90 activity 0.7GBq	Middle hepatic artery T/N ratio 1.7 Tumor mass 12g Tumor dose 85Gy Liver mass 252g Liver dose 51Gy Y90 activity 0.3GBq	N/A	Right inferior phrenic; falciform ‖	4.3% 1Gy	1.0GBq	Indeterminate; ill-defined tumor margins †

Table 3. Dosimetric data by artery-specific SPECT/CT partition modeling (continued)

Pt No.	1st Y90 RE radiation dose	Planning target volume 1	Planning target volume 2	Planning target volume 3	Artery prophylactic coil embolization	Liver-lung shunt, Gy	Total injected Y90 activity	Technical success*
8	N/A	Right hepatic artery T/N ratio 2.4 Tumor mass 266g Tumor dose 91Gy Liver mass 1465g Liver dose 38Gy Y90 activity 1.6GBq	Left hepatic artery T/N ratio 4.3 Tumor mass 23g Tumor dose 107Gy Liver mass 1044g Liver dose 25Gy Y90 activity 0.6GBq	Middle hepatic artery T/N ratio 3.2 Tumor mass 10g Tumor dose 95Gy Liver mass 356g Liver dose 30Gy Y90 activity 0.2GBq	Right gastric; gastro-duodenal #	6.1% 3Gy	2.4GBq	No; Non-implantation in caudate tumor
9	N/A	Proper hepatic artery T/N ratio 11.5 Tumor mass 1252g Tumor dose 97Gy Liver mass 755g Liver dose 8Gy Y90 activity 2.6GBq	N/A	N/A	Accessory left gastric ‖; right gastric‖; gastro-duodenal #; pancreatico-duodenal arcade #	1.7% 2Gy	2.6GBq	Indeterminate; subcentimeter lesions ¶
10	N/A	Right hepatic artery T/N ratio 10.6 Tumor mass 955g Tumor dose 97Gy Liver mass 350g Liver dose 9Gy Y90 activity 2.3GBq	N/A	N/A	No	14.5% 16Gy	2.3GBq	Indeterminate; ill-defined tumor margins; subcentimeter lesions † ¶

RE: Y90 radioembolization; T/N ratio: tumor-to-normal liver ratio; N/A: not applicable; * Technical success assessed by bremsstrahlung SPECT/CT; 'Dose': predicted mean radiation absorbed dose in Gy; † Ill-defined tumor margins cannot be reliably assessed by bremsstrahlung SPECT/CT; ‡ Planned by planar partition modeling; § Planned by sub-lesional dosimetry with radiation lobectomy intent to the left hepatic arterial territory; ‖ Coil embolization at time of mapping hepatic angiography; ¶ Subcentimeter lesions are below bremsstrahlung SPECT/CT spatial resolution; # Coil embolization at time of Y90 radioembolization
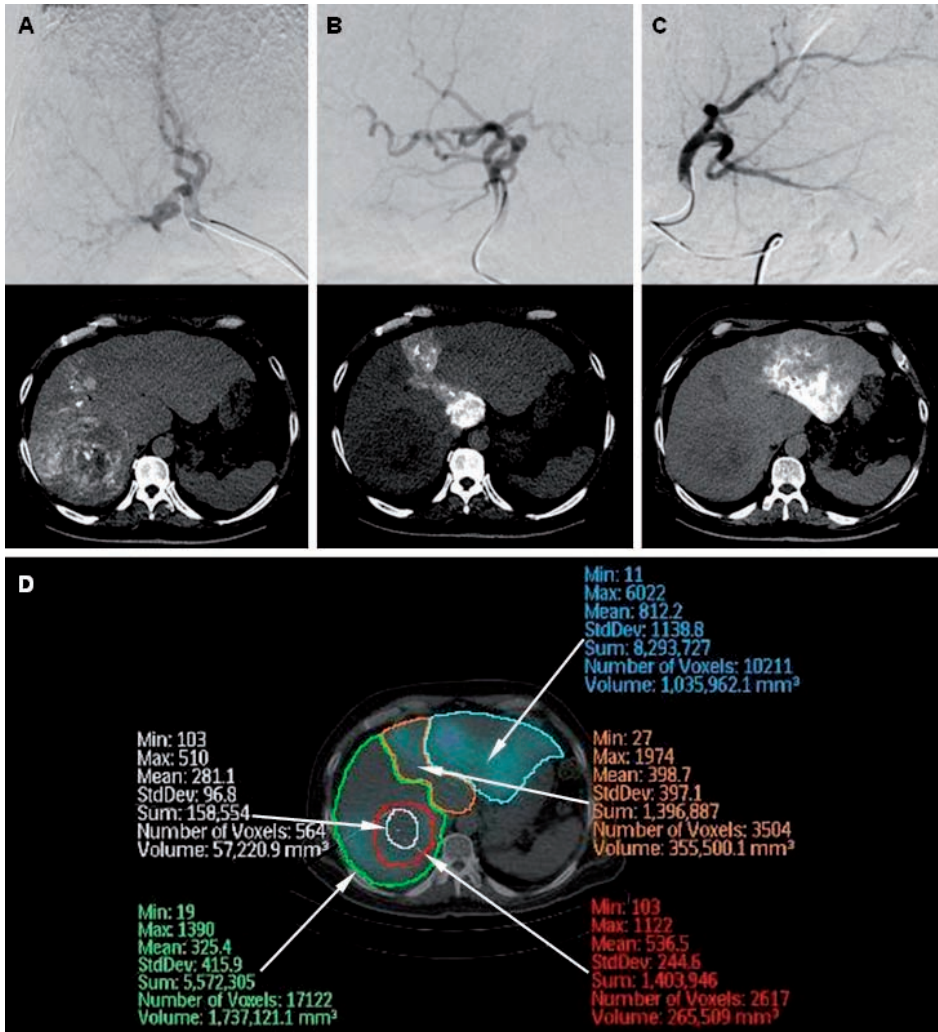
Figure 1. Example of artery-specific SPECT/CT partition modeling of 3 arterial territories. A liver with multifocal HCC supplied by the right (A), middle (B) and left (C) hepatic arteries is depicted here in digital subtraction angiography and catheter-directed CTHA respectively. Regions-of-interest (ROI) are drawn on 99mTc-MAA SPECT/CT transaxial slices representing the left (D, blue ROI), middle (D, orange ROI) and right (D, green ROI) hepatic artery planning target volumes, the implanted tumor (D, red ROI) and necrotic tumor (D, white ROI).

Y90 radioembolization was well tolerated in all patients. None developed postradio-embolization syndrome. All patients were ambulating freely by the next day and discharged within 24 hours post-radioembolization. In 8 patients, serum bilirubin, albumin, and alanine transaminase (ALT) were measured within 24 hours post-radioembolization; none developed significant biochemical toxicities.
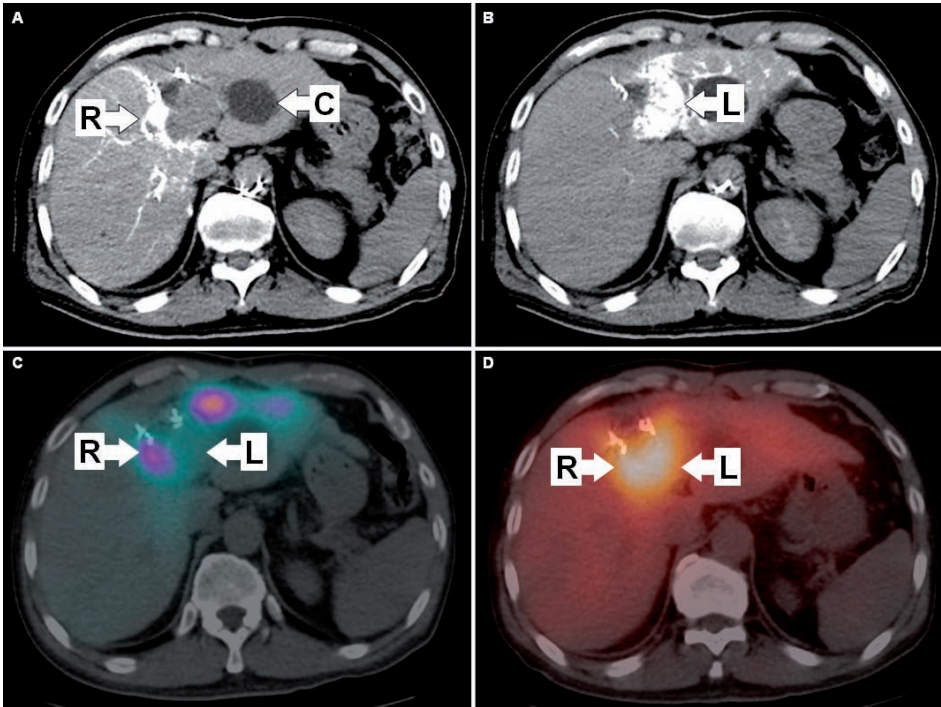
Figure 2. Patient 2: Example of sub-lesional dosimetry with left radioembolization lobectomy intent. The patient had recurrent HCC at the segment IV resection margin. Left lobe hypodensity is a cyst (A, 'C'). The tumor was supplied by the right and left hepatic arteries. Catheter-directed CTHA depicts the planning target volumes of the right (A) and left (B) hepatic arteries, dividing the dosimetric plan into two independent halves for sub-lesional dosimetry. 99mTc-MAA SPECT/CT showed good T/N ratio (6.1) of the lateral tumor portion supplied by the right hepatic artery (C, 'R'), but poor T/N ratio (1.4) of the medial tumor portion supplied by the left hepatic artery (C, 'L'). The dosimetric plan of the left hepatic artery planning target volume was deliberately escalated beyond safe limits to achieve a predicted mean radiation absorbed dose of 133 Gy to tumor and 93 Gy to non-tumorous liver, where progressive atrophy of the left lobe was the anticipated collateral effect i.e. left radioembolization lobectomy intent. Post-radioembolization bremsstrahlung SPECT/CT showed good tumoral activity in both lateral (D, 'R') and medial (D, 'L') tumor portions, indicating technical success.

At the time of this report, follow-up data was available for 8 patients. The median follow-up duration was 21 weeks (95% CI, 12-50 weeks). The other 2 patients were non-residents, returned to their home country and were lost to follow-up. Patient 3 was excluded from biochemical and survival analysis due to confounding medical issues, but was included in imaging analysis.

With the exception of Patient 3, all 7 other patients remained clinically well. None developed gastrointestinal complications or radiation pneumonitis. There were no biochemical toxicities beyond CTCAE Grade 2 within 3 months postradioembolization. Postradioembolization serum alphafetoprotein was available in 5 patients. There was an

interval decrease in alphafetoprotein in 3 patients, ranging from 32 to 95%. The remaining 2 patients had normal baseline alphafetoprotein levels, which remained un-elevated on follow-up.
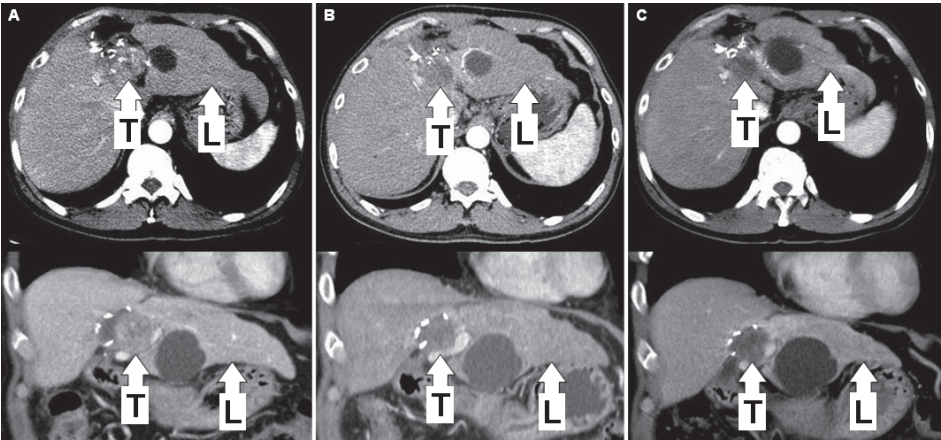

Figure 3. Patient 2: Baseline triphasic CT liver shows the recurrent HCC at the segment IV resection margin (A). Follow-up triphasic CT liver at three (B) and six (C) months post-radioembolization showed good tumor ('T'; 133 Gy) response with progressive atrophy of the left lobe ('L'; 93 Gy), in keeping with left radioembolization lobectomy intent. Right lobe volume (27 Gy) remained stable.
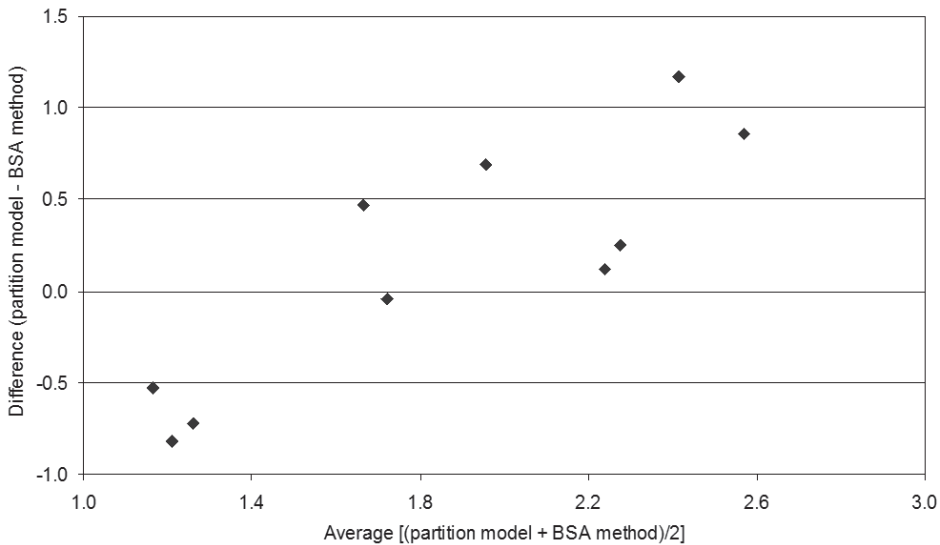

Figure 4. Bland-Altman plot of Y90 activities derived by artery-specific SPECT/CT partition modeling versus that hypothetically derived by body surface area (BSA) methodology.

Postradioembolization best imaging response was available in 8 patients. Median time-to-best imaging response was 76 days (11 weeks; 95% CI 55-114 days). When Y90 radioembolization was analyzed strictly as a brachytherapy, all 8 of 8 patients showed regression of the index tumor, with a median size decrease of 58% (95% CI, 40%-72%). None developed new tumors within planning target volumes. Seven of 8 patients achieved clinical success at the time of best imaging response. Patient 1 was a case of infiltrative HCC classified as clinical failure due to progression of existing portal vein tumor thrombosis despite significant regression of the index tumor. Otherwise, tumor thrombosis regressed or remained stable in 3 of 4 patients with baseline tumor vascular involvement.

At the time of best imaging response, extrahepatic metastases were discovered in 3 of 8 patients, involving the lungs and adrenal gland. When Y90 radioembolization was analyzed as part of a comprehensive multi-modality treatment plan, partial response was achieved in 3 of 8, stable disease in 1 of 8, and progressive disease in 4 of 8 patients; consistent across all three classifications (RECIST 1.1, WHO and 2D-EASL). Median imaging time-to-progression (TTP) and median overall survival were not reached at the time of this report. Patient 1 died 13 weeks postradioembolization and had an overall survival of 95 weeks (22 months) under comprehensive multi-modality care; all 7 other patients are still alive.

DISCUSSION

The aim of personalized predictive dosimetry is to guide decisions on radionuclide therapy in order to avoid the use of futile therapy and achieve the maximum tumor radiation absorbed dose while minimizing collateral radiation injury to normal tissue.

Precise radionuclide predictive dosimetry has the potential to yield many benefits for cancer therapy, and the need to further research into internal dosimetry has recently been emphasized (31). To our knowledge, the artery-specific SPECT/CT partition model is the first to integrate catheter-directed CTHA, 99mTc-MAA SPECT/CT and partition modeling (MIRD) into a unified, accurate, and practical form of image-guided personalized predictive dosimetry for Y90 radioembolization.

Our results show that a 100% tumor response rate can be achieved when the predicted mean tumor radiation absorbed dose was at least 91 Gy to a planning target volume. There were no significant toxicities with predicted mean radiation absorbed doses to non-tumorous liver and lungs of ≤51 Gy and ≤16 Gy, respectively. This highlights the

power of predictive radionuclide dosimetry to achieve desired outcomes when planned in accordance to dose-response relationships. The capability of artery-specific SPECT/CT partition modeling is best exemplified by patient 2, in whom sub-lesional dosimetry was successfully planned with Y90 radioembolization lobectomy intent (Figs. 2-3).

Y90 radioembolization is point-source, continuous low dose-rate brachytherapy delivered at a single time-point. Hence, its true therapeutic efficacy can only be revealed by analyzing outcomes in the context of planning target volumes and technical success. Therefore, postradioembolization appearance of new tumors within a planning target volume should not be misconstrued as clinical failure. Such lesions may represent new metastases, pre-existing micro-metastases that have enlarged, or de novo tumors arising from cirrhotic liver; all of which have little or no bearing on Y90 radioembolization as brachytherapy delivered at a single time-point. It follows that when applying standard response evaluation criterion (e.g. RECIST), which takes into account new tumors and distant metastases, one should analyze Y90 radioembolization brachytherapy as part of comprehensive multi-modality care and not in isolation.

The application of Y90 radioembolization without due regard for radiobiological principles is akin to flying an aircraft without guidance from air traffic control. Since most patients with inoperable HCC have limited prognosis, Y90 radioembolization should be carefully planned using scientifically sound methods (e.g. MIRD) to achieve the maximum desired effect for optimal, personalized cancer therapy. Our dosimetric data showed wide inter- and intra-patient variations in SPECT/CT-based mean T/N ratios (Table 3), emphasizing the importance of having a personalized dosimetric approach to Y90 radioembolization. The assumption of a standard T/N ratio for the sake of dosimetric simplification may result in over- or undertreatment, and confounds data analyses because reliable dose-response relationships cannot be established or verified (10). Despite its popularity, the BSA method has questionable radiobiological basis and is scientifically inferior to MIRD methodology (5,10). One must be cognizant that the BSA method was first published by van Hazel et al. for whole-liver Y90 radioembolization to previously untreated colorectal liver metastasis, not HCC (32). These patients did not have chronic liver disease, prior liver resection, local ablation, or selective/super-selective Y90 radioembolization. Furthermore, colorectal liver metastases are rarely bulky enough to distort liver anatomy. These features are often present in HCC, and therefore they cast doubt on the validity, safety, and efficacy of the BSA methodology for use in HCC. Our data showing a lack of agreement in total Y90 activities derived by artery-specific SPECT/CT partition modeling versus BSA method is further evidence against the routine use of BSA methodology (Figure 4).

In this report, postradioembolization bremsstrahlung SPECT/CT was used to determine technical success. This was indeterminate in 7 of 10 patients, all of whom have either sub-centimeter tumors or tumors with ill-defined margins. This finding highlights the low spatial resolution of bremsstrahlung SPECT/CT as a technical limitation by indirectly imaging Y90 biodistribution using scatter radiation. It may be possible for positron emission tomography to overcome this limitation by co-incidence imaging of yttrium-90 internal pair production (33). This is currently under investigation at our institution.

Y90 microspheres once implanted, remain permanently in place and decays to infinity in situ. This simplifies the dosimetric process because time-activity curves need not be obtained, unlike systemic radionuclide therapy. Future Y90 radioembolization dosimetric techniques must improve accuracy in several areas: delineation of arterial territory target volumes, microparticle simulation and biodistribution assessment, and predictive radiation dose-response modeling. For example, future development of positron-labeled microspheres in place of 99mTc-MAA may increase the accuracy of liver-to-lung shunt calculation, simulation of hepatic microsphere biodistribution, and improve predictive radiation modeling by voxel- or Monte-Carlo-based techniques (34-35). Y90 radioembolization will also benefit from a wealth of experience if EBRT radiobiologic models (e.g. linear quadratic model, normal tissue complication probability model) and radiation planning techniques (e.g. dose-volume histogram) can be meaningfully translated into radionuclide dosimetry models (e.g. MIRD) and vice versa. Application of the biologically effective dose (BED) concept into Y90 radioembolization dosimetry may achieve this aim (36).

In conclusion, compliance to radiobiological principles of radionuclide internal dosimetry is fundamental to Y90 radioembolization success. Image-guided personalized predictive dosimetry by artery-specific SPECT/CT partition modeling achieves high clinical success rates for safe and effective Y90 radioembolization.

REFERENCES

1. Salem R, Lewandowski RJ, Sato KT, et al. Technical aspects of radioembolization with Y90 microspheres. Tech Vasc Interv Radiol. 2007;10:12-29.

2. Gaba RC, Lewandowski RJ, Kulik LM, et al. Radiation lobectomy: preliminary findings of hepatic volumetric response to lobar yttrium-90 radioembolization. Ann Surg Oncol. 2009;16:1587-1596.

3. Riaz A, Lewandowski RJ, Kulik LM, et al. Complications following radioembolization with yttrium-90 microspheres: a comprehensive literature review. J Vasc Interv Radiol. 2009;20:1121-1130.

4. Ahmadzadehfar H, Biersack HJ, Ezziddin S. Radioembolization of liver tumors with yttrium-90 microspheres. Semin Nucl Med. 2010;40:105-121.

5. Lau WY, Kennedy AS, Kim YH, et al. Patient selection and activity planning guide for selective internal radiotherapy with yttrium-90 resin microspheres. Int J Radiat Oncol Biol Phys. 2010 Jan 1;82(1):401-407.

6. Salem R, Lewandowski RJ, Mulcahy MF, et al. Radioembolization for hepatocellular carcinoma using Yttrium-90 microspheres: a comprehensive report of long-term outcomes. Gastroenterology. 2010;138:52-64.

7. Wang SC, Bester L, Burnes JP, et al. Clinical care and technical recommendations for Y90ttrium microsphere treatment of liver cancer. J Med Imaging Radiat Oncol. 2010;54:178-187.

8. Riaz A, Gates VL, Atassi B, et al. Radiation segmentectomy: a novel approach to increase safety and efficacy of radioembolization. Int J Radiat Oncol Biol Phys. 2011;79:163-171.

9. Jakobs TF, Hoffmann RT, Fischer T, et al. Radioembolization in patients with hepatic metastases from breast cancer. J Vasc Interv Radiol. 2008;19:683-690.

10. Kao YH, Tan EH, Ng CE, Goh SW. Clinical implications of the body surface area method versus partition model dosimetry for yttrium-90 radioembolization using resin microspheres: a technical review. Ann Nucl Med. 2011;25:455-461.

11. Rhee TK, Omary RA, Gates V, et al. The effect of catheter-directed CT angiography on yttrium-90 radioembolization treatment of hepatocellular carcinoma. J Vasc Interv Radiol. 2005;16:1085-1089.

12. Pereira JM, Stabin MG, Lima FR, Guimarães MI, Forrester JW. Image quantification for radiation dose calculations - limitations and uncertainties. Health Phys. 2010;99:688-701.

13. Garin E, Rolland Y, Lenoir L, et al. Utility of quantitative Tc-MAA SPECT/CT for yttrium-labelled microsphere treatment planning: calculating vascularized hepatic volume and dosimetric approach. Int J Mol Imaging. July 28, 2011 (Epub ahead of print).

14. Kao YH, Tan EH, Teo TK, Ng CE, Goh SW. Imaging discordance between hepatic angiography versus Tc-99m-MAA SPECT/CT: a case series, technical discussion and clinical implications. Ann Nucl Med. 2011 Nov;25(9):669-676.

15. Salem R, Thurston KG. Radioembolization with 90Yttrium microspheres: a state-of-the-art brachytherapy treatment for primary and secondary liver malignancies. Part 1: Technical and methodologic considerations. J Vasc Interv Radiol. 2006;17:1251-1278.

16. Covey AM, Brody LA, Maluccio MA, Getrajdman GI, Brown KT. Variant hepatic arterial anatomy revisited: digital subtraction angiography performed in 600 patients. Radiology. 2002;224:542-547.

17. Flux G, Bardies M, Monsieurs M, Savolainen S, Strands SE, Lassmann M. The impact

of PET and SPECT on dosimetry for targeted radionuclide therapy. Z Med Phys. 2006;16:47-59.

18. Patel CN, Chowdhury FU, Scarsbrook AF. Hybrid SPECT/CT: the end of "unclear" medicine. Postgrad Med J. 2009;85:606-613.

19. Hamami ME, Poeppel TD, Müller S, et al. SPECT/CT with 99mTc-MAA in radioembolization with Y90 microspheres in patients with hepatocellular cancer. J Nucl Med. 2009;50:688-692.

20. Ahmadzadehfar H, Sabet A, Biermann K, et al. The significance of 99mTc-MAA SPECT/CT liver perfusion imaging in treatment planning for Y90-microsphere selective internal radiation treatment. J Nucl Med. 2010;51:1206-1212.

21. Gulec SA, Mesoloras G, Dezarn WA, McNeillie P, Kennedy AS. Safety and efficacy of Y90 microsphere treatment in patients with primary and metastatic liver cancer: the tumor selectivity of the treatment as a function of tumor to liver flow ratio. J Transl Med. 2007;5:15-24.

22. Flamen P, Vanderlinden B, Delatte P, et al. Multimodality imaging can predict the metabolic response of unresectable colorectal liver metastases to radioembolization therapy with Yttrium-90 labeled resin microspheres. Phys Med Biol. 2008;53:6591-6603.

23. Campbell JM, Wong CO, Muzik O, Marples B, Joiner M, Burmeister J. Early dose response to yttrium-90 microsphere treatment of metastatic liver cancer by a patient-specific method using single photon emission computed tomography and positron emission tomography. Int J Radiat Oncol Biol Phys. 2009;74:313-320.

24. Ho S, Lau WY, Leung TW, et al. Partition model for estimating radiation doses from yttrium-90 microspheres in treating hepatic tumours. Eur J Nucl Med. 1996;23:947-952.

25. Ho S, Lau WY, Leung TW, Chan M, Johnson PJ, Li AK. Clinical evaluation of the partition model for estimating radiation doses from yttrium-90 microspheres in the treatment of hepatic cancer. Eur J Nucl Med. 1997;24:293-298.

26. Sirtex Medical Limited, New South Wales, Australia. Sirtex Medical training manual (version TRN-US-03, Sirtex.com). Undated.

27. Gulec SA, Mesoloras G, Stabin M. Dosimetric techniques in Y90-microsphere therapy of liver cancer: The MIRD equations for dose calculations. J Nucl Med. 2006;47:1209-1211.

28. Salem R, Lewandowski RJ, Gates VL et al. Research reporting standards for radioembolization of hepatic malignancies. J Vasc Interv Radiol. 2011;22:265-278.

29. National Cancer Institute. Common Terminology Criteria for Adverse Events version 4.03. U.S. National Insitutes of Health. June 14, 2010.

30. Duke E, Deng J, Ibrahim SM. Agreement between competing imaging measures of response of hepatocellular carcinoma to yttrium-90 radioembolization. J Vasc Interv Radiol. 2010;21:515-521.

31. Stabin MG, Sharkey RM, Siegel JA. RADAR commentary: evolution and current status of dosimetry in nuclear medicine. J Nucl Med. 2011;52:1156-1161.

32. Van Hazel G, Blackwell A, Anderson J, et al. Randomised phase 2 trial of SIR-Spheres plus fluorouracil/leucovorin chemotherapy versus fluorouracil/leucovorin chemotherapy alone in advanced colorectal cancer. J Surg Oncol. 2004;88:78–85.

33. Gates VL, Esmail AA, Marshall K, Spies S, Salem R. Internal pair production of Y90 permits hepatic localization of microspheres using routine PET: proof of concept. J Nucl Med. 2011;52:72-76.

34. Kennedy A, Dezarn W, Weiss A. Patient specific 3D image-based radiation dose estimates for Y90 microsphere hepatic radioembolization in metastatic tumors. J Nucl Med Radiat Ther. 2011;2:1-8.

35. Gulec SA, Sztejnberg ML, Siegel JA. Hepatic structural dosimetry in (90)Y microsphere treatment: a Monte Carlo modeling approach based on lobular microanatomy. J Nucl Med. 2010;51:301-310.

36. Cremonesi M, Ferrari M, Bartolomei M. Radioembolization with Y90-microspheres: dosimetric and radiobiological investigation for multi-cycle treatment. Eur J Nucl Med Mol Imaging. 2008;35:2088-2096.

Chapter 9

Percutaneous isolated hepatic perfusion for the treatment of unresectable liver malignancies
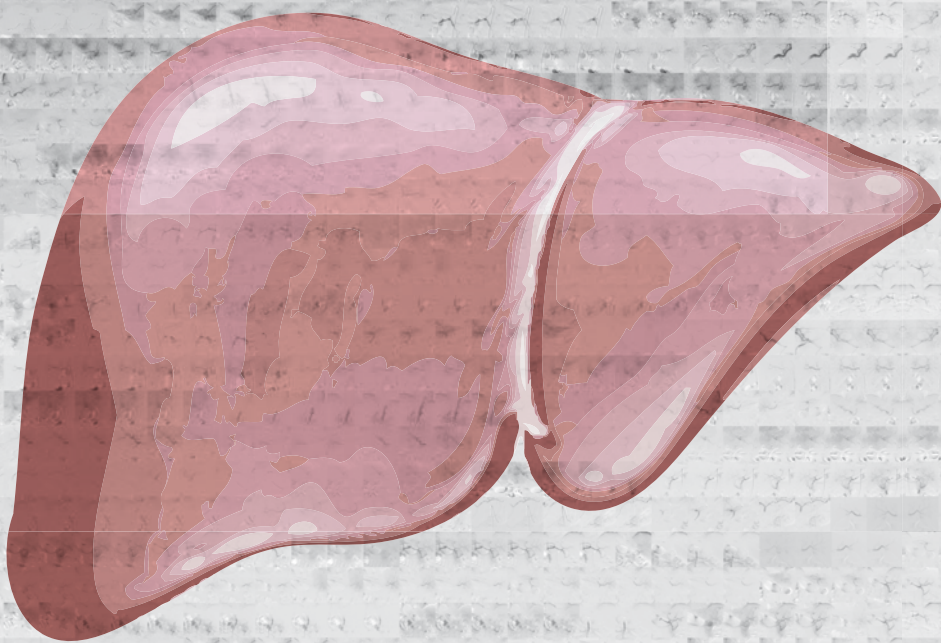
Burgmans MC, de Leede EM, Martini CH, Kapiteijn E, Vahrmeijer AL, van Erkel AR

ABSTRACT

Liver malignancies are a major burden of disease worldwide. The long-term prognosis for patients with unresectable tumors remains poor, despite advances in systemic chemotherapy, targeted agents and minimally-invasive therapies such as ablation, chemo- and radioembolization. Thus the demand for new and better treatments for malignant liver tumors remains high. Surgical isolated hepatic perfusion (IHP) has been shown to be effective in patients with various hepatic malignancies, but is complex, associated with high complication rates and not repeatable. Percutaneous isolated liver perfusion (PHP) is a novel minimally-invasive, repeatable and safer alternative to IHP. PHP is rapidly gaining interest and the number of procedures performed in Europe now exceeds 200. This review discusses the indications, technique and patient management of PHP and provides an overview of the available data.

INTRODUCTION

The liver is frequently affected by cancer. Primary liver cancer is the sixth most common cancer in the world and the third cause of cancer-related death (1). The liver is also a predilection site for metastases from various malignancies (1,2). Surgery or ablation offers the best chance of a cure in most liver malignancies, but this is often not feasible due to the extend or location of the disease. Liver malignancies have a dominant or exclusive vascular supply from the hepatic artery, whereas 70-80% of the supply of the non-tumorous liver parenchyma is derived from the portal vein (3,4). This difference in perfusion is utilized in liver-directed therapies, such as trans-arterial (chemo-) embolization or radioembolization. The unique hepatic anatomy also allows vascular isolation of the liver to deliver high doses of cytotoxic agents with minimal systemic toxicity. Isolated hepatic perfusion (IHP) is a complex surgical technique that involves clamping of the inferior vena cava (IVC) and portal vein (PV), ligation of IVC tributaries and arterial hepatico-enteric anastomoses with subsequent infusion of a high dose of chemotherapy into the proper hepatic artery (5-10). Promising results have been obtained with IHP in treating liver tumors from different histology. Response rates of 37-52% have been reported for metastatic ocular melanoma patients (11-14). In patients with liver metastases from colorectal carcinoma, response rates of 50-60% have been obtained (15-17). Despite the good response rates, the complexity and duration (up to 9 hours) of the procedure have prevented for IHP to gain wide acceptance (12). Furthermore, IHP is generally not repeatable and is associated with high morbidity and mortality rates (16,18-20).

Percutaneous isolated hepatic perfusion (PHP) is a novel alternative to IHP that enables vascular isolation and perfusion of the liver with the use of endovascular techniques (21). The minimally-invasiveness as well as the repeatability of PHP offers an important advantage over IHP. This review will describe this highly innovative technique and provide an update of current literature on PHP.

PHP PATIENT SELECTION

PHP has been performed in patients with primary tumors and various hepatic metastases (Table 1). Patients that best qualify for PHP are those that have disease of the liver only or predominantly. For obvious reasons, systemic treatment is the more appropriate therapy for patients with more extensive extra-hepatic disease, if available. As significant hemodynamic perturbations occur during PHP, patients should have a normal to high functional capacity and have no or limited cardio-pulmonary co-morbidity. Although

the most commonly used chemotherapeutic agent, melphalan chloride, has limited liver toxicity, patients with insufficient liver function are generally excluded from treatment. Portal hypertension, especially with concomitant hepatofugal portovenous blood flow, is a contra-indication for treatment. During the procedure adequate anti-coagulation with heparin is required to prevent intravascular thrombosis and clot formation in the extracorporeal circulation system. Therefore, patients with intolerance to heparin do not qualify for treatment nor do patients with an increased risk of bleeding (recent history of spontaneous internal bleeding or uncorrectable coagulation disorder). Women that are pre-menopausal should not be treated during the menstruation period or receive hormonal suppression therapy to prevent intra-procedural vaginal bleeding. It is generally recommended to perform computed tomography (CT) or magnetic resonance imaging (MRI) of the brain prior to treatment, as brain metastases with a propensity to bleed are a contra-indication to PHP. Patients should undergo arterial phase and portovenous phase contrast-enhanced abdominal CT to confirm patency of the portal vein and screen for vascular anomalies that may render PHP difficult of impossible. Variants of the hepatic arteries are usually not a contra-indication to PHP, but may require pre-emptive coil-embolization to either re-distribute hepatic flow or prevent inadvertent leakage of chemotherapeutics to the systemic circulation.

HEPATIC VASCULAR MAPPING

Prior to PHP, angiography of the celiac trunk and hepatic arteries should be performed to delineate the arterial supply of the liver (Figure 1). Angiography of the superior mesenteric artery may provide additional information and is always performed in patients with an aberrant right hepatic artery or to obtain an indirect portogram if hepatofugal or compromised portovenous flow is suspected. After mapping of the hepatic arterial circulation, a strategy for chemotherapy infusion is formulated. Infusion into the common or proper hepatic artery allows whole-liver treatment without repositioning of the catheter, but carries a higher risk of inadvertent flow of chemotherapeutic drugs into branches with supply to the gastrointestinal tract. To prevent this, coil-embolization may be indicated of arteries at risk, such as the gastroduodenal and right gastric artery. The use of cone-beam CT is recommended as this improves the detection of vascular variants, extra-hepatic enhancement and extra-hepatic vascular tumor supply (22-26). Embolization of aberrant hepatic arteries has been proven to be an effective strategy to redistribute flow in transarterial liver therapies such as radioembolization (27). Hepatic vascular mapping is generally performed several days to a week prior to PHP.
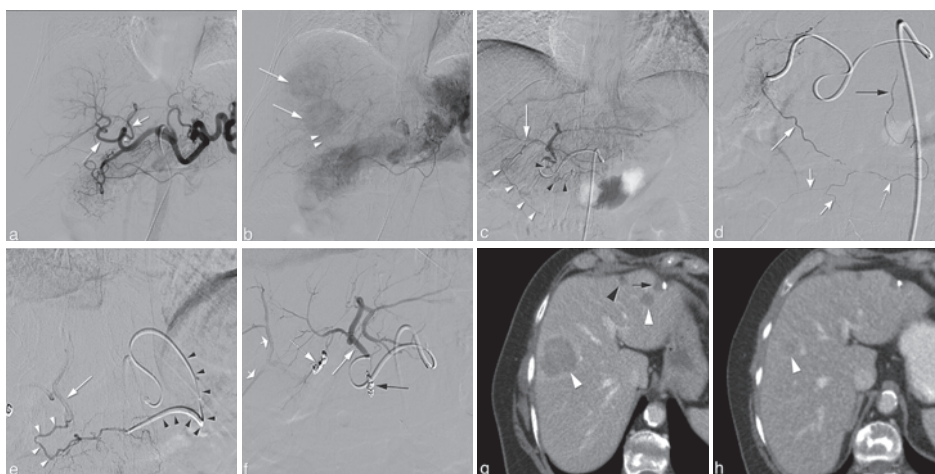
Figure 1. Hepatic vascular mapping in a 63-year old female with bilateral hepatic metastases from ocular melanoma. a. Angiographic images from the celiac trunk show a right gastric artery (asterisk) originating from the left hepatic artery (white arrow). b. In the late arterial phase, two hypervascular metastases in the right liver lobe (white arrows) are seen as well as the falciform artery (arrowheads). A treatment plan was made to perform PHP with selective infusion of melphalan chloride into the left hepatic artery (LHA) and right hepatic artery (dotted arrow in a) with pre-emptive coiling of the right gastric (RGA) and falciform artery (FA). c. Selective angiography from the LHA shows the FA (white arrowheads) to be originating from the segment 4 artery (white arrows). The RGA is also depicted (black arrowheads). d. Selective angiography of the FA (long white arrow) shows opacification of the right internal thoracic artery (black arrow) through the ensiform artery (dotted arrow) and of anterior abdominal wall arteries (short white arrows). e. Antegrade catheterization of the RGA was unsuccessful and therefore, retrograde catheterization was performed via the LGA using a 2.4F micro-catheter (arrow). Angiography shows the RGA (white arrowheads) and LHA (white arrow). f. Angiography of the LHA (white arrow) after successful coiling of the FA (dotted arrow) and RGA (black arrow) with 2mm detachable micro-coils. Some reflux of contrast is seen in right hepatic artery branches (short white arrows). g. Axial CT image in portovenous phase before treatment demonstrates two hepatic metastases (white arrowheads). A third metastasis was seen in segment 4B (not shown). In the left liver lobe a cyst is seen (black arrowhead) as well as a hypodensity caused by previous laparoscopic excisional biopsy (black arrow). h. CT in portovenous phase after two cycles of PHP shows marked reduction in size of the right liver lobe metastasis. The other two metastases showed a complete radiological response after treatment.

PHP PROCEDURE

At present, only one PHP system is commercially available (Chemosaturation Hepatic Delivery System, Delcath Systems Inc, New York, USA) and therefore some of the techniques described are specific to this system. In Japan, another double balloon catheter (4L/2B, Fuji System Co. Ltd, Tokyo, Japan) is currently used in clinical studies.

The procedure is performed under general anesthesia by a team consisting of a dedicated interventional radiologist, anesthesiologist and an extracorporeal perfusionist. A cannula is placed in the radial artery for continuous arterial pressure monitoring and a

urinary bladder catheter inserted. A triple-lumen line is placed in the left internal jugular vein (IJV) for central venous pressure monitoring and infusion of sympathomimetics and fluids. Access to the right IJV is created with a 10F vascular sheath, to the right common femoral vein (CFV) with an 18F sheath and to the left common femoral artery (CFA) with a 5F sheath (Figure 2). After all lines and sheaths have been placed, heparin is administered at an initial dose of 300 U/kg and the activated clotting time (ACT) is maintained above 400 sec during the entire procedure. Hepatic angiograms are obtained and the tip of a micro-catheter is then placed into the hepatic artery at the intended location of infusion. In a selective lobar approach, the dose of chemotherapy is split and infused

Figure 2. Schematic display of the set-up of percutaneous hepatic perfusion. Chemotherapeutic drugs are infused through a catheter placed in the hepatic artery (arrowhead) and the effluent chemosaturated blood returning through the hepatic veins is aspirated through the side-holes of the double-balloon catheter. An extracorporeal system with carbon activated filters is used to separate the chemotherapeutics from the blood, before the blood is returned through a sheath in the internal jugular vein.

into the right and left hepatic artery separately. In most patients, the ratio of the two lobes is such that 60% of total dose is to be injected into the right hepatic artery and 40% into the left hepatic artery. The disadvantage of consecutive lobar infusions is that it prolongs the time of extracorporeal circulation, as the chemotherapy infusion has to be interrupted to reposition the catheter. After placement of the infusion-catheter in the hepatic artery, a 16F double-balloon catheter (Isofuse Isolation Aspiration Catheter, Delcath Systems Inc, New York, NY) is inserted via the right CFV and positioned with its tip in the right atrium. The catheter is then connected to an extracorporeal circulation system consisting of a centrifugal pump and two drug filtration activated carbon filters. Blood is aspirated through catheter fenestrations in a segment between the two balloons, actively pumped through the filtration system and returned through the sheath in the IJV. The cranial balloon of the catheter is then inflated in the right atrium and retracted into the inferior caval vein (ICV) until the shape of the balloon resembles that of an acorn. The caudal balloon is inflated in the inferior vena cava below the level of the hepatic veins and above the level of renal veins. With both balloons inflated, a venogram is obtained by hand-injection of a contrast medium through the injection port of the double-balloon catheter (Figure 3). With adequate positioning of the double balloon catheter, flow of the effluent hepatovenous blood back to the systemic circulation is prevented by the cranial balloon at the atriocaval junction and by the caudal balloon at the level of the retrohepatic ICV.
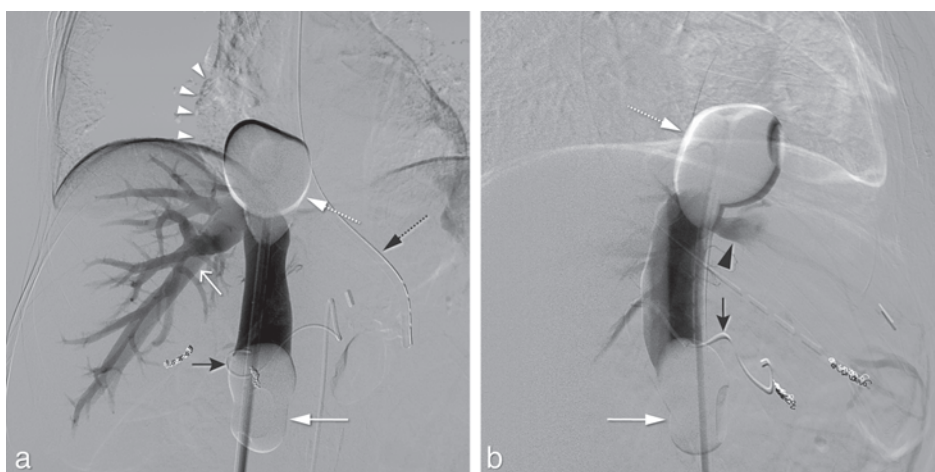

Figure 3. Same patient as in figure 1. Postero-anterior (a) and lateral (b) images during venography performed by hand-injection of non-diluted contrast medium through the size-holes of the double-balloon catheter. The cranial balloon (dotted white arrow) was positioned at the atriocaval junction to prevent flow to the right atrium (white arrowheads). The caudal balloon (white arrow) prevented retrograde flow to the infrarenal inferior vena cava. A micro-catheter (black arrow) was placed through a 5F celiac catheter and into the left hepatic artery for the infusion of melphalan chloride. Both the right hepatic vein (open white arrow) and middle hepatic vein (black arrowhead) were opacified. Also, a nasogastric tube is seen (dotted black arrow).

Once correct positioning of the two balloons is confirmed, a step-wise approach is used to start filtration of blood by the two cartridges. A centrifugal pump is used to achieve a flow rate between 0.40 and 0.75 L/min. The maximal flow rate should not exceed 0.8 L/min and pre-pump pressures should not exceed -250 mmHg to avoid the catheter to collapse or kink. The hemofiltration filters are brought online one by one, by removing the clamps. Once the cartridges are completely filled with blood, the bypass line is closed. When the hemofiltration circuit is running sufficiently and hemodynamic stability is achieved (see below), intra-arterial infusion of chemotherapeutic drugs may be started using a pump-injector and a flow rate of 0.4 ml/sec. Before and during the infusion, hepatic angiograms are obtained to ensure that hepatic blood flow is not compromised. If the angiograms show arterial spasms, this may be treated with nitroglycerine boluses of 100-200 micrograms. After the infusion, extracorporeal filtration is continued for 30 minutes ('washout period') to allow clearance of chemotherapeutics from the liver. At the end of the procedure, the effects of heparin are reversed by administration of protamine sulphate on a 1:1 basis (1 mg of protamine sulphate to antagonize 1 mg of heparine). The vascular sheaths are left in place until coagulation is sufficiently corrected, although a vascular closure device may be placed immediately after the procedure to achieve hemostasis at the arterial puncture site. The duration of the procedure is generally 3-4 hours.

ANESTHESIOLOGY AND PERFUSIONIST SUPPORT

PHP is associated with hemodynamic and metabolic changes that require monitoring and management by an experienced anesthesiologist. In early studies, the conduct of PHP under local anesthesia and sedation has been described but nowadays procedures are generally performed under general anesthesia (28,29). PHP results in significant decreases in mean arterial and central venous pressures and increases in heart rate compared to baseline (29,30). Decreases in blood pressures generally occur at two stages: upon occlusion of the IVC and when blood flow is diverted through the filters. Inflation of the balloons of the double-balloon catheter results in a decrease of central venous return and right atrium pre-load. This first drop in blood pressure is corrected by administration of fluids and norepinephrine and/or phenylephrine to maintain a mean arterial pressure above 60 mmHg. A second drop in blood pressure may be attributed to the depletion of sympathomimetics by the activated carbon filters. Infusion rates as high as 0.2-1.5 µg/kg/min for norepinephrine and 0.4-3.0 µg/kg/min for phenylephrine are generally required during the perfusion period as 67-95% of the sympathomimetics are cleared from the blood by the filters (29). A decrease in patient's body temperature is also commonly encountered during PHP and is a result of the blood flowing through the

non-heated extracorporeal circuit. In general, the hypothermia is not severe and may be reduced by using an air-warming system (30).

CHEMOTHERAPEUTIC AGENT

The majority of studies have used melphalan chloride as the chemotherapeutic agent of choice, for it has pharmacological properties to make it suitable for PHP. It can easily be administered intra-arterially, has limited liver toxicity, a high hepatic extraction rate, a very short half-life and an immediate effect on tumor cells (31,32). The currently available filtration system (Delcath hemofiltration cartridges) is specific for melphalan chloride.

Melphalan chloride is an alkylating agent of the nitrogen mustard group. Its binding to deoxyribonucleic acid (DNA) can result in cross-linking between bases on complementary strands leading to double-stranded DNA breaks and eventually cell death (8,10,33-38). In a phase I dose-escalating study with percutaneous administration, the maximum tolerated dose (MTD) of melphalan chloride was 3.0 mg/kg body weight (39). The maximum total dose is generally limited to 220 mg. Because of the short-life of melphalan chloride, the drug should be prepared in the pharmacy just prior to administration.

Several studies have used doxorubicin as the chemotherapeutic agent, mainly in patients with hepatocellular carcinoma (HCC) (29,40-43). Doxorubicin has some disadvantages over melphalan chloride as an agent for PHP. Firstly, it has a first-pass hepatic extraction fraction that is only around 60% (44). Secondly, doxorubicin is associated with considerable liver toxicity. Studies on PHP with doxorubicin have reported chemical hepatitis rates of >70% (29,40-43). The chemical hepatitis was generally mild to moderate and self-limiting. Thirdly, with the currently available filters the doxorubicin infusion time, and consequently the administered dose, is limited as prolonged infusion may lead to increased systemic exposure. In a study by Ku et al., a mean doxorubicin extraction rate of 91% was found, but the filtration rated dropped to 55% at 20 minutes (40). Nevertheless, very promising results have been obtained with doxorubicin in patients with advanced HCC with PHP as either the primary treatment or as an adjunct to surgery (see results section). The hemofiltration cartridges (DHP-1; Kuraray Co., Ltd., Osaka, Japan) used in this study differ from those in studies with melphalan chloride.

POST-PROCEDURAL CARE

Patients are monitored in a medium or intensive care unit (ICU) 12-24 hours after the procedure and are generally discharged after 2-3 days. This compares favorably to IHP for which admission to the ICU is generally several days and a mean hospital stay has been reported of 10-29 days (45). Anemia, neutropenia and thrombocytopenia may be seen early after the procedure and may (in part) reflect dilution as a result of peri-procedural fluid administration. Transfusion with fresh frozen plasma, packed red blood cells or platelets may occasionally be needed. PHP is associated with transient metabolic acidosis, but infrequently to such a degree that correction with sodium bicarbonate is required (32).

COMPLICATIONS

Table 1 provides an overview of the type and frequency of common and serious complications as reported in the literature. The most common adverse effects result from bone marrow suppression leading to neutropenia, thrombocytopenia, and/or anemia. Mild to moderate bone marrow suppression is seen in half tot three-quarters of patients. The nadir of cytopenia is generally 10–14 days after PHP. It is generally recommended to administer granulocyte colony-stimulating factor analogues (pegfilgastrim) within 48 hours after PHP to anticipate bone marrow depression. Symptomatic anemia and severe thrombocytopenia (<20.000/mm^3) may require transfusions. Regular blood tests in the first two weeks after PHP are recommended.

Complications related to multiple vascular accesses and vessel catheterization might occur. Patients are at an increased risk of puncture site bleeding as high doses of heparin are administrated during the procedure to prevent clot formation in the extracorporeal circuit. Bleeding other than from the puncture site is uncommon, but may have severe consequences (29,30,46). The hypotension associated with PHP may results in complications such as organ ischemia, but these have not been reported to date. In general, the hypotension is of short duration and responds well to administration of fluids and sympathomimetics.

The reported mortality rate of PHP is 0-13.3% (Table 1). Most of the published deaths occurred in early studies at the beginning of the learning curve and with a system that was different from the kit that is currently used. The reported IHP-related death rate is much higher than that of PHP: 5-27% (45).

LEAKAGE TO THE SYSTEMIC CIRCULATION

Bone marrow depression is a result of leakage of melphalan chloride to the systemic circulation. Increased systemic exposure to melphalan chloride may be a result of incomplete filtration of the chemotherapeutic agent by the hemofiltration filters. In a phase I dose-escalating study, pharmacological blood samples were obtained during 74 procedures in 28 patients with unresectable hepatic malignancies (38). Perfusions were performed with Hemosorba drug filtration cartridges (Asahi Medical Co, Tokyo, Japan) for which the filter extraction percentages ranged from 58.2% to 94.7%, with a mean of 77%. A 2nd generation filter system is available since 2012 and this filter was reported to have an efficiency rate of 99% in pre-clinical studies (47). Initial experiences with the 2nd generation filter seem to indicate that the degree of bone marrow depression with this filter is lower compared to that associated with previous filter systems (46).

There may be causes of melphalan chloride leakage other than through the filter system. The fact that, even with the 2nd generation filter, mild to moderate bone marrow depression is not infrequently seen seems to suggest that leakage other than through the hemofiltration system indeed occurs (46). One potential cause of leakage may be insufficient sealing of the balloon at the atriocaval junction with consequent leakage alongside the balloon. Furthermore, leakage to the systemic circulation could also be a result of the presence of collateral pathways between the IVC and azygos, hemiazygos, accessory hemiazygos, thoracolumbar and/or diaphragmatic veins. Small interconnecting veins between the aforementioned structures are not uncommon and may cause the melphalan chloride to bypass the extracorporeal filter system. Another possible mechanism may be the uptake of melphalan chloride by the hepatobiliary system and storage until the balloons are deflated, after which melphalan chloride is released systemically. However, IHP is associated with lower rates of leakage of chemotherapeutic drugs than PHP (48). Furthermore, the half-life of melphalan chloride is very short. It therefore seems less plausible that post-procedural release of chemotherapeutics by the liver is the cause of systemic toxicity.

In IHP, leakage can be monitored by injection of human serum albumin (HSA) or erythrocytes labelled with iodine-31 or technetium-99 (45,49,50). A closed, recirculating system is used in IHP and detection of labelled HSA or erythrocytes in the systemic circulation is an indication of leakage. Unfortunately, this method cannot be applied in PHP as the perfusion circuit is not a closed system and the activated carbon filters allow passage of both HSA and erythrocytes. Leakage *can* be quantified by measurement of systemic drug levels during PHP, but this does not provide real-time information as laboratory tests to determine melphalan plasma levels are rather complex and time-consuming.

Table 1. Summary of conducted studies on percutaneous hepatic perfusion.

Author	Year	No. pts (no. PHPs)	Type of hepatic malignancy (n)	Chemotherapy	Type of study	Intervention
Hughes (53)	2015	93 (max 6 per pt)	Melanoma (ocular 83; cutaneous 10)	melphalan	RCT	PHP u
Vogl (46)	2014	14 (18)	Melanoma (ocular 8; cutaneous 3), Gastric/Breast/CA (1)	melphalan	retrospective	PHP u
Fitzpatrick (57)	2014	5 (15)	Melanoma (ocular 4; cutaneous 1)	melphalan	case-series	PHP u
Fukumoto (42)	2014	68 (103)	HCC, BCLC intermediate (27) or advanced (41)	mitomycin C and/or doxorubicin	prospective,	resection + PHP
Forster (52)	2013	10 (27)	Melanoma (ocular 5; cutaneous 3, unknown 1). Sarcoma (1)	melphalan	retrospective	PHP u
Pingpank (58)	2011°	23 (68)	NET (23)	melphalan	prospective	PHP u
Miao (30)	2008	51 (136)	Melanoma (ocular 12, cutaneous 4), NET (12), CRC (7), HCC (5), RCC (4), AdrC/Breast/CA (2), Ewing (1)	melphalan	prospective	PHP u
Pingpank (39)	2005	28 (74)	Melanoma (ocular 10, cutaneous 3), CRC (2), Hepatobiliary (3), NET (4), RCC (2), AdrC/Breast/Sarcoma/PA (1)	melphalan	phase I	PHP u
Ku (59)	2004	22 (40)	HCC (22)	doxorubicin	prospective;	resection + PHP
Savier (48)	2003	4 (10)	Breast/CRC/Gastric/CA (1)	melphalan	prospective study	IHP + PHP
Ku (56)	1998	28 (39)	HCC, TNM III (1) or IV-A (27)	doxorubicin	prospective	PHP
Ku (60)	1997	16 (16)	HCC (11), CRC (1), Breast CA (1), Melanoma (1)	doxorubicin	prospective	PHP
Ku (40)	1995	15 (15)	HCC, unresectable (15)	doxorubicin	phase I	PHP
Ravikumar (29)	1994	21 (58)	HCC (5), CRC (8), Melanoma (2), Sarcoma (4), Adrenal/Pancreatic/SCLC/CA (n=1)	5-FU, doxorubin	phase I	PHP

ORR = objective response rate (complete plus partial resspone). NET = neuroendocrine tumor. HCC = hepatocellular carcinoma. CRC = colorectal carcinoma.RCC = renal cell carcinoma. AdrC = Adrenalcortical carcinoma. CA = cholangiocarcinoma. SCLC = small cell lung carcinoma. PA = periampullary carcinoma. BCLC = Barcelona Clinic Liver Criteria.

Endpoint	ORR % (n)	hPFS, median	OS, median	Complications ¶
response (primary: hPFS)	27.3% (vs 4.1% in control)	7.0 months (vs 1.6 in controls)	10.6 months (vs 10.0 in controls) W	neutropenia (85.7%), thrombocytopenia (80.0%), anemia (62.9%), self-limiting hyperbilirubinemia (14.3%), cardiac toxicity (12.9%), cerebral ischemia (1.2%), death 3.2%
response and toxicity	54 (7)	n.r.	n.r.	pancytopenia; death (7.1%; retroperitoneal hemorrhage)
feasibility and toxicity	n.r.	n.r.	n.r.	transient mild hypothermia and metabolic acidosis
response	70.6 (48)	n.r.	25 months	leukopenia (44.1%), serum AST gr. 3-4 (77.9%), hair loss (72%), gastroduodenal ulcer (4.4%)
response and toxicity	50 (5)	240 days	n.r.	bone marrow suppression; mild elevation serum troponin (70%)
response (ORR)	79	39 months	n.r.	acute transaminitis gr 3-4 (22%); neutropenia 47%, thrombocytopenia 29%, anemia (15%); death 0.04% (cholangitis)
hemodynamics and metabolic changes	n.r.	n.r.	n.r.	transient hypotension and metabolic acidosis; nasea/vomiting (10%)
MTD, toxicity, pharmacokinetics	29.6 (8)	n.r.	n.r.	neutropenia gr 3-4 (73.6%); thrombocytopenia gr 3-4 (36.8%); aneamia (21.1%)◆
efficacy	86 (19)	n.r.	1 & 5 yr OS: 86 & 47%	leukopenia (45.5%), hair loss (63.6%)
feasibility; pharmacokinetics	n.r.	n.r.	n.r.	neutropenia grade 3-4 (50%)
response and survival	63 (17)	n.r.	16 months	chemical hepatitis (71%), leukopenia (54%), hair loss (43%), thrombocytopenia (18%), hemolysis/hematuria (57%), gastroduodenal ulcer (7%), death 8% due to pancreatisis (4%) and HAT (4%)
hemodynamics, pharmacology, toxicity	n.r.	n.r.	n.r.	chemical hepatitis (75%), leukopenia (43.7%), alopecia (37.5%), thrombocytopenia (25%), hemolysis/hematuria (50%)
hemodynamics, pharmacology, toxicity, response	64 (9)	n.r.	12 months for responders (vs 5 for non-responders)	chemical hepatitis (71%), leukopenia (67%), alopecia (33%), thrombocytopenia (40%), hemolysis/hematuria (87%), gastroduodenal ulcer (14%), death 13.3% due to pancreatisis (7%) and HAT (7%)
MTD, feasibility	9.5 (2)	n.r.	n.r.	hematologic, primarily leukopenia/neutropenia; transient hypotension (78.5%)

n.r. = not reported. hPFS = hepatic progression-free survival. MTD = maximum tolerated dose. HAT = hepatic artery thrombosis. ° Only presented as an abstract. u Delcath System. ¶ List is not extensive, mortality and common complications are reported. Ω 57.1% of patients in control group crossed over to PHP. ◆ Complication rates are quoted per PHP at MTD
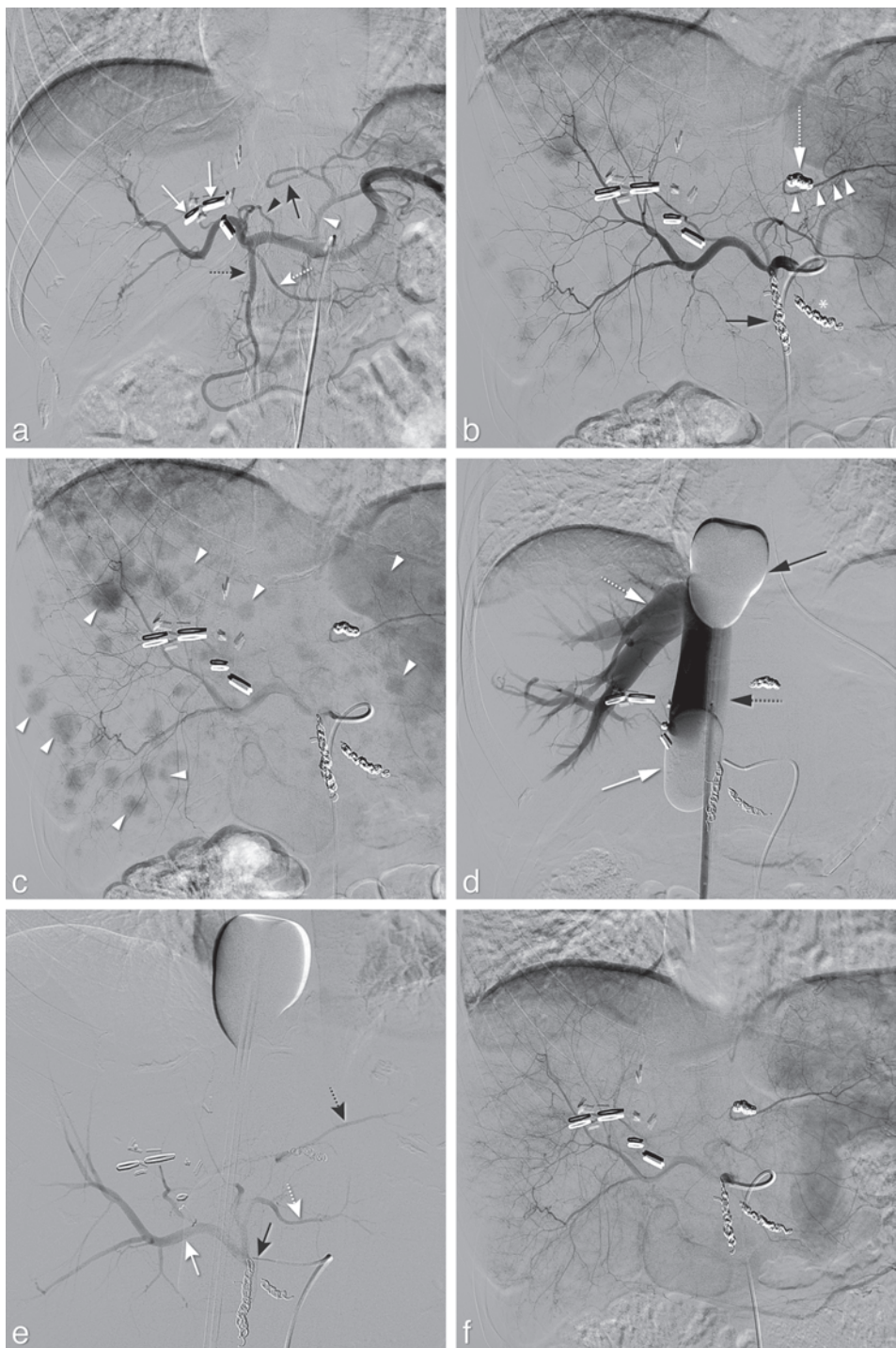
Figure 4.

RESULTS OF PHP TO DATE

The data of the efficacy of PHP is limited, and only one randomized controlled trial has been published to date. Table 1 provides an overview of PHP studies, excluding case-reports and small case-series. The number of procedures per patients varies from 1 to 3 between the different studies as the optimal treatment schedule and indications for re-treatment have not yet been established. Most studies on PHP have been conducted in patients with liver metastases from ocular melanoma (Figure 4). Patients with liver metastases from ocular melanoma are evident candidates for liver-directed locoregional therapy because of the remarkable metastatic pattern of this tumor. Metastases occur in approximately 50% of patients with ocular melanoma. In those patients with metastases, the liver is affected in 95% of patients and in 80% the disease has only spread to the liver (2,51). Ocular melanoma has a high sensitivity to melphalan chloride and there are currently no systemic therapies with proven long-term efficacy for this tumor type.

In 2005, Pingpank et al. published results of a phase I dose escalation study on PHP with melphalan chloride in 28 patients with primary and metastatic hepatic disease, establishing a MTD of 3mg/kg (39). Response and survival rates were not primary end-points, but were reported. In the 10 patients with metastases from ocular melanoma, an objective response rate (ORR) of 50% was observed: 2 complete responses (CR) and 3 partial responses (PR). In the total study group, 6 PRs were documented (21.4%). The duration of CR was 10 and 12 months and duration of PR included two patients with ongoing responses at 9 and 11 months.

← **Figure 4.** Hepatic vascular mapping and PHP in a 44-year old female with bilateral hepatic metastases from ocular melanoma. a. Angiography from the celiac trunk showed the gastroduodenal artery (GDA) (dotted black arrow), the right gastric artery (RGA) (dotted white arrow), a segment 3 artery (S3) (black arrowhead) originating from the left hepatic artery and a segment 2 artery (S2) (black arrow) originating from the left gastric artery. b. After coil-embolization of the GDA (black arrow), RGA (asterisk) and aberrant left hepatic artery (open white arrow), redistribution of flow to S2 (arrowheads) was established through intrahepatic collaterals. c. Multiple hypervascular tumors aren in both lobes (arrowheads). d. After inflation of the cranial (black arrow) and caudal (white arrow) balloon of the double-balloon catheter, the inferior caval vein (open black arrow) and right hepatic vein (white open arrow) were opacified during venography. No leakage was demonstrated alongside the balloons. e. Angiography with a micro-catheter positioned in the proper hepatic artery showed opacification of all hepatic arteries, including the right hepatic artery (white arrow), S2 (open black arrow) and S3 (open white arrow), just prior to infusion of melphalan chloride. f. At the start of the *second* PHP 6 weeks later, angiography shows complete disappearance of staining of the liver metastases. Follow-up CT and PET/CT (not shown) after two PHP procedures revealed three small residual tumors that were subsequently treated with RFA. The patient remained without evidence of disease until 1 year after the first PHP.

In a retrospective study by Forster et al., including 10 patients with hepatic metastases from ocular melanoma (n=5), cutaneous melanoma (n=3), melanoma from unknown origin (n=1) or sarcoma (n=1), nine patients (90%) had stable disease or PR on follow-up imaging (52). The median percent decrease in hepatic tumor volume was 48.6% for patients with ocular melanoma compared to 33.3% for the entire cohort. At a median follow-up of 11.5 months (range 4-55 months), median hepatic free survival was 240 days and median overall survival from the time of first PHP was 8.7 months.

A retrospective two-center study reported the results of PHP in 14 patients treated with 18 PHP procedures (46). The majority of patients (n=11; 78.5%) had liver metastases from melanoma (ocular (n=8) or cutaneous (n=3)). A 50% ORR was reported (one CR in a patient with cholangiocarcinoma and 6 PRs in patients with metastases from melanoma) and 38% patients had stable disease.

In 2016, the results were published of a multi-center, randomized controlled study comparing PHP with best alternative care (BAC) in patients with hepatic metastases from melanoma (53). The study included 93 patients with unresectable hepatic metastases from melanoma (either ocular (n=83) or cutaneous (n=10)). Patients with limited extra-hepatic disease were allowed to enter the study, although most patients (59.1 %) had metastases confined to the liver. Patients in the PHP arm (n=44) underwent a maximum of 6 isolated liver perfusions with melphalan at 4 weekly intervals. Patients in the control group (n=49) received best alternative care (BAC) with the majority of patients (81.6%) receiving active treatment such a systemic chemotherapy, chemoembolization, radio-embolization and surgery. A statistically significant improvement in hepatic progression-free survival (hPFS) and overall progression-free survival (oPFS) was demonstrated in patients treated with PHP compared to BAC. The hPFS and oPFS were 7.0 and 5.4 months respectively for the PHP group compared to 1.6 and 1.6 months respectively for the BAC group (p<0.0001). No statistically significant difference in overall survival (OS) was found between the PHP and BAC group (10.6 and 10.0 months respectively), but this was confounded by a large proportion of the patients in the BAC group (57.1 %) crossing over to receive PHP after progression of disease.

A Japanese group has published several studies on PHP in patients with HCC using a different double balloon catheter and hemofiltration system (see above). Some overlap between the patient groups in the different studies exists (42,54-56). In a prospective study, 28 patients with advanced HCC (TNM III or IV-A) underwent an average of 1.4 PHP with doxorubicin. The ORR was 63% and the OS was 16 months. The 1-, 3- and 5-year survival rates were 67.5%, 39.7% and 39.7% respectively (41). In a recent publication, the results were reported of combined reductive surgery and PHP with mitomycin C and/

or doxorubicin in 68 patients with intermediate or advanced stage HCC (42). An ORR of 70.6% was achieved with a median OS of 25 months.

FUTURE DIRECTIONS

PHP holds promise as a locoregional therapy for patients with hepatic malignancies. The ability to deliver high doses of chemotherapy with limited systemic exposure is appealing and the minimally invasive nature of the procedure offers great advantages over IHP. In phase I studies, the feasibility and toxicity profile of the procedure have been well established. Data on the efficacy of PHP is limited, but initial results are promising, especially in the treatment of liver metastases from ocular melanoma. A recent phase III trial showed superiority of PHP over BAC in patients with hepatic metastases from either

Table 2. Overview of on-going prospective studies on percutaneous hepatic perfusion

Study design	Type of hepatic malignancy	Initiation	Treatment	Estimated enrollment	End-points	Status
Phase II, single center	Ocular melanoma	Investigator[1]	PHP with melphalan 2 cycles	20	ORR, post-PHP resectibility safety, OS, HPFS, PFS, QoL	Recruiting
Phase III, multi-center	Ocular melanoma	Industry[2]	PHP with melphalan. max 6 cycles vs. BAC (dacarbazine, TACE, ipilimumab or pembrolizumab)	240	OS, PFS, ORR, HPFS, hepatic ORR, QoL	Launching 4th quarter 2015
Phase II, single center	Colorectal carcinoma	Investigator[1]	PHP with melphalan. 2 cycles	34	ORR, post-PHP resectibility safety, OS, HPFS, PFS, QoL	Recruiting
Phase II, multi-center	HCC or ICC	Industry[2]	PHP with melphalan. 2 cycles	42	ORR, safety, PFS	Recruiting
Phase II, multi-center	HCC	Industry[2]	PHP with melphalan. 3 cycles, followed by sorafenib	31	Adverse events, ORR, PFS, pharmacokinetics, QoL	Recruiting
Phase I/II	HCC	Investigator[3]	PHP followed by sorafenib	30	PFS, OS, safety	Recruiting

[1] Leiden University Medical Center, The Netherlands. [2] Delcath Systems Inc. U.S.A. [3] Kobe University, Japan. HCC= hepatocellular carcinoma. ICC= intrahepatic cholangiocarcinoma. BAC = best alternative care. TACE = transarterial chemoembolization. ORR = objective response rate. OS = overall survival. HPFS = hepatic progression-free survival. PFS = progression-free survival. QoL = Quality of Life

ocular (89.2 %) or cutaneous (10.8 %) melanoma (53). Further studies are needed to establish the role of PHP in treatment of different types of hepatic malignancies, define the optimal treatment frequency and interval and compare treatment outcomes with currently available locoregional and systemic therapies. Prospective studies on the efficacy of PHP for primary liver tumors as well as hepatic metastases from various origins are currently being conducted (Table 2).

The most frequent toxicity associated with PHP is bone marrow depression as a result of leakage of melphalan chloride. With the introduction of the 2nd generation hemofiltration system, the rate and severity of bone marrow depression appear to be reduced. To further reduce the systemic toxicity rates, further studies are needed to analyze the causes of systemic leakage of chemotherapeutics and improve the technique and hemofiltration system of PHP. Currently, melphalan chloride is the most commonly chemotherapeutic agent used for PHP. In studies using either fluorouracil or doxorubicin the affinity of the filters used was either limited or the extraction rated dropped after prolonged chemotherapy infusion (29,40). New detoxification filters factory tuned to high affinity for specific chemotherapeutics may enable more effective treatment with other drugs than melphalan chloride in the future.

In conclusion, PHP is a novel, minimally invasive and repeatable alternative to IHP. Phase I studies have demonstrated PHP to be feasible and safe. A recently published randomized controlled trial has shown improved control of liver disease compared to standard available therapy in patients with hepatic metastases from (ocular) melanoma. Further phase II and III studies are needed to define the role of PHP in the clinical management of patients with different hepatic malignancies.

REFERENCES

1. European Association for Study of THE Liver, European Organisation for Research and Treatment of Cancer. EASLEORTC clinical practice guidelines: management of hepatocellular carcinoma. Eur J Cancer. 2012;48(5):599–641.

2. Jovanovic P, Mihajlovic M, Djordjevic-Jocic J, Vlajkovic S, Cekic S, Stefanovic V. Ocular melanoma: an overview of the current status. Int J Clin Exp Pathol. 2013;6(7):1230–44.

3. Taylor I, Bennett R, Sherriff S. The blood supply of colorectal liver metastases. Br J Cancer. 1978;38(6):749–56.

4. Schenk WG Jr, McDonald JC, McDonald K, Drapanas T. Direct measurement of hepatic blood flow in surgical patients: with related observations on hepatic flow dynamics in experimental animals. Ann Surg. 1962;156:463–71.

5. van de Velde CJ, Kothuis BJ, Barenbrug HW, Jongejan N, Runia RD, de Brauw LM, et al. A successful technique of in vivo isolated liver perfusion in pigs. J Surg Res. 1986;41(6):593–9.

6. Ausman RK. Development of a technic for isolated perfusion of the liver. N Y State J Med. 1961;61:3993–7.

7. Aigner K, Walther H, Tonn J, Wenzl A, Hechtel R, Merker G, et al. First experimental and clinical results of isolated liver perfusion with cytotoxics in metastases from colorectal primary. Recent Results Cancer Res. 1983;86:99–102.

8. de Brauw LM, Marinelli A, van de Velde CJ, Hermans J, Tjaden UR, Erkelens C, et al. Pharmacological evaluation of experimental isolated liver perfusion and hepatic artery infusion with 5-fluorouracil. Cancer Res. 1991;51(6):1694–700.

9. Hafstrom LR, Holmberg SB, Naredi PL, Lindner PG, Bengtsson A, Tidebrant G, et al. Isolated hyperthermic liver perfusion with chemotherapy for liver malignancy. Surg Oncol. 1994;3(2): 103–8.

10. Marinelli A, Vahrmeijer AL, van de Velde CJ. Phase I/II studies of isolated hepatic perfusion with mitomycin C or melphalan in patients with colorectal cancer hepatic metastases. Recent Results Cancer Res. 1998;147:83–94.

11. van Etten B, de Wilt JH, Brunstein F, Eggermont AM, Verhoef C. Isolated hypoxic hepatic perfusion with melphalan in patients with irresectable ocular melanoma metastases. Eur J Surg Oncol. 2009;35(5):539–45.

12. Noter SL, Rothbarth J, Pijl ME, Keunen JE, Hartgrink HH, Tijl FG, et al. Isolated hepatic perfusion with high-dose melphalan for the treatment of uveal melanoma metastases confined to the liver. Melanoma Res. 2004;14(1):67–72.

13. Alexander HR, Libutti SK, Bartlett DL, Puhlmann M, Fraker DL, Bachenheimer LC. A phase I–II study of isolated hepatic perfusion using melphalan with or without tumor necrosis factor for patients with ocular melanoma metastatic to liver. Clin Cancer Res. 2000;6(8):3062–70.

14. Alexander HR Jr, Libutti SK, Pingpank JF, Steinberg SM, Bartlett DL, Helsabeck C, et al. Hyperthermic isolated hepatic perfusion using melphalan for patients with ocular melanoma metastatic to liver. Clin Cancer Res. 2003;9(17):6343–9.

15. van Iersel LB, Gelderblom H, Vahrmeijer AL, van Persijn van Meerten EL, Tijl FG, Putter H, et al. Isolated hepatic melphalan perfusion of colorectal liver metastases: outcome and prognostic factors in 154 patients. Ann Oncol. 2008;19(6):1127–34.

16. Rothbarth J, Pijl ME, Vahrmeijer AL, Hartgrink HH, Tijl FG, Kuppen PJ, et al. Isolated hepatic perfusion with high-dose melphalan for the treatment of colorectal

metastasis confined to the liver. Br J Surg. 2003;90(11):1391–7.

17. Alexander HR Jr, Libutti SK, Pingpank JF, Bartlett DL, Helsabeck C, Beresneva T. Isolated hepatic perfusion for the treatment of patients with colorectal cancer liver metastases after irinotecan-based therapy. Ann Surg Oncol. 2005;12(2):138–44.

18. de Wilt JH, van Etten B, Verhoef C, Eggermont AM. Isolated hepatic perfusion: experimental evidence and clinical utility. Surg Clin North Am. 2004;84(2):627–41.

19. Alexander HR Jr, Bartlett DL, Libutti SK, Fraker DL, Moser T, Rosenberg SA. Isolated hepatic perfusion with tumor necrosis factor and melphalan for unresectable cancers confined to the liver. J Clin Oncol. 1998;16(4):1479–89.

20. Facy O, Doussot A, Zinzindohoue F, Holl S, Rat P, OrtegaDeballon P. Isolated hepatic perfusion: principles and results. J Visc Surg. 2014;151(Suppl 1):S25–32.

21. Eggermont AM, van IJken MG, van Etten B, van der Sijp JR, ten Hagen TL, Wiggers T, et al. Isolated hypoxic hepatic perfusion (IHHP) using balloon catheter techniques: from laboratory to the clinic towards a percutaneous procedure. Hepatogastroenterology. 2000;47(33):776–81.

22. Burgmans MC, Kao YH, Irani FG, Dames EL, Teo TK, Goh AS, et al. Radioembolization with infusion of yttrium-90 microspheres into a right inferior phrenic artery with hepatic tumor supply is feasible and safe. J Vasc Interv Radiol. 2012;23(10):1294–301.

23. Kao YH, Hock Tan AE, Burgmans MC, Irani FG, Khoo LS, Gong Lo RH, et al. Image-guided personalized predictive dosimetry by artery-specific SPECT/CT partition modeling for safe and effective Y90 radioembolization. J Nucl Med. 2012;53(4):559–66.

24. Miyayama S, Yamashiro M, Okuda M, Yoshie Y, Sugimori N, Igarashi S, et al. Usefulness of cone-beam computed tomography during

ultraselective transcatheter arterial chemoembolization for small hepatocellular carcinomas that cannot be demonstrated on angiography. Cardiovasc Intervent Radiol. 2009;32(2):255–64.

25. Miyayama S, Yamashiro M, Hattori Y, Orito N, Matsui K, Tsuji K, et al. Efficacy of cone-beam computed tomography during transcatheter arterial chemoembolization for hepatocellular carcinoma. Jpn J Radiol. 2011;29(6):371–7.

26. Takayasu K, Muramatsu Y, Maeda T, Iwata R, Furukawa H, Muramatsu Y, et al. Targeted transarterial oily chemoembolization for small foci of hepatocellular carcinoma using a unified helical CT and angiography system: analysis of factors affecting local recurrence and survival rates. AJRAmJ Roentgenol. 2001;176(3):681–8.

27. Spreafico C, Morosi C, Maccauro M, Romito R, Lanocita R, Civelli EM, et al. Intrahepatic flow redistribution in patients treated with radioembolization. Cardiovasc Intervent Radiol. 2015;38(2):322–8.

28. Dougherty TB, Mikolajek JA, Curley SA. Safe anesthetic management of patients undergoing a novel method of treating human hepatocellular cancer. J Clin Anesth. 1997;9(3):220–7.

29. Ravikumar TS, Pizzorno G, Bodden W, Marsh J, Strair R, Pollack J, et al. Percutaneous hepatic vein isolation and high-dose hepatic arterial infusion chemotherapy for unresectable liver tumors. J Clin Oncol. 1994;12(12):2723–36.

30. Miao N, Pingpank JF, Alexander HR, Steinberg SM, Beresneva T, Quezado ZM. Percutaneous hepatic perfusion in patients with metastatic liver cancer: anesthetic, hemodynamic, and metabolic considerations. Ann Surg Oncol. 2008;15(3):815–23.

31. Rothbarth J, Koevoets C, Tollenaar RA, Tilby MJ, van de Velde CJ, Mulder GJ, et al. Immunohistochemical detection of melphalan-

DNA adducts in colon cancer cells in vitro and human colorectal liver tumours in vivo. Biochem Pharmacol. 2004;67(9):1771–8.

32.   Vahrmeijer AL, van Dierendonck JH, Keizer HJ, Beijnen JH, Tollenaar RA, Pijl ME, et al. Increased local cytostatic drug exposure by isolated hepatic perfusion: a phase I clinical and pharmacologic evaluation of treatment with high dose melphalan in patients with colorectal cancer confined to the liver. Br J Cancer. 2000;82(9):1539–46.

33.   Rothbarth J, Vahrmeijer AL, Mulder GJ. Modulation of cytostatic efficacy of melphalan by glutathione: mechanisms and efficacy. Chem Biol Interact. 2002;140(2):93–107

34.   Uzgare RP, Sheets TP, Johnston DS. Evaluation of melphalan, oxaliplatin, and paclitaxel in colon, liver, and gastric cancer cell lines in a short-term exposure model of chemosaturation therapy by percutaneous hepatic perfusion. Anticancer Res. 2013;33(5):1989–2000.

35.   de Vries MR, Borel Rinkes IH, van de Velde CJ, Wiggers T, Tollenaar RA, Kuppen PJ, et al. Isolated hepatic perfusion with tumor necrosis factor alpha and melphalan: experimental studies in pigs and phase I data from humans. Recent Results Cancer Res. 1998;147:107–19.

36.   Ku Y, Saitoh M, Iwasaki T, Tominaga M, Maekawa Y, Shiki H, et al. Intraarterial infusion of high-dose adriamycin for unresectable hepatocellular carcinoma using direct hemoperfusion under hepatic venous isolation. Eur J Surg Oncol. 1993;19(4):387–92.

37.   van Iersel LB, de Leede EM, Vahrmeijer AL, Tijl FG, den Hartigh J, Kuppen PJ, et al. Isolated hepatic perfusion with oxaliplatin combined with 100 mg melphalan in patients with metastases confined to the liver: a phase I study. Eur J Surg Oncol. 2014;40(11):1557–63.

38.   Rothbarth J, Tollenaar RA, Schellens JH, Nortier JW, Kool LJ, Kuppen PJ, et al. Isolated hepatic perfusion for the treatment of colorectal metastases confined to the liver: recent trends and perspectives. Eur J Cancer. 2004;40(12):1812–24.

39.   Pingpank JF, Libutti SK, Chang R, Wood BJ, Neeman Z, Kam AW, et al. Phase I study of hepatic arterial melphalan infusion and hepatic venous hemofiltration using percutaneously placed catheters in patients with unresectable hepatic malignancies. J Clin Oncol. 2005;23(15):3465–74.

40.   Ku Y, Fukumoto T, Iwasaki T, Tominaga M, Samizo M, Nishida T, et al. Clinical pilot study on high-dose intraarterial chemotherapy with direct hemoperfusion under hepatic venous isolation in patients with advanced hepatocellular carcinoma. Surgery. 1995;117(5):510–9.

41.   Ku Y, Iwasaki T, Fukumoto T, Tominaga M, Muramatsu S, Kusunoki N, et al. Induction of long-term remission in advanced hepatocellular carcinoma with percutaneous isolated liver chemoperfusion. Ann Surg. 1998;227(4):519–26.

42.   Fukumoto T, Tominaga M, Kido M, Takebe A, Tanaka M, Kuramitsu K, et al. Long-term outcomes and prognostic factors with reductive hepatectomy and sequential percutaneous isolated hepatic perfusion for multiple bilobar hepatocellular carcinoma. Ann Surg Oncol. 2014;21(3):971–8.

43.   Ku Y, Fukumoto T, Tominaga M, Iwasaki T, Maeda I, Kusunoki N, et al. Single catheter technique of hepatic venous isolation and extracorporeal charcoal hemoperfusion for malignant liver tumors. Am J Surg. 1997;173(2):103–9.

44.   Chen HS, Gross JF. Intra-arterial infusion of anticancer drugs: theoretic aspects of drug delivery and review of responses. Cancer Treat Rep. 1980;64(1):31–40.

45. Christoforidis D, Martinet O, Lejeune FJ, Mosimann F. Isolated liver perfusion for non-resectable liver tumours: a review. Eur J Surg Oncol. 2002;28(8):875–90.

46. Vogl TJ, Zangos S, Scholtz JE, Schmitt F, Paetzold S, Trojan J, et al. Chemosaturation with percutaneous hepatic perfusions of melphalan for hepatic metastases: experience from two European centers. Rofo. 2014;186(10):937–44.

47. Moeslein FM, McAndrew EG, Appling WM, Hryniewich NE, Jarvis KD, Markos SM, et al. Evaluation of Delcath Systems' Generation 2 (GEN 2) melphalan hemofiltration system in a porcine model of percutaneous hepatic perfusion. Cardiovasc Intervent Radiol. 2014;37(3):763–9.

48. Savier E, Azoulay D, Huguet E, Lokiec F, Gil-Delgado M, Bismuth H. Percutaneous isolated hepatic perfusion for chemotherapy: a phase 1 study. Arch Surg. 2003;138(3):325–32.

49. Runia RD, de Brauw LM, Kothuis BJ, Pauwels EK, van de Velde CJ. Continuous measurement of leakage during isolated liver perfusion with a radiotracer. Int J Rad Appl Instrum B. 1987;14(2):113–8.

50. Rothbarth J, Pijl ME, Tollenaar RA, Tijl F, Ivancev G, Mulder GJ, et al. An experimental minimally invasive perfusion technique for the treatment of liver metastases. Eur J Surg Oncol. 2003;29(9):757–63.

51. Woodman SE. Metastatic uveal melanoma: biology and emerging treatments. Cancer J. 2012;18(2):148–52.

52. Forster MR, Rashid OM, Perez MC, Choi J, Chaudhry T, Zager JS. Chemosaturation with percutaneous hepatic perfusion for unresectable metastatic melanoma or sarcoma to the liver: a single institution experience. J Surg Oncol. 2014;109(5):434–9.

53. Hughes MS, Zager J, Faries M, Alexander HR, Royal RE, Wood B, et al. Results of a randomized controlled multicenter phase III trial of percutaneous hepatic perfusion compared with best available care for patients with melanoma liver metastases. Ann Surg Oncol. 2016 Apr;23(4):1309-19.

54. Ku Y, Saitoh Y. Extracorporeal carbon chemofiltration under hepatic venous isolation for high-dose intraarterial chemotherapy of the liver. Surgery. 1994;116(5):941.

55. Ku Y, Saitoh Y. Percutaneous technique of hepatic venous isolation and charcoal hemoperfusion with a dual-balloon vena cava catheter. Surgery. 1996;119(3):360.

56. Ku Y, Tominaga M, Iwasaki T, Fukumoto T, Muramatsu S, Kusunoki N, et al. Efficacy of repeated percutaneous isolated liver chemoperfusion in local control of unresectable hepatocellular carcinoma. Hepatogastroenterology. 1998;45(24):1961–5.

57. Fitzpatrick M, Richard Alexander H, Deshpande SP, Martz DG Jr, McCormick B, Grigore AM. Use of partial venovenous cardiopulmonary bypass in percutaneous hepatic perfusion for patients with diffuse, isolated liver metastases: a case series. J Cardiothorac Vasc Anesth. 2014;28(3):647–51.

58. Pingpank JF, Royal RE, Kammula US, Kam AW, Wood BJ, Libutti SK, et al. Chemo-saturation with percutaneous hepatic perfusion (CS:PHP) using Melphalan for unresectable neuroendocrine tumor liver metastases (MNET). Abstract CIRSE 2011; FP2109.

59. Ku Y, Iwasaki T, Tominaga M, Fukumoto T, Takahashi T, Kido M, et al. Reductive surgery plus percutaneous isolated hepatic perfusion for multiple advanced hepatocellular carcinoma. Ann Surg. 2004;239(1):53–60.

60. Kawai S, Tani M, Okamura J, Ogawa M, Ohashi Y, Monden M, et al. Prospective and randomized trial of lipiodol-transcatheter

arterial chemoembolization for treatment of hepatocellular carcinoma: a comparison of epirubicin and doxorubicin (second cooperative study). The Cooperative Study Group for Liver Cancer Treatment of Japan. Semin Oncol. 1997;24(2 Suppl 6):S6-38–45.

Chapter 10

Prospective clinical and pharmacological evaluation of the Delcath System's second generation (GEN2) hemofiltration system in patients undergoing percutaneous hepatic perfusion with melphalan
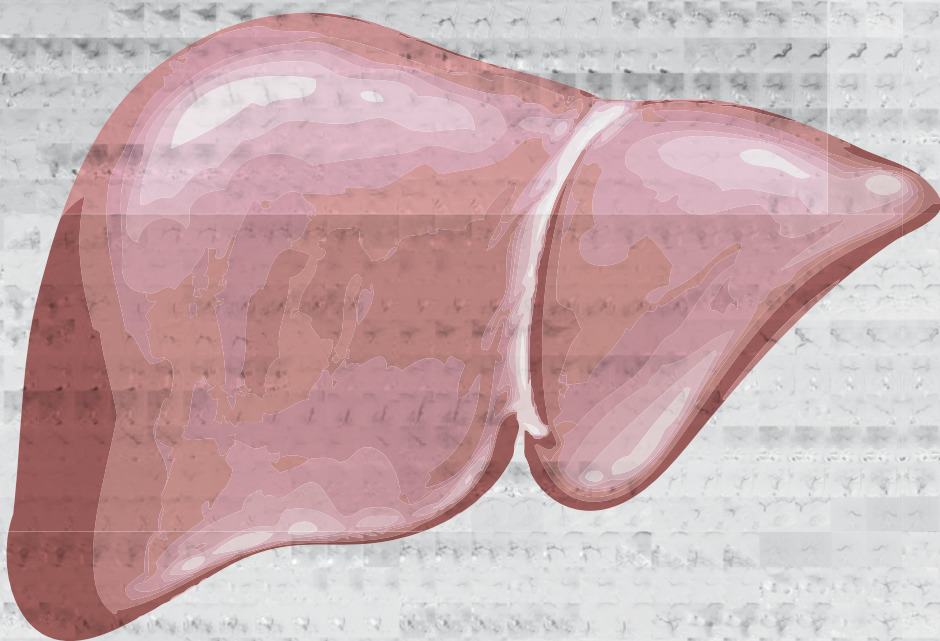
de Leede EM[*], Burgmans MC[*], Meijer TS, Martini CH, Tijl FGJ, Vuijk J, van Erkel AR, van de Velde CJH, Kapiteijn E, Vahrmeijer AL

*Both authors equally contributed to this manuscript

ABSTRACT

Purpose
Percutaneous hepatic perfusion (PHP) with melphalan is an effective treatment for patients with hepatic metastases, but associated with high rates of bone marrow depression. To reduce systemic toxicity, improvements have been made to the filtration system. In pre-clinical studies, the Delcath System's GEN2 filter was superior to the first generation filters. In this clinical study, we analysed the pharmacokinetics and toxicity of PHP using the new GEN2 filter.

Methods
Starting February 2014, two prospective phase II studies were initiated in patients with hepatic metastases from ocular melanoma or colorectal cancer. In 10 PHP procedures performed in the first 7 enrolled patients, blood samples were obtained to determine filter efficiency and systemic drug exposure. PHP was performed with melphalan 3mg/kg with a maximum of 220 mg. Complications were assessed according to CTCAE v4.03. Response was assessed according to RECIST 1.1.

Results
Pharmacokinetic analysis of blood samples showed an overall filter efficiency of 86% (range 71.1 - 95.5%). The mean filter efficiency decreased from 95.4% ten minutes after the start of melphalan infusion to 77.5% at the end of the procedure (p=0.051). Bone marrow depression was seen after up to 80.0% of 10 procedures, but was self-limiting and mostly asymptomatic. No hypotension-related complications or procedure related mortality occurred.

Conclusions
The GEN2 filter has a higher melphalan filter efficiency compared to the first generation filters and a more consistent performance. PHP with the GEN2 filter appears to have an acceptable safety profile, but this needs further validation in larger studies.

INTRODUCTION

Percutaneous hepatic perfusion (PHP) is an innovative, minimally invasive procedure that is gaining interest as a therapeutic option for patients with hepatic malignancies. A recently published randomized controlled trial (RCT) has shown superiority of PHP over best alternative care in patients with hepatic metastases from ocular and cutaneous melanoma (1). Furthermore, small prospective cohort studies have shown promising results in patients with secondary liver tumours as well as primary liver tumours (2-7). Wide acceptance of PHP in clinical practice has been halted due to concerns about the safety profile of PHP. The most notable complication of PHP is bone marrow depression resulting in anaemia, neutropenia and/or thrombocytopenia. Reported rates of complications related to bone marrow depression vary from 43.7% to 85.7% (8). In PHP, the liver vasculature is isolated from the systemic circulation using percutaneously inserted catheters. A micro-catheter is placed in the hepatic artery to deliver a high dose of the chemotherapeutic agent melphalan. Prior to the start of infusion of the chemotherapeutic drug, a double-balloon catheter is placed in the inferior caval vein (ICV). The balloons prevent leakage of chemotherapeutics to the systemic circulation by occluding the ICV at the level of the atrio-caval junction and infra-hepatic ICV. Through catheter side-holes located in between the two balloons, the chemosaturated blood returning through the hepatic veins is aspirated and the blood is then pumped through an extra-corporeal filtration system. After filtration, the blood is returned to the patient through a catheter in the internal jugular vein (8). The high rate of bone marrow depression associated with PHP indicates that systemic exposure to chemotherapeutic drugs does occur. This may result from failure to achieve complete isolation of the liver vasculature or from incomplete extraction of chemotherapeutics by the hemofiltration system. In a phase I trial including 28 patients treated with PHP, pharmacological analyses of blood samples demonstrated a mean filter extraction rate of 77% (range 58.2% - 94.7%) (9). In this study, and most of the other published studies, PHP was performed using a first generation hemofiltration system. In 2012, a second generation detoxification cartridge (GEN 2 filter; Delcath Systems, New York, NY, USA) was made commercially available. Compared to the first generation hemofiltration system, the GEN 2 filter has been modified in several ways to improve the filter extraction rate. The activated carbon particles have been changed in shape (from granular to spherical), density (from 0.600 – 0.560g/ml to 0.195 - 0.185 g/mL), size (mean ± standard deviation from 1363 ± 457 μm to 720 ±102 μm) and volume per cartridge (from 500ml to 550ml). In a porcine study, the extraction rate of the GEN 2 filter was 99 ± 0.4% (10). Initial clinical experiences seem to indicate that the use of the GEN 2 filter may indeed reduce systemic toxicity (7). In 2014, we initiated two phase II trials investigating PHP with the GEN 2 filter in patients with hepatic metastases from either ocular melanoma or colorectal carcinoma. As part of these trials, we obtained

blood samples in a subset of patients to investigate the pharmacokinetics of PHP with the GEN 2 filter. Our hypothesis was that the use of the GEN 2 filter would result in a higher filter extraction rate and lower incidence of bone marrow depression compared to those reported after PHP with the first generation filter. The primary objective of this pharmacological study was to determine the melphalan filter efficiency of the GEN 2 filter. The objective of the phase II studies was to analyse the safety and efficacy of PHP with melphalan.

METHODS

Study design and patients

In this pharmacological study the first consecutive seven patients treated with PHP were included as part of the aforementioned phase II studies. In the first three patients, pharmacological samples were also obtained during the second PHP procedure.

Thus, pharmacological data of 10 PHP procedures in 7 patients was analysed. The phase II studies and the presented pharmacological study were approved by the Local Medical Ethics Committee of the Leiden University Medical Centre. Patients were potential candidates for one of the two phase II studies, if they had histologically proven, unresectable metastases confound to the liver from either ocular melanoma or colorectal carcinoma. Patients were ineligible for surgical resection because of diffusely spread of liver disease or a metastasis not accessible for surgical resection or radiofrequency ablation, as evaluated by a multidisciplinary liver team of hepatic surgeons, medical oncologists and interventional radiologists.

Both phase II studies had similar inclusion criteria: life expectancy > 4 months, resection of the primary tumour > 4 weeks prior to PHP, aspartate aminotransferase (AST), alanine aminotransferase (ALT) and alkaline phosphatase ≤ 5 times upper limit of normal, leucocyte count ≥ 3,0 ×10^9/l, platelet count ≥ 100 × 10^9/l and estimated GFR ≥ 40 ml/min. Exclusion criteria were a World Health Organization (WHO) performance status of ≥ 2, age <18 and > 65 years, less than 40% healthy liver tissue based on computed tomography (CT) or magnetic resonance imaging (MRI), evidence of extrahepatic disease or coagulation disorders: activated partial thromboplastin time (APTT) > 32,5 seconds and prothrombin time (PT) > 13,7 seconds. Contrast-enhanced CT of chest, abdomen (arterial and venous phase) and brain were performed to exclude extra-hepatic disease and detect vascular variants precluding PHP. All patients underwent pre-procedural angiography with cone-beam CT. The later was used to exclude extrahepatic enhancement and vascular tumor supply from extrahepatic collaterals. All patients provided written informed consent for

the study. Patients were routinely scheduled to undergo two PHP procedures with a six-week interval, in case there was no progression of disease after the first PHP.

PHP procedure

Details of the PHP procedure have been described previously (8). The following description is a summary of the most relevant parts of the procedure. Procedures were performed under general anesthesia in the angiography room by a dedicated team of an interventional radiologist, anesthesiologist and perfusionist. After creation of vascular accesses to both internal jugular veins, the right common femoral vein and left hepatic artery, heparin was administrated to achieve an activated clotting time (ACT) of > 400 sec. A 2.7F microcatheter (Progreat, Terumo, Tokyo, Japan) was placed in the hepatic artery to deliver melphalan. A double balloon catheter (Isofuse Isolation Aspiration catheter, Delcath Systems Inc., New York, USA) was positioned in the ICV and the balloons were inflated to prevent the flow of chemosaturated blood to the systemic circulation (Figure 1). During set-up and initiation of the extracorporeal filtration circuit, sufficient blood pressure was maintained by the anesthesiologist by administration of fluids and intravenous infusion of norepinephrine and/or phenylephrine. All PHP procedures were performed with the GEN 2 filtration system. Melphalan (Alkeran, Aspen, Dublin, Ireland) was infused at a dose of 3mg/kg (with a maximum of 220mg) at a rate of 0.4 ml/sec in about 30 minutes. After melphalan infusion, extracorporeal circulation of blood returning through the hepatic veins was maintained for an additional 30 minutes ('wash-out' period). At the end of the procedure, protamine sulphate was administrated to reverse the effects of heparin. Patients were monitored in a medium or intensive care unit 12-24 hours after the procedure. Patients were discharged from the hospital at day 3 after PHP.

Pharmacological sampling

Blood samples were taken simultaneously from the median cubital vein as well as of the tubing before and after the filter of the extracorporeal system starting 10 minutes after commencement of melphalan infusion (T_{10}), at the end of melphalan infusion ($T_{end\ infusion}$) and at the end of the wash-out period ($T_{end\ wash-out}$) (Figure 1). In addition to this, venous (systemic) blood samples were obtained 10 and 20 minutes after the start of the wash-out period, at the end of the wash-out period and 5, 30, 60 and 120 minutes after the end of the wash-out period. Blood was drawn in 10 mL sodium heparin tubes and placed in ice immediately after collection. Directly after the PHP procedure, the blood samples were centrifuged for 10 minutes at 1000G at room temperature. After centrifugation, the plasma was split into two aliquots and stored in cryovials at -70ºC until analysis. All samples were analysed for melphalan by a high-performance liquid chromatographic analysis with ultraviolet detection as previously described (11). The detection limit of
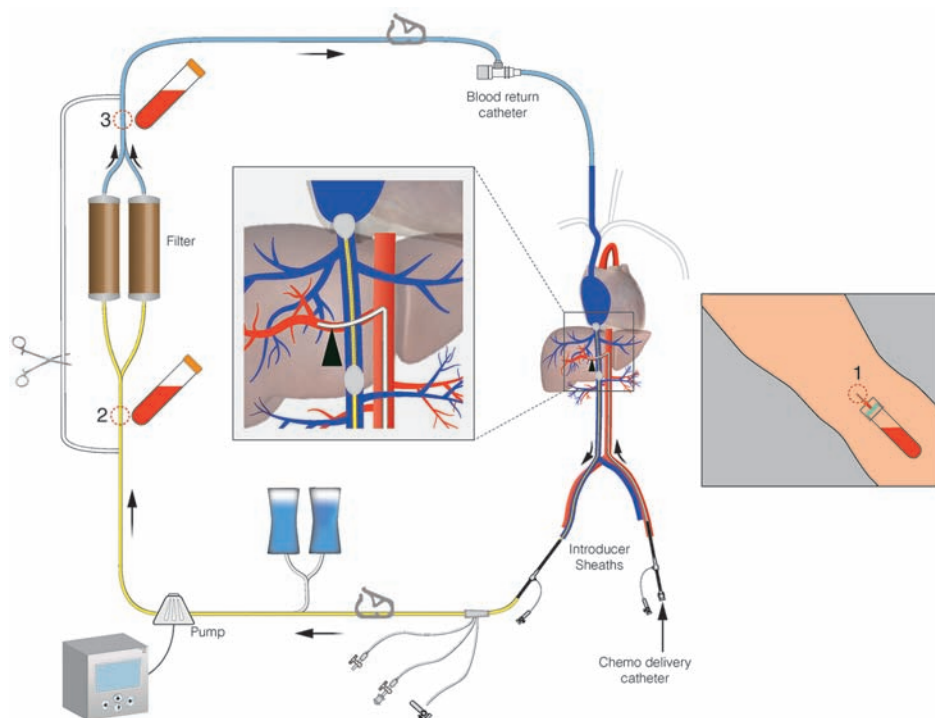
Figure 1. Schematic overview of PHP circuit. Indicated are the pharmacokinetic sampling points

melphalan in plasma was 0.5 µg/ml. The intra-assay coefficients of variation were 2,5% for melphalan in plasma in the concentration range of 0.5 -5.0 µg/ml and the inter-assay coefficients of variation were 12.4% for melphalan in plasma in the concentration range of 0.5 µg/ml, and 3.6% for melphalan in plasma in the concentration range of 5.0 µg/ml.

Safety and efficacy of PHP

Blood tests were performed on each patient prior to treatment, on day 1, 2, 3, 9, 12, 15 and 18 after PHP and then weekly, until both blood cell count and liver function tests were normalized or reduced to grade I-II toxicity according to the common terminology criteria for adverse events v4.03 (CTCAE v4.03). Routine study blood tests included: full blood count, APTT, PT, international normalized ratio (INR), glucose, creatinine, sodium, potassium, bilirubin, amylase, alkaline phosphatase, ALT, AST, lactate dehydrogenase (LDH), γ-glutamyl transferase, protein, albumin, bicarbonate. Routine follow-up included visits to the outpatient clinic at 1 and 6 weeks and then every three months as well as telephonic consultation at day 9, 12, 15 and 18. Patients underwent CECT of the abdomen and chest (including arterial phase of the liver) 4 and 12 weeks after the first PHP procedure and every 3 months thereafter. In patients with poor visibility of metastases

on CT, multiphase MRI of the liver was performed instead of CECT of the abdomen. If the CECT at 4 weeks post-PHP did not demonstrate disease progression and no complications occurred during the first PHP that contra-indicated repeated treatment, patients underwent a second PHP procedure as per protocol.

Outcome assessment

Technical success was defined as the successful delivery of the prescribed dose of melphalan.

The mean filter efficiency of the GEN 2 filters was determined by calculation of the difference between the areas under the plasma melphalan concentration-time curves (AUC) before and after the filter. The AUCs were calculated with the trapezoidal rule. The overall mean filter efficiency was calculated as follows: ((prefilter AUC) – (postfilter AUC)/ (prefilter AUC)) x100. For the filter efficiency at a specific time point, the filter efficiency was calculated using the pre- and post filter concentrations ((prefilter concentration T_x) – (postfilter concentration T_x)/(prefilter concentration T_x)) x100. The maximum concentration (Cmax) was defined as the peak systemic concentration of melphalan during a PHP procedure. Post-procedural blood test abnormalities, toxicity and adverse events were assessed according to CTCAE v4.03. Haematological laboratory disorders occurring within 3 days after PHP were categorized as 'early' and those occurring more than 3 days after PHP as 'late'. Early haematological complications were considered to be related to the procedure itself, i.e. to the dilution of blood as a result of fluid administration and/ or to haemolysis by the hemofiltration system. Late haematological complications were most likely attributable to bone marrow depression as a result of melphalan toxicity. CT and MRI scans were assessed by an independent abdominal radiologist according to Response Evaluation Criteria for Solid Tumors version 1.1 (RECIST 1.1). Time to progression and overall survival were assessed.

Statistical analysis

The filter extraction rates for all perfusions at different time points are expressed as mean ± standard deviation (SD). The mean filter efficiency rates and mean melphalan plasma concentration were compared using a paired t-test. Time-to-progression and overall survival was expressed in months as mean and median ± SD. All data were analysed using SPSS software for Windows version 20 (SPSS, Chicago, Illinois, USA). Graphs were created using GraphPad Prism 6 Software for Windows (GraphPad Software, La Jolla California USA). A difference was considered significant when p<0.05.

RESULTS

Patients and procedure

Patients and tumour characteristics of the 7 patients are listed in Table 1. Median age at time of treatment was 57 years (range 42-64 years); 5 patients were males. All patients received previous treatment for their hepatic metastases, such as systemic chemotherapy, radiofrequency ablation (RFA) or immunotherapy in a clinical trial. Four out of the seven patients underwent two technically successful PHP procedures as per protocol, however not all these procedures were included in this pharmacological study. Three patients underwent only one PHP procedure. One patient was reluctant to undergo a second PHP as the first procedure was complicated by pancytopenia with severe bacterial pharyngitis. In another patient, the CT 6 weeks after the first procedure showed progression of colorectal hepatic metastases and this patient did therefore not undergo a second PHP procedure. The third patient developed a pulmonary embolus three weeks after the procedure and was reluctant to undergo a second PHP. All ten PHP procedures were technically successful. Median duration of infusion for all procedures was 45 minutes (range 39 – 55 minutes). The overall mean duration of the entire PHP procedure was 4:02 hours (range 3:26 – 4:45h). The perfusion parameters are listed in Table 2. All patients were successfully treated with the planned dose of 3 mg/kg body weight, with a maximum dose of 220 mg of melphalan. The median follow-up was 24 months (interquartile range 9.0-26.5 months).

Pharmacokinetic analysis

Heparinized blood samples were successfully obtained during all ten PHP procedures as per protocol. A summary of the Cmax, Area Under the Curve (AUC) and filter efficiency is shown in Table 3. The overall mean filter efficiency during 10 PHP procedures was 86.0% (range 71.1 %–95.5%). No significant differences were observed in filter efficiency and systemic concentrations between the first and second procedure in the patients that underwent two procedures. Figure 2 illustrates the changes in filter efficiency during the 10 PHP procedures. The mean filter efficiency at specific time points decreased from 95.4% (range 82.7-100%) at T_{10} to 77.5% (range 30-100%) at $T_{end\ washout}$ (p=0.051).

Figure 3 displays the mean plasma concentration of melphalan of all patients during the PHP procedure. The systemic concentration increases rapidly during the infusion period. The mean peak melphalan plasma (Cmax) was 1.1 μg/ml (range 0,5-1,8 μg/ml). In the majority of the procedures (67%), Cmax occurred at $T_{end\ infusion}$. The melphalan plasma concentration decreased rapidly after cessation of infusion and was undetectable in the blood samples in all patients 2 hours after the start of the infusion.
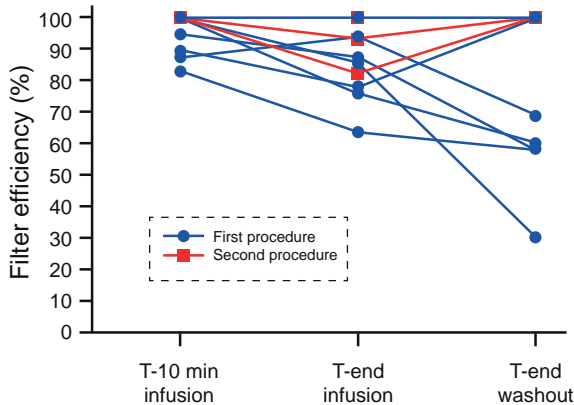
Figure 2. Filter efficiency per patient at different time-points during the procedure.
The mean filter efficiency was calculated at three time points during the 10 procedures. First at ten minutes after the start of the melphalan infusion, than at the end of the melphalan infusion and at the end of the wash-out period.
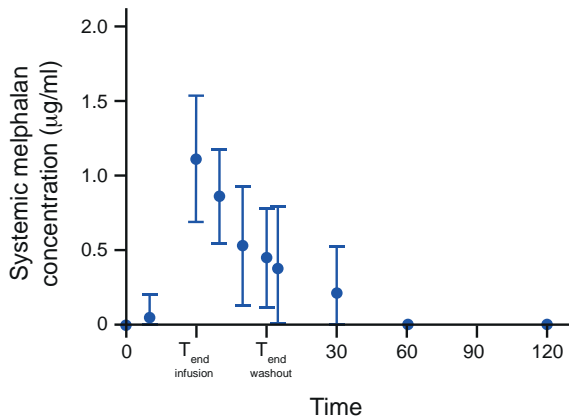

Figure 3. Mean systemic concentration of melphalan of all patients over time.
A mean concentration of systemic melphalan was calculated at different time points, for all ten procedures, the bars indicate the standard deviation (SD). The horizontal dotted line at 0.5 µg/ml indicates the detection limit of melphalan in plasma.

Safety of PHP

Procedure-related adverse events in all 10 PHP procedures are summarized in Table 3. This excludes peri-procedural transient hypotension, which was seen and managed successfully by the anesthesiologist in all patients and did not result in any hypotension-related complications. Haematological laboratory disorders were the most common post-procedural complication. Early (<3 days) anaemia and thrombocytopenia grade III occurred after 10% of the procedures. No early grade III or IV leukopenia or neutropenia were observed, but asymptomatic early grade III (40%) or IV (10%) lymphocytopenia occurred after half of the perfusions. Late haematological complications, indicative of bone marrow depression, were observed in the majority of patients in our study. Late grade III/IV leukopenia, neutropenia and thrombocytopenia were observed after 80.0%, 80.0% and 40.0% of perfusions respectively. After the first two procedures, pancytopenia occurred: the first patient was asymptomatic, but the second patient was admitted to the IC because of a bacterial pharyngitis. After this, the protocol was amended; dur-

Table 1. Characteristics of 7 patients with unresectable liver metastases treated with percutaneous hepatic perfusion.

PT	Sexe/ Age	Type of cancer	Time between first diagnosis and PHP (months)	Time between diagnosis liver metastases and PHP months)	No. PHP's	Best response	Time to progr. (months)	Location of progression	Status	Follow up after first perfusion (months)
1	M, 57	UM	105	34	2	PR	28	Liver	Alive	28†
2	F, 62	UM	36	6	1	PR	9	Liver	Dead	11
3	M, 42	UM	36	3	1	PR	11	Bone, liver	Alive	26
4	M, 58	CRC	34	34	1	SD	1	Lymph node, LTR	Dead	7
5	M, 46	CRC	28	27	2	PR	5	Lung	Alive	27
6	F, 43	UM	40	16	2	PR	14	Liver	Alive	25‡
7	M, 64	CRC	30	30	2	SD	5	Lung	Alive	24

Abbreviations: PT = patient; PHP = percutaneous hepatic perfusion; UM = uveal melanoma; CRC = colorectal cancer; LTR = local tumor recurrence at colonic anastomosis
† 2nd perfusion was followed by radiofrequency ablation (RFA) of 6 small residual tumors.
‡2nd perfusion was followed by RFA of 3 small residual tumors. Because of hepatic progression another 2 perfusions were performed.

Table 2. Treatment parameters for the ten procedures

Procedure	Dose melphalan (mg)	Duration PHP procedure (hours)	Duration of melphalan infusion (min)	Duration of filtration (min)	Location of infusion
1	220	3:58	NR	75	PHA
2	180	3:26	51	88	RHA
3	220	3:05	50	85	PHA
4	220	3:28	40	81	LHA (180mg) and RHA (40mg)
5	165	3:54	40	82	PHA
6	210	3:59	39	98	PHA
7	220	4:44	43	79	Anterior branch RHA (110 mg) and LHA (110 mg)
8	220	4:45	45	80	PHA (110 mg) and replaced RHA (110mg)
9	210	3:55	40	95	PHA
10	220	4:15	55	84	PHA (110 mg) and replaced RHA (110mg)

NR = not recorded. PHA = proper hepatic artery. LHA = left hepatic artery.

ing subsequent procedures 6 mg of granulocyte colony-stimulating factor (GCSF) was administered 48 hours after the treatment. Four patients received blood transfusion to

Table 3. Outcomes of filter efficiency in 10 procedures

Parameter (n=10)	Cmax (µg/ml)	AUC (h.mg/L)		Filter efficiency*	Filter efficiency at time T_x (%) $\pm$			
		Pre-filter	Post-filter	Overall	$T_{10}^{\$}$	$T_{end\,infusion}^{\$}$	$T_{end\,washout}^{\$}$	Mean
Mean	1,13	4,29	0,57	86,0	95,4	85,9	77,5	86,3
SEM	0,13	0,28	0,0	2,5	2.1	3.6	8.1	3,7
Median	1,15	4,55	0,49	87,2	100	86,3	84.4	86,2
Minimum	0,50	2,20	0,23	71,1	82.7	63,6	30,0	68.2
Maximum	1,80	5,20	1,30	95,5	100	100	100	100
Range	1,30	3,00	1,07	24,4	17.2	36.4	70	31.8

SEM = standard error of the mean

*$((AUC_{prefilter}- AUC_{postfilter})/AUC_{prefilter})$ x 100

±$((prefilter\ concentration) – (postfilter\ concentration)/(prefilter\ concentration))$ at time T_x

$\$$t10 versus t30: p=0,013; t30 versus t60: p=0,290; t10 versus t60: p=0,051. (p for significance is p<0.017)

correct post-procedural blood cell abnormalities. No relation was found between the occurrence of grade III-IV haematological complications and the administered melphalan dose. In all patients haematological laboratory values had returned to baseline within 3 weeks. Mean time for blood cell count to return to normal was 8.3 days (range 3-20) for thrombocytes (normal lab value 150-400 $\cdot10^9$/L) and 13 days (range 5-18) for leukocytes (normal lab value 40-10 $\cdot10^9$/L).

Efficacy of PHP

Although response and survival rates were not the primary endpoints of this pharmacological study, all patients were assessable for response evaluation. The results are displayed in Table 1. A partial response was achieved in all patients with ocular melanoma liver metastases (n=4). The mean TTP in these patients was 15.5 months (range: 9-28 months). In the patients with CRC metastases (n=3), partial response was achieved in one patient (33.3%) and the mean TTP of this patient was 4.3 months (range: 1-5 months).

DISCUSSION

In our study, we demonstrated an overall mean filter efficiency of 86.0% in patients undergoing PHP with the GEN 2 filter. The efficacy of this filter compares favorably to that of first generation PHP-filters. As mentioned in the introduction, the mean filter extraction rate of the first generation filter (Hemosorba; Asahi Medical, Tokyo, Japan) was found to be 77% in a phase I study (9). Apart from a better filter efficiency, also a more consistent performance of the GEN 2 filter was observed. The filter extraction rate varied from 71.1% to 95.5%, whereas a considerably wider range has been reported with the

Table 4. Main procedure-related adverse events by severity in all perfusions (n=10), categorized as early phase (day 0-3) and late phase (day 4-6 weeks after perfusion).

CTCAE*		All grades (n)	Grade 3 (n)	Grade 4 (n)
Hematologic events				
Anemia	*Early*	9	1	-
	Late	9	1	-
Thrombocytopenia	*Early*	9	1	-
	Late	9	-	4
Leukopenia	*Early*	3	-	-
	Late	8	1	7
Neutropenia	*Early*	-	-	-
	Late†	8	-	8
Lymphocytopenia	*Early*	8	4	1
	Late†	9	6	1
Hepatic events				
Elevated AST level	*Early*	5	-	-
	Late†	3	-	-
Elevated ALT level	*Early*	3	-	-
	Late†	2	-	-
Elevated serum bilirubine level	*Early*	1	-	-
	Late†	2	-	-
Other				
Fever		2	-	-
Thromboembolic event‡		1	1	-
Post-procedural hemorrhage±		2	-	-
Pharyngitis≠		1	1	-
Alopecia		1	-	-
Nausea		2	-	-
Edema limbs€		1	-	-

Abbreviations: CTCAE, Common Terminology Criteria for Adverse Events; AST, aspartate aminotransferase; ALT, alanine aminotransferase.
* Grades of adverse events were defined according to CTCAE (version 4.0).
† Not determined in 1 perfusion.
‡ Pulmonary emboli (PE) was diagnosed in one patient 17 days after PHP. Symptoms resolved in after treatment with low-molecular weight heparin.
± Bleeding from puncture site groin, managed conservatively.
≠ Sepsis based on bacterial pharyngitis for which intravenous antibiotics and immunoglobulins were given, followed by aspiration of retropharyngeal abscess.
€ As a result of administration of intravenous fluid during procedure.

Hemosorba filter (range 58.2% - 94.7%). The mean filtration rate in our study was lower than that obtained in in-vivo, pre-clinical studies. In a study including 6 pigs treated with PHP with the first generation filter, the filter extraction rate was 99% (10). Clearly,

outcomes of a well-controlled laboratory animal experiment may differ from PHP in a clinical setting. Furthermore, the lower filter efficacy in our study may be related to differences between pigs and humans in liver volume and hepatic blood flow rates and volumes. In our study the mean efficiency dropped from 95.4% at T_{10} to 77.5% at $T_{end\ infusion}$, although the difference did not reach statistical significance. Pre-clinical studies have also shown that the filter efficiency decreases during the perfusion (10). We hypothesize that the filter is more saturated at the end of the procedure. Based on this study finding, we recommend shortening the time that a patient is on the extracorporeal filtration system. This requires optimal coordination between members of the team performing the procedure and timely ordering of melphalan, as the short half-life of the drug mandates preparation shortly before the start of infusion. Furthermore, infusion time can be shortened by coil-embolization of variant hepatic arteries during the pre-procedural angiography. By this so-called consolidation of hepatic arterial inflow, the locations of infusion can be reduced and thus the need for repositioning of the catheter during the procedure. This strategy has been well established in the treatment of liver tumors with radioembolization (12,13). The low percentage of early grade III/IV anaemia, leukopenia, neutropenia and thrombocytopenia indicates that the modified activated carbon of the GEN 2 filter does not cause significant haemolysis. After half of the perfusions early grade III /IV lymphocytopenia occurred. As decreases in number were much less frequent for other blood cells, the observed early lymphocytopenia may also be related to causes other than haemolysis by the filter. Factors such as pre-procedural fasting, peri-procedural stress or administration of corticosteroids and fluids may play in role in causing lymphocytopenia.

Late haematological complications, indicative of bone marrow depression related to systemic exposure to melphalan, were observed in the majority of patients in our study. The rates of bone marrow depression in our study are comparable to those reported after PHP with the first generation filter (8). Our study findings thus indicate that the improved filtration rate of the GEN 2 filter does not translate to lower rates of grade III/IV haematological complications. It is important to note though, that grading of leukopenia, neutropenia and thrombocytopenia according to CTCAE v4.03 is based on laboratory investigations, not on symptoms. The second patient included in our study, developed pancytopenia complicated by bacterial pharyngitis. All consecutive patients received gCSF and none experienced symptoms related to bone marrow depression. Furthermore, in all patients haematological disorders were transient. There has been some speculation over the cause of systemic exposure to melphalan in patients undergoing PHP. It has been suggested that systemic toxicity may be related to causes other than incomplete filtration by the hemofiltration system (8). In a small prospective study by Savier et al, 4 patients underwent surgical isolated liver perfusion followed by one or

two consecutive percutaneous liver perfusions (2). For the percutaneous procedures, a closed circuit was created using thread-occlusion of the hepatic artery and portal vein occlusion with a transhepatic occlusion-balloon. Blood returning from the hepatic veins was pumped into the hepatic artery and no hemofiltration system was used. In all percutaneous liver perfusions, leakage of melphalan was seen and grade III or IV neutropenia occurred after two-thirds of the procedures. In the surgical procedures, systemic levels of melphalan were almost undetectable and no grade III or IV hematological complications occurred. The authors postulated that leakage may occur alongside the balloons or though veins around the common bile duct or the diaphragmatic veins. In our study, systemic exposure to melphalan may have been caused by either incomplete filtration and/or leakage due to incomplete isolation of the hepatic circulation. Unfortunately, we were unable to differentiate between these two different causes of systemic exposure to melphalan.

Clearly, the toxicity of PHP with melphalan has to be balanced against the potential benefits. To date, there are limited treatment options for patients with metastatic ocular melanoma. No standard systemic therapy is available and chemotherapy, immunotherapy or targeted therapies have not yet been able to show improved survival (14). Radio-embolization and transarterial chemoembolization are effective locoregional therapies for patients with primary and secondary liver tumors, but the results in patients with liver metastases from ocular melanoma has only been described in retrospective, small cohort studies (15,16). The superiority of PHP with melphalan over best alternative care (BAC) has been demonstrated in a multi-center RCT including 93 patients with unresectable hepatic metastases from either ocular (n = 83) or cutaneous (n = 10) melanoma (1). The hepatic progression-free survival (hPFS) and overall progression-free survival (oPFS) in the PHP group were 7.0 and 5.4 months respectively, compared to 1.6 and 1.6 months respectively for the BAC group (p < 0.0001). Given the potential benefit, we consider the safety profile of PHP to be acceptable in patients with hepatic metastases from ocular melanoma and PHP should therefore be considered as a first line therapy for these patients. For patients with colorectal cancer metastases several other treatment options are available, such as chemotherapy, radio-embolisation or targeted therapy. Therefor the place of PHP as treatment option for these patients has yet to be determined.

The small sample size is the most important limitation of our study. Another limitation is related to the difficulties of melphalan analysis, which precluded immediate assessment of melphalan levels during the procedure and only allowed detection of melphalan above a threshold of 0.5 μg/ml. The inability to detect melphalan levels below 0.5 μg/ml may have led to overestimation of the filter efficiency at the different time-points. Yet,

this limitation had little influence on determination of the overall filter efficiency as this was measured as area under the curve using the trapezoid method.

In conclusion, our study demonstrates that the filtration rate of the GEN 2 hemofiltration system performs better than the first generation filtration system. The filter efficiency decreases during the PHP procedure. Despite the improved filtration rate, haematological laboratory disorders grade III/IV are common, but these are transient and usually asymptomatic.

REFERENCES

1. Hughes MS, Zager J, Faries M, Alexander HR, Royal RE, Wood B et al. Results of a Randomized Controlled Multicenter Phase III Trial of Percutaneous Hepatic Perfusion Compared with Best Available Care for Patients with Melanoma Liver Metastases. Annals of surgical oncology. 2016;23(4):1309-19.

2. Savier E, Azoulay D, Huguet E, Lokiec F, Gil-Delgado M, Bismuth H. Percutaneous isolated hepatic perfusion for chemotherapy: a phase 1 study. Archives of surgery. 2003;138(3):325-32.

3. Ku Y, Iwasaki T, Tominaga M, Fukumoto T, Takahashi T, Kido M et al. Reductive surgery plus percutaneous isolated hepatic perfusion for multiple advanced hepatocellular carcinoma. Annals of surgery. 2004;239(1):53-60.

4. Miao N, Pingpank JF, Alexander HR, Steinberg SM, Beresneva T, Quezado ZM. Percutaneous hepatic perfusion in patients with metastatic liver cancer: anesthetic, hemodynamic, and metabolic considerations. Ann Surg Oncol. 2008;15(3):815-23.

5. Forster MR, Rashid OM, Perez MC, Choi J, Chaudhry T, Zager JS. Chemosaturation with percutaneous hepatic perfusion for unresectable metastatic melanoma or sarcoma to the liver: a single institution experience. J Surg Oncol. 2014;109(5):434-9.

6. Fitzpatrick M, Richard Alexander H, Deshpande SP, Martz DG, Jr., McCormick B, Grigore AM. Use of partial venovenous cardiopulmonary bypass in percutaneous hepatic perfusion for patients with diffuse, isolated liver metastases: a case series. Journal of cardiothoracic and vascular anesthesia. 2014;28(3):647-51.

7. Vogl TJ, Zangos S, Scholtz JE, Schmitt F, Paetzold S, Trojan J et al. Chemosaturation with percutaneous hepatic perfusions of melphalan for hepatic metastases: experience from two European centers. RoFo : Fortschritte auf dem Gebiete der Rontgenstrahlen und der Nuklearmedizin. 2014;186(10):937-44.

8. Burgmans MC, de Leede EM, Martini CH, Kapiteijn E, Vahrmeijer AL, van Erkel AR. Percutaneous Isolated Hepatic Perfusion for the Treatment of Unresectable Liver Malignancies. Cardiovascular and interventional radiology. 2016;39(6):801-14.

9. Pingpank JF, Libutti SK, Chang R, Wood BJ, Neeman Z, Kam AW et al. Phase I study of hepatic arterial melphalan infusion and hepatic venous hemofiltration using percutaneously placed catheters in patients with unresectable hepatic malignancies. J Clin Oncol. 2005;23(15):3465-74.

10. Moeslein FM, McAndrew EG, Appling WM, Hryniewich NE, Jarvis KD, Markos SM et al. Evaluation of Delcath Systems' Generation 2 (GEN 2) melphalan hemofiltration system in a porcine model of percutaneous hepatic perfusion. Cardiovascular and interventional radiology. 2014;37(3):763-9.

11. Sparidans RW, Silvertand L, Dost F, Rothbarth J, Mulder GJ, Schellens JH et al. Simple high-performance liquid chromatographic assay for melphalan in perfusate, rat liver and tumour tissue. Biomedical chromatography : BMC. 2003;17(7):458-64.

12. Abdelmaksoud MH, Louie JD, Kothary N, Hwang GL, Kuo WT, Hofmann LV et al. Consolidation of hepatic arterial inflow by embolization of variant hepatic arteries in preparation for yttrium-90 radioembolization. Journal of vascular and interventional radiology : JVIR. 2011;22(10):1364-71.

13. Borggreve AS, Landman AJ, Vissers CM, De Jong CD, Lam MG, Monninkhof EM et al. Radioembolization: Is Prophylactic Embolization of Hepaticoenteric Arteries Necessary?

A Systematic Review. Cardiovascular and interventional radiology. 2016;39(5):696-704.

14. Luke JJ, Triozzi PL, McKenna KC, Van Meir EG, Gershenwald JE, Bastian BC et al. Biology of advanced uveal melanoma and next steps for clinical therapeutics. Pigment cell & melanoma research. 2015;28(2):135-47.

15. Eschelman DJ, Gonsalves CF, Sato T. Transhepatic therapies for metastatic uveal melanoma. Seminars in interventional radiology. 2013;30(1):39-48.

16. Valpione S, Aliberti C, Parrozzani R, Bazzi M, Pigozzo J, Midena E et al. A retrospective analysis of 141 patients with liver metastases from uveal melanoma: a two-cohort study comparing transarterial chemoembolization with CPT-11 charged microbeads and historical treatments. Melanoma research. 2015;25(2):164-8.

PART III

PATIENT MANAGEMENT
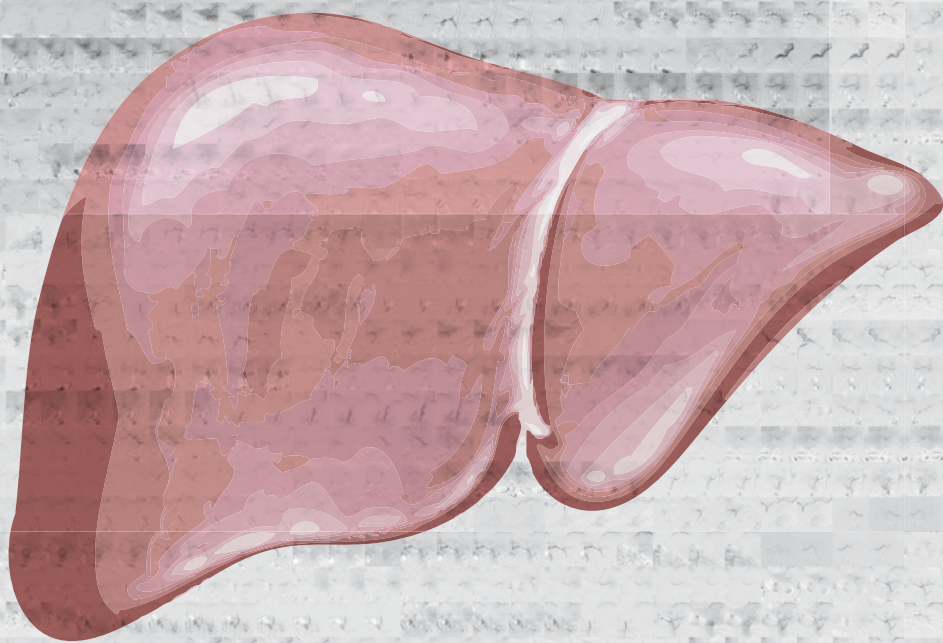
Chapter 11

Impact on patient safety and satisfaction of implementation of an outpatient clinic in interventional radiology (IPSIPOLI-study): a quasi-experimental prospective study
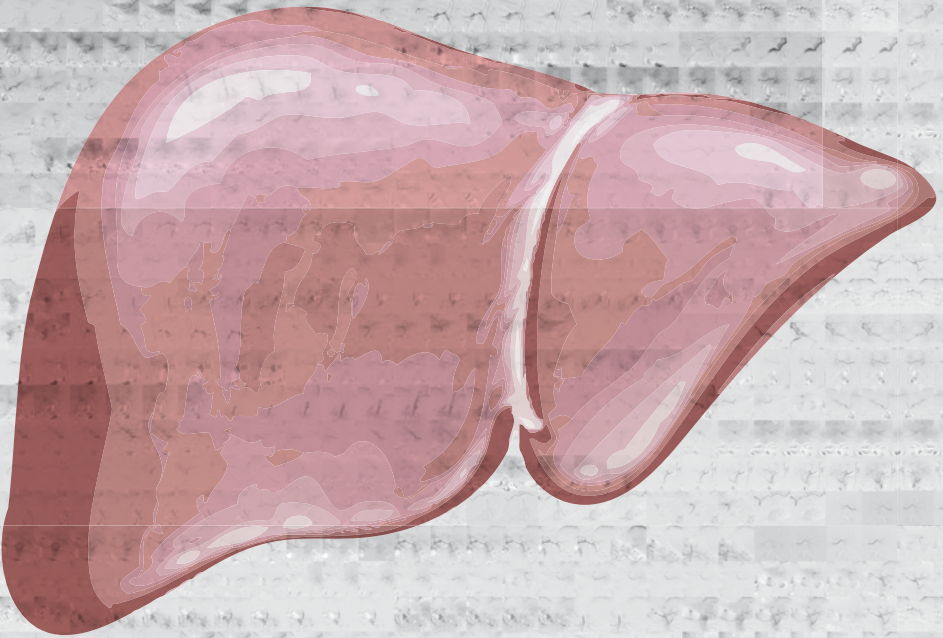
Lutjeboer J*, Burgmans MC*, Chung K, van Erkel AR

ABSTRACT

Purpose

Interventional radiology (IR) procedures are associated with high rates of preparation and planning errors. In many centers, pre-procedural consultation and screening of patients is performed by referring physicians. Interventional radiologists have better knowledge about procedure details and risks, but often only get acquainted with the patient in the procedure room. We hypothesized that patient safety (PS) and patient satisfaction (PSAT) in elective IR procedures would improve by implementation of a pre-procedural visit to an outpatient IR clinic.

Methods

IRB approval was obtained and informed consent was waived. PS and PSAT were measured in patients undergoing elective IR procedures before (control group; n=110) and after (experimental group; n=110) implementation of an outpatient IR clinic. PS was measured as the number of process deviations. PSAT was assessed using a questionnaire measuring Likert scores of three dimensions: interpersonal care aspects, information/communication and patient participation. Differences in PS and PSAT between the two groups were compared using an independent *t*-test.

Results

The average number of process deviations per patient was 0.39 in the control group compared to 0.06 in the experimental group (p<0.001). In 9.1% patients in the control group, no legal informed consent was obtained compared to 0% in the experimental group. The mean overall Likert score was significantly higher in the experimental group compared to the control group: 2.68 (SD 0.314) versus 2.48 (SD 0.381) (p<0.001).

Conclusions

PS and PSAT improve significantly if patients receive consultation and screening in an IR outpatient clinic prior to elective IR procedures.

INTRODUCTION

In 1964 Charles Dotter performed the first percutaneous transluminal angioplasty (PTA) in a patient with a superficial femoral artery stenosis (1). This was the beginning of a new medical specialty: interventional radiology (IR). For years, transarterial therapies such as PTA and stent placement have been the hallmark of IR. Over the past two decades, many new IR procedures have been introduced for indications other than atherosclerotic occlusive disease. Thanks to technological innovations, the realm of IR now offers a wide variety of minimally invasive treatments such as uterine artery embolization, biliary stenting, percutaneous ablation, transarterial (chemo)embolization, radioembolization, vertebroplasty, and etcetera. In contrast to the technological revolution of IR, organization of patient care in many IR departments has seen limited change since the days of Charles Dotter. Many IR centers have not taken full responsibility for the care of patients and still rely on the referring physician to organize aspects of care other than the procedure itself. Such practice is questionable in a time where procedure complexity and indications have expanded to such an extent that few physicians other than the interventional radiologist will have sufficient insight into the potential benefits and harms of a procedure.

Studies have shown that IR procedures are associated with high rates of preventable errors related to pre-planning and patient preparation (2,3). Such errors may result in treatment delay or last-minute postponement and could jeopardize patient safety (2,3). Also, the way informed consent is currently obtained for many IR procedures raises legal concerns. In many centers, patients will only get acquainted with the interventional radiologist performing the procedure once they have arrived at the procedure room (4).

Improvements have been made in many hospitals by the introduction of IR safety checklists, as it has in our institution (2,5). Yet, we hypothesized that further improvements could be made if patients undergoing elective IR procedures would be screened and consented preoperatively in an IR outpatient clinic. We therefore conducted a prospective study with the aim to compare patient safety and patient satisfaction between patients who were subjected to a pre-procedural visit to an IR outpatient clinic (experimental group) and those who were not (control group).

METHODS

Design

The study was conducted in accordance with the ethical standards of the institutional review board (IRB) and with the 1964 Helsinki declaration and its later amendments. Informed consent was waived by the IRB.

The study was designed as a single center, non-randomized, and prospective study. Patient safety and patient satisfaction were assessed prospectively in patients undergoing elective IR procedures. Outcomes were assessed in a group of patients before implementation of the IR outpatient clinic (control group) and then compared to those in a group of patients who were treated after implementation of the IR outpatient clinic and had made a visit to the clinic. The primary purpose of the study was to compare patient safety associated with elective IR procedures between the experimental group and the control group. The secondary purpose was to compare patient satisfaction between the two groups.

Power-analysis (Medclac version 12.4.0.0; Medcalc software) was based on a type 1 error of 0.05, a power of 80% and the assumption that implementation of an IR outpatient clinic would lead to a 14% reduction in the number of process deviations. This resulted in a calculated sample size of 220 patients with 110 patients in each group.

Particpants

Patients undergoing an elective IR procedure during the study period were eligible if they were older than 16 years and mentally capable to fill out the Dutch questionnaire. Patients undergoing one of the following procedures were excluded: peripheral vascular interventions and endovascular aortic repair (EVAR), cerebral interventions, non-elective interventions, change of drainage catheter or contrast injection through a drainage catheter, combined surgical and IR procedure, ultrasound-guided biopsy, or bone biopsy (Figure 1). At the time of commencement of the study a close collaboration existed in our institution between interventional radiologists and vascular surgeons. Interventional radiologists were already involved in screening and consenting of patients in the vascular clinic, vascular surgeons were participating in peripheral vascular interventions in the angiography room and all EVARs were performed by a team of interventional radiologists and vascular surgeons. We therefore excluded patients undergoing peripheral vascular interventions or EVAR. The second category of patients was not included as cerebral interventions in our institution were already routinely preceded by outpatient consultation by a neuro-interventionalist. Ultrasound-guided biopsy and bone biopsy were excluded in order not to cause any diagnostic delay. Our institution is committed to a

national program that guarantees a diagnosis within 48 h for 80 % of patients suspected to have one of 23 pre-defined cancer types.

Prior to their appointment for an elective IR treatment, patients were informed of the details and intent of the study by letter. Patients in the experimental group were invited for a visit to the outpatient clinic. All patients were asked to fill out a questionnaire after the procedure at a voluntary basis. If patients indicated that they were unwilling to visit the IR outpatient clinic or fill out the questionnaire, they were excluded from the study (Figure 1).
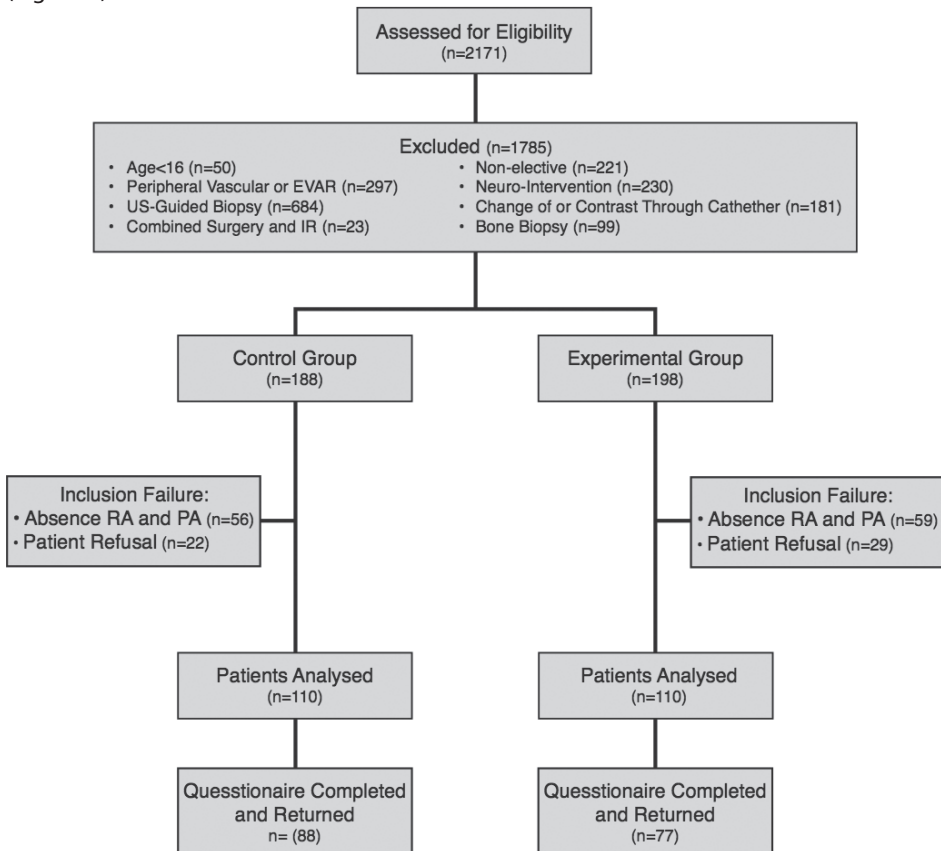
Figure 1. Flow diagram showing total number of patients screened, exclusion numbers and reasons, and per group analysis. RA research assistant, PA physician assistant

Intervention

Patients in the experimental group were scheduled for an appointment in the IR outpatient clinic 2-14 days prior to the IR-procedure. During the appointment patients would be screened for risk factors and provided with information about the procedure by an interventional radiologist or physician assistant. In the same setting informed consent

would be obtained. A key point list was used to ensure screening and consenting was performed adequately (Table 1). All relevant matters discussed were recorded in the electronic patient records (EZIS, Chipsoft, The Netherlands).

Patients in the control group were not routinely screened or consented by medical IR staff prior to the procedure. Before the procedure, one of two IR administrative assistants would perform a pre-procedural check to verify whether blood tests had been taken in accordance with IR protocols and whether anesthesiological support and specific tools were ordered as requested by the interventional radiologist. If the administrative assistant felt that blood tests were abnormal or missing, they would inform the interventional radiologist who would then contact the referring physician. The administrative assistant would also check whether the patient was using anti-coagulants and contact the patient by telephone to verify that instructions were given to temporarily stop the medication if deemed necessary. Prior to the procedure both the IR technician and interventional radiologist would assess different items of an IR safety checklist to ensure that the procedure could commence safely. Upon arrival at the procedure room, patients were asked whether the procedure and complication risks had been explained to them sufficiently. If a patient or the interventional radiologist felt that insufficient information had been provided, additional information was given. If the referring physician had recorded in the patient records that informed consent had been obtained, the informed consent was considered to be sufficient (written informed consent is not mandated in the Netherlands).

Outcome assessment

Baseline characteristics that were recorded included age, sex and the type of procedure.

The primary outcome patient safety was assessed by measurement of the number of process deviations. A process deviation was defined as 'an aspect of healthcare not executed correctly or not in accordance with IR protocols'. Process deviations were assessed using an IR safety checklist containing sections related to 'pre-procedural planning' and 'sign-in' (Figure 2). The checklist was derived from the IR patient safety checklist of the Cardiovascular and Interventional Radiological Society of Europe (CIRSE) (5). Each section of the checklist was assessed by an independent research assistant or physician assistant at the time of the IR procedure. When there was some overlap between process deviations in two sections, only one process deviation could be scored in one of both sections. For example, a patient not having fastened before the procedure may have been a result of either a lack of information (Fasting Order Given in 'Pre-procedural planning') or the wrong instructions being given (Patient Fasting in 'Sign-in').

Table 1. Key point information and outpatient screening list

Information	Discussed		
Procedure			
Indication	☐ Yes	☐ No	
Method of anaesthesia	☐ Yes	☐ No	
Procedure details explained	☐ Yes	☐ No	
Procedure length discussed	☐ Yes	☐ No	
Expected treatment outcome explained	☐ Yes	☐ No	
Complications			
Bleeding	☐ Yes	☐ No	☐ N.A.
Infection	☐ Yes	☐ No	☐ N.A.
Thrombus/embolus	☐ Yes	☐ No	☐ N.A.
Neurogenic complications	☐ Yes	☐ No	☐ N.A.
Non-Target	☐ Yes	☐ No	☐ N.A.
Allergy	☐ Yes	☐ No	☐ N.A.
Pneumothorax	☐ Yes	☐ No	☐ N.A.
Other	☐ Yes	☐ No	☐ If yes, specify:
Post-procedure			
Puncture site care	☐ Yes	☐ No	☐ N.A.
Drain management	☐ Yes	☐ No	☐ N.A.
Suture management	☐ Yes	☐ No	☐ N.A.
Pain management	☐ Yes	☐ No	☐ N.A.
Admission Time	☐ Yes	☐ No	☐ N.A.
Other	☐ Yes	☐ No	☐ If yes, specify:
Screening	Checked		
Contra-indications	☐ Yes	☐ No	
Contrast allergy	☐ Yes	☐ No	
Renal function	☐ Yes	☐ No	
Anti-coagulation	☐ Yes	☐ No	
Other medication	☐ Yes	☐ No	
Other allergy	☐ Yes	☐ No	

The secondary endpoint patient satisfaction was assessed by means of a validated questionnaire. The design and content of the questionnaire was based on the Consumer Quality Index (CQI)-measurement instruments on outpatient care (6). The questionnaire included 19 questions in Dutch measuring three dimensions: interpersonal aspects of care (5 items; α=0.82; 1 factor), information and communication (7 items; α=0.85; 1 factor) and patient participation (3 items; α=0.63; 1 factor). Examples of the questionnaire were: "Did the doctor listen carefully to you?" and "Did the doctor explain things

in an understandable way?". The items were assessed on a 4-point Likert scale (strongly disagree, somewhat disagree, somewhat agree, and strongly agree). Four questions did not correlate with these three dimensions and were measured separately (Table 4). The answers of individual patients were anonymized for interventional radiologists and referring physicians.

Figure 2. IR patient safety checklist

Statistical analysis

Data from the PS checklists and the questionnaires was analyzed using IBM SPSS Statistics 20 software (Chicago, IL, USA). Differences in baseline characteristics between the two groups were compared using a Chi-Square test. For patient safety, differences in the mean process deviations between the two groups were tested using an independent t-test.

Patient satisfaction scores were calculated for each dimension. The total Likert score for the three dimensions were calculated by adding up the score of each dimension (α > 0.60). The scores of the separate questions were assessed per question. Differences in the mean scores between the two groups were tested using an independent *t*-test. All statistical analyses were two-tailed and values of p<0,05 were considered significant.

RESULTS

Participants

The study was conducted from April 2013 till January 2014. After inclusion of patients in the control group, a 4-week period was used to implement the IR outpatient clinic. Inclusion of patients in the experimental group commenced after these 4 weeks. The patient characteristics are listed in Table 2.

Table 2. Baseline characteristics for control and experimental group

Characteristic	Control group (n = 110)	Experimental group (n = 110)	p
Age (mean ± SD)	56.6 ± 16.1	57.9 ± 14.7	0.514
Sex (N)			0.050
Male	63	77	
Female	47	33	
Questionnaires response (N %)	88 (80.0%)	77 (70.0%)	
Type of procedure (N %)			0.011
Ablations	27 (24.5%)	29 (26.5%)	
Biopsy	33 (30.0%)	43 (39.1%)	
Drainages	15 (13.5%)	4 (3.6%)	
Embolization	15 (13.5%)	24 (21.8%)	
Central venous access	15 (13.5%)	5 (4.5%)	
Stents / PTA non -arterial	5 (4.5%)	5 (4.5%)	

The number of female patients in the experimental group was significantly lower than in the control group: 33 versus 47 (p=0.050). Also, there was a significant difference in the type of procedure between the groups (p = 0.011).

Patient safety

The differences in patient safety between the two groups are listed in Table 3 and 4. The number of process deviations per patient was significantly lower in the experimental group compared to the control group: 0.06 versus 0.39 (p < 0.001). Significant differences in the number of process deviations were seen between the two groups in both

sections of the IR safety checklist, 'pre-procedural planning' and 'sign-in'. No process deviations were seen in 'pre-procedural planning' in the experimental group, whereas 0.22 process deviations per patient occurred in this section in the control group (p < 0.001). All patients in the experimental group had given legal informed consent, whereas 9.1% (n=10) of patients in the control group had not been consented adequately. Significant differences between the two groups were also seen in the section 'sign in': 0.06 process deviation per patient in the experimental group versus 0.17 in the control group (p = 0.021). Most process deviations in the section 'sign in' were related to the administration of antibiotics. Four patients in the experimental group and 7 patients in the control group received prophylactic antibiotics prior to ablation of a liver tumor, while this was deemed unnecessary according to IR protocols. The doctors prescribing the antibiotics had followed the preoperative protocol used for surgical liver resection. Five patients in the control group arrived at the angiography room for a percutaneous gastrostomy without administration of prophylactic antibiotics as mandated by IR protocols.

In the experimental group, there were no delays in treatment and 3 (2.7 %) postponements. In 2 of the 3 procedures that were postponed, the coagulation profile was unknown and blood tests had to be ordered before the procedure could be safely commenced. In the third patient, the creatinin or estimated glomerular filtration rate had not been determined prior to the procedure. In the control group, 19 (17.3 %) of the procedures where delayed to allow time to correct for process deviations. In 17 (15.5 %) procedures, the process deviation could not be corrected with the patient in the procedure room and the procedure was postponed to a later time or date. The causes for the postponement were: indication insufficiently discussed with the referring physician or in a multidisciplinary team (n = 2), missing relevant medical history (n = 2), absence of specific tools or material (n = 4), failure to stop anticoagulation medication (n = 2), fasting order not given (n = 3) or not correctly executed (n = 3), unknown coagulation profile (n = 1).

Patient satisfaction

The results of the questionnaires are summarized in table 5. Total patient satisfaction showed a significance difference between the two groups in favor of the experimental group (p<0.001). Significant improvement in patient satisfaction was seen after implementation of the IR outpatient clinic in all dimensions. The largest difference between the two groups occurred in the dimension 'Information and communication': an increase in the Likert scale score of 0.26 was seen after implementation of the IR outpatient clinic (p<0.001).

Table 3. Process deviations per item of both sections for control and experimental group

Characteristic	Control group (n = 110)	Experimental group (n = 110)
Items process deviations (N)		
Pre-procedural planning		
Discussed referring Physician / MDT	2	0
Imaging studies reviewed	1	0
Relevant Medical history	2	0
Informed Consent/ complications discussed	10	0
CIN prophylaxis	0	0
Specific Tools present/ordered	4	0
Fasting Order Given	3	0
Relevant lab test ordered	0	0
Anaesthesiologist necessary	0	0
Anticoagulation medication stopped	2	0
Post interventional (ICU) bed required	0	0
Treatment limitation checked	0	0
Total Pre-procedural planning	24	0
Sign In		
All records with patient	0	0
Correct patient/side/site	0	0
Patient fasting	3	0
IV access	3	0
Coagulation checked	1	1
CIN checked	0	2
Other lab tests checked	0	0
Allergies and/or prophylaxis checked	0	0
Antibiotics/ other drugs administered	12	4
Total Sign In	19	7
Total Pre-procedural planning and Sign in	43	7

Table 4. Overall number of process deviations per patient

Characteristic	Control group (n = 110)	Experimental group (n = 110)	p
Process deviations (Mean ± SD)			
Pre-Procedural planning	0.22 ± 0.531	0.00 ± 0.000	< 0.001
Sign In	0.17 ± 0.425	0.06 ± 0.245	0.021
Pre-Procedural + Sign In	0.39 ± 0.779	0.06 ± 0.245	< 0.001

Table 5. Questionnaire outcomes: average score per dimensions of patient satisfaction, for separate questions and overall score per group

Characteristic	Control group (n = 88)	Experimental group (n = 77)	p
Dimensions of patient satisfaction			
Interpersonal Aspects	2.73 ± 0.402	2.89 ± 0.291	0.005
Information and communication	2.57 ± 0.571	2.83 ± 0.262	< 0.001
Participation	2.38 ± 0.754	2.59 ± 0.613	0.067
Separate questions (Mean ± SD)			
Interpersonal aspect			
Was Doctor knowledgeable?	2.88 ± 0.357	2.87 ± 0.380	0.770
Information and communication			
Information was consistent with the actual treatment?	2.57 ± 0.770	2.75 ± 0.520	0.075
Information about duration of the treatment in accordance with the actual treatment?	2.34 + 0.887	2.53 ± 0.644	0.120
Properly informed about preparation of the treatment	2.51 ± 0.919	2.65 ± 0.762	0.262
Overall Patient Satisfaction			
Patient satisfaction without separate questions	2.45 ± 0.398	2.67 ± 0.301	< 0.001
Patient satisfaction	2.48 ± 0.381	2.68 ± 0.314	< 0.001

DISCUSSION

In our study, we investigated the impact of implementation of a pre-procedural visit to an IR outpatient clinic for patients undergoing an elective IR procedure. The results show that patient safety and patient satisfaction improve significantly when patients receive preoperative screening and consultation in such a clinic.

In patients who were not seen in the clinic, a high rate of process deviations occurred: 0.39 per patient. After implementation of the clinic the number of process deviations was reduced to 0.06 per patient.

A study by Koetsier et al. has shown that the number of process deviations associated with IR procedures decreases when an IR safety checklist is used (2). Such a checklist was used for all patients in our study. The use of the checklist allowed detection and correction of process deviations prior to commencement of the procedure in most patients in our study. Yet, it did not prevent delay and postponement of procedures in 17.3% and 15.5% of patients, respectively. After implementation of an IR outpatient clinic the

percentage of delays and postponements was reduced to 0% and 2.7% respectively. The results of this study thus indicate that an IR outpatient clinic has additional value to IR safety checklists and implementation of such a clinic may lead to further improvements in patient safety.

Furthermore, implementation of the clinic resolved another important matter. Adequate informed consent had not been obtained prior to arrival of the patient at the procedure room in 9.1% (n=10) of patients in the control group. This high rate of inadequate informed consent in patients undergoing IR procedures is consistent with other reports. A survey by O'Dwyer et al. revealed that in 56% of patients consent or re-consent for IR procedures is obtained in the procedure room and only 22% of patients are consented in an outpatient clinic (4). Requirements for legal informed consent vary per country, but the following three concepts of legal medical informed consent are widely accepted (7). Medical treatment can only be started after a patient's permission. Secondly, in order for the patient to make a decision, information about the patient's medical condition, the treatment purposed and alternatives should be given in lay terms. Finally, the expected benefits and potential harms of the treatment should be explained to the patient. Legislation is usually not very specific on how these matters should be achieved, but obviously consent should be given in a proper manner, in an appropriate environment and in the presence of appropriate and relevant information (7). Most people would affirm that consent for elective procedure should be obtained some time before the procedure and in an outpatient setting. Patients should be given time to think about the information provided to them and to read additional information from booklets or any other accessible medium. It seems reasonable to assume that interventional radiologists have better knowledge about details of an IR procedure than referring physicians and should therefore be the ones discussing relevant details with a patient. In our study, the number of patients without timely and adequate informed consent decreased to zero percent after implementation of an IR outpatient clinic.

Patient satisfaction is of paramount importance in building a good relationship between doctors and patients. In our study, patient satisfaction improved significantly by the implementation of an IR outpatient clinic. All aspects of patient care that were investigated (interpersonal aspects of care, information and communication and participation) improved after the IR clinic was implemented. The largest improvement in patient satisfaction was perceived in matters related to 'patient information and communication'. The provided information on pre-procedural preparation, procedural details and the length of the procedure was also perceived to be more accurate in patients in the experimental group compared to the control group. This may not only have a positive effect on the

relationship between doctors and patients, but may also have consequences for the legitimacy of the informed consent.

Over the last decades, IR has ridden the tidal wave of technological innovation to become a well-recognized medical specialty offering treatment for a variety of indications. Long gone are the days when interventional radiologists were the plumbers of the human vascular system with vascular surgeons being their main contractors. IR now caters to many different medical specialists offering a variety of therapies for many different indications. Despite the evolution of IR, in many centers the interventional radiologist has retained the traditional role between the stage scenes as a technician applauded for his catheter skills. A growing number of radiologists are now urging interventional radiologists to enter the stage as clinicians (8-10). Our study shows that indeed both patient safety and patient satisfaction improve when IR takes on the responsibility to perform screening and provide information for patients undergoing IR procedures. It was Charles Dotter who said that the radiologist 'who enters into treatment …can now play a key role, if he is prepared and willing to serve as a true clinician' (1). It is time for interventional radiologists to pay tribute to the father of IR by following his advice. This will also require diagnostic colleagues and hospital administrators to recognize the role of interventional radiologists as clinicians, allocating them time to perform the duties that come with it.

Our study has some limitations. Firstly, we were not able to account for the Hawthorne effect (11). IR staff may have enhanced their efforts to reduce process deviations or to satisfy patients, knowing that they were being observed. Secondly, regression-to-the-mean may have had impact on the study results. Thirdly, the impact of the IR outpatient clinic was assessed in a quasi-experimental experiment. Thus, it is possible that the observed changes were to some extend affected by changes in time. Yet, the study period was only 7 months during which only minimal changes in policy and IR staff occurred. Fourthly, we measured a surrogate outcome, process deviations, to assess patient safety. A study comparing the complication rate between the experimental and control group would have required a much larger sample size. The majority of process deviations in the control group could be corrected before commencement of the procedure, but not without causing delay or postponement in many patients. Finally, we excluded patients undergoing peripheral vascular interventions, EVAR or neuro-interventions from our study for reasons explained above. These patients make up a large portion of all IR patients. Although our study results cannot automatically be extrapolated to these patients, it seems reasonable to assume that similar principles apply in these subgroups of patients. We acknowledge the fact that practices may vary from country to country and even from institution to institution. It may therefore not be possible to extrapolate

our study findings to all institutions, but we believe the outcomes of our study to be applicable to many IR centers.

In conclusion, our study shows that the number of process deviations associated with elective IR procedures can be significantly reduced when patients are consulted in an IR outpatient clinic prior to the procedure. Also, by providing pre-procedural patient consultation in an outpatient setting IR can improve the satisfaction of patients. More patients will perceive the pre-procedural information provided by them as adequate and the number of patients in whom informed consent is inadequate can be reduced to zero. After the completion of our study, we have implemented a visit to the IR outpatient clinic for patients undergoing elective IR procedures of moderate to high complexity. Patients undergoing elective procedures of low complexity, such as routine biopsies, venous catheters or drainages, are receiving telephone consultation.

REFERENCES

1. Dotter CT. Transluminal angioplasty: a long view. Radiology. 1980 Jun;135(3):561-4.

2. Koetser IC, de Vries EN, van Delden OM, Smorenburg SM, Boermeester MA, van Lienden KP. A checklist to improve patient safety in interventional radiology. Cardiovasc Intervent Radiol. 2013 Apr; 36(2):312-319.

3. Morbi AH, Hamady MS, Riga CV, Kashef E, Pearch BJ, Vincent C, et al. Reducing error and improving efficiency during vascular interventional radiology: implementation of a preprocedural team rehearsal. Radiology. 2012 Aug; 264(2):473-483.

4. O'Dwyer HM, Lyon SM, Fotheringham T, Lee MJ. Informed consent for interventional radiology procedures: a survey detailing current European practice. Cardiovasc Intervent Radiol. 2003 Sep-Oct;26(5):428-433.

5. Lee MJ, Fanelli F, Haage P, Hausegger K, Van Lienden KP. Patient safety in interventional radiology: a CIRSE IR checklist. Cardiovasc Intervent Radiol. 2012 Apr; 35(2):244-246.

6. Delnoij DM, Rademakers JJ, Groenewegen PP. The Dutch Consumer Quality Index: an example of stakeholder involvement in indicator development. BMC Health Serv Res. 2010;10:88.

7. Cannavale A, Santoni M, Mancarella P, Passariello R, Arbarello P. Malpractice in radiology: what should you worry about? Radiol Res Pract. 2013:219259.

8. Introduction to clinical interventional radiology. Murphy TP. Semin Intervent Radiol. 2005 Mar;22(1):3-5.

9. Soares GM, Murphy TP. Clinical interventional radiology: parallels with the evolution of general surgery. Semin Intervent Radiol. 2005 Mar;22(1):10-14.

10. Practice Guideline for Interventional Clinical Practice. American College of Radiology; American Society of Interventional and Therapeutic Neuroradiology; Society of Interventional Radiology; J Vasc Interv Radiol. 2005 Feb;16(2 Pt 1):149-155.

11. Fernald DH. An assessment of the Hawthorne Effect in practice-based research. J Am Board Fam Med. 2012 Jan-Feb;25(1):83-86.

Chapter 12

General discussion
and future perspectives
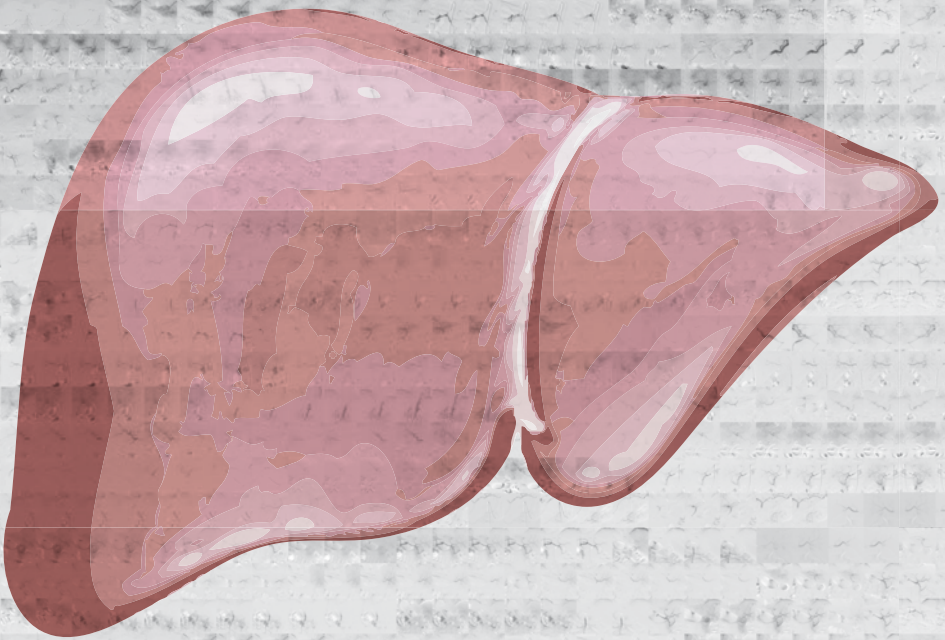
INTRODUCTION

When thinking about ways to cure cancer, the human brain is tempted to oversimplify. The idea that we will one day find the perfect solution to treat cancer is appealing and conceivable, but unlikely given the historical facts. In the past, doctors (mostly surgeons) believed we might be able to eradicate cancer by radical surgery. Yet, despite the tremendous contribution surgery has made to improve the life-expectancy of cancer patients on a whole, even aggressive surgery provides little chance of a cure in metastatic cancer. For long, people have been hopeful that chemotherapy would provide a definitive solution to metastatic cancer. In the past century, a multitude of clinical trials have been conducted in many different cancer types, often with ever-intensified regimes of combination chemotherapy. We now know that chemotherapy provides a cure in some and palliation in many patients, but there still are many cancer patients that are desperately in need of better therapies. Over recent years we have turned our hopes on targeted molecular therapies, propelled by the successes in unraveling the genetics of oncogenesis. Despite the many promising trials that have been conducted over recent years, there is a lesson to be learned from the past. It is very likely that we will see some spectacular breakthroughs in cancer treatment in the coming years, but it is unlikely that targeted or molecular drugs will solve it all. The battle against cancer will need to be fought along many lines of medical research. Some inventions will have a tremendous impact on the life of cancer patients, whereas other research will only have limited effect. Yet, the only way we stand a chance to defeat cancer is by trying in many different ways. By bringing together the ingenuity and efforts of many, we will change the perspective of cancer patients of the future. This thesis is a contribution, albeit small, to the fight against cancer. This thesis focuses on patients with hepatic malignancies.

PART 1. RADIOFREQUENCY ABLATION

Improvements in outcomes after percutaneous ablation may be achieved in different ways. Identifying and selecting those patients that will benefit most from RFA is an important first step. The study presented in **Chapter 2** demonstrates that the survival rate between patients from distinct geographical regions may differ as a result of differences in baseline parameters and patient selection. As demonstrated in this study, tumor size >3cm and tumor number >1 are independent risk factors for recurrence (csHR = 1.568; 95% CI: 1.083-2.271 and 1.494; 95%CI: 1.031-2.163 respectively). This finding is consistent with previous reports in the literature (1-3). As shown in our study, patients from a Northern-European country have a higher cumulative incidence of death despite

lower recurrence rates. This underlines the importance of factors such as the etiology of underlying liver disease and disease stage at the time of treatment.

Further advances in the field of RFA may be achieved through improvements in tumour targeting. As discussed in **Chapter 3**, co-registration of US and CT/MRI images can be performed using manual, semi-automatic or automatic co-registration. Our phantom study with the GE Logiq E9 navigation software demonstrated that the accuracy of automatic co-registration is inferior to manual co-registration and semi-automatic co-registration. The mean registration mismatch was ≤ 2.5mm for both manual and semi-automatic co-registration in our study. This is consistent with other phantom studies using similar image fusion technology (4). Unfortunately, the accuracy of co-registration is lower in a clinical setting as a result of factors such as the deformability of tissue, breathing and movement. New image fusion technology should compensate for such factors as well as provide ways to obtain easier and faster image fusion.

A third way to improve the outcome after RFA is through the combination of ablation with other therapies, such as TACE, radioembolization or systemic treatment (see below). Also, other ablation techniques may prove to be a solution to the limitations of RFA, as they are less (microwave ablation) or non-dependent (irreversible electroporation) on thermal conductivity of tissue.

In **Chapter 4**, we investigated the use of TACE as an adjuvant treatment to RFA in HCC >3cm. Unfortunately, the combination of RFA with adjuvant drug eluting bead-TACE was associated with low rates of local tumor control and survival. The 3-year local tumor progression free-survival and overall survival after combined treatment was 17.9% and 59.4% respectively. This compares unfavorable with results obtained with RFA with neo-adjuvant TACE, but comparison of results is problematic, as the different studies have been conducted in distinctly different patient cohorts.

PART 2. TRANSARTERIAL LIVER THERAPIES

TACE is generally considered as a palliative treatment, as complete tumor necrosis is often not achieved. Incomplete tumor necrosis may be a result of incomplete tumor treatment or incomplete response to treatment. Better imaging techniques have led to lower rates of incomplete tumor treatment. The use of cone-beam computed tomography (CBCT) and computed tomography hepatic arteriography (CTHA) enable improved identification of all arteries with blood supply to a tumor. Previous studies have shown that the use of these imaging modalities results in improved outcomes (5-7). In **Chapter**

5, we demonstrated that catheter-directed contrast-enhanced ultrasound (CCEUS) provides similar multi-planar information on tumor enhancement as CTHA without exposing a patient to iodinated contrast media or additional radiation. Unfortunately, practical limitations have hampered the implementation of CCEUS into routine clinical practice.

Radioembolization is generally used to treat patients with advanced stages of disease. In large tumors, delivering a tumoricidal radiation dose to the entire tumor is challenging. As demonstrated in **Chapter 6**, in patients with unresectable hepatocellular carcinoma up to 37% of patients may have extra-hepatic vascular tumor supply. Identifying extra-hepatic feeders is essential to ensure complete tumor treatment and improve outcomes. Other studies have reported extrahepatic arterial tumor supply in 17-30.8% (8-11). In these studies, angiography and CBCT were used to identify extrahepatic tumor supply. In our study, we used CTHA and this may have led to better detection of extrahepatic feeders as CTHA has better spatial resolution and a larger field of view. Furthermore, the superior image quality of CTHA proved to be essential in enabling safe radioembolization through the right inferior phrenic artery. In **Chapter 7**, we demonstrated the superiority of CTHA over angiography and Tc99m-macroaggregated albumin single photon emission computed tomography with integrated computed tomography (Tc99m-MAA SPECT/CT) in the detection of the falciform artery. Despite this and other studies on the superior image quality of CTHA, this imaging modality has not been widely adopted outside of Japan, mainly because of the higher costs compared to CBCT. Further studies will need to investigate whether the higher costs of CTHA are counterbalanced by the superior image quality.

CTHA was also used to develop artery-specific SPECT/CT partition modeling in radioembolization, as described in **Chapter 8**. This technique allows individualized patient treatment with a reduced risk of under-treatment of tumor areas. Based on dose calculations using integrated CTHA, we estimated that a target volume dose of >90 Gy is associated with complete radiological response. Other studies have suggested that radiation doses of at least 100-120 Gy are required for complete response. Yet, estimating the relationship between radiation dose and response is complicated by the fact that distribution of microspheres in inhomogeneous and tissue radiation dose can only be measured indirectly. Better insight in dose-response relationships in radioembolization may be provided by post-treatment imaging with positron emission tomography (PET) or with the use of new generation microspheres.

PHP is a novel minimally invasive treatment for patients with hepatic malignances. **Chapter 9** provides an overview on the currently available literature on PHP. The rec-

ognition of PHP as a first line therapy for patient with hepatic metastases from ocular melanoma is growing, but further research is needed in order to optimize treatment protocols and reduce systemic toxicity. In **Chapter 10**, we demonstrated that the second generation Delcath hemofiltration system has a higher and more consistent chemotherapy filtration rate compared to earlier generation filters. In the future, new detoxification filters factory tuned to high affinity for specific chemotherapeutics may further reduce systemic exposure to chemotherapeutic drugs or enable more effective treatment with other drugs than melphalan chloride.

PART 3. PATIENT MANAGEMENT

New biochemical drugs and technological discoveries with great promise for the future are often at the center of the attention of researchers and funding agencies. This may divert the attention away from research projects that may seem less innovative and exciting. Nevertheless, projects that investigate everyday practise may have an important impact on the wellbeing of patients. In **Chapter 11**, we demonstrated that both patient safety and satisfaction improve significantly when patients are seen in an interventional radiology outpatient clinic prior to an intervention. With the increasing number and complexity of procedures, it is important that interventional radiologists take greater responsibility over the peri-procedural management of patient undergoing minimally invasive image-guided therapies.

FUTURE PERSPECTIVES

Percutaneous RFA offers important advantages over surgery. It is associated with lower morbidity and mortality rates, shorter hospital stays and lower costs. Yet, recurrence rates after RFA tend to be higher than after surgery, especially in larger tumors. Future research should aim to reduce recurrence rates after percutaneous ablation to make it a therapy that is as effective as surgery. Other ablation techniques, such as microwave ablation or irreversible electroporation, have been developed in order to overcome the limitations of RFA, but so far studies have failed to provide evidence that these newer ablation methods are superior to RFA. Limitations that apply to RFA often also apply to other percutaneous ablation techniques.

An important limitation of percutaneous ablation is the absence of histological confirmation of treatment success. Whereas the surgeon will get confirmation from the pathologist whether a tumor has been removed successfully with sufficient margins, the

interventional radiologists relies on post-procedural imaging. We therefore need better ways to assess tumor necrosis and ablation margins with medical imaging. Our research team is currently investigating post-processing software that allows fusion of pre- and post-ablation cross-sectional images to better define ablation margins. With the use of such software, we may be able to identify patients that are likely to have microscopic residual tumor. Patients with increased risk of incomplete tumor ablation may then be re-ablated before recurrence actually occurs.

Another important cause of recurrence after percutaneous ablation may be the presence of micro-metastases. These frequently occur in close proximity to the primary tumor, but may not be coagulated during the ablation. Our research group has initiated a research project to investigate segmental radioembolization as an adjuvant treatment to RFA. Findings in experimental animal studies have demonstrated increased tumor necrosis and improved animal survival after combined treatment with RFA and radiation therapy when compared with either therapy alone (12,13). Preliminary clinical studies in primary lung malignancies have confirmed the synergistic effects of these therapies (14). Potential causes for the synergy include the sensitization of viable tumor cells to subsequent radiation owing to the increased oxygenation resulting from hyperthermia-induced increased blood flow to the tumor (15). Another possible mechanism, which has been seen in animal tumor models, is a radiation-induced inhibition of repair and recovery and increased free radical formation (16). It is unknown what radiation dose should be used when combining RFA with adjuvant radioembolization. This will be investigated in a dose-finding study that is financially supported with a research grant from Health Holland and the Maag Lever Darm stichting.

Conclusions

1. Midterm recurrence and death rates after radiofrequency ablation (RFA) differ between hepatocellular carcinoma (HCC) patients in South-East Asian and Northern-European populations as a result of differences in baseline patient characteristics and patient selection.
2. The accuracy of manual and semi-automatic co-registration of ultrasound (US) and computed tomography (CT) images is better than that of automatic co-registration, based on experiments with the General Electric Logiq E9 navigation platform in a phantom.
3. Local tumor progression-free survival rates after combined RFA and drug-eluting bead transarterial chemoembolization (DEB-TACE) for HCC >3 are low compared to the results reported after combination therapy of conventional transarterial chemoembolization (TACE) followed by RFA.

4. Catheter-directed CEUS is a potentially valuable imaging tool in adjunction to DSA when performing TACE and may provide similar information as catheter-directed computed tomography hepatic arteriography (CTHA).

5. Delivery of Y90 microspheres through the right inferior phremic artery (IPA) is feasible and safe with the use of CTHA in addition to digital subtraction angiography and Tc-99m macroaggregated albumin (MAA) single photon emission computed tomography/integrated computed tomography (SPECT/CT).

6. The hepatic falciform artery detection rate of CTHA is superior to that of DSA and 99mTc-MAA SPECT/CT.

7. Image-guided personalized predictive dosimetry by artery-specific SPECT/CT partition modeling achieves high clinical success rates for safe and effective Y90 radioembolization.

8. Percutaneous hepatic perfusion should be considered as a first line treatment in patients with liver metastases from ocular melanoma

9. The Delcath Systems' second generation (GEN2) hemofiltration system has a higher melphalan filter efficiency compared to the first generation filters and a more consistent performance.

10. Patient safety and satisfaction improve significantly if patients receive consultation and screening in an interventional radiology (IR) outpatient clinic prior to elective IR procedures.

REFERENCES

1. EASL-EORTC clinical practice guidelines: management of hepatocellular carcinoma. European Association for Study of Liver; European Organisation for Research and Treatment of Cancer. Eur J Cancer. 2012 Mar;48(5):599-641

2. Weis S, Franke A, Mössner J, Jakobsen JC, Schoppmeyer K. Radiofrequency (thermal) ablation versus no intervention or other interventions for hepatocellular carcinoma (Review). The Cochrane Library 2013, Issue 2

3. Tiong L, Maddern GJ. Systematic review and meta-analysis of survival and disease recurrence after radiofrequency ablation for hepatocellular carcinoma. Br J Surg. 2011 Sep;98(9):1210-24.

4. Ewertsen C, Ellegaard K, Boesen M, Torp-Pedersen S, Bachmann Nielsen M. Comparison of Two Co-Registration Methods for Real-Time Ultrasonography Fused with MRI: a Phantom Study. Ultraschall in Med 2010; 31:296–301.

5. Miyamaya S, Yamashiro M, Okuda M et al. Usefullness of cone-beam computed tomography during ultraselective transcatheter arterial chemoembolization for small hepatocellular carcinomas that cannot be demonstrated on angiography. Cardiovasc Intervent Radiol. 2009; 32:255-264.

6. Miyamaya S, Yamashiro M, Hattori Y et al. Efficacy of cone-beam computed tomography during transcatheter arterial chemoembolization for hepatocellular carcinoma. Jpn J Radiol. 2011; 29:371-377.

7. Takayasu K, Muramatsu Y, Maeda T, et al. Targeted transarterial oily chemoembolization for small foci of hepatocellular carcinoma using a unified helical CT and angiography system: analysis of factors affecting local recurrence and survival rates. American Journal of Roentenology 2001; 176:681-688.

8. Miyayama S, Matsui O, Taki K, et al. Extrahepatic Blood Supply to Hepatocellular Carcinoma: Angiographic demonstration and Transcatheter Arterial Chemoembolization. Cardiovasc Intervent Radiol 2006; 29:39–48.

9. Chung JW, Kim HC, Yoon JH, et al. Transcatheter arterial chemoembolization of hepatocellular carcinoma: prevalence and causative factors of extrahepatic collateral arteries in 479 patients. Korean J Radiol 2006; 7:257–266.

10. Abdelmaksoud MHK, Louie JD, Kothary N, et al. Embolization of Parasitized Extrahepatic Arteries to Reestablish Intrahepatic Arterial Supply to Tumors before Yttrium-90 Radioembolization. J Vasc Interv Radiol 2011; 22:1355-1362.

11. Miyayama S, Yamashiro M, Okuda M, et al. The March of Extrahepatic Collaterals: Analysis of Blood Supply to Hepatocellular Carcinoma Located in the Bare Area of the Liver After Chemoembolization. Cardiovasc Intervent Radiol 2006; 29:39–48.

12. Solazzo S, Mertyna P, Peddi H, Ahmed M, Horkan C, Goldberg SN. RF ablation with adjuvant therapy: comparison of external beam radiation and liposomal doxorubicin on ablation efficacy in an animal tumor model. Int J Hyperthermia. 2008 Nov;24(7):560-7.

13. Horkan C, Dalal K, Coderre JA, Kiger JL, Dupuy DE, Signoretti S et al. Reduced tumor growth with combined radiofrequency ablation and radiation therapy in a rat breast tumor model. Radiology. 2005 Apr;235(1):81-8.

14. Dupuy DE, DiPetrillo T, Gandhi S, Ready N, Ng T, Donat W et al. Radiofrequency ablation followed by conventional radiotherapy for

medically inoperable stage I non-small cell lung cancer. Chest. 2006 Mar;129(3):738-45.

15. Mayer R, Hamilton-Farrell MR, van der Kleij AJ, Schmutz J, Granström G, Sicko Z et al. Hyperbaric oxygen and radiotherapy. Strahlenther Onkol. 2005 Feb;181(2):113-23.

16. Solazzo SA, Ahmed M, Schor-Bardach R, Yang W, Girnun GD, Rahmanuddin S et al. Liposomal doxorubicin increases radiofrequency ablation-induced tumor destruction by increasing cellular oxidative and nitrative stress and accelerating apoptotic pathways. Radiology. 2010 Apr;255(1):62-74.
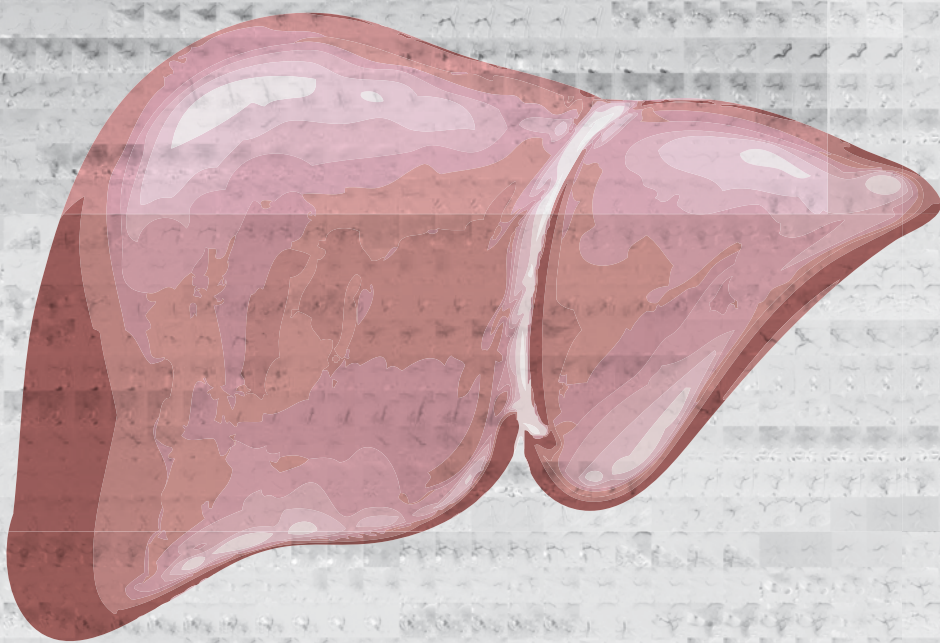
Appendix

NEDERLANDSE SAMENVATTING

Interventie oncologie is een deelspecialisme van de interventieradiologie dat sterk in opkomst is. Bij oncologische interventies wordt gebruik gemaakt van moderne beeldvormende technieken, zoals angiografie, computer tomografie (CT) of magnetische resonantie imaging (MRI). Die beeldvormende technieken maken het mogelijk heel gericht een gezwel te behandelen en de schade aan de rest van het lichaam beperkt te houden. Een ander kenmerk van oncologische interventies is dat ze minimaal invasief zijn. Er is doorgaans niet meer nodig dat een klein prikgaatje om een behandeling uit te voeren. Oncologische interventies bieden belangrijke voordelen voor patiënten boven chirurgische ingrepen en systemische chemotherapie. Omdat de behandelingen gericht en minimaal-invasief zijn, is de kans op complicaties beperkt, het herstel doorgaans sneller en zijn de kosten lager.

Technologische ontwikkelingen hebben in de voorbije twee decennia verschillende nieuwe behandelingen mogelijk gemaakt en bestaande therapieën verbeterd. Dit proefschrift is een bundeling van wetenschappelijk onderzoek dat is verricht naar verschillende nieuwe radiologische interventies bij de behandeling van patiënten met kanker in de lever. De meeste studies in dit proefschrift zijn verricht bij patiënten met kanker welke is ontstaan uit levercellen, zogenaamd hepatocellulair carcinoom (HCC). Jaarlijks overlijden circa 800.000 mensen in de wereld aan leverkanker en de kansen op genezing zijn klein voor personen bij wie de ziekte wordt geconstateerd.

Deel 1 Radiofrequentie ablatie

In dit deel staat radiofrequentie ablatie (RFA) centraal. Bij radiofrequentie ablatie wordt onder beeldgeleide een naald geplaatst in een gezwel. De naald wordt vervolgens aangesloten op een stroombron en door middel van een wisselstroom worden moleculen in het gezwel in trilling gebracht. Door de trilling van de moleculen ontstaat wrijvingswarmte en zo kan de tumor worden verhit tot temperaturen die de tumorcellen niet overleven. Een gezwel kan zo als het ware worden weggebrand. Deze techniek is met name bij patiënten met HCC een aantrekkelijk alternatief voor een operatie. Circa 90% van de patiënten met HCC hebben een onderliggende leverziekte, zoals chronische leverontsteking (hepatitis) of cirrose. Als gevolg daarvan is het operatief verwijderen van een leverkankergezwel risicovol en soms zelfs onmogelijk. RFA is acht keer veiliger dan het operatief verwijderen van een HCC, maar met name bij grotere gezwellen is de kans na een operatie groter dat het gezwel in totaliteit is verwijderd.

In **hoofdstuk 2** worden de resultaten besproken van een onderzoek naar RFA in een groep patiënten met HCC in Singapore en Nederland. Hoewel in beide landen eenzelfde

internationale richtlijnen worden gehanteerd en dezelfde techniek en apparatuur wordt gebruikt, werden duidelijk verschillen gezien in uitkomsten tussen de Aziatische en Europese groep. Risicofactoren voor het terugkomen van de ziekte in de lever waren een gezwelgrootte van meer dan 3 centimeter en het hebben van meer dan 1 gezwel. De kans dat opnieuw een leverkankergezwel uitgroeide was 1.3 maal groter bij de Aziatische patiënten, maar toch was de sterfte na 5 jaar onder Aziatische patiënten bijna driemaal lager (4.9% versus 21.0% in de Europese groep). Mogelijke verklaringen voor de verschillen in uitkomst waren een hoger percentage in de Europese groep met een verder gevorderd ziektestadium, alcoholmisbruik als oorzaak voor de onderliggende leverziekte en verschillen in patiëntenselectie.

In **hoofdstuk 3** beschrijft een studie naar fusie-imaging, een techniek die helpt om met grotere precisie een RFA naald in een gezwel te plaatsen. Echografie is het best bruikbaar om een RFA naald op de juiste plaats te brengen, maar soms is een gezwel niet of slecht zichtbaar op echografie beelden. Er kan dan gebruik gemaakt worden van zogenaamde fusie-imaging. De beelden van een eerder gemaakte CT of MRI scan kunnen worden gekoppeld met de echografie beelden zodat toch kan worden bepaald waar de naald moet worden geplaatst. In een fantoom studie werden drie verschillende methoden van fusie imaging onderzocht: handmatige fusie, semi-automatische fusie en automatische fusie. De eerste twee methoden bleken meer accuraat dan de automatische fusie en de meest betrouwbare fusie werd verkregen door handmatige identificatie van multipele overeenkomstige anatomische locaties op echografie beelden enerzijds en CT/MRI beelden anderzijds.

Zoals in hoofdstuk 2 werd aangetoond, is het risico dat een HCC terugkomt groter bij gezwellen groter dan 3 centimeter. In **hoofdstuk 4** wordt combinatie behandeling van RFA en transarteriële chemoembolisatie (TACE) onderzocht bij patiënten met een HCC groter dan 3 cm. TACE is een behandeling waarbij via het slagaderlijk bloedvatstelsel een weg wordt gezocht naar de leverslagader en lokaal bolletjes met chemotherapie worden geïnjecteerd. Deze behandeling heeft op twee verschillende manieren effect op het gezwel: de bolletjes sluiten de bloedtoevoer van het gezwel af en geven geleidelijk het chemotherapeuticum af zodat de kankercellen gedurende dagen tot weken hieraan worden blootgesteld. In een retrospectieve studie vergeleken we de resultaten van RFA bij patiënten met een HCC ≤3 centimeter met die van RFA + TACE bij patiënten met een HCC > 3 centimeter. Ondanks de toevoeging van TACE bleken patiënten met een groter HCC een duidelijk slechtere prognose te hebben. Er is derhalve een blijvende noodzaak tot verbetering van de minimaal invasieve behandelmogelijkheden van patiënten met een HCC van >3 centimeter.

Deel 2 Transarteriële therapieën

In dit deel van het proefschrift staan TACE, radioembolisatie en percutane leverperfusie centraal. Hierboven werd al TACE genoemd, waarbij bolletje geladen met chemotherapie via het slagaderlijk bloedstelsel tot in een gezwel worden gebracht. TACE is de therapie van keuze bij patiënten met meerdere HCCs in de lever zonder uitzaaiingen buiten de lever. **Hoofdstuk 5** beschrijft de resultaten van een pilot studie bij HCC patiënten die TACE ondergingen met een nieuwe beeldvormende methode. Digitale subtractie angiografie (DSA) is de standaard beeldvormende techniek om de bolletjes chemotherapie op de juiste plek te krijgen. Bij DSA wordt gebruik gemaakt van röntgenstralen en worden de bloedvaten zichtbaar gemaakt door contrastmiddel te injecteren. Een nadeel van DSA is dat de verkregen beelden alleen tweedimensionale informatie geven. Driedimensionale informatie kan wel verkregen worden door een CT scan te maken tijdens de injectie van contrastmiddel in de slagaderen. Deze techniek heet catheter-directed computed tomography hepatic arteriography (CTHA). Een nadeel is dat het gepaard gaat met relatief hoge dosis röntgenstraling. In de beschreven pilot studie werd aangetoond dat vergelijkbare driedimensionale informatie kon worden verkregen met behulp van echografie en injecties van echo-contrastmiddel. Deze techniek, catheter-directed contrast-enhanced ultrasound (CCEUS) genoemd, gaat niet gepaard met schadelijke röntgenstraling. Bovendien geeft het echografie contrastmiddel geen risico op nierfunctieverlies, in tegenstelling tot het jodium-houdend contrastmiddel dat gebruikt wordt bij DSA en CTHA.

Radioembolisatie is een andere en nieuwere transarteriële therapie Hierbij wordt via het slagaderlijk bloedvatstelsel een dunne katheter geplaatst in de leverslagader om vervolgens bolletjes te laten inlopen welke zijn geladen met het radiotherapeutisch middel yttrium-90. Enkele dagen voor de eigenlijke behandeling ondergaat een patient angiografie waarbij een eiwit aggregaat wordt geïnjecteerd dat is gekoppeld aan technetium-99. Dit eiwit aggregaat, technetium 99m-macro-aggregated albumin (Tc99m-MAA), heeft een vergelijkbare grootte als yttrium-90 bolletjes. Wanneer na injectie van Tc99m-MAA een scan wordt gemaakt, kan de verdeling van yttrium-90 bolletjes worden voorspelt en de benodigde dosis radiotherapeutisch materiaal worden berekend. De scantechniek die hierbij wordt gebruikt heet single photon emission computed tomography with integrated computed tomography (SPECT/CT). Wanneer de verdeling van de 'test'-dosis Tc99m-MAA zichtbaar wordt gemaakt, wordt de scan aangeduid als Tc99m-MAA SPECT/CT.

Een gevreesde complicatie van radioembolisatie is dat de bolletjes met yttrium-90 buiten de lever terecht komen en zo stralingsschade veroorzaken aan de darmen of

longen. Er is veel informatie over hoe radioembolisatie veilig kan worden verricht via de leverslagader. Het is echter niet ongewoon dat een levergezwel ook bloed ontvangt via andere slagaders dan de leverslagader. In **hoofdstuk 6** wordt aangtoond dat bij grote HCC gezwellen er in ruim eenderde van de gevallen ook een bloedvoorziening is van buiten de lever. Meest voorkomend bleek bloedtoevoer via de slagader van het middenrif, de arteria frenica inferior. In hoofdstuk 6 wordt in een kleine patientengroep aangetoond dat injectie van yttrium-90 bolletjes via de slagader van het middenrif veilig kan als in aanvulling op DSA ook gebruik gemaakt wordt van hoog geavanceerde beeld- vormende technieken, zoals de hierboven genoemde CTHA en Tc99m-MAA SPECT/CT.

Ook in **hoofdstuk 7** spelen DSA, CTHA en Tc99m-MAA SPECT/CT een belangrijke rol. In een retrospectieve studie bij HCC patienten wordt onderzocht hoe goed elk van de genoemde beeldvormende techniek in staat is om de arteria falcifome te identificeren. De arteria falciforme is een heel kleine slagader die verloopt van de lever naar de buik- wandhuid. Als bij injectie van yttrium-90 in de leverslagader een deel van de bolletjes via deze slagader in de buikwand terecht komen kan dat leiden tot bestralingsschade aan de huid. Aangetoond wordt dat CTHA veel beter in staat is de arteria falciforme te identificeren dan DSA en Tc99m-MAA SPECT/CT: met CTHA werd bijna vier keer zo vaak een arterie falciforme gevonden. Uit deze studie bleek evenwel ook dat het zelden noodzakelijk is om extra voorzorgsmaatregelen te nemen bij patiënten met een kleine arteria falciforme.

Hoofdstuk 8 onderzoekt een nieuwe methode voor de planning van radioembolisatie en bepaling van de benodigde stralingsdosis yttrium-90. Meestal wordt een leverge- zwel van bloed voorzien door verschillende aftakkingen van de leverslagader. Wanneer bolletjes yttrium-90 worden geïnjecteerd op een positie stroomopwaarts van de vertak- kingen, is moeilijk te voorspellen hoeveel bolletjes elk afzonderlijk bloedvat instromen. Het kan dan zijn dan een deel van het gezwel een hoge stralingsdosis ontvang en een ander deel (te) weinig. De methode die onderzocht wordt in hoofdstuk 8 maakt het mo- gelijk een meer voorspelbare en gelijkmatige verdeling van de yttrium-90 bolletjes te verkrijgen. De voedende slagaderen worden afzonderlijk gekatheteriseerd waarna met behulp van CTHA en Tc99m-MAA SPECT/CT de optimale dosis voor de elk stroomgebied apart wordt bepaald.

De laatste twee hoofdstukken van deel 2 handelen over onderzoeken naar percutane geïsoleerde leverperfusie, ookwel aangeduid met de engelse naam percutaneous he- patic perfusion (PHP). Bij deze therapie wordt de bloedvoorziening van de lever als het ware gescheiden van die van de rest van het lichaam met behulp van verschillende katheters. Op die manier wordt het mogelijk een hoge dosis chemotherapie te geven

aan levergezwellen zonder de rest van het lichaam bloot te stellen aan die hoge dosis toxische medicatie.

Hoofdstuk 9 geeft een overzicht van de techniek van PHP, de huidige indicaties en gepubliceerde wetenschappelijke studies. Op basis van beschikbare studies kan worden geconcludeerd dat PHP een effectieve therapie is bij de behandeling van leveruitzaaiingen van oogmelanoom. Bij de meerderheid van de patiënten treedt beenmergdepressie op veroorzaakt door een (beperkte) mate van blootstelling van het lichaam aan chemotherapie. De beenmergdepressie leidt in veel gevallen niet tot symptomen en zelden tot ernstige complicaties. In **hoofdstuk 10** worden de eerste resultaten beschreven van twee klinische studies naar PHP. In genoemde studies werd gebruik gemaakt van een vernieuwd filter, waarmee het bloed uit de lever wordt gezuiverd alvorens het bloed terug gepompt wordt naar de centrale bloedsomloop. Het nieuwe filter bleek effectiever en betrouwbaarder dan eerder gebruikte filtratiesystemen. Desondanks kwam toch een deel van de chemotherapie terecht in de centrale bloedsomloop en trad bij 80% van de patiënten beenmergdepressie op. Ook in deze studie hadden patiënten veelal geen klachten van de beenmergdepressie en waren ernstige complicaties zeldzaam.

Deel 3 Patiëntenzorg

Deel 3 van dit proefschrift bevat slechts één hoofdstuk, **hoofdstuk 11**, en betreft geen onderzoek wat zich specifiek richt op behandelingen van kanker in de lever. Vanwege het belang van het onderwerp is het toch in dit proefschrift opgenomen. De radiologie heeft zich in de voorbije decennia geconcentreerd op het leveren van efficiënte en kwalitatief hoogstaande diagnostiek en het verlenen van peri-procedurele zorg is niet gaan behoren tot haar kerntaken. Ondanks de toename in aantal en complexiteit van radiologische interventies, beschikken de meeste afdelingen radiologie niet over een eigen polikliniek en opnameafdeling. In de meeste centra is de zorg rondom radiologische interventies grotendeel uitbesteed aan verwijzend specialisten. In 2013 is de afdeling radiologie in het Leids Universitair Medisch Centrum (LUMC) gestart met een polikliniek interventieradiologie. In een observationele studie werd gedurende 3 maanden voor en na implementatie van de polikliniek de zorg rondom radiologische interventies geëvalueerd. De polikliniek interventieradiologie bleek een positief effect te hebben op de verleende zorg. Er werden na invoering van de polikliniek minder fouten gemaakt in de voorbereiding op de ingreep en patiënten waren tevredener over de behandeling omdat ze zich beter geïnformeerd en gehoord voelden.

Slotwoord

RFA wordt veelvuldig ingezet bij de behandeling van HCC, maar wordt veelal gezien als alternatief voor patienten waarbij een operatie niet haalbaar is. RFA biedt evenwel

belangrijke voordelen (lagere kosten, minder complicaties en sneller herstel) en zou derhalve bij bepaalde patienten moeten gelden als eerste keus therapie. Op basis van gepubliceerd wetenschappelijk onderzoek is het aannemelijk dat RFA even effectief is als operatieve verwijdering bij patienten met een HCC kleiner dan 2 centimer, maar goede vergelijkende studies ontbreken nog. De resultaten van RFA bij grotere gezwellen dienen te worden verbeterd om het te maken tot een eerste keus therapie. Inmiddels is in het LUMC een start gemaakt met de HORA EST HCC studie. Hierbij worden patiënten met grotere HCCs behandeld met een combinatie van RFA en radioembolisatie met Holmium-166. Verder is gestart met onderzoek dat is gericht op verbeteringen in het evalueren van de zogenaamde ablatie marge, hetgeen een maat is voor hoe ruim een gezwel is weggebrand.

De transarteriële therapieën TACE en radioembolisatie worden frequent ingezet als palliatieve therapie bij patiënten met HCC. De in dit proefschrift opgenomen onderzoeken zijn er met name op gericht geweest met betere beeldvormende technieken te komen tot betere resultaten. Het gebruik van CTHA bij de planning en dosisberekening voor radioembolisatie heeft bewezen meerwaarde, maar er zijn nog weinig centra die de benodigde apparatuur tot hun beschikking hebben. Mogelijk biedt cone-beam computed tomography (CBCT) een goed alternatief voor CTHA. Deze techniek is wel beschikbaar in de meeste centra en dankzij technologische verbeteringen benadert de beeldkwaliteit van CBCT inmiddels die van CTHA. De in het LUMC verrichtte onderzoeken naar PHP hebben geleid tot een acceptatie van PHP als eerste lijns palliatieve behandeling bij patiënten met leveruitzaaiingen van oogmelanoom. In een volgende studie hopen we PHP te combineren met immunotherapie om zo te komen tot betere lange termijn resultaten.

Het is vrijwel ondenkbaar dat een patiënt voor een operatie verschijnt in de operatiekamer zonder vooraf gezien te zijn door een chirurg (in opleiding). Het is echter aan de orde van de dag dat een patiënt pas in de behandelkamer kennis maakt met de interventieradioloog. De studie in hoofdstuk 11 van dit proefschrift heeft aangetoond dat het voeren van een polikliniek interventieradiologie leidt tot een vermindering van fouten in de voorbereiding van een ingreep en tot meer patienttevredenheid. Desondanks behoort een polikliniek interventieradiologie in de meeste centra niet tot de gangbare praktijk en is er geen eenduidige vergoedingssystematiek voor een consult interventieradiologie. Het is aan de huidige generatie interventieradiologen om daar verandering in te brengen.

CURRICULUM VITAE

Mark Burgmans was born on 24 March 1972 in Leiden, the Netherlands. He studied Medicine, Dutch Studies and Philosophy at the University of Amsterdam and received his Medical Degree in 1999. Before obtaining his Master's degree, he spent six months at Yale University in the USA to conduct basic research on expression cloning of the potassium channel gene.

After residencies in Surgery and Orthopedics in the Leiden University Medical Center and St. Lucas-Andreas Hospital, he commenced training in Radiology in the Gelre ziekenhuizen in 2003. In 2005, he continued his training in the University Medical Center Utrecht (UMCU) and worked in the Komfo Anyoke Teaching Hospital in Ghana for 2 months. In 2008, Mark was registered as a radiologist and worked in the UMCU as a fellow in interventional radiology. To further develop his skills as an interventional radiologist, he entered the 1-year fellowship program of the Leiden University Medical Center (LUMC) in Leiden and HAGA hospitals in Den Hague.

After his training, Mark joined Singapore General Hospital in Singapore as a consultant in Interventional Radiology. In 2011, he took on the position of Deputy-director of Research of the department of Radiology, whiched spurred on his interest in clinical research. During this time, he completed a prospective trial on contrast-enhanced ultrasonography-guided TACE and initiated the Singapore INfra-Genicular Angioplasty with PAclitaxel-eluting balloon for Critical Limb Ischaemia (SINGA-PACLI) trial that was granted a competitive research grant from the National Medical Research Council Singapore.

Mark returned to the Netherlands in 2012 to join the LUMC as an interventional radiologist. That same year, he commenced his work as a PhD candidate under professor dr. Albert de Roos. Over recent years, he developed his own line of research and managed to obtain grants from industrial partners, the Dutch Cancer Society and ZonMW. Mark is currently a principle investigator in prospective trials on percutaneous isolated liver perfusion and combination therapy of radiofrequency ablation and radioembolization.

In 2016, Mark joined the board of the Dutch Society of Interventional Radiology and has taken on the role of Chairman since Arpil 2017. He is a member of the board of the Dutch Hepatocellular and Cholangiocarcinoma Group since 2015. Mark has been an invited speaker for various national and international congresses and is a reviewer for

Cardiovascular and Interventional Radiology and Journal of Vascular and Interventional Radiology.

Mark is married to Annemieke Littooij and has two children, Noor and Zoë. His favorite pastime is to ride his racing bike.

LIST OF PUBLICATIONS

Scientific journal publications

1. Drug Eluting Stents in Infrapopliteal Arterial Disease: A Pilot Safety Study in an Asian Population. Damodharan K, Patel A, Irani FG, Burgmans MC, Gogna A, Tay KH, Lo RH, Too CW, Leong S, Venkatanarasimha N, Chan S, Win HH, Sivanathan C, Tan BS. Ann Acad Med Singapore. 2017 Apr;46(4):155-159

2. Percutaneous Endovascular Treatment to Salvage Non-Maturing Arteriovenous Fistulas in a Multiethnic Asian Population. Tham WP, Burgmans MC, Tan BS, Tay KH, Irani FG, Gogna A, Patel A, Lo RHG, Chng SP, Choong HL, Chan SXJM. Ann Acad Med Singapore 2017;46:64-71

3. Phantom study investigating the accuracy of manual and automatic image fusion with the General Electric Logiq E9: implications for use in percutaneous liver interventions. Burgmans MC, Harder JM, Meershoek P, van de Berg NS, Chan SJXM, van Leeuwen FWB, van Erkel AR. Cardiovasc Interv Radiol. 2017 Jun;40(6):914-923

4. Prospective clinical and pharmacological evaluation of the Delcath System's second generation (GEN2) hemofiltration system in patients undergoing percutaneous hepatic perfusion with melphalan. de Leede EM, Burgmans MC, Meijer TS, Martini CH, den Hartig J, Tijl FGJ, Vuyk J, van Erkel AR, van de Velde CJH, Kapiteijn E, Vahrmeijer AL. Cardiovasc Interv Radiol. 2017 Aug;40(8):1196-1205

5. Differences in patient characteristics and mid-term outcome between Asian and European patients treated with radiofrequency ablation for hepatocellular carcinoma. Burgmans MC, Too CW, Fiocco M, Kerbert A.J.C., Lo RH, Schaapman JJ, van Erkel AR, Coenraad MJ, Tan BS. Cardiovasc Intervent Radiol. 2016 Dec;39(12):1708-1715

6. Isolated (hypoxic) hepatic perfusion with high-dose chemotherapy in patients with unresectable liver metastases of uveal melanoma: results from two experienced centres. de Leede EM, Burgmans MC, Kapiteijn E, Luyten GP, Jager MJ, Tijl FG, Hartgrink HH, Grünhagen DJ, Rothbarth J, van de Velde CJ, Verhoef C, Vahrmeijer AL. Melanoma Res. 2016 Aug 10

7. Percutaneous Hepatic Perfusion (PHP) with Melphalan as a Treatment for Unresectable Metastases Confined to the Liver. de Leede EM, Burgmans MC, Martini CH, Tijl FG, van Erkel AR, Vuyk J, Kapiteijn E, Verhoef C, van de Velde CJ, Vahrmeijer AL. J Vis Exp. 2016 Jul 31;(113).

8. Percutaneous isolated hepatic perfusion for the treatment of unresectable liver malignancies. Burgmans MC, de Leede EM, Martini CH, Kapiteijn E, Vahrmeijer AL, van Erkel AR. Cardiovasc Interv Radiol. 2016 Jun;39(6):801-14

9. In Vivo Proof of Superselective Transarterial Chemoembolization with 40-μm Drug-Eluting Beads in a Patient with Hepatocellular Carcinoma. She HL, Burgmans MC, Coenraad M, Saraqueta AF. Cardiovasc Intervent Radiol. 2016 Jan;39(1):137-40

10. Gastric variceal hemorrhage in a non-cirrhotic patient treated with Balloon-Occluded Retrograde Transvenous Obliteration. Ottevanger J, van Rijswijk CSP, van Hoek B, Burgmans MC. Cardiovasc Intervent Radiol. 2015 Aug;38(4):1060-3.

11. Impact on Patient Safety and satisfaction of ImPlementation of an Outpatient cLinic in Interventional radiology (IPSIPOLI-study): a quasi-experimental prospective study. Lutjeboer J, Burgmans MC, Chung K, van Erkel AR. Cardiovasc Interv Radiol. 2015 Jun;38(3):543-51

12. Pilot study evaluating catheter-directed contrast-enhanced ultrasound compared to catheter-directed computed tomography arteriography as adjuncts to digital subtraction angiography to guide transarterial chemoembolization. Burgmans MC, van Erkel AR, Too CW, Coenraad MJ, Lo RHG, Tan BS. Clin Radiol. 2014 Oct;69(10):1056-61

13. Survival and Pattern of Tumor Progression with Yttrium-90 Microsphere Radioembolization in Predominantly Hepatitis B Asian Patients with Hepatocellular Carcinoma. Khor AYK, Toh Y, Allen JC, Ng DCE, Kao YH, Zhu S, Choo SP, Lo RHG, Tay KH, Teo JY, Goh BKP, Burgmans MC, Irani FG, Goh ASW, Chow PKH. Hepatology International. 2014 Jul; 8 (3): 395-404

14. Post-radioembolization yttrium-90 PET/CT - part 1: diagnostic reporting. Kao YH, Steinberg JD, Tay YS, Lim GK, Yan J, Townsend DW, Takano A, Burgmans MC, Irani FG, Teo TK, Yeow TN, Gogna A, Lo RH, Tay KH, Tan BS, Chow PK, Satchithanantham S, Tan AE, Ng DC, Goh AS. EJNMMI Res. 2013 Jul 25;3(1):56.

15. Post-radioembolization yttrium-90 PET/CT - part 2: dose response and tumor predictive dosimetry for resin microspheres. Kao YH, Steinberg JD, Tay YS, Lim GK, Yan J, Townsend DW, Budgeon C, Boucek JA, Francis RJ, Cheo TS, Burgmans MC, Irani FG, Lo RH, Tay KH, Tan BS, Chow PK, Satchithanantham S, Tan AE, Ng DC, Goh AS. EJNMMI Res. 2013 Jul 25;3(1):57.

16. Computed tomography hepatic arteriography has a hepatic falciform artery detection rate that is much higher than that of DSA and 99mTc-MAA SPECT/CT: implications for planning Y90 radioembolization? Burgmans MC, Too CW, Kao YH, Goh ASW, Chow PKH, Tan BS, Tay KH, Lo RHG. Eur J Radiol. 2012 Dec;81(12):3979-84

17. Radioembolization with infusion of Y90 microspheres into a right inferior phrenic artery with hepatic tumor supply is feasible and safe. Burgmans MC, Kao YH, Irani FG, Dames E, Teo TK, Goh ASW, Chow PKH, Tay KH, Lo RHG. J Vasc Interv Radiol. 2012 Oct;23(10):1294-301

18. Radioembolization after portal vein embolization in a patient with multifocal hepatocellular carcinoma. Burgmans MC, Irani FG, Chan W, Teo T, Kao YH, Goh ASW, Chow PKH, Lo HG. Cardiovasc Intervent Radiol. 2012 Dec;35(6):1519-23.

19. Image-guided personalized predictive dosimetry by artery-specific SPECT/CT partition modeling for safe and effective Yttrium-90 radioembolization. Kao YH, Tan AEH,

Burgmans MC, Irani FG, Khoo LS, Lo RHG, Tay KH, Tan BS, Chow PKH, Ng DCE, Goh ASW. J Nucl Med. 2012 Apr;53(4):559-66

20. Image quality assessment of the right ventricle with three different delayed enhancement sequences in patients suspected of ARVC/D. Plaisier AS, Burgmans MC, Vonken EPA, Prakken NH, Cox MGPJ, Hauer RN, Velthuis BK, Cramer MJM. Int J Cardiovasc Imaging. 2012 Mar;28(3):595-601

21. Pacemaker lead induced severe tricuspid valve stenosis. Uijlings R, Kluin J, Salomonsz R, Burgmans M, Cramer MJ. Circ Heart Fail. 2010 May 1;3(3):465-7.

22. Septic thrombosis of the inferior vena cava treated with percutaneous mechanical thrombectomy. Burgmans MC, Rommes JH, Spronk PE, van Nidek RJ, Bouma WH, Gratama JW J Vasc Interv Radiol. 2006 Oct;17(10):1697-702

23. State of the art treatment of comminutive femoral shaft fractures: evidence-based case report. Poolman RW, Burgmans MC, Ultee JM. Dutch Journal of Traumatology. 2002 Dec;10:168-175

Book chapter

Burgmans MC, et al. Interventionen bei Hämodialyse-Shunts. In: Chavan A, ed. Vaskuläre Interventionen. George Thieme Verlag AG. 2016;ISBN: 9783131532015. p 274-284.

DANKWOORD

De basis voor dit proefschrift is gelegd in Singapore. Gedurende twee jaar was ik met veel plezier werkzaam in Singapore General Hospital (SGH). De beslissing om in Singapore te gaan werken was een van de betere beslissingen uit mijn leven. De beste beslissing was de keuze voor mijn vrouw Annemieke, maar daarover later meer. Het was verplicht in de angiokamer in SGH een operatiepak te dragen dat het meest weg had van een pyjama. Er gingen vele etmalen voorbij waarbij ik alleen in bed *geen* pyjama droeg...

De gebundelde expertise van interventieradiologen uit allerlei windstreken en uitstekende faciliteiten maakten het mogelijk de grenzen van de interventie radiologie te verkennen. Daarmee groeide ook de notie dat innovatie en onderzoek onmisbaar zijn om die grenzen te verleggen. En dus besloot ik daaraan mijn steentje bij te gaan dragen.

Dear Bien Soo, you have been an inspiration in many ways. You have shown me that hard work and persistance are the key elements to reset boundaries and accomplish goals. You tought me to push the envelope and I probably would not have written this thesis without your encouragements to initiate research projects.

Dear Kiang Yong, I have often been amazed by your speed and skills in the angiosuite. Puncturing the peroneal artery under fluoroscopic guidance? You make it look so easy... Your energy and devotion to interventional radiology seem endlessly and have been an inspiration.

Dit proefschrift heeft pas echt vorm gekregen in Leiden. Beste professor Bloem, beste Hans, dank dat je bij mijn aanstelling de weg en tijd vrij hebt gemaakt om mijn promotie vorm te geven. Beste professor de Roos, beste Albert, dankzij jouw pragmatisme is het hele traject vlot verlopen: het was bij benadering de beoogde blitzkrieg.

Beste Arian, je bent een belangrijke reden geweest om na mijn verblijf in Singapore terug te keren in het LUMC en jouw bijdrage aan dit proefschrift is groot geweest. Je bent een bekwaam interventie radioloog, maar bovenal een prettig persoon met oog voor cohesie en menselijke maat en belangrijk klankbord voor ideeën.

Beste Carla en Rutger, met een promotie ben je vele anderen tot last, maar ik heb van jullie nooit gemor gehoord... Ik ben blij zulke prettige (en competente) collegae te hebben!

Beste Jacob, beste PA van Nederland, wat een positieve invloed heeft jouw aanwezigheid op sectie 5! Dankzij jou (en Kaman!) is de IPSIPOLI studie een succes geworden.

De meeste projecten in dit proefschrift zijn tot stand gekomen dankzij nauwe en plezie-rige samenwerking met vele medisch specialisten in het LUMC. In het bijzonder dank ik Minneke Coenraad, Ellen Kapiteijn en Alexander Vahrmeijer; jullie inbreng is onmisbaar geweest bij de tot stand komen van de publicaties van dit proefschrift!

Geachte leden van de beoordelingscommissie, prof. dr. Lioe-Fee de Geus-Oei, prof. dr. Otto van Delden, prof. dr. Willem Mali, dr. Minneke Coenraad en dr . Alex vahrmeijer: veel dank voor het lezen en beoordelen van mijn proefschrift!

Noor en Susan, dank voor al jullie inspanningen voor de PHP studies. Hopelijk volgt jullie eigen proefschrift snel! Annarein Kerbert, Jelle Schaapman, Marta Fiocco, Ron Wolterbeek, Fijs van Leeuwen, Chiel Harder, Pip Meershoek, Chris Martini, Jaap Vuijk, Fred Tijl en Gerrit Kracht: dank voor jullie bijdragen aan dit proefschrift.

Verder heb ik bij verschillende onderzoeksprojecten nauw samengewerkt met voorma-lig collegae uit Singapore. Many thanks to the IRs in SGH who collaborated on some of the research projects of this thesis: Farah (my IR buddy), Richard, Chow Wei, Shaun, Terence and Li Ser. Special thanks to Yung Hsiang Kao, who has been the driving force for the projects on radioembolization.

Bassie, Tammo, dank dat ik jullie op mag zadelen met de uitvoerende taken van een paranimf. Ik heb U lief!

Lieve Ad, dank dat je de weg naar het Academie gebouw op het Rapenburg al geplaveid hebt! Ik zal kijken of ik nog een plek op de muur kan vinden om je naam alsnog bij te schrijven...

Lieve mama, overtreffende trap van onvoorwaardelijke moederliefde, dank voor alle liefde en zorg waarmee je mij (en mijn gezin) al vele jaren ondersteunt. Love you to the moon and back.

Lieve Annemieke, geen twijfel over mogelijk: ik heb met mijn zelfgemaakte Sushi en krijt op de juiste stoep gestaan! Er zijn vele hoogtepunten geweest de afgelopen jaren, nu weer deze dubbelpromotie, maar ook bij de ontij van dit jaar staan we samen sterk. Aan energie heb ik geen gebrek, maar ik dank het aan jou dat het ook nog ergens toe leidt!

Lieve Noor en Zoë, dank je dat ik zo vaak heb mogen "You-tuben" van jullie, zodat ik dit proefschrift kon voltooien..... Wat een feest dat jullie er zijn!